

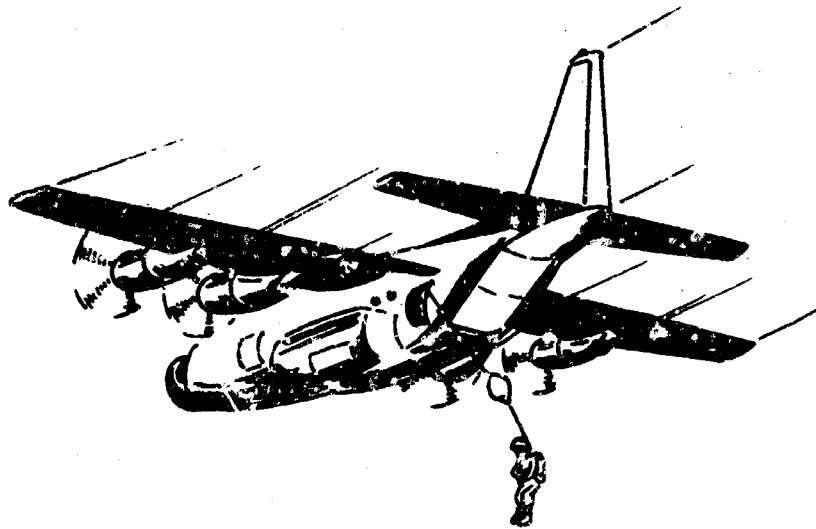
GER-12888

30 December 1966

Copy No. 8

AD 667401

**PRELIMINARY INVESTIGATION OF CONCEPTS
FOR LOW-ALTITUDE AIRDROP OF
PERSONNEL - EXPLORATORY DEVELOPMENT
(FINAL REPORT)**



Prepared by Richard A. Lau
Goodyear Aerospace Corporation, Akron, Ohio
for
U.S. Army Natick Laboratories, Natick, Mass.
Contract No. DA 19-129-AMC-855(N)

This document has been approved for public release and sale; its distribution is unlimited.

The findings in this report are not to be construed as an official Department of the Army position unless so designated by other authorized documents.

Citation of trade names in this report does not constitute an official endorsement or approval of the use of such items.

Destroy this report when no longer needed. Do not return to the originator.

UNCLASSIFIED

AD 667 401

PRELIMINARY INVESTIGATION OF CONCEPTS FOR
LOW-ALTITUDE AIR DROP OF PERSONNEL - EXPLORATORY
DEVELOPMENT

Richard A. Lau

Goodyear Aerospace Corporation
Akron, Ohio

30 December 1966

Processed for . . .

DEFENSE DOCUMENTATION CENTER
DEFENSE SUPPLY AGENCY



U. S. DEPARTMENT OF COMMERCE / NATIONAL BUREAU OF STANDARDS / INSTITUTE FOR APPLIED TECHNOLOGY

THIS REPORT HAS BEEN APPROVED FOR
PUBLICATION AND ITS DISTRIBUTION
IS UNLIMITED.

GOODYEAR AEROSPACE CORPORATION

AKRON, OHIO 44315

TR 68-43-AD

PRELIMINARY INVESTIGATION OF
CONCEPTS FOR LOW-ALTITUDE AIR -
DROP OF PERSONNEL - EXPLORATORY
DEVELOPMENT (FINAL REPORT)

GER-12888

30 December 1966

Richard A. Lau

Goodyear Aerospace Corporation, Akron, Ohio

for

U.S. Army Natick Laboratories, Natick, Mass.

Contract No. DA 19-129-AMC-855(N)

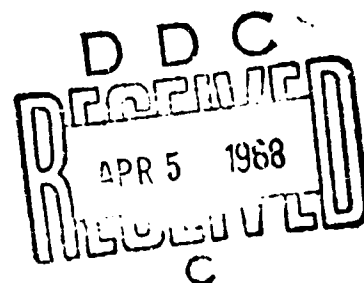


TABLE OF CONTENTS

	<u>Page</u>
FOREWORD	ii
LIST OF ILLUSTRATIONS	v
LIST OF TABLES	ix
SUMMARY	xi

<u>Section</u>	<u>Title</u>	
I	INTRODUCTION	1
	1. General	1
	2. System Concepts	1
	3. Scope and Constraints	1
	4. Design Criteria and Performance Goals	3
	5. Concept Evaluation Criteria	4
	6. Summary of Aerial Delivery Applications	7
II	PERSONNEL AERIAL DELIVERY CONCEPT ANALYSIS	9
	1. General	9
	2. Drag Concepts	9
	a. General	9
	b. BALLUTE/Parachute Concept	10
	c. Internal Canopy System	14
	d. Ballistic Parachute	17
	e. Drag Cone	22
	f. Canopy/Explosive System	28
	3. Thrust-Lift Concepts	31
	a. General	31
	b. Rotating Decelerators	31
	c. Powered Lifting Devices	40
	4. Gliding Concepts	44
	a. General	44
	b. Parawings	45
	c. Gliding Parachutes	63
	d. Ring Wing Airfoil	78
	e. Total System Design and Performance	84

TABLE OF CONTENTS

<u>Section</u>	<u>Title</u>	<u>Page</u>
III	SYSTEM CONCEPT RECOVERY PROFILES	97
1.	General	97
2.	Functional Operations	97
a.	BALLUTE/Parachute	97
b.	Internal Canopy System	98
c.	Ballistic Parachute	98
d.	Drag Cone	127
e.	Canopy/Explosive System	127
f.	Rotating Decelerator	128
g.	Powered Lifting Systems	128
h.	Parawing	129
i.	Gliding Parachutes	130
j.	Ring Wing Airfoil	130
IV	CONCEPT EVALUATION	133
1.	General	133
2.	Performance and Operational Suitability	133
3.	Nonoperational Suitability and Reliability	136
V	CONCLUSIONS AND RECOMMENDATIONS	143
	LIST OF SYMBOLS	145
	LIST OF REFERENCES	155
<u>Appendix</u>		
A	PERFORMANCE CHARACTERISTICS OF THE T-10 PERSONNEL DELIVERY SYSTEM	159
B	INFLATION SYSTEM STUDY	165

LIST OF ILLUSTRATIONS

<u>Figure</u>	<u>Title</u>	<u>Page</u>
1	System Concepts	5
2	Computer Analysis of First-Stage BALLUTE	11
3	Opening Time and Opening Force Related to Characteristic Value of the Original Parachute	15
4	UPP Opening Time versus Velocity	18
5	Calculated Inflation Time versus Deployment Velocity (UPF)	18
6	Ballistic Personnel Parachute Inflation Time versus Velocity	20
7	Ballistic Parachute Load versus Time	20
8	Estimated C_{D_B} versus Cone Semiapex Angle	23
9	Ballistic Coefficient versus Equilibrium Descent Velocity	23
10	Sample Drag Cone Schematic	24
11	Attenuator History	27
12	Rotor Drag Coefficient versus Advance Ratio	33
13	Descent Velocity versus Rotor Diameter	34
14	$(L/D)_R$ versus Advance Ratio for 45-Ft Diameter Rotor	35
15	$(L/D)_T$ Variation with Parasite Body Drag (C_{D_P}) and Advance Ratio (μ)	36
16	Performance Parameters for Collective Flare	37

LIST OF ILLUSTRATIONS

Figure	Title	Page
17	Estimated Recovery-System Weight versus Descent Velocity for a Rocket-Cushioning, Ground-Proximity Device	44
18	Lift-to-Drag Performance for 50-Deg Swept Conical and Cylindrical Parawings Having Rigid Frames and a Limp Parawing	47
19	Aerodynamic Characteristics of Conical Canopy (Parawing Alone)	49
20	Aerodynamic Characteristics of Cylindrical Canopy (Parawing Alone)	50
21	Aerodynamic Characteristics of Limp Parawing Configuration (NASA Fabric Test Model)	51
22	Aerodynamic Characteristics of Limp Parawing ($1/8 C_R$ Nose Cut, Canopy Alone)	52
23	Static Stability Characteristics (Parawing Alone)	54
24	Center-of-Gravity Location for Trim versus Angle of Attack	55
25	Static Lateral Stability	56
26	Conical Parawing Weight versus Reference Area for Structural Integrity	62
27	Estimated Conical Parawing Weight for Recovering a 300-Lb Composite System	64
28	Estimated Limp Parawing Weight for Recovering a 300-Lb Composite System	64
29	Maximum Lift-to-Drag Ratio for Three Gliding Parachute Configurations	65
30	Normal and Tangent Force Coefficients for Parasail Test Configuration	68
31	Aerodynamic Characteristics of Cloverleaf Parachute	69
32	Aerodynamic Characteristics of Wing-Alone Configuration	70

LIST OF ILLUSTRATIONS

<u>Figure</u>	<u>Title</u>	<u>Page</u>
33	Aerodynamic Characteristics of Parasail Canopy. . .	71
34	Aerodynamic Characteristics of Cloverleaf Parachute (Canopy Alone) without Lines	72
35	Estimated Gliding Parachute Weight versus Reference Area	76
36	Estimated Parasail Weight with Suspension Lines versus Nominal Reference Area	77
37	Estimated Cloverleaf Weight with Suspension Lines versus Reference Wetted Area	77
38	Radius-to-Chord Ratio versus Aspect Ratio for a Ring Wing Airfoil	80
39	Aerodynamic Characteristics of a Ring Wing Airfoil .	81
40	Aerodynamic Characteristics of a Ring Wing Airfoil (Ring Alone)	83
41	Alternate Ring Wing Airfoil Design	84
42	Computed Paraglider Flare Trajectories	85
43	Allowable Landing Velocities	89
44	Angle of Attack versus Lift Coefficient (Conical Para- wing)	93
45	Angle of Attack versus Lift Coefficient (Cylindrical Parawing)	93
46	Angle of Attack versus Lift Coefficient (Limp Para- wing)	94
47	Angle of Attack versus Lift Coefficient (Parafoil)	91
48	Flap Extension versus Lift Coefficient (Cloverleaf)	95
49	BALLUTE/Parachute Operational Profile	101
50	Internal Canopy System Operational Profile	103

LIST OF ILLUSTRATIONS

<u>Figure</u>	<u>Title</u>	<u>Page</u>
51	Ballistic Parachute Operational Profile	105
52	Drag Cone Operational Profile	107
53	Canopy/Explosive System Operational Profile	109
54	Rotating Decelerator Operational Profile	111
55	Lift Platform Operational Profile	113
56	Conical Parawing Operational Profile	115
57	Limp Parawing Operational Profile	117
58	Parafoil Parachute Operational Profile	119
59	Parasail Parachute Operational Profile	121
60	Cloverleaf Parachute Operational Profile	123
61	Ring Wing Airfoil Operational Profile	125
62	Opening Time versus Airspeed (T-10 System, MC-1 Canopy)	134
63	Inflation Time versus Airspeed	134
A-1	Opening Time Characteristics of the MC-1	160
A-2	Estimated Altitude Lost versus Aircraft Delivery Speed for a 300-Lb System	161
A-3	Characteristics of a 10-Percent Extended-Skirt Canopy (Type MC-1, 35-Ft D_0)	162
A-4	Characteristics of a 24-Ft D_0 Solid Flat Canopy	163
B-1	Inflation System Weights	166

LIST OF TABLES

<u>Table</u>	<u>Title</u>	<u>Page</u>
I	Summary Description of System Concepts	2
II	BALLUTE/Parachute Weight Estimates	13
III	Typical Packaging Factors and Volume Requirements	14
IV	Opening Characteristics of Conventional and Internal Canopy Systems	16
V	Estimated Weight of 35-Ft D ₀ Ballistic Parachute System	22
VI	Test Results Using Timed Multiple Charges	30
VII	Calculated Results Based on Table VI	30
VIII	Estimated Rotor System Component Weights	40
IX	Weight Estimates for Teeter-Rotor and Jet-Reaction Lifting Platforms	43
X	Summary Description of Gliding Concepts	46
XI	Available Weight and Size Data for Parafoil Configurations	79
XII	Estimated Reference Area Requirements for Two Landing Velocities at Two Ground-Level Altitudes	87
XIII	Parameter Values for Descent and Landing with C_L at Landing = $C_{L_{max}}$	90
XIV	Estimated Reference Area Requirements for a 19-fps Total Landing Velocity at Two Ground-Level Altitudes	90

LIST OF TABLES

Table	Title	Page
XV	Parameter Values for Various System Landings Without Flare at $(L/D)_{\max}$	91
XVI	Effects of Attached Payload Parasite Drag Area, $(C_D S)_P$, on $(L/D)_{\max}$	92
XVII	System Sequence and Operations	99
XVIII	Estimated Performance Characteristics of System Concepts for Delivery at 130 Knots	137
XIX	Estimated Operational Suitability Characteristics	139
XX	Nonoperational Suitability and Reliability of System Concepts	141
B-1	Typical Packaging Factors	167

SUMMARY

Ten different system concepts for the low-altitude air-delivery of personnel have been investigated for their current practicality, applicability, and economy. These concepts included rotating and jet-reaction thrust-lift devices, various parawing and gliding parachute designs, and drag designs. The primary objective was the preliminary evaluation and comparison for mass air-assault operations from 500 ft or less. Basic evaluation criteria have been low-altitude delivery capability, apparent system simplicity and reliability, personnel and cargo compatibility, cost effectiveness, and overall suitability to mass airdrop applications.

The results have indicated that some of the concepts have an apparent advantage over the current T-10 personnel delivery system in low-altitude capability but may not be satisfactory in other respects.

In general, thrust-lift devices are excessive in weight and are not compatible with airdrop operations.

Some of the gliding concepts are capable potentially of satisfying the low-altitude requirement and offer the advantages of aircraft "stand-off" deployment capability and high troop saturation of the drop zone. Gliding systems, however, may not be suitable for high-density troop deployment where a minimum collision rate among deployed personnel is highly important.

Of the drag concepts investigated, only two - the ballistic parachute and the BALLUTE^a/parachute - appear to reduce the total altitude requirement. The ballistic parachute may open faster than the BALLUTE/parachute, particularly at relatively low deployment velocities, but appears less suitable in weight, operational simplicity, and inherent safety.

For potentially suitable configurations, the nominal opening characteristics should be experimentally verified and other effects, which cannot be readily or reliably ascertained analytically, determined. Currently, a large altitude margin is necessary with the T-10 system to compensate for those cases where a delayed opening, several line twists, and/or a canopy malfunction are experienced and emergency procedures must be applied. For any potentially suitable configuration, then, further experimental investigation is required to determine the extent and effects of the nominal opening characteristics.

^aTM, Goodyear Aerospace Corporation, Akron, Ohio.

SECTION I - INTRODUCTION

1. GENERAL

Hazards involved to both men and equipment in tactical assault operations have pointed up a need for a reliable airdrop system with a low-altitude delivery capability. The development of a suitable system with repeatable opening characteristics within an altitude of 500 ft would reduce substantially the vulnerability of the delivery aircraft and would provide for less trooper dispersion and more rapid assembly in the drop zone.

The current T-10 personnel delivery system has a minimum standard altitude capability of 750 to 1000 ft, although the indicated nominal opening characteristics of the MC-1 canopy are compatible with a 500-ft delivery altitude (see Appendix A). The difference in these values can be primarily attributed to delayed openings, line twists, and canopy malfunctions, where a time and altitude margin are necessary, based on a minimum acceptable risk, for using personnel to make the proper adjustment.

2. SYSTEM CONCEPTS

The basic personnel aerial delivery system concepts are listed in Table I. Table I also includes a summary description of the individual systems, a list of their major components, and a brief résumé of their potential advantages for personnel delivery application. Representative illustrations of each concept are shown in Figure 1.

3. SCOPE AND CONSTRAINTS

This program was initiated to investigate preliminarily 10 different system concepts to determine how well the concepts conform to desirable low-altitude design and performance goals. From this analysis, an evaluation of each concept was made, and a preliminary comparison of their individual suitability was obtained. To facilitate the analysis, an investigation of the T-10 personnel delivery system also was conducted (see Appendix A). This appendix provides a basic reference system for evaluating and comparing the various system concepts.

Based on the system concepts listed in Table I, this low-altitude airdrop

SECTION I - INTRODUCTION

TABLE I - SUMMARY DESCRIPTION OF SYSTEM CONCEPTS

System concept	Description	Primary components	Indicated advantages
Drag systems			
1. BALLUTE [®] /parachute	BALLUTE at apex of 35-ft D ₀ extended-skirt canopy	BALLUTE, primary canopy	First-stage stabilization and deceleration, faster more positive filling of canopy
2. Quick-opening parachute	35-ft D ₀ extended-skirt canopy with internal canopy inflation aid	Primary canopy, internal canopy	Faster filling, more positive filling
3. Ballistic parachute	35-ft D ₀ extended-skirt canopy with ballistic spreading device	Primary canopy, gas-actuated spreading device and slugs	Faster filling, more positive filling
4. Canopy/explosive	Explosive charges within a 24-ft D ₀ extended-skirt canopy	Primary canopy, several small explosive charges	Faster downtime, lower touchdown velocities
5. Drag cone	Man-enveloping fabric cone, apex attenuator	Fabric cone, pressurized torii, nose attenuator	Quicker downtime, land or water landing capability, smaller-sized configuration
Thrust-lift systems			
6. Rotating decelerator	Autorotating configuration with flexible blades	Pressurized rotating lifting surfaces	Glide capability, maneuverability, collective and cyclic flare touchdowns
7. Powered lifting devices	Powered teeter-rotor and jet-reaction lifting platforms, rocket lift systems	Lifting element, power source and fuel, support and frame attachment elements	Large range capability, controllable, low touchdown velocities
Gliding systems			
8. Parawings:			
Conical	Double-lobed configuration, conical surfaces with straight large leading edge booms and a central keel	Fabric membrane, pressurized booms and keel, control lines	Maneuverability, flared landing capability, glide capability
Cylindrical	Double-lobed configuration, cylindrical surfaces with helical large leading edge booms and a central keel	Fabric membrane, pressured booms and keel, control lines	Glide capability, maneuverability, flared landing capability, high-performance configuration
Limp	Double-lobed configuration with 1/8-keel nose cut, parawing rigging	Fabric membrane, "fan-patch" suspension line attachments, control lines	Glide capability, maneuverability, flared landing capability, parachute-like structure
9. Gliding parachutes:			
Parasail	Multislotted, triconical-shaped canopy	Parasail canopy, control flaps	Glide capability, maneuverability, parachute-type structure
Parafoil	Ram-air fabric wing, opened leading edge	Symmetrical fabric airfoil, control lines	Glide capability, maneuverability, no pressurized components, flared landing capability
Cloverleaf	Three-lobed compartmental-type canopy	Cloverleaf canopy, extendable control flaps	Glide capability, maneuverability, parachute-type structure
10. Ring wing airfoil	Ring-shaped fabric airfoil decelerator	Pressurized AIR-MAT [®] or fabric membrane with pressurized leading edge torus and chordwise tubes	Glide capability, high-performance configuration, maneuverable, flared landing capability

[®]TM. Goodyear Aerospace Corporation, Akron, Ohio. (Use of trade names does not constitute government endorsement)

SECTION I - INTRODUCTION

study encompasses a wide variety of possible techniques for personnel and cargo recovery. Various geometrical and structural designs are involved not only between the 10 concept classifications but also within the spectrum of the individual concepts themselves. Due to the number of concepts involved and the preliminary nature of this report, an investigation and an evaluation of all possible designs are not considered practical. Consequently, the approach used is to present general concept design and performance data followed by more detailed information for selected representative and/or promising designs.

When available, experimental documented results for each system concept were used as the bases for the analyses. Since not all systems or subsystems have been investigated previously or tested to the same degree, some comparison between experimentally based data and theoretical data is unavoidable. The assumptions made and the data sources used, therefore, will be referenced for comparing the system concepts.

4. DESIGN CRITERIA AND PERFORMANCE GOALS

The technical analysis conducted was performed in accordance with U. S. Army Contract DA 19-129-AMC-885(N). Design criteria and performance goals for candidate systems are described in Article 1, Statement of Work, and are summarized as follows:

1. Altitude delivery capability - 500 ft
2. Aircraft delivery speed - 40 to 150 knots
3. Ground winds - 0 to 15 knots
4. Reliability - 0.9993
5. Circular error probability (CEP) - 100 m
6. Operational capability under adverse environmental conditions and night and day operations
7. Operational and nonoperational compatibility with operations using mass aircraft formation and mass troop and cargo deployment
8. Maximum vertical impact velocity of 19 fps from sea level to 5000 ft. Composite system weight is 300 lb
9. Compatible with standard emergency and survival equipment
10. Maximum compatibility with standard individual equipment
11. Recovery-system weight of 50 lb or less

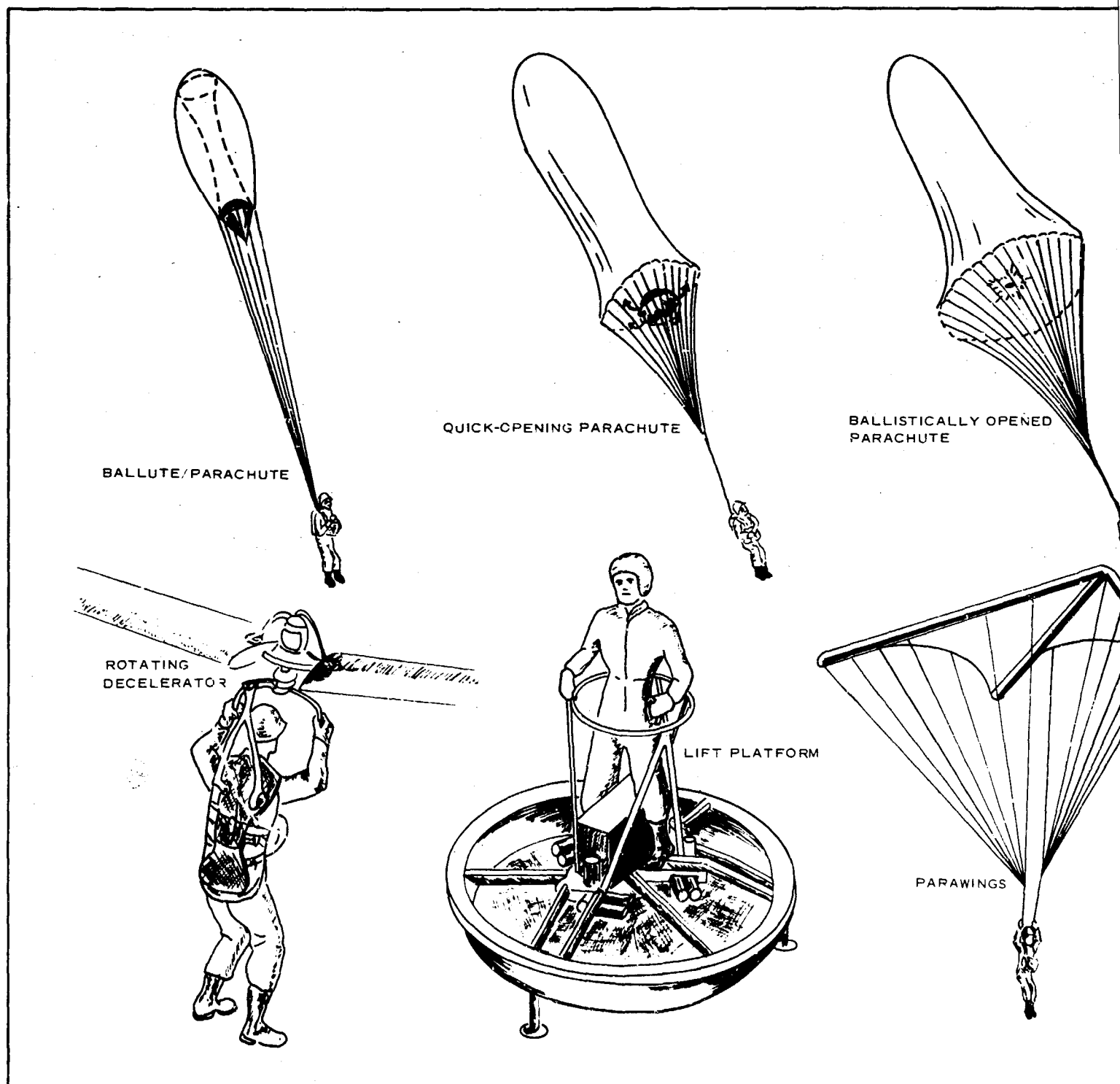
SECTION I - INTRODUCTION

12. Cargo delivery capability
13. Minimum drop zone preparations and restrictions
14. Compatible with existing aircraft
15. Minimum manipulation requirements in operation
16. Minimum restrictions on rapid assembly of personnel in the drop zone, including immediate access to individual weapons and equipment
17. Minimum operational hazards for using personnel
18. Minimum operational and nonoperational complexities
19. Minimum training requirements for using personnel
20. Simple to adjust, fit, inspect, and operate
21. Maximum service life and minimum user maintenance
22. Maximum deceleration forces not to exceed those currently encountered with the T-10 system
23. System safety factor of 2
24. No restriction on flight safety of personnel
25. Economical to develop, manufacture, replace, and repair

5. CONCEPT EVALUATION CRITERIA

In selecting suitable criteria for evaluating system concepts, consideration must be given to established design and performance goals for personnel air delivery systems. Criteria developed for this study, therefore, were formulated primarily from these goals and constituted a representative cross section of performance capability, design simplicity, operational and nonoperational suitability, reliability, maintenance and service, and cost effectiveness. Evaluation criteria are as follows:

1. Minimum operational altitude
2. Target intercept capability
3. Performance sensitivity
4. Compatibility with mass air-assault operations (including aircraft, men, and equipment)
5. System weight



A.

SECTION I - INTRODUCTION

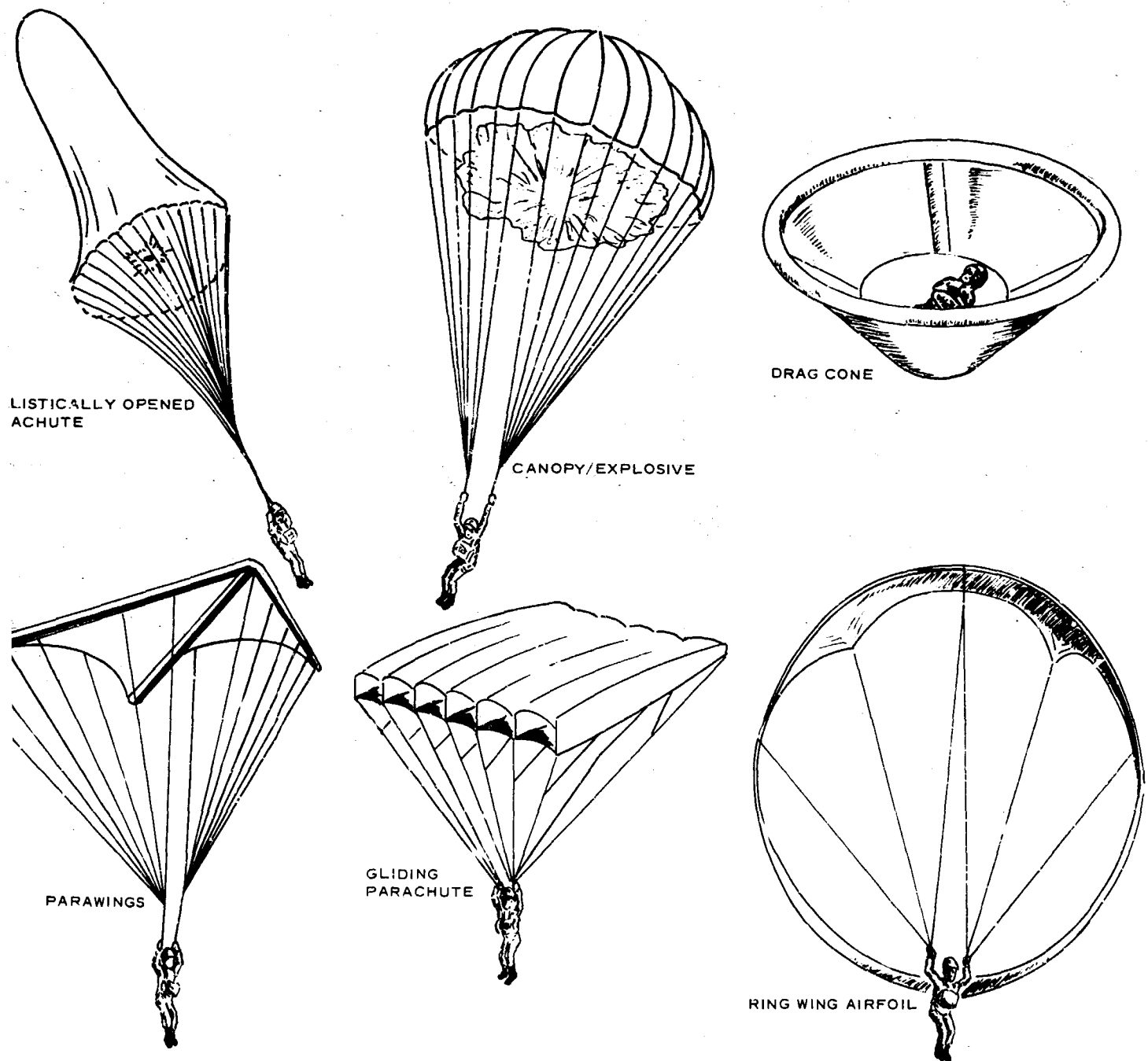


Figure 1 - System Concepts

SECTION I - INTRODUCTION

6. Geographical independence at landing
7. System stowed size and bulk
8. Range capability
9. Equipment complexity
10. Sensitivity to functioning
11. Imposed loads
12. Operational safety and compatibility with emergency procedures
13. Operational complexity
14. Training requirements
15. Inspection, replacement, repair
16. Reliability
17. Compatibility with existing aircraft and other hardware
18. Stowage, handling, readiness for operation
19. Development, manufacturing, service/training costs

The above criteria are considered applicable generally to all concepts. Other criteria applicable to specific concepts also will be used in the evaluation.

6. SUMMARY OF AERIAL DELIVERY APPLICATIONS

Past and present aerial delivery applications are significant historically to this low-altitude airdrop study. The type of application of a system and the success achieved are indicative of the system's state of the art. A review of available literature reveals that several personnel system delivery concepts are comprised primarily of systems that have been applied to aerial delivery operations in general and personnel delivery operations in particular. This fact is especially true of the parachute concepts, where the parachute itself is the primary recovery unit. For these systems, the concept involved is essentially an auxiliary device that potentially enhances the parachute's performance. In general, most of the auxiliary devices have been tested and used successfully. The ram-air BALLUTE has been extensively and successfully applied in both subsonic and supersonic operations. One configuration has been man-rated for recovering the Gemini astronauts during an emergency capsule abort. The internal canopy system and the ballistically opened parachute system also have been very successful. The internal canopy has been

SECTION I - INTRODUCTION

used in cargo parachute delivery, while the ballistically opened canopy principle has been developed into a reserve parachute system. Canopies containing explosive charges have been tested successfully, but the obvious hazards involved with explosives have prevented their general application.

Various gliding systems considered also have been investigated for aerial delivery applications. The conical parawing, for example, has been studied rather extensively and tested over the years, including the design, development, and testing of a personnel system by Ryan Aeronautical Co. Problems associated with weight and deployment, however, have not been resolved satisfactorily. Cylindrical parawings have been both wind-tunnel and flight tested, but deployable configurations have not been developed. In addition, the cylindrical parawing itself has demonstrated typically poor stability characteristics, which has necessitated additional stabilizing surface for successful flight operations. More recent completely limp gliding designs, such as the limp parawing and the Parasail, Parafoil, and Cloverleaf gliding parachutes, have demonstrated adequate flight characteristics and appear more amenable to packaging and deployment. The limp parawing, capitalizing on the knowledge and experience gained with the conical and cylindrical parawings, has been quite successful in its limited cargo and personnel delivery applications. The limp parawing more closely resembles the original Rogallo concept than either the conical or cylindrical designs resemble it. The three gliding parachute designs have enjoyed much success in limited applications and are being tested and evaluated as potential missile and spacecraft recovery systems.

The other systems considered involve concepts either not previously considered for personnel air delivery or concepts using untested designs. Douglas Aircraft has studied the drag cone concept but has done no known development or testing. Various types of lifting systems have been examined by government agencies and industries for providing temporary air mobility to individual troops for special tactical applications. Lifting systems, however, generally have been connected with ground-to-ground maneuvers and not with air-to-ground operations.

SECTION II - PERSONNEL AERIAL DELIVERY

CONCEPT ANALYSIS

1. GENERAL

This section contains design and performance data relevant to the investigation of the various concepts for personnel aerial delivery applications. Appropriate aerodynamic and structural data resulting from a survey of the available literature are presented to establish the basic criteria for size, shape, and weight estimation. Nominal performance characteristics of each system are examined for operational suitability and applicability. Weight data are for the basic system concept and are comparable to the basic MC-1 canopy weight of approximately 15 lb. Packing density, unless otherwise indicated, is considered the same as the density used for MC-1 canopy in the T-10 assembly (approximately 18 pcf).

For convenience, concepts will be broadly classified into three basic categories - drag, thrust-lift, and gliding. Classification is based on the steady-state operations of the primary recovery unit. Drag concepts include the drag cone, the quick-opening parachute, the ballistic parachute, the BALLUTE/parachute, and the canopy-contained explosive parachute. Thrust-lift concepts include rotating decelerators and powered lifting systems. Gliding concepts include parawings, gliding parachutes, and the ring wing airfoil.

2. DRAG CONCEPTS

a. General

The drag systems (see Items 2 b through 2 f, below) can be classified further according to their conceptual function as either rapid-opening systems or rapid-descent systems. Configurations classified as rapid-opening systems include the BALLUTE/parachute system, the internal canopy parachute system, and the ballistic parachute system. All three concepts tend to promote a faster, more positive, more repeatable canopy inflation process. Rapid-descent concepts include the drag cone and the canopy/explosive system. In both, the equilibrium descent velocity presumably can be higher than the equilibrium descent velocity of a standard personnel canopy, since each system provides for additional deceleration at or just prior to impact.

SECTION II - CONCEPT ANALYSIS

Sizing of the primary recovery unit for drag concepts can be accomplished readily by equating the total weight and drag under equilibrium descent conditions and then solving the drag equation for size. Since the effects of the inflation aids in the rapid-opening systems are considered negligible following canopy inflation, a standard-sized personnel canopy is required to limit the landing velocity to 19 fps at sea level. Consequently, further evaluation of these systems assumes a 35-ft D_0 extended-shirt canopy (MC-1 type). Sizing of the primary recovery unit for the rapid-descent drag concepts, however, is less straightforward, since an equilibrium descent velocity is not defined initially. For these concepts, sizing will be discussed in Items 2 e and 2 f, below.

b. BALLUTE/Parachute Concept

(1) BALLUTE Size and Inlet Requirements

In the two-stage BALLUTE/parachute system, the BALLUTE opens first to decelerate and stabilize the system for subsequent deployment of the canopy. Thus, the BALLUTE must be designed and sized for its application as a first-stage decelerator. This requirement can be satisfied using a configuration shape similar to the man-rated unit described in Reference 1. Extensive analysis of that program has shown a 4-ft configuration to be a conservative selection for deceleration and stabilization of personnel in both subsonic and supersonic flow regimes. In Reference 2, a 0.7-ft diameter BALLUTE with an inlet area of 0.015 sq ft was shown to inflate in 0.156 sec at a dynamic pressure (q) of 50 psf. If these parameters are to be scaled to a 4-ft configuration deployed at 130 knots, a realistic inflation time of 0.25 sec requires an inlet area of approximately 1.54 sq ft. For a single inlet, this inflation time corresponds to an inlet diameter of 1.4 ft. The inflation time requirement varies with deployment velocity and inlet-flow alignment. Therefore, at lower deployment speeds, a larger inlet area is required to maintain the 0.25-sec inflation time. Alternately, an auxiliary inflation system can be used to obtain an inflation time that is independent of inlet size or deployment conditions. A consistent inflation time of about 0.25 sec or less can be achieved using this technique.

Following stabilization of the trooper, the primary canopy, already at full-line stretch, is released and inflated. During this operation, the BALLUTE serves as an inflation aid in a manner similar to the internal canopy system discussed in Item 2 c, below.

(2) BALLUTE Trajectory Analysis

Figure 2 presents results of a point-mass computer analysis of the first-stage BALLUTE. The two cases presented, (a) and (b), represent initial jump velocities of 130 knots (220 fps) and 40 knots (68 fps), respectively. Deployment of the BALLUTE and subsequent inflation can

SECTION II - CONCEPT ANALYSIS

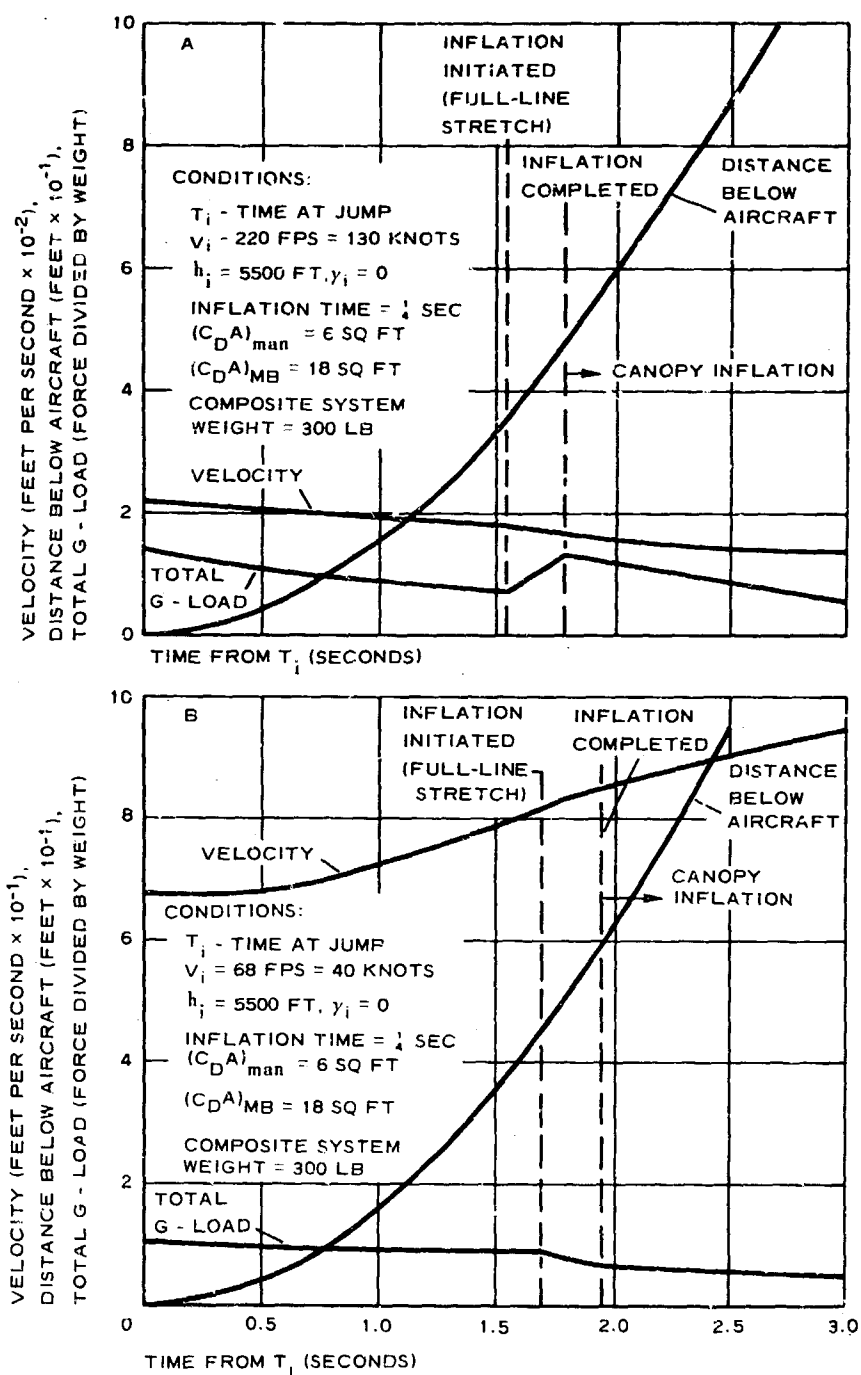


Figure 2 - Computer Analysis of First-Stage BALLUTE

SECTION II - CONCEPT ANALYSIS

be initiated prior to the complete deployment of the primary canopy, since the BALLUTE is much smaller in size. BALLUTE inflation is assumed to begin where the standard canopy normally reaches full-line stretch - that is just as the canopy becomes fully deployed. Full-line stretch occurs when the total separation distance between the man and the aircraft is approximately 45 to 50 ft. For these conditions, and assuming a man free-fall drag area $[(C_D A)_{\text{man}}]$ of six square feet, the approximate time lapse between the jump and the beginning of the BALLUTE inflation process is indicated in Figure 2. During inflation, the drag area of the BALLUTE is assumed to increase linearly from 0 to 12 sq ft over the 0.25-sec inflation time. Inflation of the primary canopy follows and is aided by the BALLUTE's presence. The entire sequence is described more fully in Section III, Item 2a.

Total G-load, plotted in Figure 2, represents the vector sum of gravitational acceleration and the acceleration due to the flow drag. Gravity is considered since the flow drag is relatively small in both cases. Thus, at equilibrium, total G-load is zero. The maximum G's due to flow drag alone are 1.9 and 0.87 for cases (a) and (b), respectively.

(3) Inflation Techniques (see Appendix B)

Since the BALLUTE design is readily adaptable either to ram-air inflation or to internal source pressurization, two possible internal source pressurization techniques will be discussed - compressed gas in pressure vessels and gas generation by burning fuel (see Appendix B.) The former probably is the most widely used method of internal source pressurization, and the design of a reliable system is well within the state of the art. Pressure bottles are readily available as off-the-shelf items in various shapes and materials. Bottle pressures from 3000 to 5000 psi are commonly used.

The gas generation system is of two types - the hot-gas generator and the cool-gas generator. Gas generators typically are not available as off-the-shelf items; their development is not so advanced as the development of the pressure bottles. Hot-gas generator systems have been used in the Mercury and Gemini programs to deploy the first-stage drogue recovery parachute. Use of the hot-gas generator system for the Mercury and Gemini programs indicates that it is reliable and feasible.

For a 4-ft diameter BALLUTE operating at 130 knots under sea level conditions ($q = 58$ psf), an internal inflation energy (the product of the internal pressure and the inflatable volume) of approximately 90,000 ft-lb is required. This value is obtained using the enclosed volume of 41 cu ft and an internal pressure of 2174 psf ($2116 + 58$), since the BALLUTE's inflatable shape is maintained adequately when the structure

SECTION II - CONCEPT ANALYSIS

is ram-air inflated. To ensure adequate pressurization, an inflation energy margin of approximately 10 percent is added to the required 90,000 ft-lb. The result is a total inflation energy of approximately 100,000 ft-lb.

An inflation energy of 100,000 ft-lb apparently does not impose any unusual problems for either gas-generation inflation method. However, either type of system imposes certain disadvantages with respect to weight and system complexity. Their use may be justified by improving the total system's low-altitude capability. Testing of a ram-air inflated configuration, therefore, is necessary to determine if its opening characteristics provide a satisfactory low-altitude capability over the entire spectrum of possible deployment conditions.

(4) Estimated System Weight

For a BALLUTE/parachute system using a ram-air inflated BALLUTE, canopy weight is estimated at 17 lb. This weight allows approximately 2 lb for the BALLUTE subsystem and 15 lb for the primary canopy, which presumably is a 35-ft D_0 extended-skirt canopy. Use of an internal-source inflation system adds additional weight. Weight estimations are summarized in Table II.

TABLE II - BALLUTE/PARACHUTE WEIGHT ESTIMATES

Item	BALLUTE inflation technique			
	Ram-air (lb)	Pressure bottle [†] (lb)	Cool-gas generator (lb)	Hot-gas generator [‡] (lb)
Inflation system*	0	10 to 28	11	7.5
BALLUTE/ parachute	17	17	17	17.0
Total	17	27 to 45	28	24.5

*See Appendix B

[†]Includes weight of air as pressurizing gas

[‡]Includes weight estimate of piping required to cool gas for entry into BALLUTE

SECTION II - CONCEPT ANALYSIS

The volume requirement of an inflation system depends on the system used. From typical packing factors and the results of Appendix B, the volume of the inflation system was calculated for each type of system (see Table III).

**TABLE III - TYPICAL PACKAGING FACTORS AND
VOLUME REQUIREMENT**

Type of system	Density (pcf)	Estimated Volume (cu in.)
Hot-gas generator	60	216
Cool-gas generator	95	200
Fiberglass sphere, air at 3000 psi	35	640
Titanium sphere, air at 7000 psi	59	220
Steel bottle, air at 3000 psi	63	690

c. Internal Canopy System

(1) Internal Canopy Design

Reference 3 documents the test results on extended-skirt canopies with internal parachute systems. In these tests, the primary canopy was initially reefed and sting-mounted with its inlet normal to the flow. The internal canopy was located at variously measured distances behind the inlet of the primary.

Figure 3 presents nominal performance results of one series of tests as a function of internal canopy location. The internal canopy system exhibited a maximum reduction in opening time over the extended-skirt canopy alone of about 18 percent, although an increase in opening force also was exhibited.

In another series of tests using a 6.2-in. D_p guide-surface internal canopy and a 10 percent extended-skirt primary, significantly different inflation characteristics were exhibited over the comparatively small range of internal canopy locations (5.8 to 8.3). Again, similar time reduction was exhibited, with a maximum value of about 18 percent obtained. A 4 to 9 percent reduction in opening force with respect to the primary canopy alone also was exhibited.

These results are directly applicable to the MC-1 canopy under similar

SECTION II - CONCEPT ANALYSIS

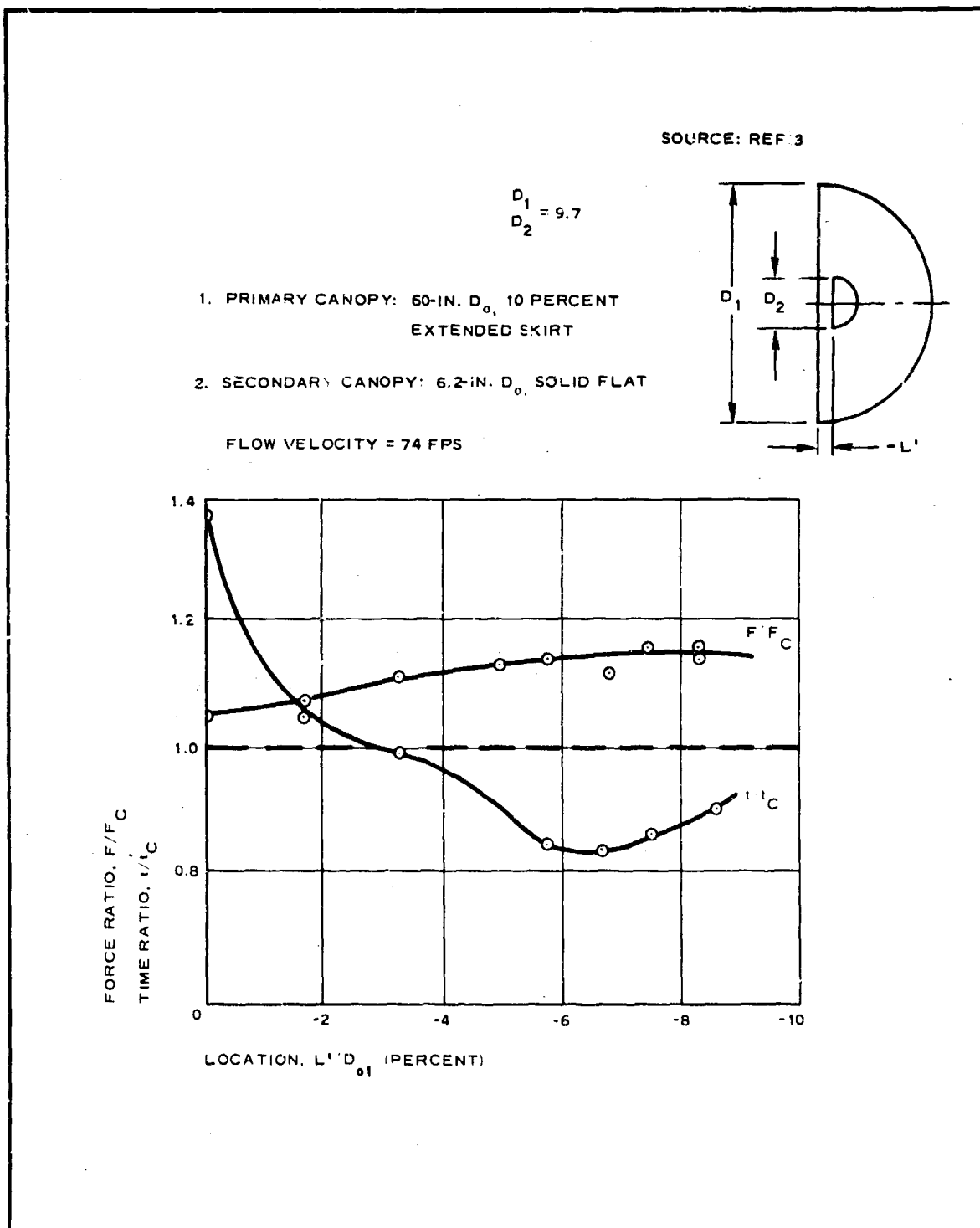


Figure 3 - Opening Time and Opening Force Related to Characteristic Value of the Original Parachute

SECTION II - CONCEPT ANALYSIS

deployment conditions and with the same geometrical relationships. With a 35-ft D_0 canopy, a 4.5-ft D_0 solid flat or a 4.5-ft D_p guide surface would be used.

(2) Repeatability

The above data indicate the nominal design and performance characteristics of the two internal canopy systems. Since several tests were performed at each location for both systems, a measure of the system repeatability is available. Results of the tests are given in Table IV.

TABLE IV - OPENING CHARACTERISTICS OF CONVENTIONAL
AND INTERNAL CANOPY SYSTEMS

	$(t/t_C)_{\min}$	Location (L/D_{01}), %	Standard deviation (%)
10 percent extended-skirt canopy alone	1.0	. . .	± 5.9
10 percent extended-skirt canopy with solid flat secondary	0.826	-6.67	± 3.6
10 percent extended-skirt canopy with guide-surface secondary	0.818	-7.50	± 4.7

The test results given in Table IV were obtained under infinite mass conditions without the deployment dynamics typically experienced in personnel jumps. Consequently, the parameter values are considered only as qualitative measures of the internal canopy system's effectiveness when applied to the air delivery of personnel. These results apparently indicate that the opening time of an internal canopy system would be more repeatable than the opening time of the standard system.

(3) Estimated System Weight

The weight penalty resulting from incorporating an internal canopy within a standard MC-1 parachute is estimated at about one pound. The canopy includes a 4.5-ft diameter secondary canopy and a riser and attachments. Total canopy weight is estimated to be about 16 lb.

SECTION II - CONCEPT ANALYSIS

d. Ballistic Parachute

(1) Performance and Design

Use of a ballistically deployed parachute system with a ballistic canopy-spreading device can substantially reduce the opening-time requirements, especially at low deployment velocities. Tests of various ballistic systems at deployment velocities ranging from essentially zero to more than 600 knots verify this last statement.

Tests were conducted on the ultrafast opening parachute type XMP-2. Both back-style and platform-mounted configurations were used to evaluate the effectiveness of the ballistic parachute concept for personnel usage (see Reference 4). The back-style configuration mounted directly to the operator and was activated by a rip cord. The platform-mounted configuration was designed for use with either the Hiller flying platform or the deLackner aerocycle. The back-style configuration was attached to an anthropomorphic dummy and was tested on the ground and from a helicopter at airspeeds of from near zero to 70 knots.

The platform-mounted configuration was tested, using an articulated dummy, from a special wooden tower at three different altitudes - 16, 27 and 42 ft. Tests were conducted at speeds from 10 to 50 knots.

The conclusions of Reference 4, based on the test results of the XMP-2, pointed out that the back-style configuration did not meet basic requirements of the personnel system; its further usage was not recommended. The platform-mounted configuration did not perform satisfactorily but appeared superior to the back-style. At certain altitudes and speeds, the platform-mounted configuration seemed feasible.

A more recent development of the Stencil Aeronautical Engineering Corp. is the ultraprecision parachute (UPP), which offers significant improvements over the XMP-2 configuration and conceivably could be more appropriate for personnel delivery applications. This type of parachute is being incorporated into ejection-seat recovery systems and has been developed recently into a reserve parachute system. The standard UPP is both ballistically deployed and ballistically opened. For personnel delivery applications, a static-line deployment presumably could be used to eliminate the weight and complexity of a projection gun and slug.

Figure 4 indicates the opening-time characteristics of a 28-ft D_0 solid flat canopy (LS-1 ballistic parachute system) under a 200 to 235-lb load with respect to the velocity at projection. The canopy inflation time is estimated in Figure 5 and allows an estimated projection time of 0.2 sec as indicated by the load-time results of reference. For application to a conventional-sized personnel parachute system under a design load of 300 lb, these data must be converted by correcting deviations in payload weight, canopy diameter, and deployment mode. If inflation time is

SECTION II - CONCEPT ANALYSIS

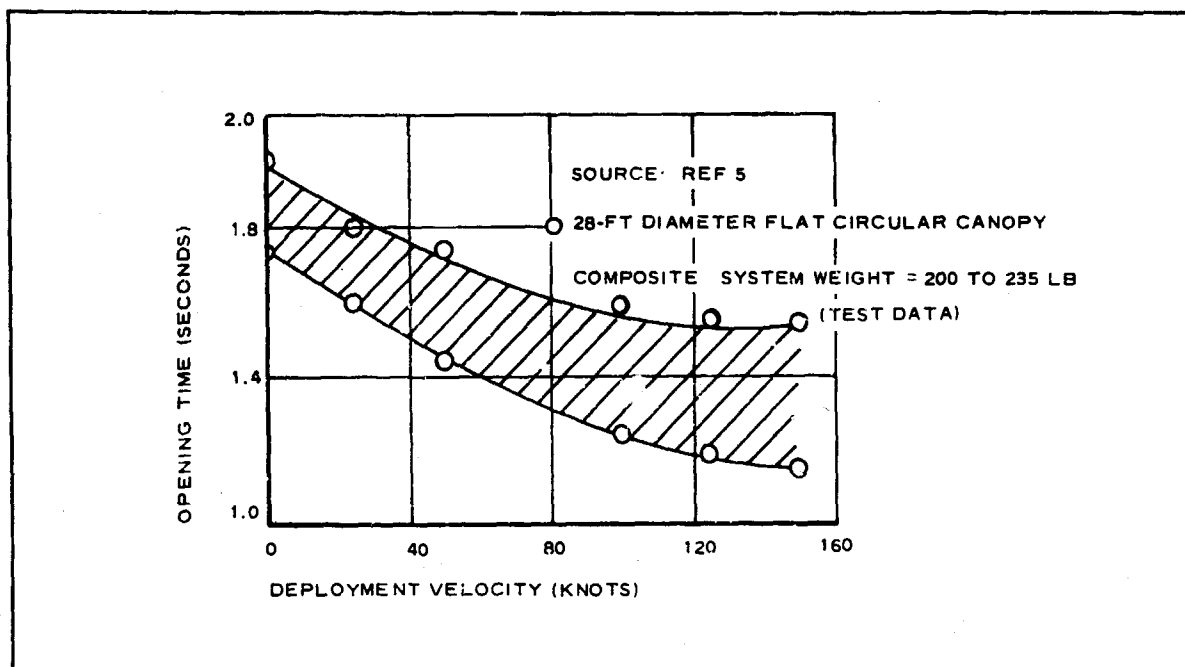


Figure 4- UPP Opening Time versus Velocity

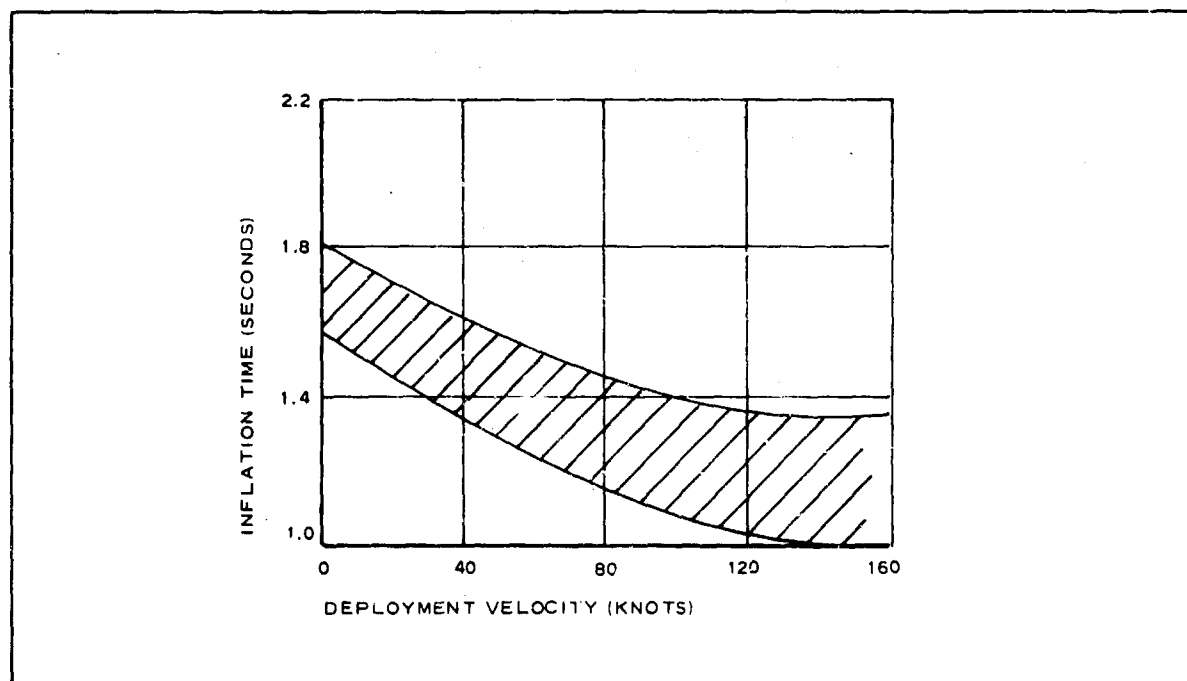


Figure 5 - Calculated Inflation Time versus Deployment Velocity (UPP)

SECTION II - CONCEPT ANALYSIS

considered a function of canopy volume and mass flow rate, the filling time of a 35-ft D_0 canopy can be approximated from the results of Figure 5 under the same deployment conditions. Thus, at corresponding velocities and assuming the deceleration rate during inflation of both systems to be essentially the same (since the canopy loading for both systems is approximately equal) the filling time is estimated by

$$\frac{t_2}{t_1} = \left(\frac{\bar{v}_2}{\bar{v}_1} \right) \left(\frac{A_{i1}}{A_{i2}} \right) \cong \frac{D_{o2}}{D_{o1}}, \quad (1)$$

and

$$t_2 = 1.25 t_1 .$$

With this approach and the results of Figure 5, an estimated inflation time versus velocity can be calculated for the 35-ft D_0 ballistic parachute (see Figure 6). An indication of the ballistic parachute's repeatability also is given in Figure 6 and is based on Figure 4.

A trace of experimental G-load versus time is presented in Figure 7 (see Reference 5) for the LS-1 system. To convert this data to a conventionally sized personnel system, the previous assumption that the two systems will experience equivalent deceleration rates is again used. Thus,

$$G_1 \left(\frac{W_1}{m_1} \right) = -a_1 = -a_2 \quad (2)$$

and

$$\left(\frac{m_2}{W_2} \right) (-a_2) = G_2 . \quad (3)$$

Therefore,

$$G_2 = \left(\frac{W_1}{m_1} \right) \left(\frac{m_2}{W_2} \right) G_1 , \quad (4)$$

where

SECTION II - CONCEPT ANALYSIS

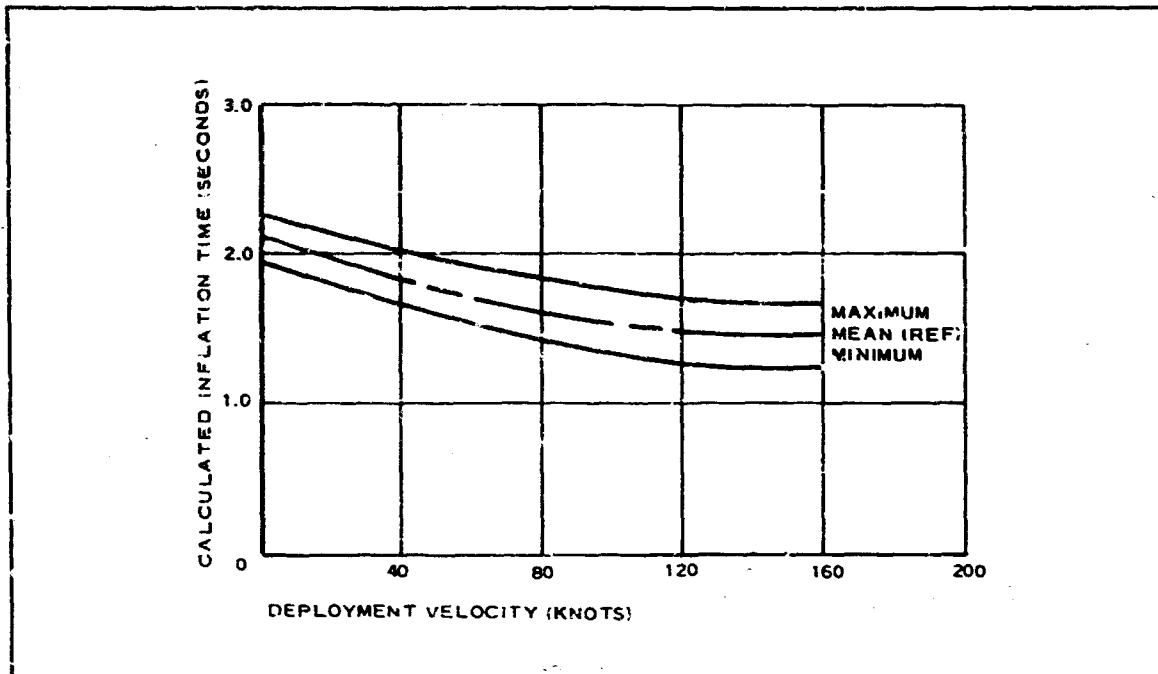


Figure 6 - Ballistic Personnel Parachute Inflation Time versus Velocity

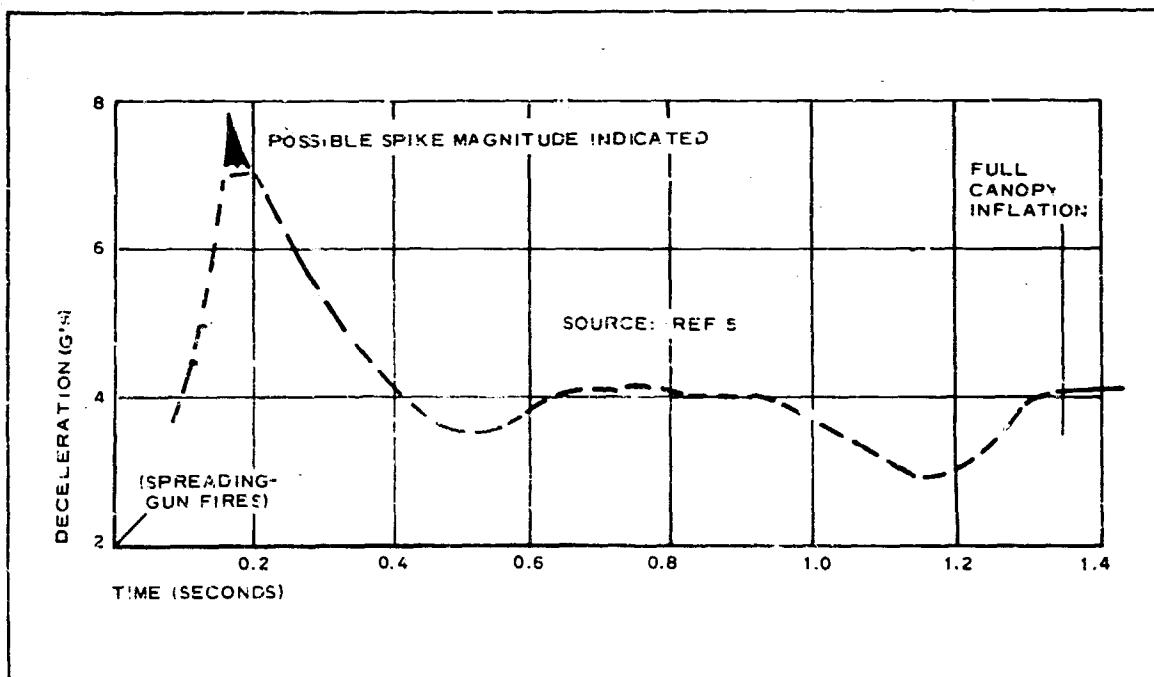


Figure 7 - Ballistic Parachute Load versus Time

SECTION II - CONCEPT ANALYSIS

G = the deceleration level in g's,

W = the composite system weight,

m = the composite system mass,

a = the deceleration rate, and

subscripts 1 and 2 denote quantities associated with the LS-1 and the personnel systems, respectively

But,

$$\frac{W_1}{m_1} = g,$$

$$\frac{m_2}{W_2} = 1/g, \quad (5)$$

which implies that $G_2 = G_1$.

Based on the above analysis, the trace of Figure 7 also is considered representative of a personnel system design.

(2) Estimated System Weight

To maintain the same mass balance between the LS-1 ballistic parachute system and the required personnel system, the known values of the LS-1 are adjusted by the ratio of the canopy weights. Reference 6 gives the weights of 28-ft D_0 solid flat and 35-ft D_0 extended skirt as approximately 12 and 15 lb, respectively. The ratio of these numbers is 1.25. The projected weight of the LS-1 system, including the projection slug, the spreading mechanism and slugs, and the canopy, is 18 lb (see Reference 5). Thus, for the 35-ft D_0 ballistic parachute, the projected weight is estimated at 23 lb. Allowing approximately 1 lb for the projection gun, the total estimated weight for the canopy and ballistic equipment is approximately 24 lb. For a static line deployed system using only a ballistic spreading mechanism, the weight is estimated at 19 lb.

Table V summarizes the estimated weights.

SECTION II - CONCEPT ANALYSIS

TABLE V - ESTIMATED WEIGHT OF 35-FT D₀
BALLISTIC PARACHUTE SYSTEM

Item	Estimated weight (lb)
Canopy	15
Spreader and slugs	4
Deployment gun	1
Deployment slug	4
Total	24

e. Drag Cone

(1) General

The drag cone is the only drag-type configuration considered that would not utilize a parachute system during the terminal recovery phase. Instead, the drag of a large man-enveloping cone is used to achieve the desired impact velocity. At impact, a nose-attenuator system presumably limits the landing shock to a value acceptable by using personnel.

Application of the drag cone for personnel delivery is not well defined and considerable analysis would be required to establish an optimum system. The various tradeoffs involved include deployment velocity; pressurization and component size; apex angle and cone size; composite system stability; and attenuator pressure and design. To provide a preliminary indication of the concept suitability for personnel delivery application, a simplified analysis will be made and a sample design evaluated. To facilitate the analysis, performance of the drag cone is assumed virtually the same as the performance of a regular cone, regardless of the deviation in the nose-attenuator section. Thus, Figure 8 is considered representative of the indicated parameters. Required drag cone size then can be determined from Figure 9 for desired terminal descent conditions.

(2) Sample System Design

To indicate the suitability of the drag cone design for personnel delivery applications, a sample system design will be developed. This design is based on the concept analysis of Douglas Aircraft in Reference 7. From

SECTION II - CONCEPT ANALYSIS

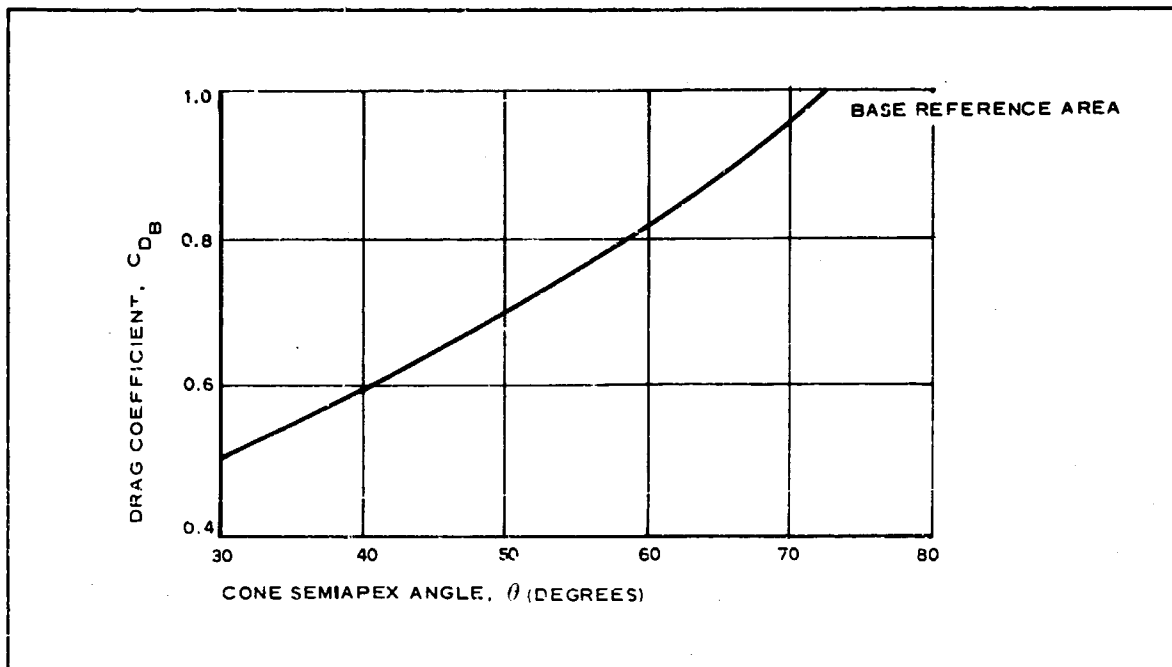


Figure 8 - Estimated C_{DB} versus Cone Semiapex Angle

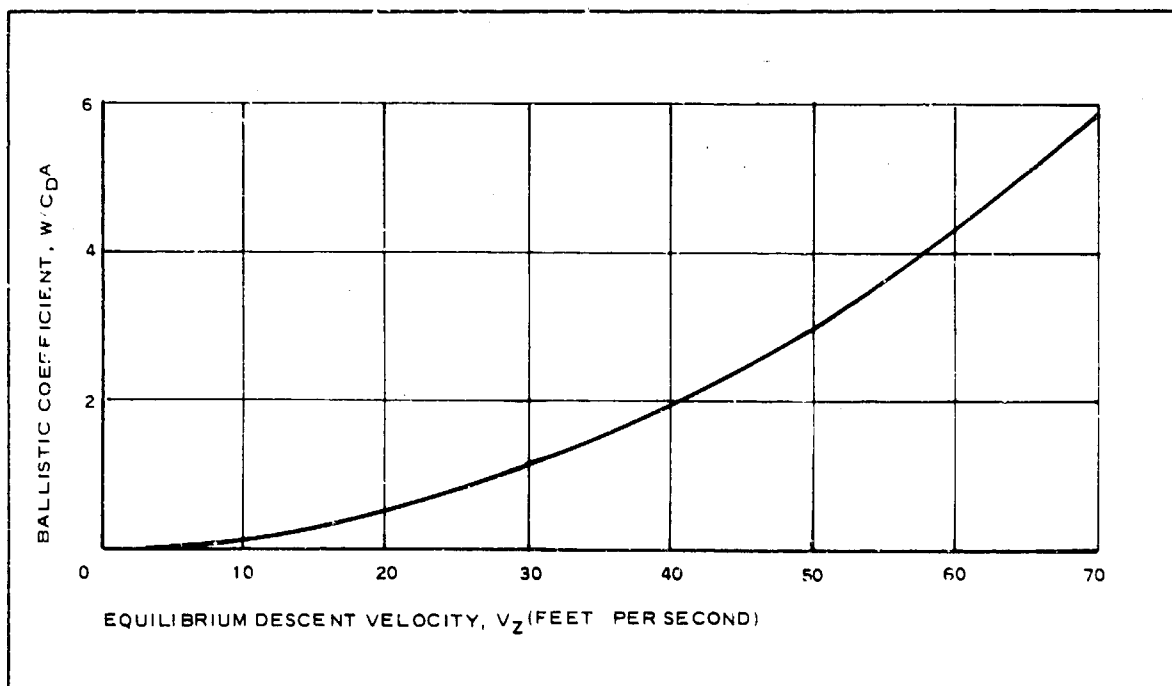


Figure 9 - Ballistic Coefficient versus Equilibrium Descent Velocity

SECTION II - CONCEPT ANALYSIS

Reference 7 and the composite system design weight, the following design parameters are obtained:

1. Composite system weight - 300 lb
2. Vertical impact velocity - 50 fps
3. Attenuator stroke requirements (for a right-circular conical attenuator) - 3 ft

The composite cone configuration shown in Figure 10 satisfies these design conditions and provides for a reasonably efficient compromise between stability and drag effectiveness. The base is approximately 15 ft in diameter, the apex (attenuator section) cone angle is 90 deg, and the composite cone angle is 80 deg. The composite cone angle of 80 deg places the center of pressure well aft of the approximate center-of-gravity location and renders the design statically stable.

(3) Stress and Loads

As indicated in Figure 10, the drag cone is supported in the cone shape

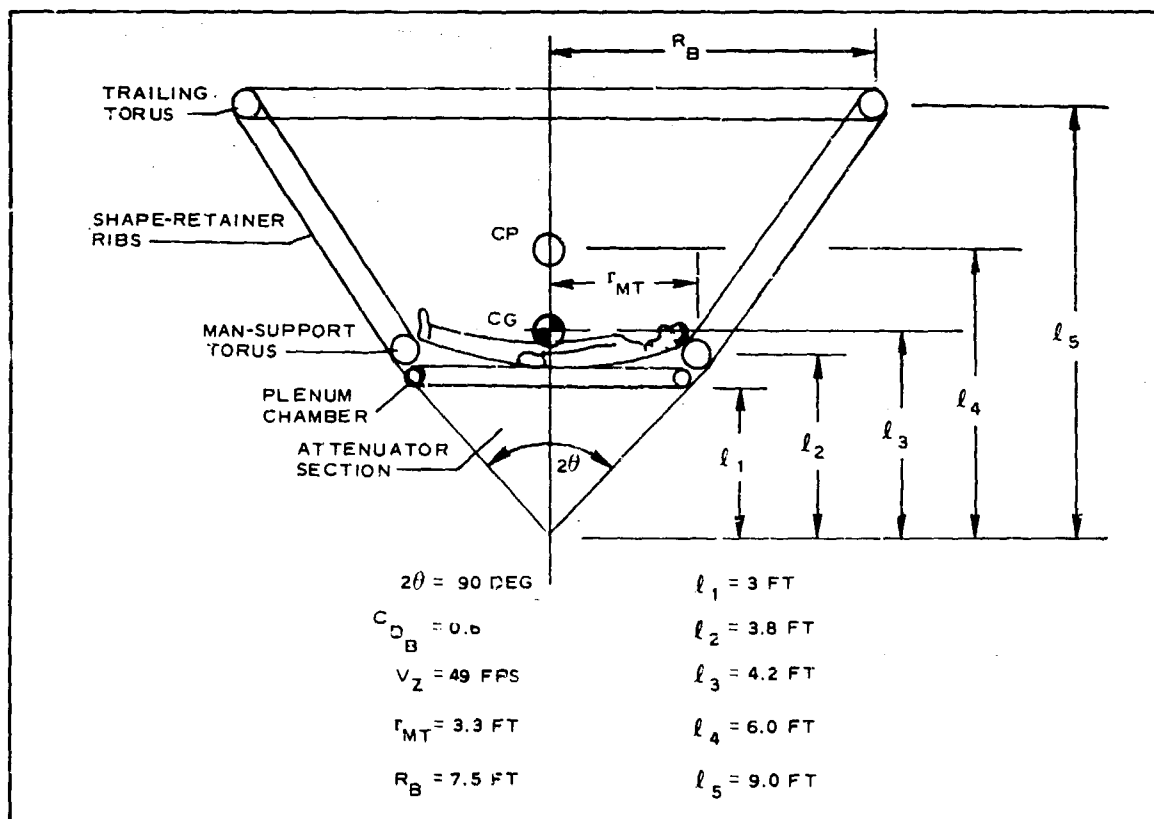


Figure 10 - Sample Drag Cone Schematic

SECTION II - CONCEPT ANALYSIS

under load by several support torii. From Reference 7, the aerodynamic compressive loads in the radial torri are given by

$$L_C = Aqa/12\pi D \text{ (lb/in.)}, \quad (6)$$

where

A = equivalent flat-plate area (sq ft),

q = dynamic pressure (psf),

a = cone angle factor,

D_T = torus diameter (ft), and

L_C = compressive load (lb/in.).

The critical load is given by

$$\begin{aligned} P_{cr} &= 3EI/R_T^3 \\ &= \frac{3E\pi r_t^3 t}{R_T^3}, \end{aligned} \quad (7)$$

where

E = modulus of elasticity,

I = moment of inertia,

r_t = tube radius (in.)

t = material thickness (in.)

R_T = torus radius (in.), and

P_{cr} = critical load (lb/in.).

Solution of these equations (for the man-support torus, the compressive load due to the man also must be added to determine the total value at the desired deployment velocity) permits the design of the required torii.

SECTION II - CONCEPT ANALYSIS

Since the loading per square foot on the fabric curtain is relatively small, a minimum weight material can be used (perhaps a 2.2 oz/sq yard low permeability laminate).

For structural integrity and high attenuator efficiency an initial inflation pressure of approximately 3 psi is assumed in the attenuator. Figure 11 presents an attenuator history diagram for three composite system weights.

As shown in Figure 11, the peak estimated G-load imposed on the sample drag cone system is excessive. Three modifications of the sample design are available. These modifications either individually or collectively could presumably lower the impact G-level. They are (1) reducing the attenuator pressure and lengthening the stroke, (2) increasing the base diameter, and (3) increasing the total apex angle. The first method theoretically would provide for a longer but less severe attenuation while the latter two techniques would lower the impact velocity. The first approach is not considered practical, since any significant pressure reduction in combination with a longer stroke may render the attenuator ineffective. Landing while drifting with a ground wind and/or landing on a slope, for example, would subject the attenuator to both a normal and a shearing load. Then, sufficient rigidity must be available to resist deflection. The second approach also is considered unacceptable due to the weight penalties involved. As will be shown under Item (4), below, the sample design already has an estimated weight of 40 lb compared with the 15-lb MC-1 canopy. The final approach, increasing the apex angle, may offer the best practical solution to reducing the impact load level. Wind-tunnel tests with cones having apex angles as great as 120 deg have indicated these configurations still to be dynamically stable. Using Figure 8 and considering cone angles of 80 (sample design), 100 and 120 deg, impact velocities of 50, 46, and 43 fps, respectively, would be obtained with cones having a base diameter of 15 ft and a composite system weight of 300 lb. If the attenuating force varies directly with the impact kinetic energy for the small changes in velocity, the approximate associated G-level for each case then would be 40, 34, and 29, respectively.

Thus, the higher cone-angle configurations do reduce the impact G's but apparently not to an acceptable level.

(4) Estimated System Weight

The drag cone weight requirement can be minimized by deployment of the drag cone at a relatively low dynamic pressure (see Equations 6 and 7). This minimizing is possible since a first-stage deceleration system is already necessary to stabilize and orient the composite personnel system for subsequent drag cone deployment. The larger the first-stage decelerator, however, the greater the weight of that device. Therefore,

SECTION II - CONCEPT ANALYSIS

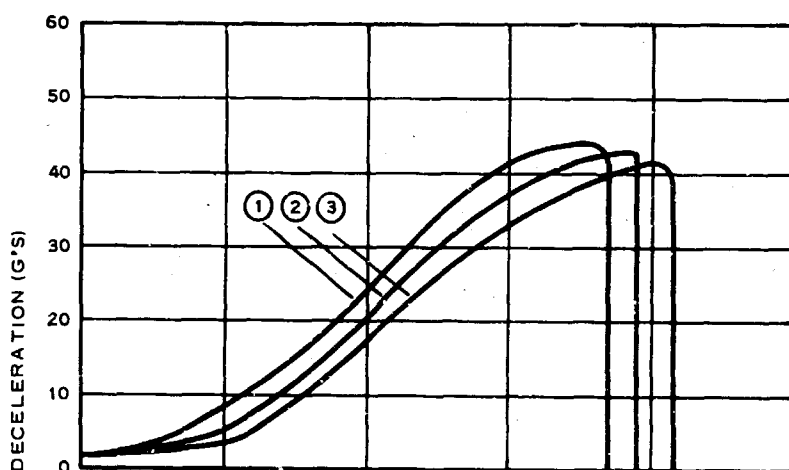
DRAG CONE CONFIGURATION
SOURCE: REF 7

ASSUMPTIONS:

RIGHT-CIRCULAR
CONICAL ATTENUATOR
INITIAL PRESSURE - 3 PSIG
LIMIT PRESSURE - 3.5 PSIG
INITIAL VELOCITY - 50 FPS
COMPOSITE SYSTEM WEIGHT

- ① 250 LB
- ② 300 LB
- ③ 350 LB

(A) DECELERATION VERSUS TIME



(B) VELOCITY TIME

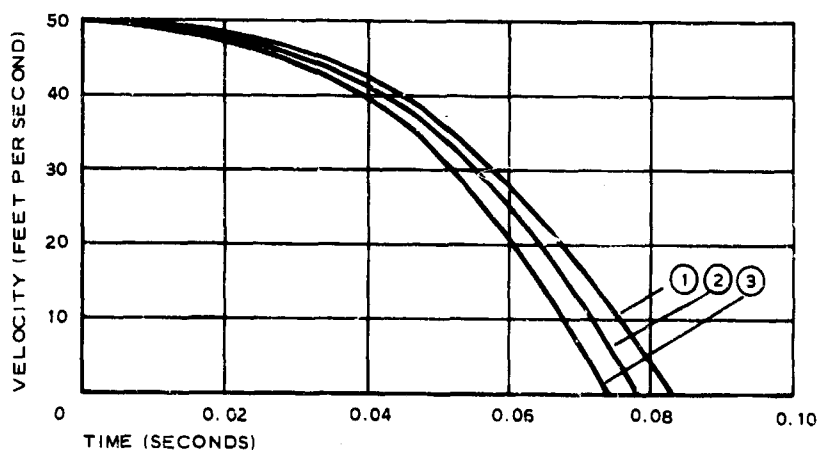


Figure 11 - Attenuator History

SECTION II - CONCEPT ANALYSIS

a tradeoff between drag cone weight and initial decelerator weight is indicated to establish the minimum weight system. A weight estimate can be obtained if the torus inflation pressure is assumed to be the same as the initial attenuator pressure - that is, 3 psig. This approach seems reasonable, at least from a design standpoint, since it would eliminate the need for multistage pressure regulators. Elimination of the pressure regulators would reduce the design and operational complexities. For this case the limiting values of dynamic pressure for the fully inflated sample design can be calculated using Equation 6. For the trailing torus, the most critical component (see Reference 7), the limiting value, is calculated to be 18 psf corresponding to a velocity of 120 fps. Even these values, however, do not appear to be critical for deployment, since considerable deceleration would occur during the inflation process. As a result, a relatively small first-stage decelerator, approximately 3 to 5 ft in diameter, should be satisfactory. If 8-in. tube diameter torii are used, the approximate gas requirement for landing under standard sea level conditions is 76 standard cubic feet. To provide a 10 percent pressure margin, 84 standard cubic feet of gas are considered appropriate. Assuming air as the pressurizing gas, the estimated weight becomes 40 lb for a 250-lb composite system. This weight is based on the component weights of Reference 7 and on the estimated weight of a fiberglass sphere pressure bottle as obtained from Appendix B.

Increasing the cone apex angle while maintaining the same base size would not have a significant effect on the weight. At most, a slightly larger first-stage decelerator would be required to reduce the cone deployment dynamic pressure by approximately 3 to 4 pcf for the 120-deg cone.

f. Canopy/Explosive System

(1) Design and Performance

Experiments conducted with parachute canopies incorporating explosive charges have indicated that this system may be an efficient means of providing terminal deceleration. The technique is to explode a charge under a parachute canopy, creating a positive pressure shock front that is captured by the parachute and results in a force larger than the aerodynamic force that would exist normally.

In a series of feasibility tests conducted by the Boeing Company in 1964 (see Reference 8), 5-, 8-, 10-, and 15-gram charges were fired at the center of an inflated 8-ft diameter cargo parachute. Measured loads were 660, 1690, 2260, and 3110 lb, respectively, with peak shock front pressures ranging between 4 and 12 psi. From these data, it was estimated that the 350,000-lb system being delivered by four 200-ft extended-skirt canopies could be decelerated from its equilibrium descent rate of 60 fps to approximately 9.3 fps in 0.3 sec, with the total charge weight

SECTION II - CONCEPT ANALYSIS

of 720 lb fired over 26 time increments. These values indicate that an average of 4.05×10^{-5} lb of charge are required to reduce the velocity of 1 lb of weight by 1 fps (720/350,000/50.7).

For a 300-lb man (in equilibrium free-fall at approximately 190 fps), a 15-lb, 35-ft D_0 extended-skirt canopy is required to change the descent rate to 18.7 fps at sea level ($\Delta V = 171$ fps). This change represents an average of 2.92×10^{-4} lb of decelerator required to reduce the velocity of 1 lb of weight by 1 fps (15/300/171). From these values, the explosive charges are indicated to be 88 percent more efficient for their weight than the extended-skirt canopy.

Although the weights associated with the booster-recovery analysis are significantly greater than those encountered with a personnel system, they were obtained from the results of tests conducted by Boeing and were extrapolated without regard to the unknown scale effects. Consequently, the extrapolated results, applied directly from the above indicated test values, are considered appropriate for the comparative weight analysis.

An earlier test conducted by Radioplane using weights and sizes approximately the same as those encountered with personnel delivery is given in Reference 9. This reference presents data on a 24-ft D_0 extended-skirt parachute equipped with single explosive charges ranging from 0.25 to 3 lb. Test results indicated that the maximum charge weight for which no canopy damage occurred following explosion was 2 lb. For the 2-lb charge then, the effective linear impulse was 36 lb-sec, the peak explosion force was 3080 lb, and the application time was 0.033 sec. The computed change in velocity is obtained as follows:

$$\begin{aligned} F\Delta t &= m_{C.S.} \Delta V \\ 36 &= (300/32.2) (28 - V_f) \\ V_f &= 24 \text{ fps.} \end{aligned} \tag{8}$$

The maximum G-load is given by

$$\begin{aligned} G &= F_{\max}/C.S.W. \\ &= (3080)/(300) \\ &= 10.2. \end{aligned} \tag{9}$$

As shown by Equations 8 and 9, a single explosive charge will not provide satisfactory performance. However, Reference 9 also records

SECTION II - CONCEPT ANALYSIS

test results using timed multiple charges. Table VI gives these test results for three and four charges per canopy.

TABLE VI - TEST RESULTS USING TIMED
MULTIPLE CHARGES

Item	Number of charges	
	3	4
Peak retarding force (lb)	1540	1405
Effective linear impulse	51.8	48.8
Total charge weight (lb)	1.87	2.00
Δ velocity (fps)	8	10.9
Parachute diameter (ft)	24	24
Payload weight (lb)	310	310

From Table VI, the following results can be calculated assuming the same retarding force and velocity change for a personnel system:

TABLE VII - CALCULATED RESULTS BASED ON
TABLE VI

Item	Number of charges	
	3	4
Total system weight (lb)	300	300
Maximum G-load	5.14	4.7
Final landing velocity (fps) (initial velocity = 28 fps)	20	17.1

(2) Estimated System Weight

Based on this design and performance analysis, the canopy/explosive system offers good potential for air-dropped personnel recovery application. The weight of a 24-ft D_0 canopy is estimated at 9 lb. The required charge weight, from the above data, is approximately 2 lb, for

SECTION II - CONCEPT ANALYSIS

a total decelerator weight of 11 lb. This total represents a weight savings of about 4 lb over the conventional 35-ft D₀ canopy. Alternately, an impact velocity of approximately 9 fps could be achieved using explosive charges in a standard-sized canopy. For this case, the weight is approximately 2 lb greater than the weight used with present systems, or about 17 lb.

The above weight estimates do not include the weight of an actuator probe, timing mechanism, and other necessary equipment. These weights, however, are considered to be relatively small.

3. THRUST-LIFT CONCEPTS

a. General

Lifting concepts include flexible rotary decelerators, teeter-rotor platforms, jet-reaction platforms, and "rocket belt"-type lifting devices. With the exception of rotary decelerators, which are considered to be autorotating devices, all systems generate their lift from some auxiliary power source.

In general, lifting systems using the thrust-lift concept have several possible advantages that warrant preliminary consideration. First, they offer the potential capability of a controlled orderly descent through modulating the lifting force or, in the case of the rotary decelerators, through modulating the lift-to-drag ratio. Each system is conceptually capable of providing, at the user's option, controlled descent in either a pure vertical mode or in a lateral-vertical mode. Rotating decelerators have a gliding capability obtainable by cyclically pitching the individual rotor blades or, possibly, by tilting the rotor shaft. Powered lifting devices conceivably could be controlled to provide either independent or collective lateral and vertical motion by proper thrust vectoring. A second potential advantage is the soft landings possible. Rotating decelerators are capable of converting kinetic energy to rotation energy to reduce the landing velocity substantially by effecting a transient increase in lift. Controlled landing of the powered devices is possible through modulating the thrust.

b. Rotating Decelerators

(1) Design and Performance

Rotating decelerators potentially are capable of delivering personnel in either a vertical or a gliding descent mode. Autorotative characteristics in a vertical descent mode result in the same performance that is experienced with drag configurations. Consequently, the relationship existing between descent rate, the effective rotor drag coefficient, and

SECTION II - CONCEPT ANALYSIS

the projected rotor disk area is defined by the general drag equation. Gliding capability is obtained through a cyclic pitch maneuver and is comparable to that of passive gliding devices, such as parawings and gliding parachutes.

Typical vertical descent performance characteristics of an autorotating rotary decelerator are presented in Figure 12 as a function of advance ratio. The results of Figure 12 indicate the lowest solidity value of 10 percent to be the most efficient in terms of weight, since the rotor drag coefficient does not increase proportionally with the solidity. As a result, only the 10 percent solidity case will be considered further. The maximum drag coefficient obtainable is approximately 1.4, which corresponds to an advance ratio of 0.1. From the general drag equation under equilibrium conditions then, the relationship between rotor size and descent velocity can be obtained. Figure 13 gives a plot of these parameters for the optimum drag coefficient for recovery at both sea level and 5000 ft.

An L/D capability can be obtained for a rotary decelerator by incorporating cyclic pitch. The potential of the decelerator alone is indicated by the wind-tunnel results shown in Figure 14 (see Reference 10). For the configuration of Figure 14, the effects of parasite drag on $(L/D)_R$ are indicated for various advance ratios in Figure 15. Since the parasitic drag of a personnel system probably would equal at least the maximum value shown (5.2 sq ft), $(L/D)_T$ values of two or less would be anticipated.

The results of Reference 11 indicate that rotating decelerators in axial descent are essentially free of flight instabilities at low subsonic speeds and low rotor velocities. For gliding flight, some type of additional stabilization probably would be required.

(2) Rotor Size and Structural Analysis

The rotor configuration considered most applicable for personnel delivery application consists of autorotating fabric lifting elements that are inflated from their packaged state to effect the delivery operation. Blades fabricated from lightweight AIRMAT with symmetrical airfoil cross sections have demonstrated the feasibility of fabric rotor blades capable of being folded and stowed within a small volume. Auxiliary inflation equipment is, however, required for this type of construction as well as a drogue/spinup device for blade deployment and initial system stabilization. In operation, maneuvers conceivably could be performed by either cyclic pitch or by tilting the rotor shaft. The former technique is the generally accepted approach but may not be amenable to a simple design. The latter method, however, has never been applied to flexible blades, and its effectiveness is not known.

SECTION II - CONCEPT ANALYSIS

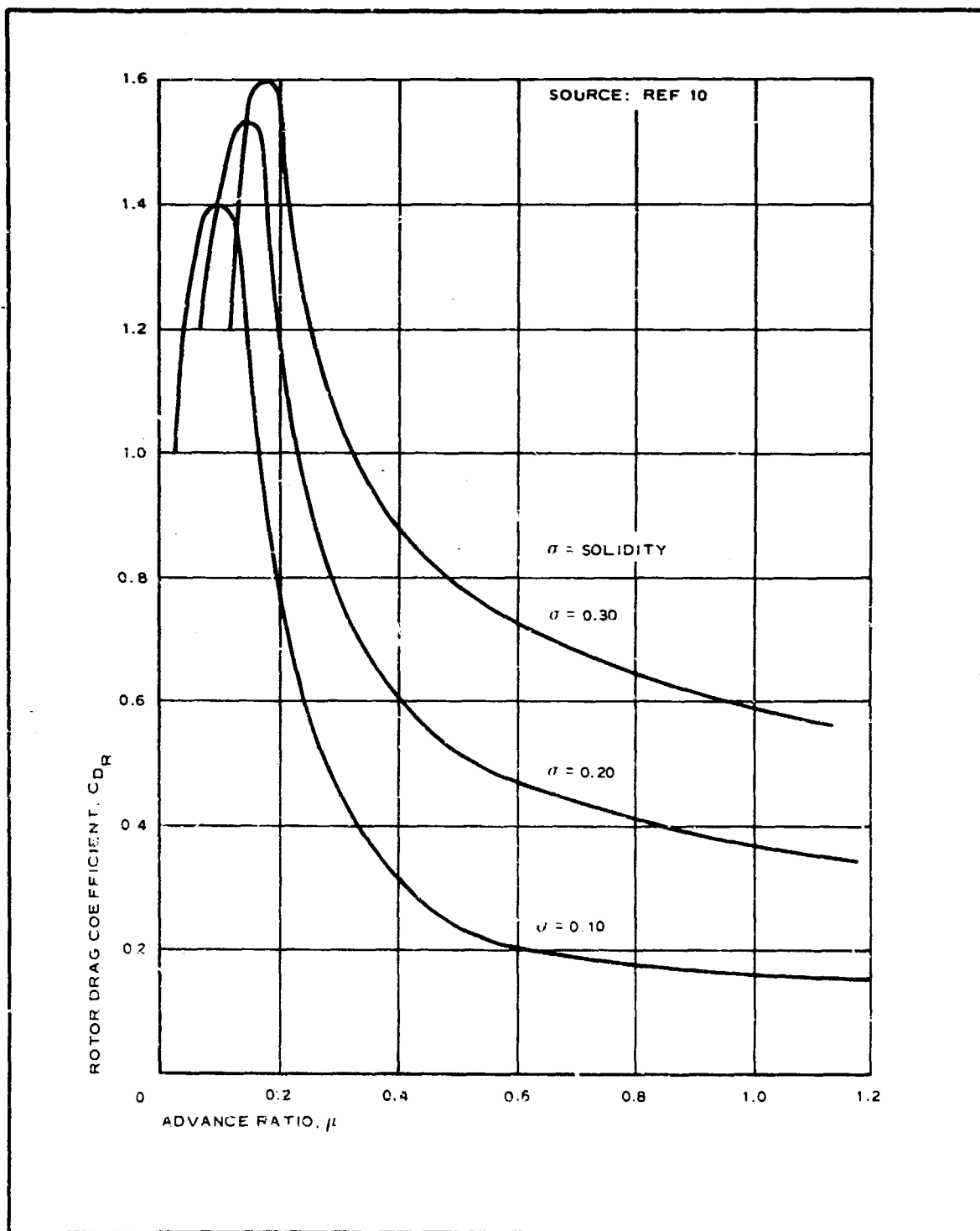


Figure 12 - Rotor Drag Coefficient versus Advance Ratio

SECTION II - CONCEPT ANALYSIS

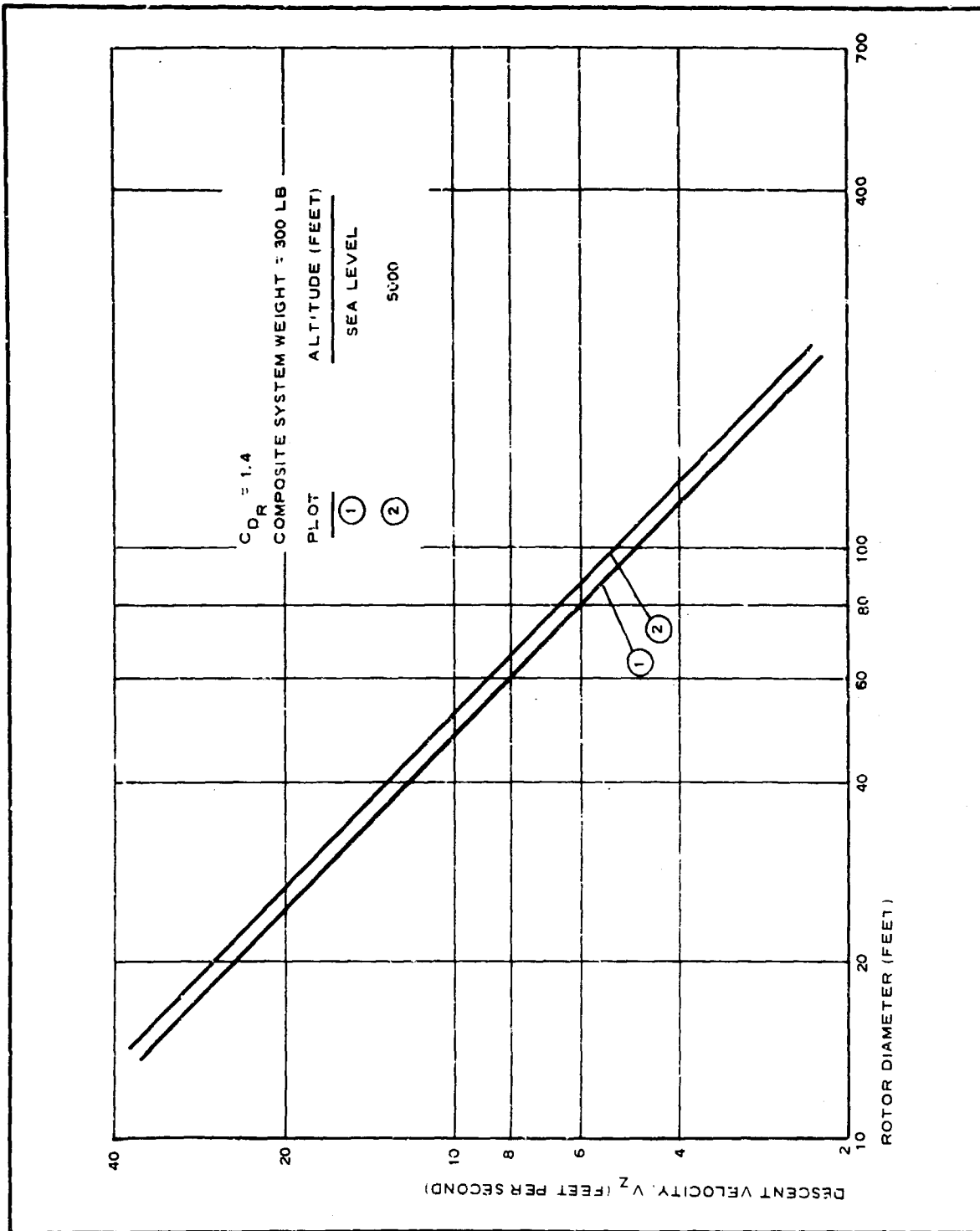


Figure 13 - Descent Velocity versus Rotor Diameter

SECTION II - CONCEPT ANALYSIS

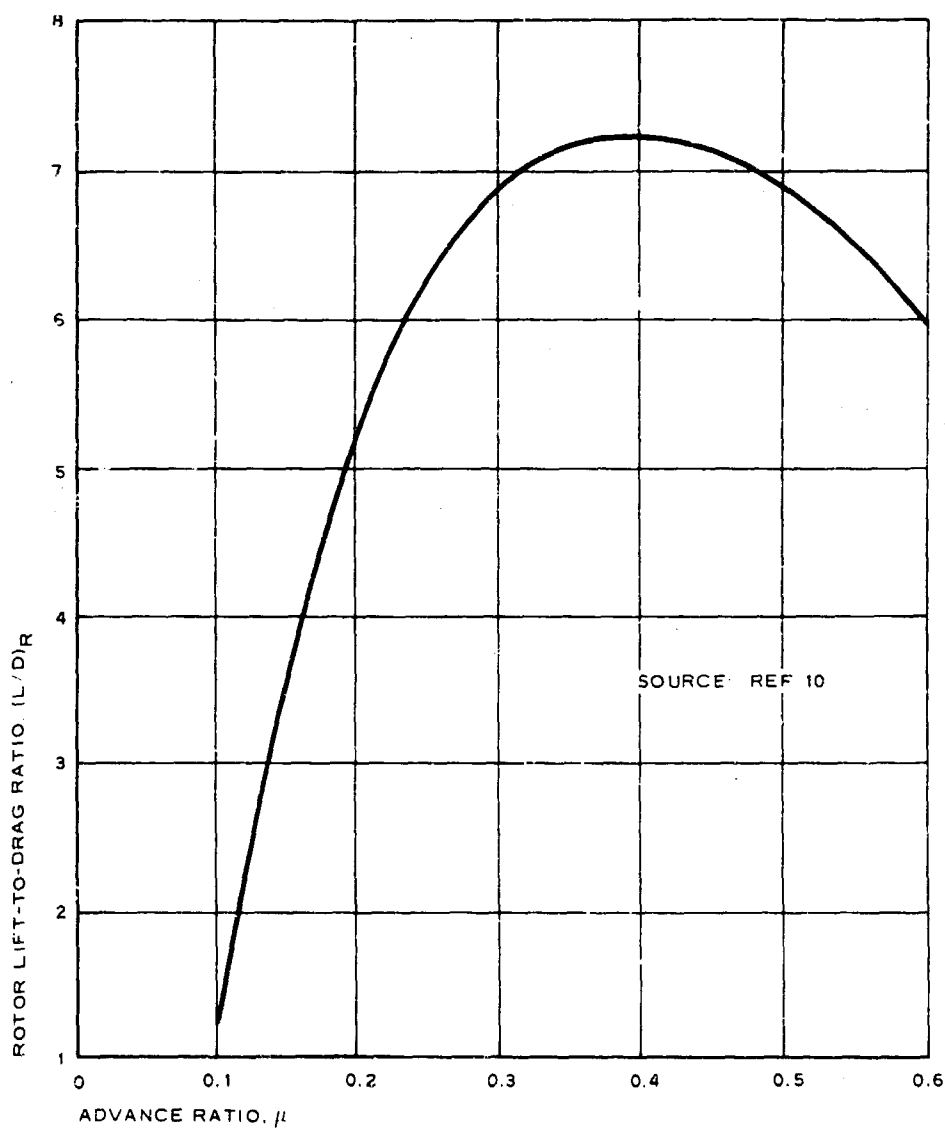


Figure 14 - $(L/D)_R$ versus Advance Ratio for 45-Ft Diameter Rotor

SECTION II - CONCEPT ANALYSIS

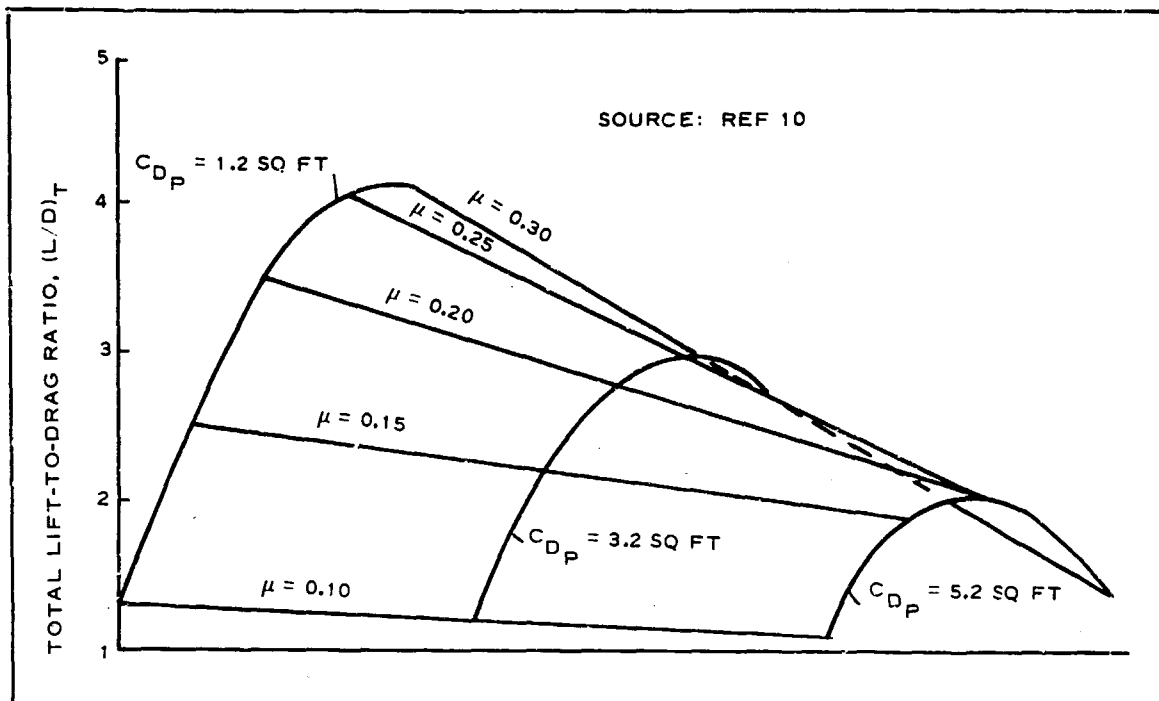


Figure 15 - $(L/D)_T$ Variation with Parasite Body Drag (C_{DP}) and Advance Ratio (μ)

For the axial descent case with no flare maneuver for landing, the required rotor disk diameter (see Figure 13) is 28 ft to limit the impact velocity to the design value of 19 fps at 5000 ft. A considerable reduction in this size can be obtained by utilizing the composite system's kinetic energy to attain a collective flare. In this case, an additional requirement of the rotor system is that the preflare ratio between thrust coefficient and solidity be less than 1 - that is,

$$\frac{C_T}{\sigma} < 1.$$

Therefore, for $\sigma = 0.1$, $C_T < 0.01$. This requirement is necessary to preclude blade stall during the collective flare maneuver (see Reference 11).

The required relationships between disk loading and blade weight for collective flares are depicted in Figure 16 for a rotor C_{DR} of about 1.4.

The weight ratio parameter in Figure 16 was determined from the preflare kinetic energy of rotation required to obtain a collective flare deceleration to a 19 fps vertical impact velocity. The equations used in

SECTION II - CONCEPT ANALYSIS

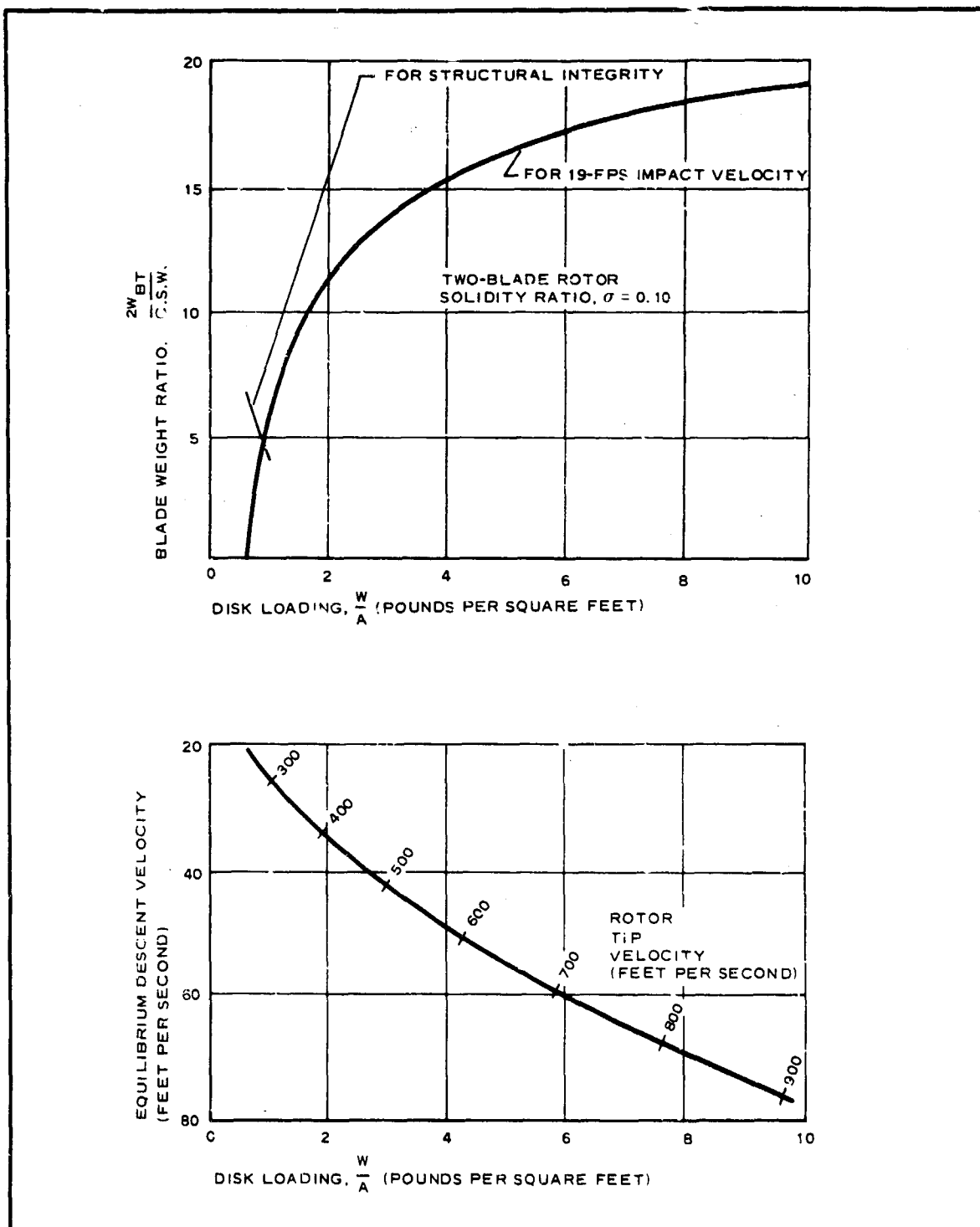


Figure 16 - Performance Parameters for Collective Flare

SECTION II - CONCEPT ANALYSIS

obtaining this curve are given in Reference 12. As shown in Figure 16, an increase in disk loading by, for example, decreasing the rotor diameter for a given weight results in an increase in the required blade weight. The weight required for structural integrity, however, is not necessarily equal to the weight required for collective flare performance. The weight of the theoretically optimum axial descent system is defined by the lowest weight ratio value for structural integrity not exceeded by the corresponding value for collective flare performance at the same disk loading.

To provide an estimated weight and volume requirement for the fabric rotor blades, the shape and pressurization requirements must be specified. An NACA 0012 airfoil will be assumed because (1) its symmetrical shape is obtained easily with an AIRMAT construction and (2) it has exhibited good performance characteristics. To maintain structural rigidity during operation, an internal gage pressure of 10 psi is adequate.

For the above conditions, the estimated blade weight can be determined by the method in Reference 13. The required AIRMAT blade weight for pressure is given by

$$W_{BB} = \frac{(2.046 \times 10^{-3})}{N^2} R_R^3. \quad (10)$$

The air weight required to inflate the enclosed volume to 10 psi is

$$W_{air} = \frac{(1.03 \times 10^{-3})}{N^2} R_R^3, \quad (11)$$

where N and R are number of blades and rotor radius, respectively. The weight of the coating, W_C , is assumed to be equal to 0.6 of the AIRMAT weight. Then the total weight for mass balance, is given by

$$W_B = W_1 + W_2,$$

where

$$W_2 = 3/4 W_{BB} + 3/4 W_{air} + 3/4 W_C \quad (12)$$

and

$$W_1 = 3W_2.$$

For a rotor radius of 14 ft, the required parameters are:

SECTION II - CONCEPT ANALYSIS

$$W_{BB} = 1.4 \text{ lb}$$

$$W_{\text{air}} = 0.705 \text{ lb}$$

$$W_C = 0.84 \text{ lb}$$

$$W_2 = 1.05 + 0.22 + 0.63 = 1.90 \text{ lb}$$

$$W_1 = 3 \times 1.9 = 5.7 \text{ lb}$$

$$W_B = 8.0 \text{ lb per blade}$$

The tip weight requirement for centrifugal tension is given by

$$Q = \frac{0.7427 L_B - W_B \left[0.5 \cos \beta \left(\frac{V_t^2 \tan \beta}{3R_R g} \right) \right]}{\cos \beta + \frac{V_t^2 \tan \beta}{R_R g}}, \quad (13)$$

where

Q = required tip weight per blade,

L_B = total lift per blade,

W_B = blade weight without tip weight,

V_t = tip velocity, and

β = coning angle.

Substituting appropriate values into the tip weight equation, the tip weight per blade, Q , is found to be 2.4 lb.

(3) Estimated System Weight

From the preceding structural analysis, the estimated weight of two blades without a collective flare landing maneuver is about 21 lb. Using the same analysis, an optimized blade weight of about 7.5 lb can be achieved by using a collective flare maneuver from an initial disk loading

SECTION II - CONCEPT ANALYSIS

of 0.9. The 0.9 disk loading corresponds to a rotor disk diameter of 20.6 ft and an initial descent velocity of 24 fps. The root fittings and hub, inflation system, initial drogue, collective flare (if used) initiation and actuation equipment, and the payload suspension system also contribute to the rotor system weight. Estimated weight of the components are provided in Table VIII.

TABLE VIII - ESTIMATED ROTOR SYSTEM
COMPONENT WEIGHTS

Item	Weight (lb)
Blades (2)	15
Root fitting and hub	3
Inflation system	4
Equipment for collective flare	1
Initial drogue	2
Suspension system	5
Total	30

The above weights are based on using the collective flare, since the predicted descent velocity prior to its use is not excessive for landing should a collective flare failure occur. The inflation system is assumed arbitrarily to be a fiberglass pressure bottle, with an appropriate weight value from Appendix B. For the suspension system, a rigid attachment is considered necessary to prevent contact between the man and rotor system at landing. Then, the weight value used includes the estimated weight of rigid connection between the man and the rotor and a rigid attachment frame.

The blade weight for structural integrity in the collective flare case has been estimated and assumes a collective flare peak loading factor of 2 and, from Reference 13, a safety factor of 4. Thus, a safety factor of 2 should be maintained under deployment peak loadings not in excess of 4. This statement is particularly true if the peak loading in deployment occurs before the blades are fully extended.

c. Powered Lifting Devices

(1) Stand-on Platforms

Powered lifting devices are designed generally to be kinesthetically

SECTION II - CONCEPT ANALYSIS

controlled in flight. Early investigations by NACA in 1951 (see Reference 14) demonstrated that this concept was indeed feasible for personnel in connection with stand-on platforms supported by either a jet-reaction device or a powered teeter-rotor. At that time, it was found that, while hovering in calm air, the flyer's natural balancing reactions tended to provide a stable flight situation. Subsequent investigations of rotor-supported platforms have verified the early NACA results and have shown kinesthetic control to be an easy and natural means of operation while hovering in calm air. Unfortunately, man's control power with stand-on platforms under practical flight conditions was found to be generally insufficient for any reasonably sized machine, while trim requirements, instabilities, and sensitivities to turbulence were quite large. To alleviate some of these problems and improve the basic flight characteristics of platforms, Hiller Aircraft Corp. embarked on an extensive development and evaluation program (see Reference 15). Its efforts resulted in the development of a platform supported by a 7-ft diameter ducted rotor system. Flight characteristics were somewhat improved by a vertically raised center-of-gravity position and by the addition of a gyro-bar stabilization system. Hovering flights in calm and gusty air and forward flights up to 18 mph were made. But these machines still remained limited in their general application to practical flight conditions.

Then, in 1962, the National Aeronautics and Space Administration conducted tests to determine if more effective operations could be achieved by providing the flyer with aircraft-type stick control (see Reference 16). Four differentially operated air jets, located about the periphery of the platform at 90-deg intervals, were provided. This stick-control system exhibited improved flight characteristics, especially when operated by personnel with previous flight experience. The machines, however, were found still to have inherent dynamic instabilities, and unrestricted forward flight under varied wind conditions was not possible. Thus, the stand-on platforms, relatively easy to fly while hovering in calm air, remain currently impractical for general use in forward flight or operations in turbulent air.

(2) Small Rocket Lift Device

A second type of powered device that has achieved considerable success using kinesthetic control for personnel mobility is the small rocket lift device (SRLD). This device, developed by the Bell Aerosystems Co., uses a 90 percent hydrogen peroxide fuel to obtain thrust. The bulk of the system is attached to the user's back, with the control and throttle arm assemblies installed in two rigid "arms" that extend in front of him. Control in roll and pitch is obtained kinesthetically by the operator's muscular movements. Yaw control is obtained by a jetavator thrust-vectoring system operated by a rotary control in the man's left hand. A rotary handle in the operator's right hand provides throttle control. Recent man flights, at a composite system weight of about 300 lb, have

SECTION II - CONCEPT ANALYSIS

demonstrated the following capabilities of the system (see Reference 17).

1. Maximum flight duration - 30 sec
2. Flight range - 800 to 1000 ft
3. Forward speed - 60 to 70 mph
4. Altitude capability - 100 ft

In addition, the SRLD has demonstrated the capability of hovering, soft landing, hill climbing, and 180-deg coordinated turns. Estimated flight time requirement for learning to operate adequately the SRLD is approximately 15 min.

(3) Retrorocket System

A third thrusting-type concept that presumably could be used to augment a parachute in decelerating personnel for landing is a retrorocket system. A general survey of Reference 18 was conducted to find available solid propellant rocket motors that could be used for personnel delivery application. The results of Reference 18 are classified; however, several motors are available that are appropriate for personnel application. Individual motors were found that provide total impulses as low as 40 lb-sec. Eleven different motors were found that weigh less than 10 lb and are capable of effecting a velocity change of up to 82 fps for a 300-lb system, without inducing an excessive deceleration level.

(4) Estimated System Weight

Component weights and total platform weights for various powered teeter-rotor and jet-reaction platforms are provided in Table IX. These weight estimates do not include any provisions for a stabilization system or an initial drogue device, which would be necessary to achieve any type of success with the retrorocket concept. They do, however, indicate the unfavorable weight penalties associated with this type of device even when only the basic system requirements are considered. That these weights are optimistic is evidenced by the fact that the Hiller platforms weigh more than 300 lb. Component weights given in Table IX were determined from the support thrust requirements obtained from Reference 14 and the specific impulses of the indicated fuels.

The weight penalties associated with the other powered devices are, in general, also excessive for this application. The weight of the SRLD, for example, without any allowance for an initial drogue device is about 115 lb when fueled. The parachute/retrorocket system is capable apparently of meeting the basic weight requirements but only under very unfavorable conditions. Figure 17 (see Reference 19) is a general plot of percent weight required for a parachute/retrorocket configuration to effect a final impact velocity of zero from the indicated initial descent

SECTION II - CONCEPT ANALYSIS

TABLE IX - WEIGHT ESTIMATES FOR TEETER-ROTOR AND
JET-REACTION LIFTING PLATFORMS

Configuration and power source	Weight (lb)						
	Frame and support	Lift element (8-ft diam)	Propulsion unit with tanks	Fuel	Throttle and controls	Drive and mounting	Total device Payload
Internal combustion engine shaft-driven teeter-rotor, 40 bhp	10	6.5	58.0	0.25	3	10	88.0 237.0
H ₂ O ₂ tip jets, 52-lb thrust at 4-ft radius	10	6.5	6.5	10.4	3	10	46.4 278.6
H ₂ O ₂ turbine shaft-driven rotor, 40 bhp	10	6.5	25.0	15.0	3	10	69.5 255.5
Compressed-air tip jets, 52-lb thrust at 4-ft radius	10	6.5	142.8	30.0	3	10	202.3 122.7
Solid-fuel jet reaction, $I_{SP} = 220$ sec	5	...	26.0	39.0	2	5	77.0 248.0
Liquid oxygen alcohol rocket, $I_{SP} = 240$ sec	5	...	32.3	40.7	1	5	84.0 241.0

SECTION II - CONCEPT ANALYSIS

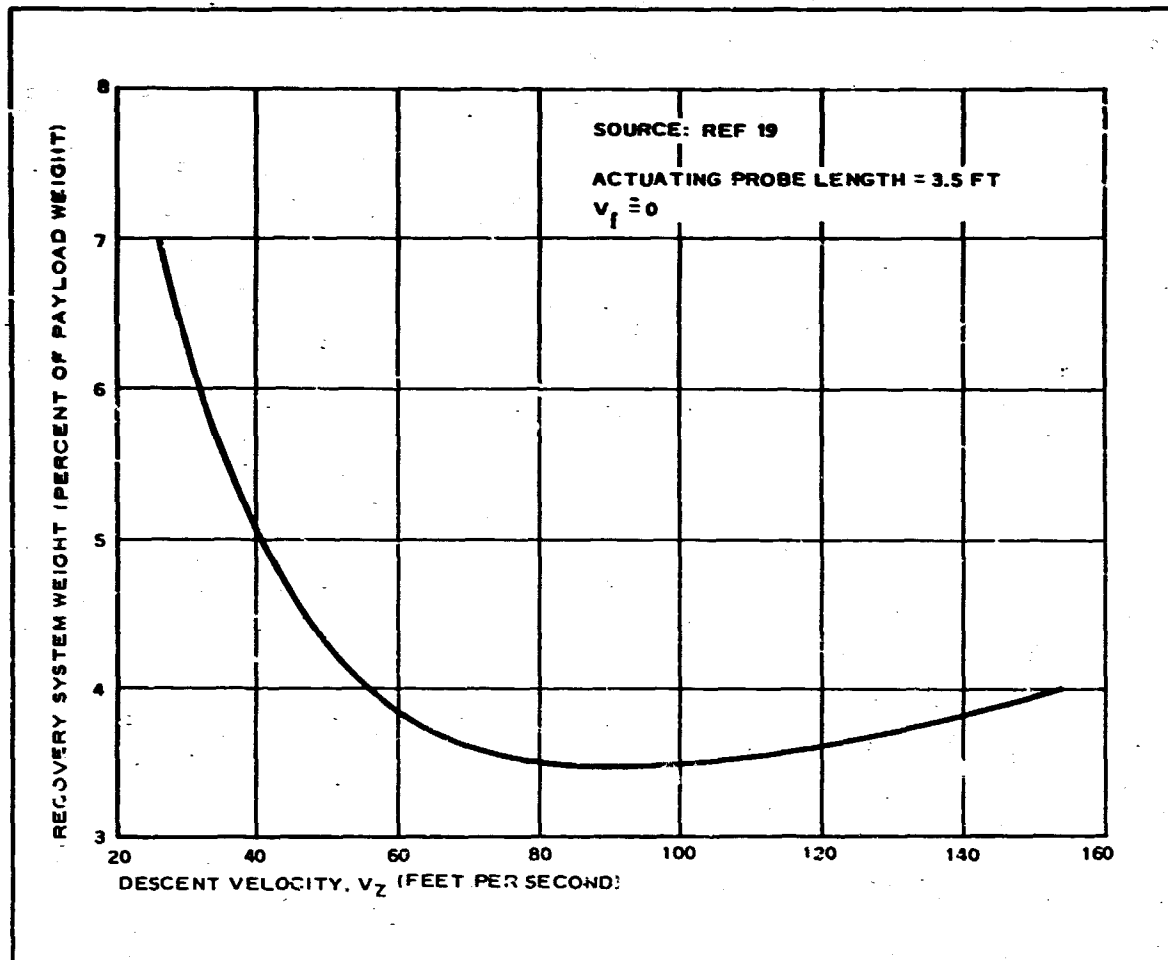


Figure 17 - Estimated Recovery-System Weight versus Descent Velocity for a Rocket-Cushioning, Ground-Proximity Device

velocity. The optimum performance systems are those systems that have an initial descent velocity of about 80 fps. Since the retrorockets would be activated close to the ground, emergency equipment, in the event of malfunction of the rockets, could not be used. Consequently, a lower initial descent velocity is considered more reasonable, in which case the system becomes inefficient.

4. GLIDING CONCEPTS

a. General

Seven different passive-type gliding concepts also have been investigated, including conical, cylindrical, and limp parawings; Parafoil, Parasail,

SECTION II - CONCEPT ANALYSIS

and Cloverleaf gliding parachutes; and the ring wing airfoil. The ring wing airfoil has advantages over the powered concepts in weight, cost, and operational complexity. Gliding concepts can be used to obtain a controlled descent with a limited range capability. Thus, a high degree of target accuracy is potentially possible. In addition, flare maneuvers at landing can reduce substantially the preflare kinetic energy and, thereby, provide a soft touchdown with a relatively small decelerator. The gliding capability of the systems also could be used to negate or to reduce substantially ground wind effects.

In the gliding concept analysis, performance coefficient and aspect ratio of passive gliding concepts are based on the concept reference area, which is not necessarily equal to the flat pattern fabric area. Table X differentiates between the various gliding devices and indicates the reference areas to be used throughout the rest of this report. Attached payloads are assumed to effect the total profile drag and not the total lift. Thus, the total system drag coefficient and the wing drag coefficient will be different, but the corresponding lift coefficients will be the same - that is, the wing alone value.

b. Parawings



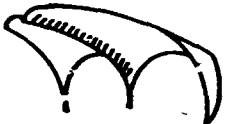

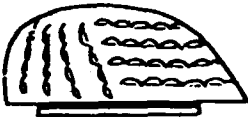
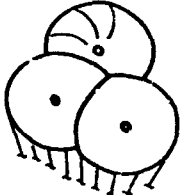
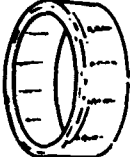
(1) Lift-to-Drag Performance Spectrum

Reference 20 summarizes the maximum lift-to-drag ratios (see Figure 18) for the three parawing configurations at the conditions indicated. These values, with the exception of the limp parawing, were obtained from tests using rigid-frame models. The large leading edge configurations were designed to simulate inflatable tube configurations. The higher L/D values obtained with the cylindrical wing reflect the lower profile drag of this configuration resulting from the absence of airfoil camber and twist. The comparatively low lift-to-drag ratio of the limp parawing can, in general, be attributed to its low aspect ratio design necessitated by the absence of a pressurized support structure. The use of a pressurized support structure on both the conical and cylindrical wings also allows some potential design freedom as to the size of the support structure (leading edge and keel), the planform shape, lobe height, and range of possible aspect ratios.

Since so many variations of the conical and cylindrical configurations are possible, specific configurations must be selected for further analyses to maintain a realistic frame of reference. Consequently, the rest of this report will apply to the selected designs unless otherwise specified. The conical configuration will be a large untapered leading edge design, primarily the individual drop glider (IDG) design (see Reference 21.) The conical configuration was selected due to its development as a personnel delivery system and since data are available on its deployment and delivery capability. In addition, this configuration is known to have relatively good stability.

SECTION II - CONCEPT ANALYSIS

TABLE X - SUMMARY DESCRIPTION OF GLIDING CONCEPTS

Concept	Description	Configuration	Reference area
Conical parawing	Fabric membrane, conical lobes; inflatable leading edges and keel		Projected planform area
Cylindrical parawing	Fabric membrane, cylindrical lobes; large leading edges and keel		Projected planform area
Limp parawing	Fabric membrane, 1/8-keel nose cut; parachute-type structure, parawing rigging		Total flat pattern surface area
Parafoil	Fabric compartmented structure, two layers of cloth with symmetrical airfoil cross section		Projected planform area
Parasail	Triconical parachute structure slotted for L/D and control		Nominal surface area
Cloverleaf	Trilobed parachute structure, extendable flaps for L/D modulation and control		Upper surface wetted area
Ring wing airfoil	Fabric ring with inflatable leading edge (torus) and chordwise ribs		Elliptical flat plate of span b and area $S = (\pi/2) b C$, where b and C are ring wing radius and chord respectively

SECTION II - CONCEPT ANALYSIS

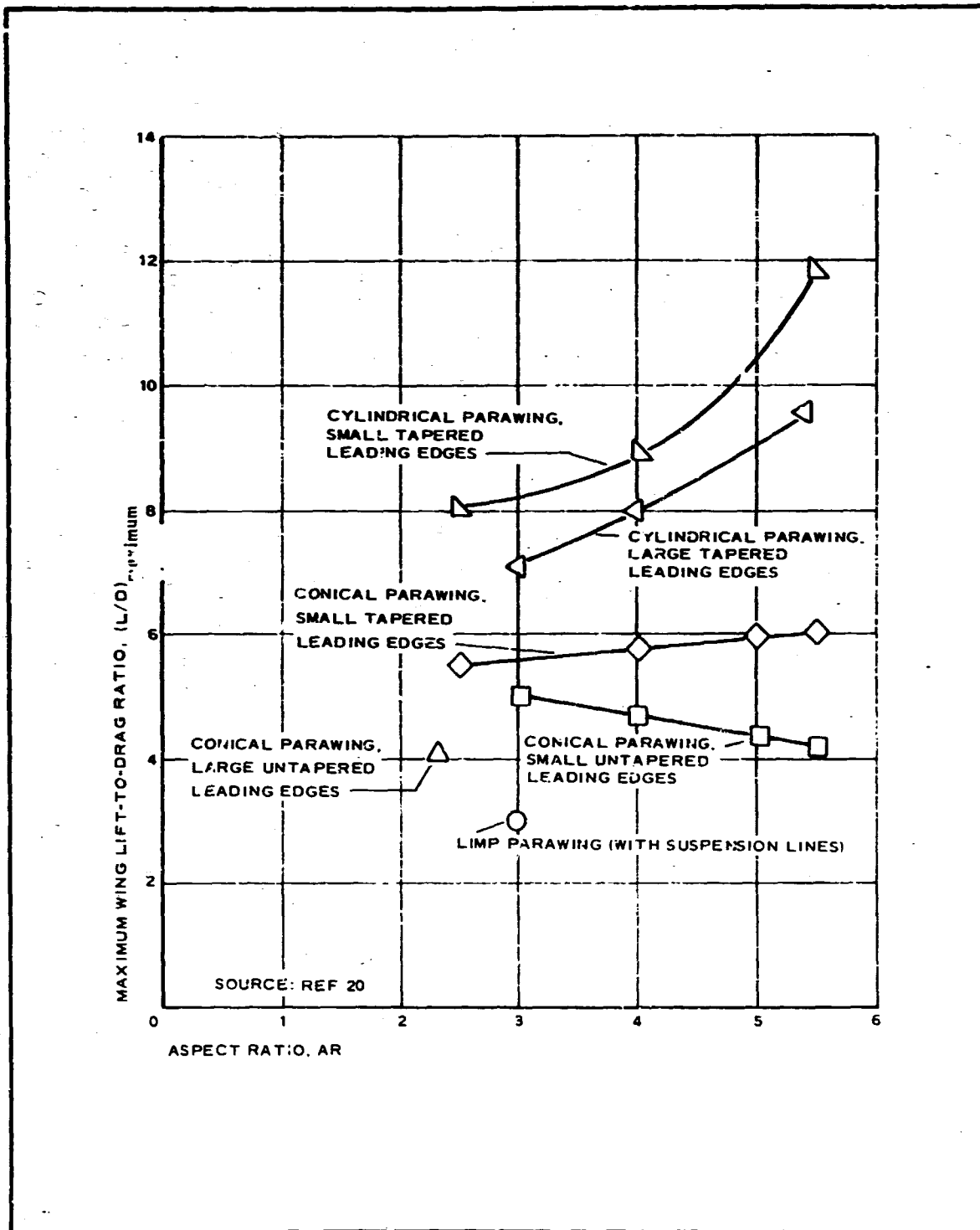


Figure 18 - Lift-to-Drag Performance for 50-Deg Swept Conical and Cylindrical Parawings Having Rigid Frames and a Limp Parawing

SECTION II - CONCEPT ANALYSIS

The selection of a cylindrical design is less straightforward than the selection of the conical, but its one apparent advantage over other gliding systems is its comparatively high L/D capability. Consequently, a design was selected to emphasize this performance while maintaining a configuration capable of being deployed. Thus, a low-lobed high aspect ratio design with large inflatable booms and keel will be used.

(2) Aerodynamic Characteristics and L/D Modulation

Aerodynamic characteristics of the selected conical and cylindrical configurations are presented in Figures 19 and 20. Data for the conical design were obtained from Reference 21. Data for the cylindrical design were obtained primarily from Reference 22 for a configuration with small leading edges. An adjustment for the parasitic drag of large leading edges was derived then from the simulated inflatable tube design of Reference 20. The L/D values were adjusted accordingly to form the curve in Figure 19.

Considerably less data are available on the limp parawing, although a few live drop tests have been conducted. Data presented are based on the limited analysis conducted by NASA and documented in Reference 20. Figure 21 presents the data of Figure 22 but includes the estimated effects of cable drag.

Figures 19, 20, and 22 show that the conical and limp parawings have a more restricted operating range than the cylindrical design does. At low positive angles of attack, canopy flutter problems become characteristic of the conical design, while the limp parawing design has a tendency toward nose tuck.

(3) Control and Maneuverability

The three parawing designs can be controlled by differentially operating the control lines connected to either control flaps located within the lifting surface or attached to the aft portion of the leading edges. Flaps located within the lifting surface are used by Ryan Aeronautical Co. in the current precision drop glider (PDG) system, a more up-to-date configuration similar in size, shape, and operation to Ryan's IDG. When maneuvering with this PDG configuration, the unattached end of the flap is pulled away from the lifting surface, thus creating an increase in form drag on the affected side of the canopy. This pull also deflects the lifting surface, which results in a slight lift reduction. This combination results in a rolling and yawing moment toward the affected side and results in a coordinated turn. By the downward deflection of the aft outboard tip of the lifting surface itself, the same basic result is obtained. By putting a line toward the payload, lift on the affected portion is spoiled while drag is increased, and a turn in the direction of the deflected panel is obtained.

SECTION II - CONCEPT ANALYSIS

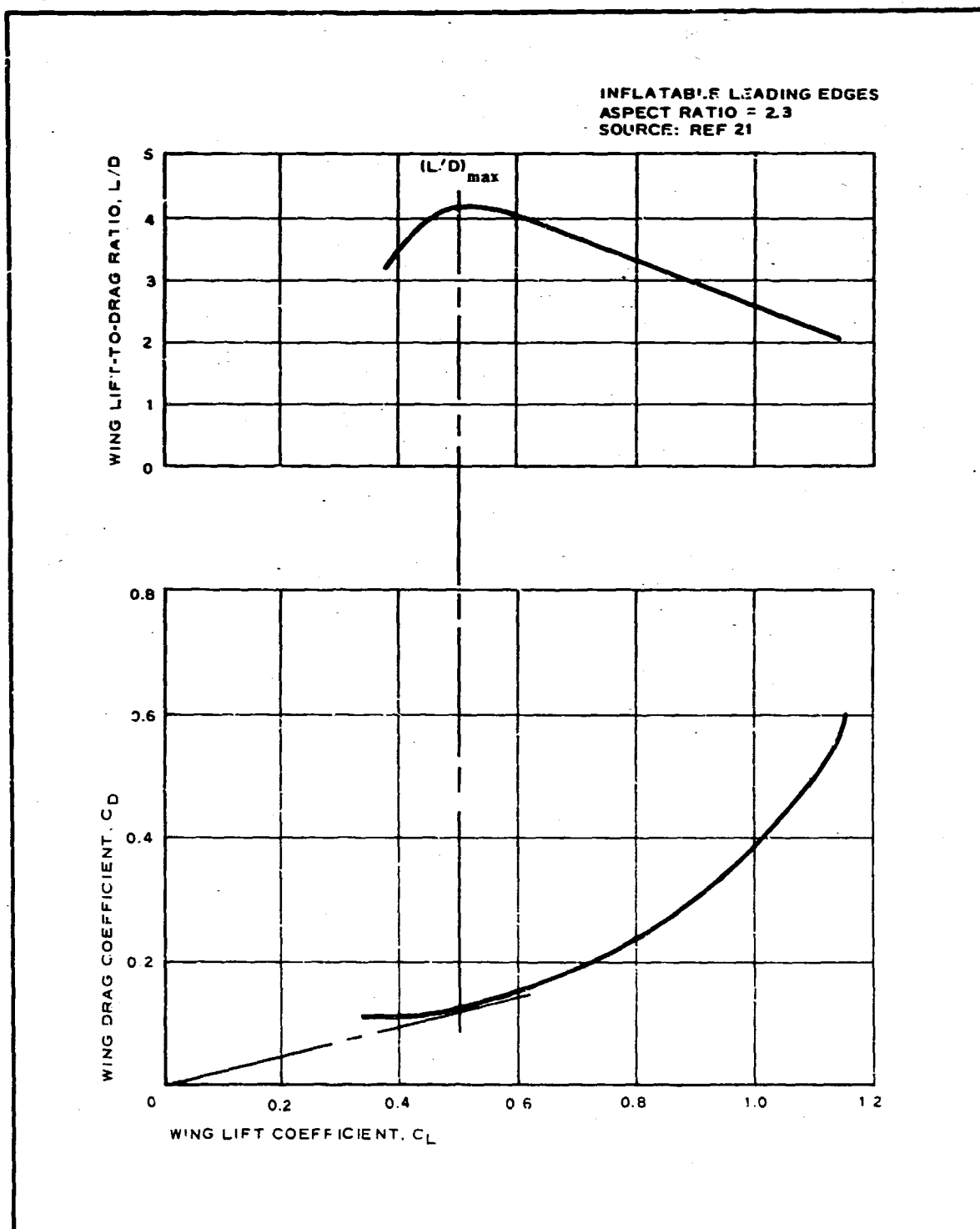


Figure 19 - Aerodynamic Characteristics of Conical Canopy (Parawing Alone)

SECTION II - CONCEPT ANALYSIS

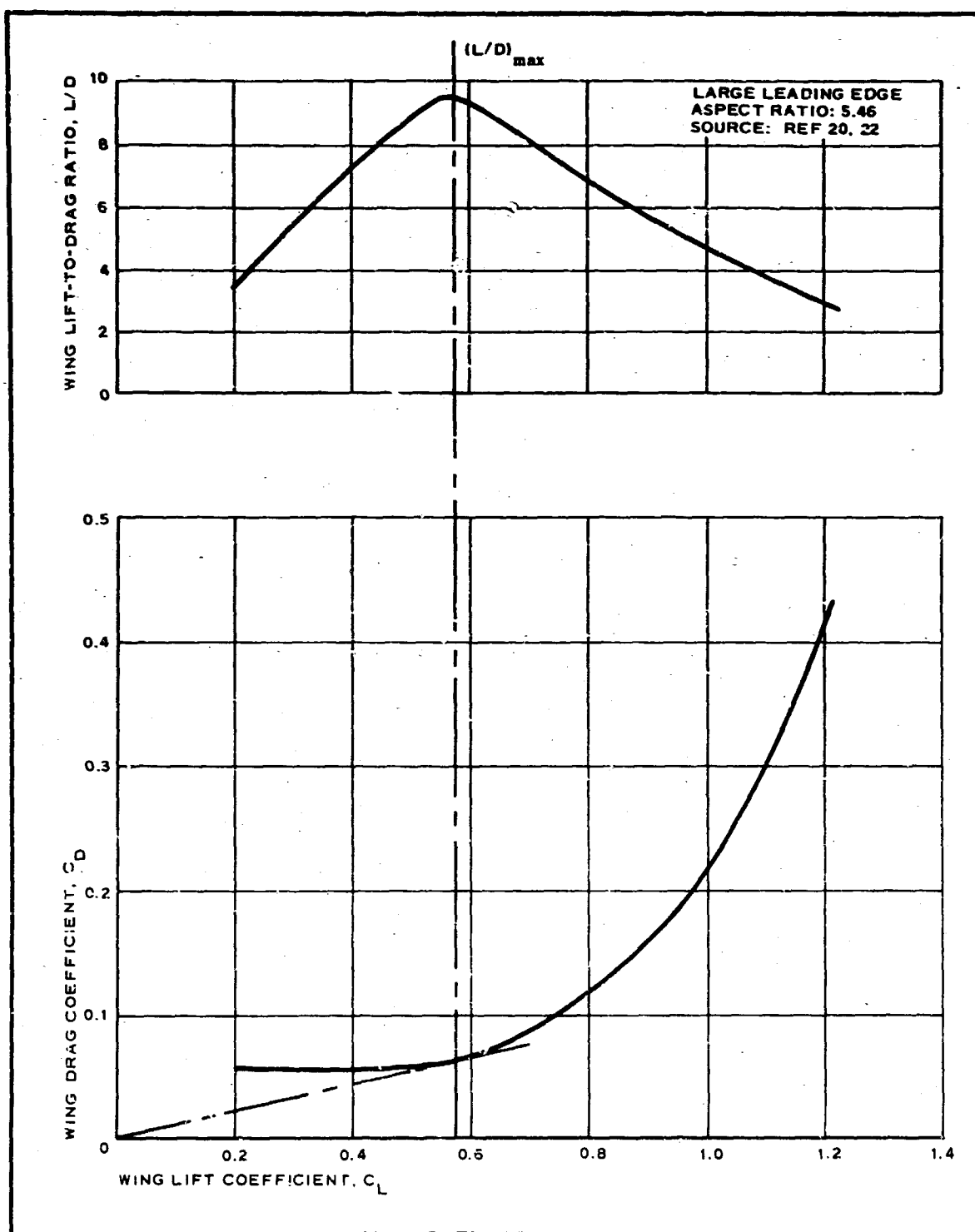


Figure 20 - Aerodynamic Characteristics of Cylindrical Canopy (Parawing Alone)

SECTION II - CONCEPT ANALYSIS

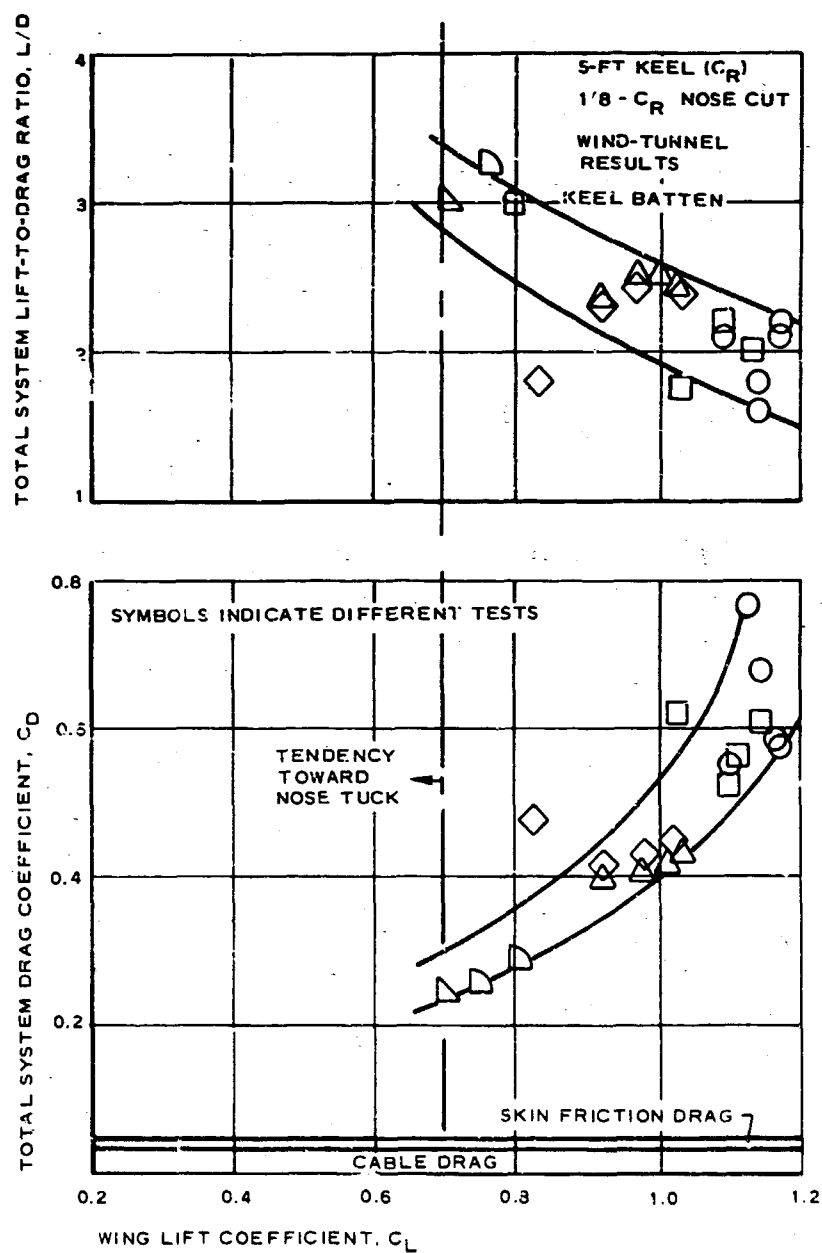


Figure 21 - Aerodynamic Characteristics of Limp Parawing Configuration (NASA Fabric Test Model)

SECTION II - CONCEPT ANALYSIS

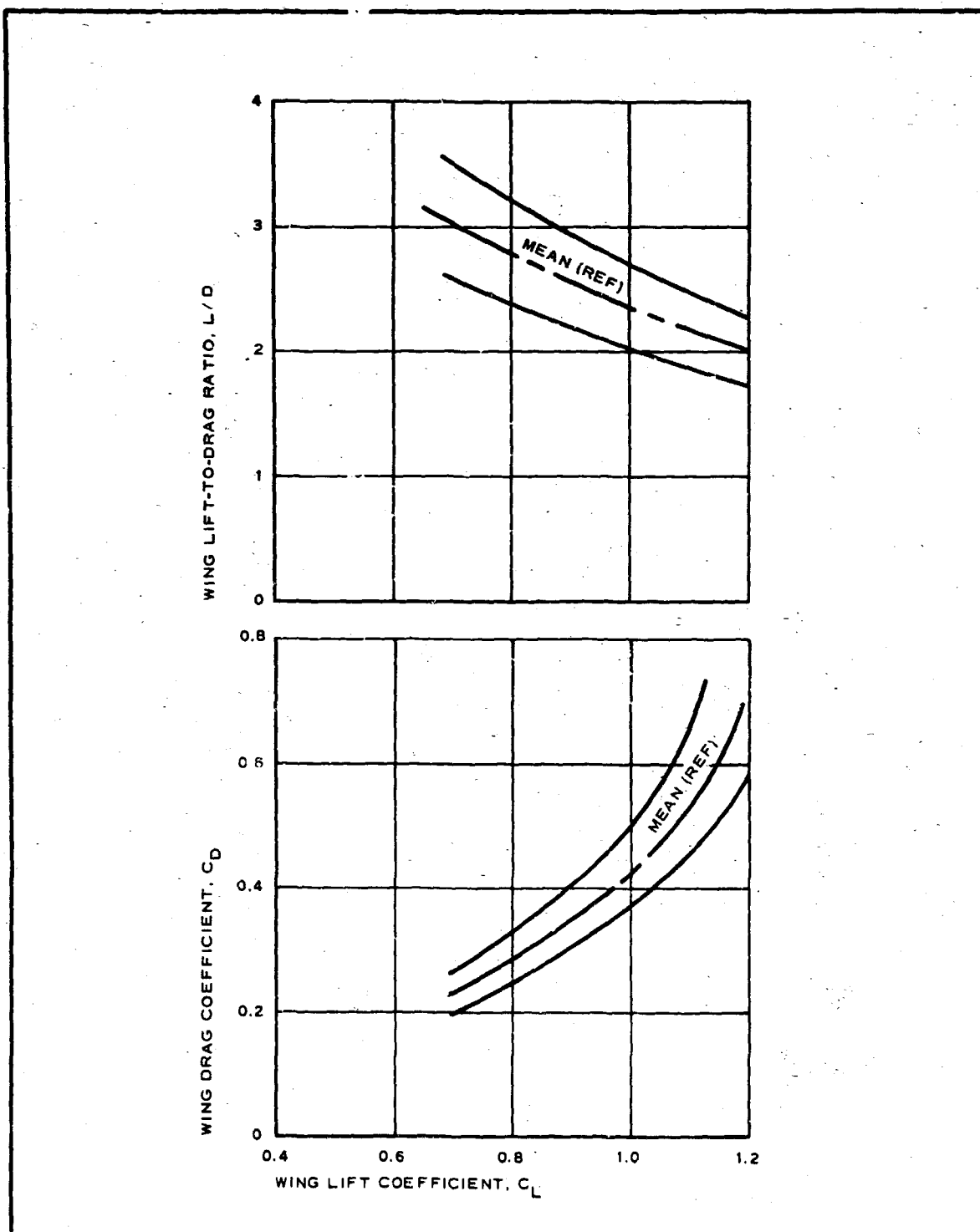


Figure 22 - Aerodynamic Characteristics of Limp Parawing
($1/8 C_R$ Nose Cut, Canopy Alone)

SECTION II - CONCEPT ANALYSIS

(4) Stability

Figure 23 presents pitching moment characteristics for the conical and cylindrical designs alone. A trimmed system for each configuration and for the limp parawing configuration can be obtained by suspending the payload below the wing. An example of the required relationships for the conical wing is shown in Figure 24 for the conditions indicated. Thus, the parawings can be trimmed for operations at more than one C_L value. This trimming is advantageous if, for example, it is desirable to flare the wing from C_L at $(L/D)_{\max}$ to $C_{L \max}$ for landing purposes. The proper relationship between X_{CG}/\bar{c} , Z_{CG}/\bar{c} , and $\alpha_{\bar{c}}$ would have to be maintained at the two corresponding C_L values. Lateral and directional stability of the three parawing configurations as used in a complete system is considerably more difficult to ascertain. Some insight into their relative stability, however, can be obtained by considering the static lateral and directional derivatives. Figure 25 indicates the relationship existing between these derivatives for configurations representative of the type of conical and cylindrical designs being considered. These plots indicate the conical design to have generally satisfactory stability, a conclusion generally verified by flight tests. Poor dutch roll stability and large side force coefficients are indicated for the cylindrical design, which indicates the possible need for auxiliary surfaces for satisfactory dynamic lateral stability. Static derivatives of low aspect ratio cylindrical wings also indicate this configuration to have poor dynamic lateral stability.

Lateral-directional derivatives for the limp parawing design are not available, but wind-tunnel and flight tests have indicated this configuration to have satisfactory lateral-directional stability when used in a complete system.

(5) Estimated System Weight

A complete parawing delivery system would include necessarily some type of first-stage decelerator to provide initial composite system stabilization and to effect a smooth transition to the gliding descent phase. For comparison of the three candidate parawing concepts, it will be assumed that first-stage deceleration would be provided by deploying the parawings themselves into a parachute mode. This technique was used by Ryan in developing the IDG and seems suited ideally to the parawing design, particularly to the conical and cylindrical configurations. Three advantages of this technique are (1) the need for only one recovery device, (2) the ability of the system to initiate inflation of the inflatable tubes while in the parachute mode, and (3) the reduced opening loading obtained. Since the limp parawing design has no inflatable tube structure, direct deployment to the parawing mode is possible theoretically. To provide a comparative weight estimation, an initial parachute mode is assumed for all three parawing designs.

SECTION II - CONCEPT ANALYSIS

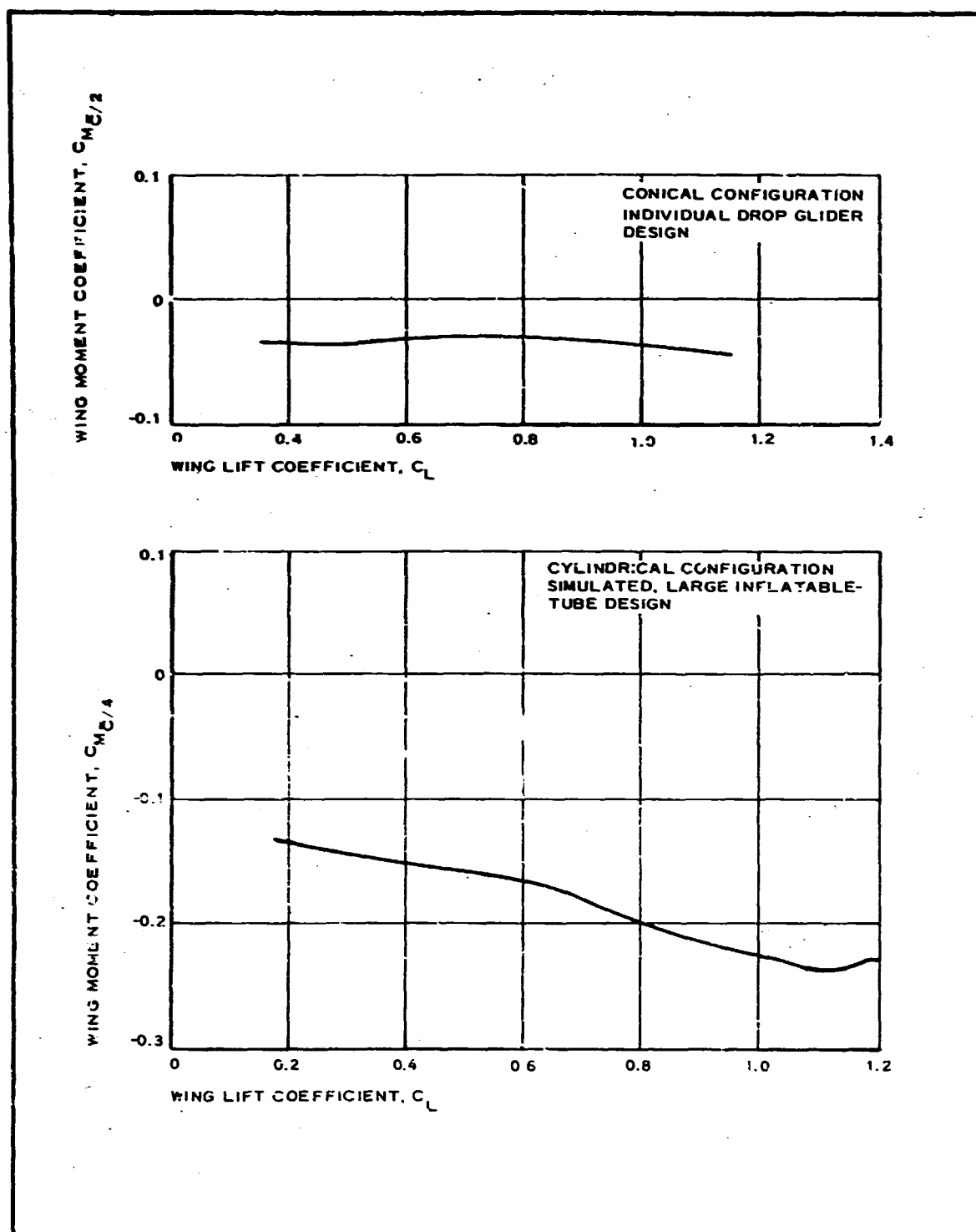


Figure 23 - Static Stability Characteristics (Parawing Alone)

SECTION II - CONCEPT ANALYSIS

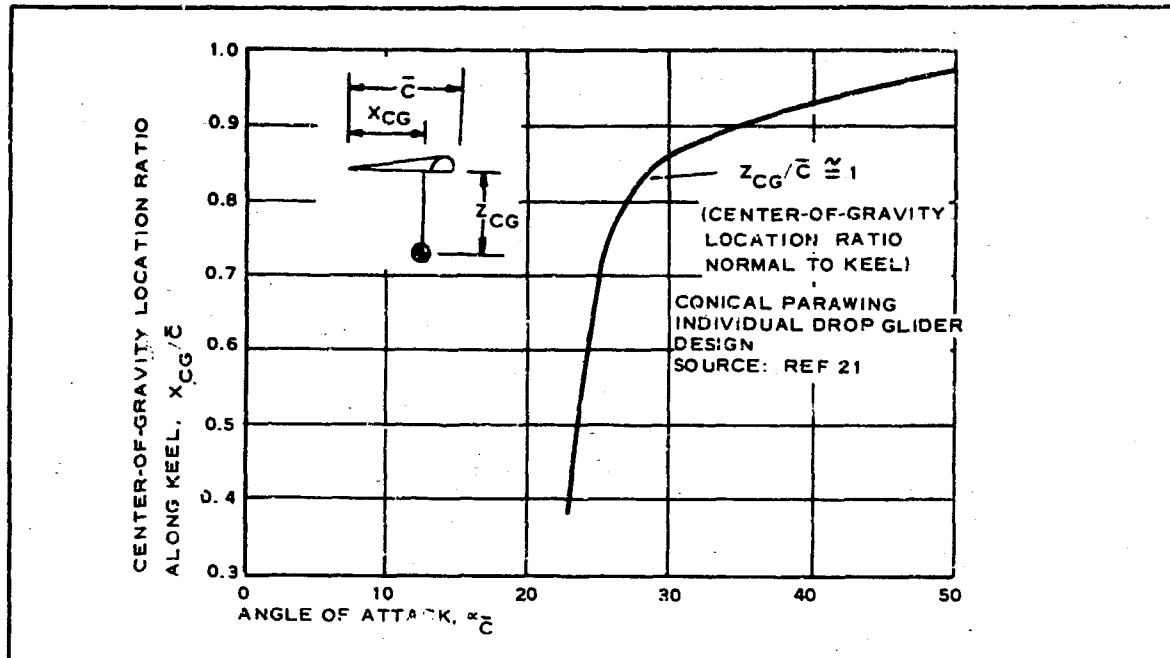


Figure 24 - Center-of-Gravity Location for Trim versus Angle of Attack

The weights of the various parawing systems depend on the size of the lifting surfaces, which must be obtained from the landing requirements. In general, many different sizes can be used to satisfy the basic landing requirements, primarily depending upon whether the wing is flared for landing. Consequently, various sizes are possible for obtaining the same landing results; therefore, weight as a function of size will be obtained in the following analysis. Sizing will be discussed more thoroughly in Item 4e, below.

In the following analysis, a proportional theoretical relationship between system weight for structural integrity and decelerator reference area will be established. The following parameters for the IDG, obtained from Reference 21, then will be used to determine the constants of proportionality from which plots of weight versus reference area will be constructed.

The parameters to be used are:

1. Composite system weight - 300 lb
2. Reference area - 278 sq ft
3. Design load limit - 8 G's (2400 lb)
4. Transition load limit - 2.26 G's
5. Deployed shape - parachute mode

SECTION II - CONCEPT ANALYSIS

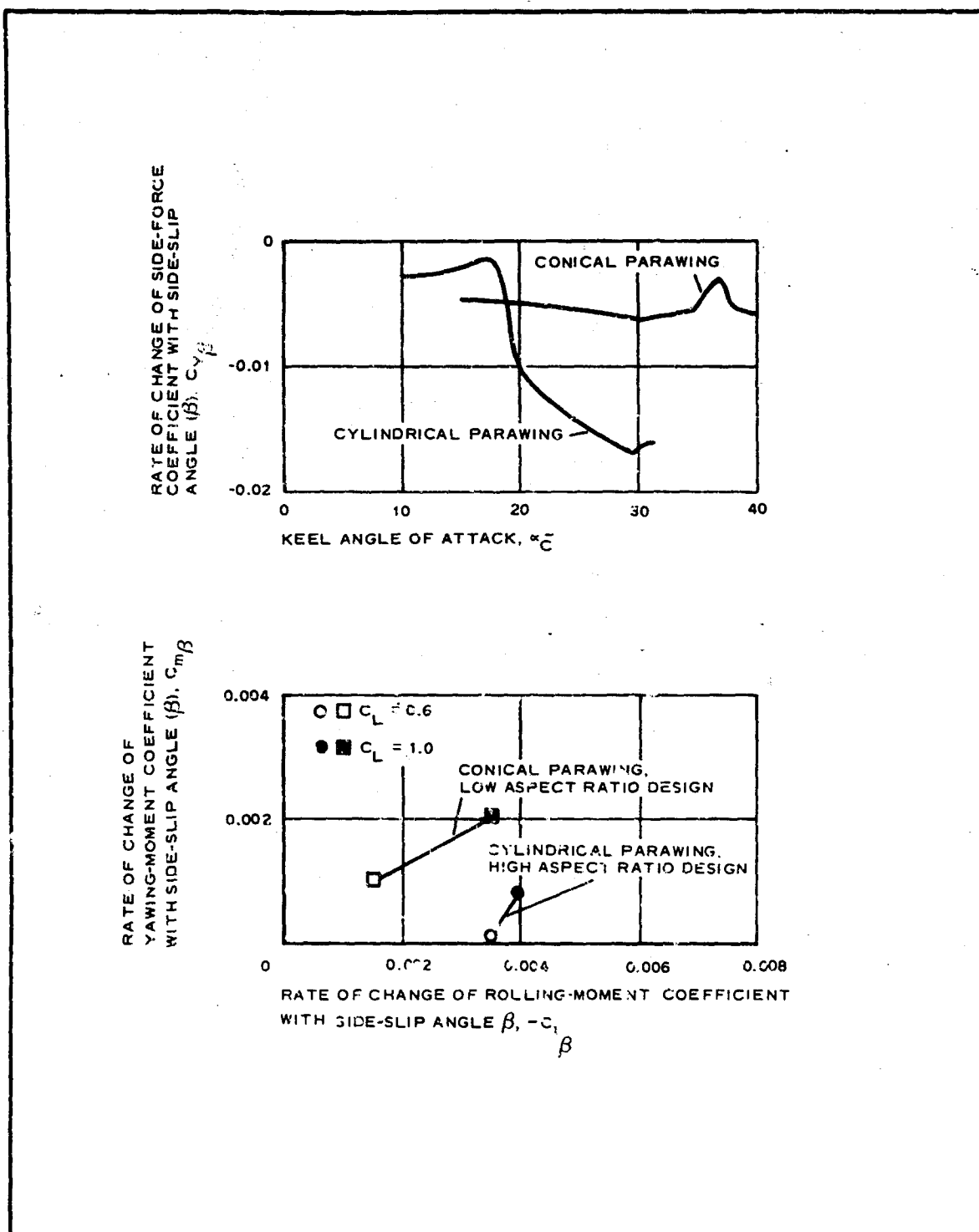


Figure 25 - Static Lateral Stability

SECTION II - CONCEPT ANALYSIS

6. Safety factor - 2
7. Membrane weight - 9.63 lb
8. Booms (2) - 3.56 lb
9. Keel - 1.30 lb
10. Miscellaneous (glue and hardware) - 8.8 lb

In Reference 21, the fabric hoop load in the membrane (in units of force per unit length) is given by

$$f_m = p_m R_m, \quad (14)$$

where p_m is the force per unit area (pressure) on the membrane and R_m is the lobed membrane radius. By expressing the pressure and the radius as functions of the force and reference area, the equation can be given by

$$f_m \propto \left(\frac{F}{S}\right) (S)^{1/2}, \quad (15)$$

where $R_m \propto (S)^{1/2}$ and α denotes a proportional relationship. The weight of the membrane is given by

$$W_m = \frac{f_m S}{k} \quad (16)$$

or

$$W_m \propto \left(\frac{F}{S}\right) (S)^{1/2} \left(\frac{S}{k}\right); W_m \propto \left(\frac{F}{k}\right) (S)^{1/2}, \quad (17)$$

where k is the strength-to-weight ratio of the fabric.

The critical load occurs at deployment into the parachute mode (see Reference 21), where for the IDG the design load limit is approximately 2400 lb. Since a coated Dacron construction is assumed, the membrane weight can be expressed as

$$W_m = C_1 (S)^{1/2}, \quad (18)$$

where C_1 is the product of the constant value F/k and the constant of proportionality. The weight of the booms and keel as a function of the size can be determined in a similar manner. Since the keel structure is the most critical, the keel will be analyzed and the resulting weight multiplied by three to include the two booms. From Reference 21, the internal keel

SECTION II - CONCEPT ANALYSIS

pressure requirement is given by

$$p_{\bar{C}} = \frac{M_{\bar{C}}}{R_{\bar{C}}^3} \quad (19)$$

where M is the maximum bending moment and $R_{\bar{C}}$ is the keel radius. The maximum moment, $M_{\bar{C}}$, is given by

$$M_{\bar{C}} = \frac{W' x^2}{\bar{C}} \quad (20)$$

where W' is a load parameter, \bar{C} is the keel length, and $x = 0.136 \bar{C}$. Again, taking advantage of the geometrical relationships,

$$M_{\bar{C}} \propto W' R_{\bar{C}} \quad (21)$$

Therefore

$$p_{\bar{C}} \propto \frac{W' R_{\bar{C}}}{R_{\bar{C}}^3} \propto \frac{W'}{S} \quad (22)$$

Now, the hoop stress in the keel is given by

$$f_{\bar{C}} = p_{\bar{C}} R_{\bar{C}}$$

and

$$f_{\bar{C}} \propto \left(\frac{W'}{S} \right) (S)^{1/2}$$

and

$$W_{\bar{C}} \propto \left(\frac{W'}{S} \right) (S)^{1/2} \left(\frac{S}{k} \right) \quad (23)$$

Since the construction, size, and shape of the booms are the same as those of the keel, the weight of all three keel tubes can be expressed as

$$W_t \propto (3) \left(\frac{F}{S} \right) (S)^{1/2} \left(\frac{S}{k} \right)$$

or

SECTION II - CONCEPT ANALYSIS

$$W_t = C_2 S^{1/2} \quad (24)$$

By the same reasoning, the weight of miscellaneous glue and hardware for the conical design can be expressed as

$$W_{\text{misc}} = C_3 S^{1/2} \quad (25)$$

Finally, the weight of the inflation system and inflatant must be determined. By determining the total inflation energy ($p_t V_t$) requirement, this weight can be obtained by using the plot given in Appendix B,

$$V_t \propto (S)^{3/2} \quad (26)$$

It was previously shown that

$$p_t \propto \frac{W'}{S} \quad (27)$$

Therefore,

$$p_t V_t \propto \left(\frac{W'}{S} \right) (S)^{3/2},$$

or

$$p_t V_t = C_4 (S)^{1/2} \quad (28)$$

The inflation system weight is obtained then from the Appendix B plot. The inflatant weight (assuming air) is obtained from

$$W_{\text{air}} = \frac{p_t V_t}{p_{\text{atm}}} \times m_{\text{air}}, \quad (29)$$

where p_{atm} is the atmospheric pressure and m_{air} is the weight per unit volume.

In summary, the relationships obtained are:

1. Membrane - $W_m = C_1 (S)^{1/2}$
2. Tubes - $W_t = C_2 (S)^{1/2}$
3. Miscellaneous - $W_{\text{misc}} = C_3 (S)^{1/2}$

SECTION II - CONCEPT ANALYSIS

4. Inflation energy - $p_t V_t = C_4 (S)^{1/2}$

5. Air - $W_{air} = p_{atm} \times m_{air}$ (30)

The design parameters of the IDG now can be used to determine constants C_1 , C_2 , C_3 , and C_4 as follows:

$$C_1 = \frac{W_m}{S^{1/2}} \Big|_{IDG}$$

$$= \frac{9.63}{(278)^{1/2}} = 0.577$$

$$C_2 = \frac{W_t}{(S)^{1/2}} \Big|_{IDG}$$

$$= \frac{4.86}{(278)^{1/2}} = 0.291$$

$$C_3 = \frac{W_{misc}}{(S)^{1/2}} \Big|_{IDG}$$

$$= \frac{8.8}{(278)^{1/2}} = 0.526$$

$$C_4 = \frac{pV}{(S)^{1/2}} \Big|_{IDG}$$

$$= \frac{(3015)(144)(205/1738)}{(278)^{1/2}} = 3070 \quad (31)$$

Therefore, the size-weight relationships are:

$$W_m = 0.577(S)^{1/2}$$

$$W_t = 0.291(S)^{1/2}$$

$$W_{misc} = 0.526(S)^{1/2}$$

SECTION II - CONCEPT ANALYSIS

$$p_t V_t = 3070(S)^{1/2} \quad (32)$$

The estimated parawing weight as a function of size is plotted in Figure 26. Due to the lack of more specific data, an assumed 8-G load limit was used, since this limit is comparable to the maximum opening shock experienced with the T-10 assembly. Unfortunately, the actual relationship between G-load, size, and weight is not known; however, this relationship should be governed by the design. Drop tests of the IDG conducted by Ryan indicated the actual opening loads to be approximately three times those loads expected at the corresponding dynamic pressure levels. This statement suggests that possibly additional reefing or some other technique would be required to reduce the opening loads, especially at higher deployment velocities. Reducing the opening loads would affect the weight estimates of Figure 26. Additional reefing, for example, would lower the load in the membrane at deployment in the parachute mode and, thus, theoretically lower the membrane weight requirement. At transition into the glider mode, however, the load induced into the booms and keel would be increased, which suggests that an increase in weight would be necessary for these components. The net result may not appreciably affect the total weight in Figure 26, although the individual component weights could be affected significantly.

The cylindrical configuration at corresponding reference areas would be significantly heavier than the conical configuration due, primarily, to the increased weight requirement of the booms and the necessity of stabilizer surfaces. The heavier booms are required to offset their structurally less efficient helical shape, compared with the straight boom characteristic of the conical parawing. The stress analysis of helically shaped inflatable booms is extremely complex and is not presented here. With the stabilizer surfaces and the heavier booms, however, the cylindrical parawing, for any reasonably sized configuration, would be considerably heavier than 50 lb.

The limp parawing configuration would be the lightest of the three parawings when deployed and operated under similar conditions. The absence of a pressurized support structure and an inflation system suggests that the limp parawing weight would be comparable with the membrane weight of the conical configuration (see Figure 26). In recent personnel drop tests with NASA-designed 400 sq ft configurations, a six-pound parawing was used to deliver a composite system weight of about 200 lb. By maintaining the same canopy load-weight relationship, a 400-sq ft configuration weighing nine pounds would be required for a 300-lb composite system under similar test conditions. Design parameters for these test configurations are not known, but the previous statement suggests that the membrane weight in Figure 26 may be unduly conservative for the limp parawing membrane without lines.

An additional advantage of the limp parawing is its potential capability of

SECTION II - CONCEPT ANALYSIS

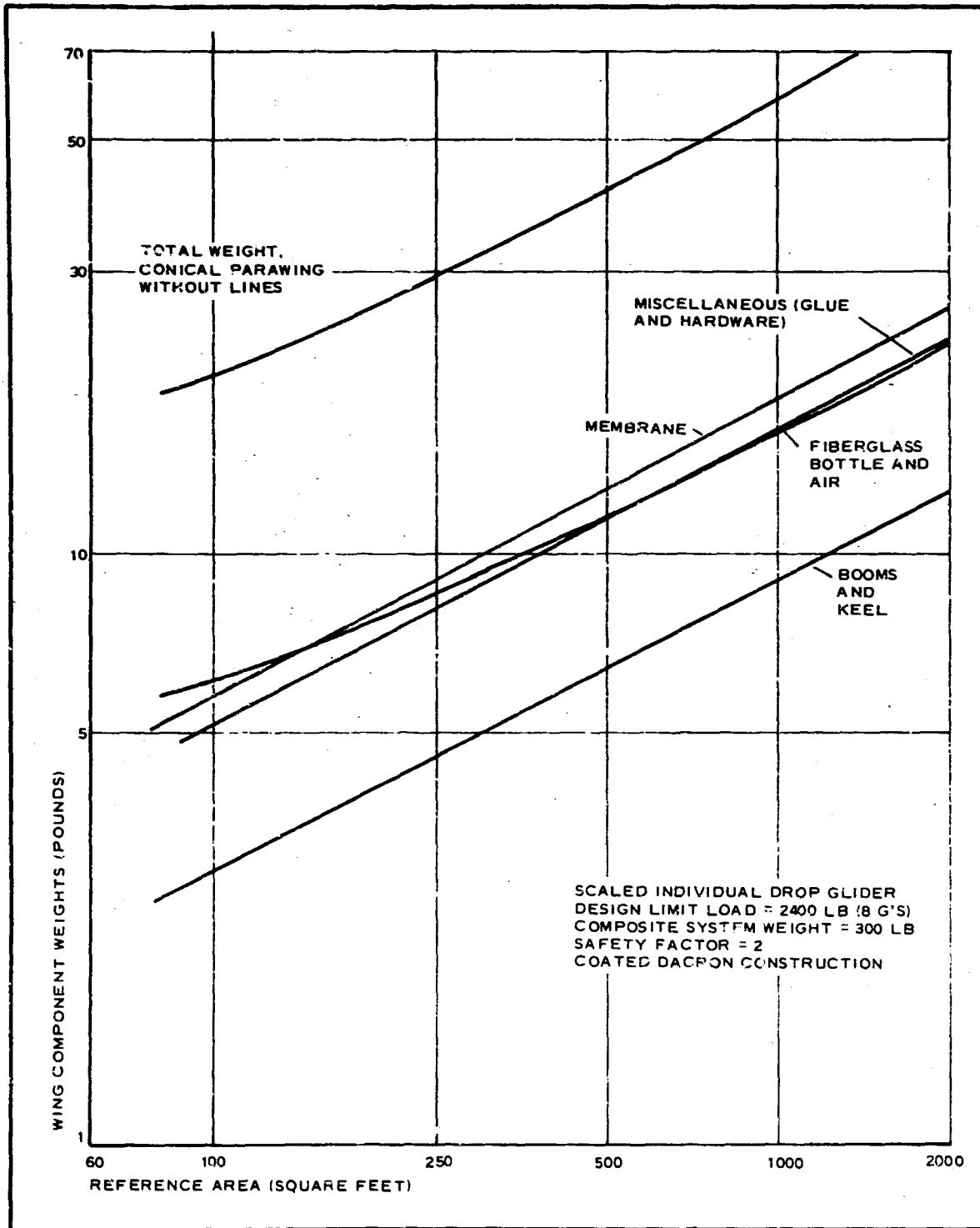


Figure 26 - Conical Parawing Weight versus Reference Area for Structural Integrity

SECTION II - CONCEPT ANALYSIS

being directly deployed to the parawing mode. Since the limp parawing has no pressurized structure, the transient parachute mode would not be required for boom and keel inflation but would be required with the conical and cylindrical configurations. Further analysis of this deployment technique would be required to determine whether an acceptable opening shock load could be attained and to determine its stability under rather adverse high-speed deployment conditions.

Two aspects that have not been considered in this weight analysis are the suspension system weight and the effects of minimum gage requirements. Standard personnel parachute lines weigh 0.0095 lb per running yard and have a tensile strength of 375 lb. Thus, to maintain a safety factor of 2 with a payload of approximately 300 lb, a minimum of about 13 lines is required. For the limp parawing, one line for every foot of keel length will be assumed, and the line length will be considered equal to one keel length. (In recent drop tests with a 400-sq ft limp parawing delivering a payload of about 200 lb, the approximate keel length, line length, and number of lines were 24 ft, 24 ft, and 23, respectively.) For the IDG, sixteen lines 22 ft long are considered appropriate for a 278-sq ft configuration having a 22-ft keel length. If the above relationships are used (and noting that the keel length varies directly with the square root of the reference area), an approximate suspension line weight as a function of reference area can be obtained (not less than 13 suspension lines). This weight is added to the appropriate membrane weights to yield the total values depicted in Figures 27 and 28.

Figures 27 and 28 also show plots of weight versus reference area for configurations assumed fabricated with minimum gage fabrics. For a light-weight fabric impregnated with an elastomer to achieve the desired permeability, a value of 2.2 oz/sq yd was used arbitrarily as a practical minimum. The weight of the suspension system, inflation system, etc., where required, was added to the estimated minimum gage fabric weight to form the minimum gage plots shown in Figures 27 and 28. From these curves, the weight was determined by the structural integrity requirements for small and medium-sized wings and by the minimum gage requirements for large wings.

c. Gliding Parachutes

(1) Lift-to-Drag Performance Spectrum

The maximum lift-to-drag ratios experimentally obtained with the three gliding parachutes were obtained from References 23 and 24 and are presented in Figure 29. These ratios include the additional drag contribution of the suspension system and, in some cases, a suspended payload, which results in a lower value than the value for the membrane alone. The indicated trend in L/D_{\max} is, however, still valid, since the additional drag

SECTION II - CONCEPT ANALYSIS

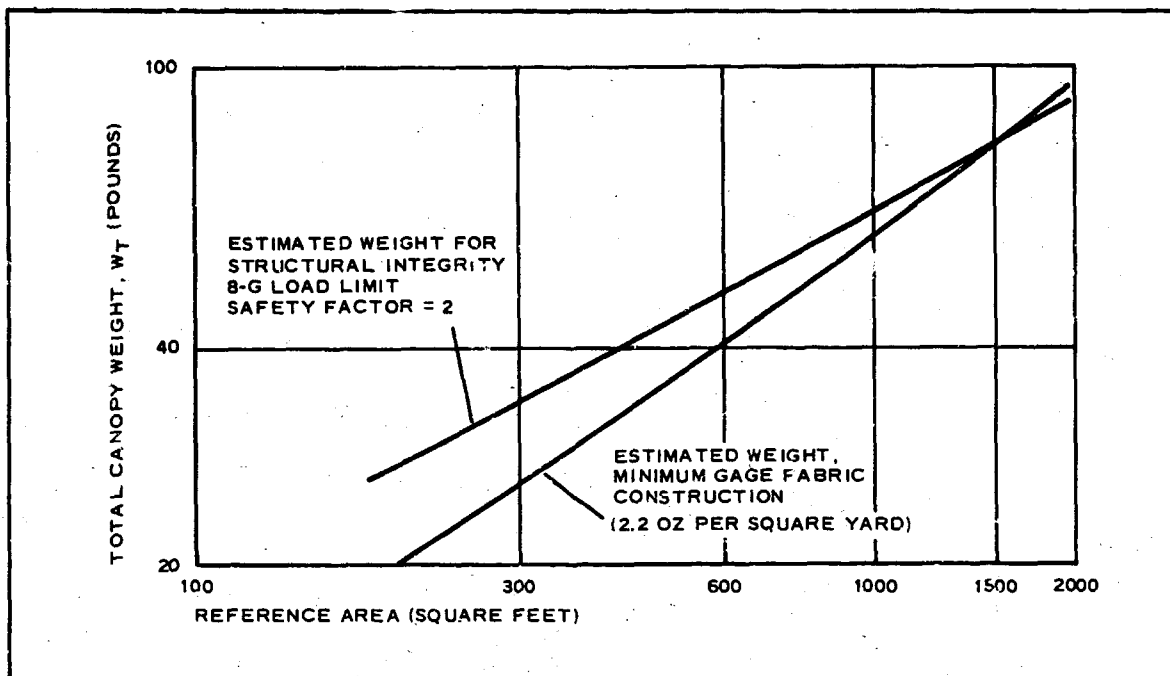


Figure 27 - Estimated Conical Parawing Weight for Re-covering a 300-lb Composite System

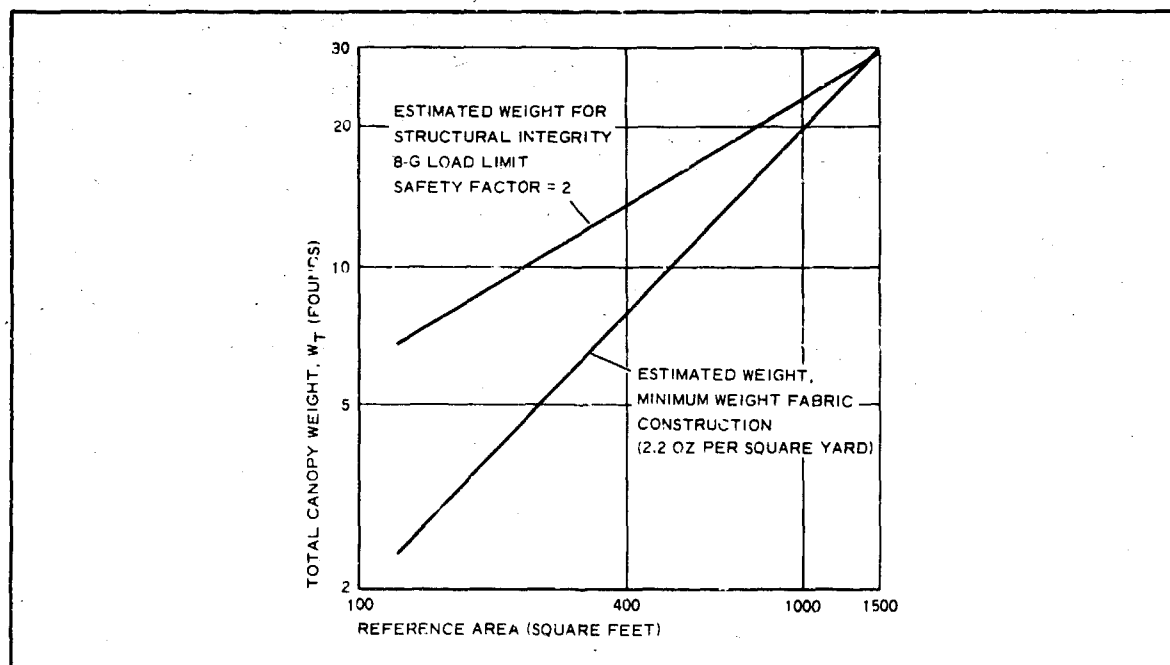


Figure 28 - Estimated Limp Parawing Weight for Re-covering a 300-lb Composite System

SECTION II - CONCEPT ANALYSIS

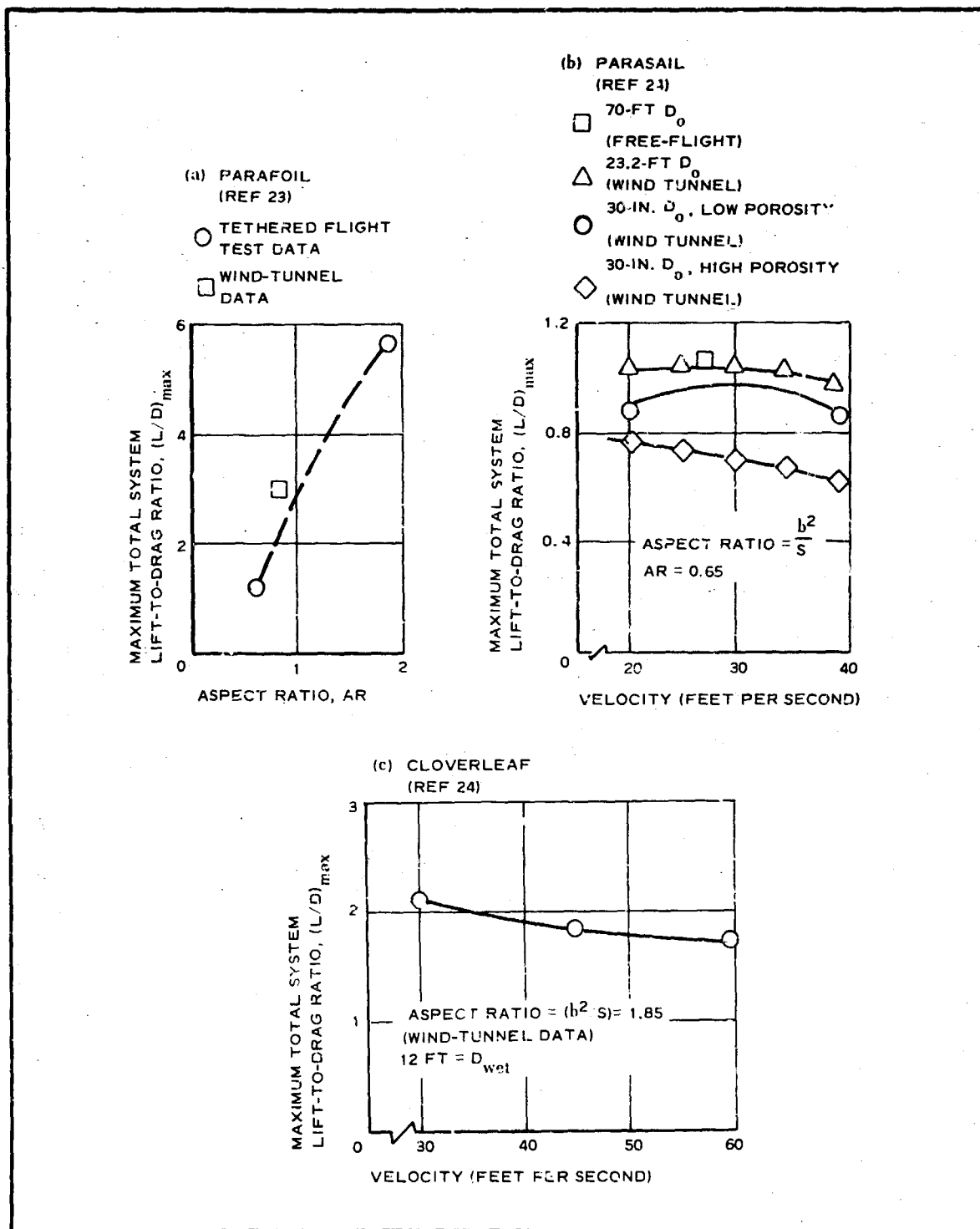


Figure 29 - Maximum Lift-to-Drag Ratio for Three Gliding Parachute Configurations

SECTION II - CONCEPT ANALYSIS

is relatively constant and is small compared with the drag of the lifting membrane.

Figure 29a shows the effect of aspect ratio on the lift-to-drag performance of typical Parafoil configurations having a symmetrical airfoil cross section and a 20 percent chord thickness. The increase in $(L/D)_{\max}$ with increase in aspect ratio is consistent with airfoil theory. For structural reasons, however, this configuration is aspect-ratio limited to the approximate range of values shown in Figure 29a. At higher aspect ratios, a tendency toward spanwise buckling becomes prevalent due to the line-induced, inward-directed forces. The actual limiting aspect ratio depends on such factors as wing loading, the included angle between the suspension lines and the local span line, and the operating angle of attack (since at low angles of attack the ram-air pressure in the compartmented structure is relatively low). For personnel and cargo applications, the above structural consideration is not considered a disadvantage since low landing velocities will dictate relatively low wing loadings and since the maximum lift-to-drag ratio, even at very low aspect ratios, is moderately high.

Figure 29b shows the Parasail's lift-to-drag performance as a function of velocity, size, and porosity. Some care is required in interpreting the results of these curves, since aeroelastic effects, profile drag of the suspension system and payload, and Reynolds number effects all contribute to the indicated performance characteristics. The increase in $(L/D)_{\max}$

with size, for example, could reflect the effect of payload and line profile drag and is not solely indicative of the canopy alone without lines. In addition, the higher Reynolds number associated with the larger size could result in a slight increase in lift coefficient without a corresponding increase in total drag. If the small variations in fabrication variations in testing techniques used, and the fact that the Parasail is a nonrigid structure are considered, the $(L/D)_{\max}$ variations with size are not pronounced.

The generally small decline in $(L/D)_{\max}$ with increased velocity can be reasonably attributed to deformation of the nonrigid structure. For the small operating velocity range associated with personnel and cargo delivery (see Item 4e, below), this effect is considered negligible.

In performance, primary disadvantages of the Parasail are its comparatively low $(L/D)_{\max}$ and its high turn rate (for an 80-ft D_0 Parasail under a wing loading of approximately one, the turn rate is approximately 50 to 60 deg/sec; see Reference 25). Primary advantages are its advanced developmental status with respect to the Cloverleaf and Parafoil and its demonstrated stability under load.

Figure 29c plots the maximum lift-to-drag ratio as a function of velocity for the Cloverleaf parachute. Like the Parasail, a net loss in $(L/D)_{\max}$

SECTION II - CONCEPT ANALYSIS

is experienced with an increase in velocity. This net loss again will be disregarded for the present application since both the net loss and the operating velocity range are small. The Cloverleaf has not been tested so extensively as the Parasail, but results indicate that it is a stable configuration.

Based on the test results with large configurations, a slower turn rate can be achieved with the Cloverleaf than with the Parasail. For a 56-ft D_{wet} configuration under a wing loading of approximately two, a turn rate of about 20 deg/sec has been demonstrated (see Reference 25).

The Cloverleaf's maximum lift-to-drag ratio is not so high as the Parafoil ratio, but it is higher than the same value for the Parasail.

(2) Aerodynamic Characteristics and L/D Modulation

Figures 30 and 31 (see References 26 and 24, respectively) present aerodynamic data for the Parasail and Cloverleaf designs. These figures indicate the operational range of the two configurations. From these data, the applicable L/D and C_L range can be obtained and are presented, along with similar data for the Parafoil configuration, in Figures 32, 33, and 34. For the Parasail canopy, C_L and C_D were obtained from C_X and C_Z using the indicated geometrical relationships that yield the following equations:

$$C_L = C_X \cos \theta + C_Z \sin \theta$$

$$C_D = -C_X \sin \theta + C_Z \cos \theta \quad (33)$$

Data for the Cloverleaf parachute in Figure 34 were obtained from Figure 31 using an estimated correction for line drag given in Reference 24. The Parafoil data were obtained from Reference 23. These data were used since they were available and since the low aspect ratio should render this design structurally acceptable for personnel applications.

Based on Figures 32, 33, and 34, the Parafoil configuration has a definite advantage over the other two configurations in that the Parafoil develops positive lift over a wide angle of attack range without luffing, collapse, or pitch instability. In this respect, the Parafoil has an advantage over the parawings, since these configurations also are limited in their operational angle-of-attack range.

(3) Control and Maneuverability

By using either control flap or deflection of the canopy itself, the three gliding parachutes can be controlled. In all cases, control lines are used to activate the control surfaces.

SECTION II - CONCEPT ANALYSIS

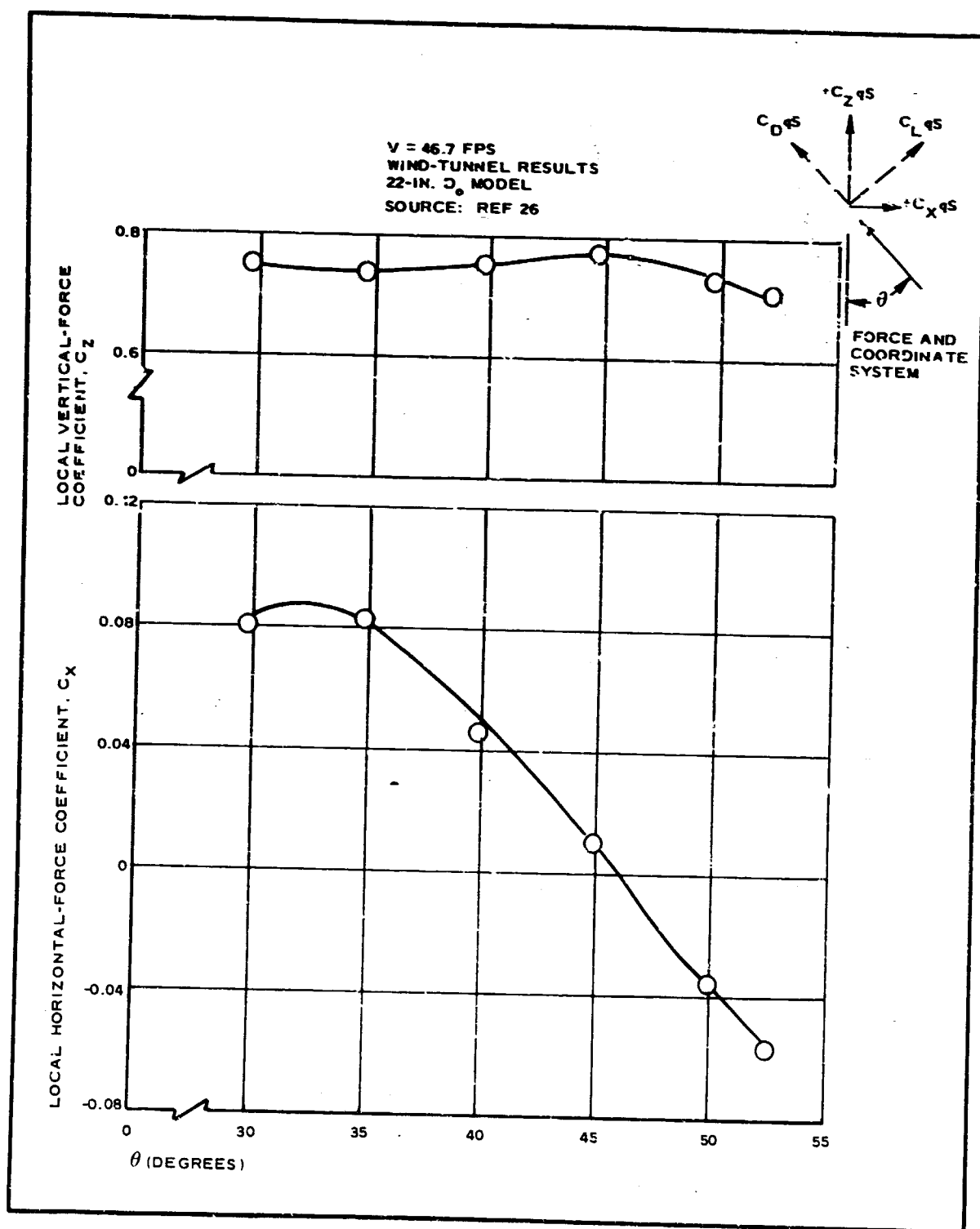


Figure 30 - Normal and Tangent Force Coefficients for Parasail Test Configuration

SECTION II - CONCEPT ANALYSIS

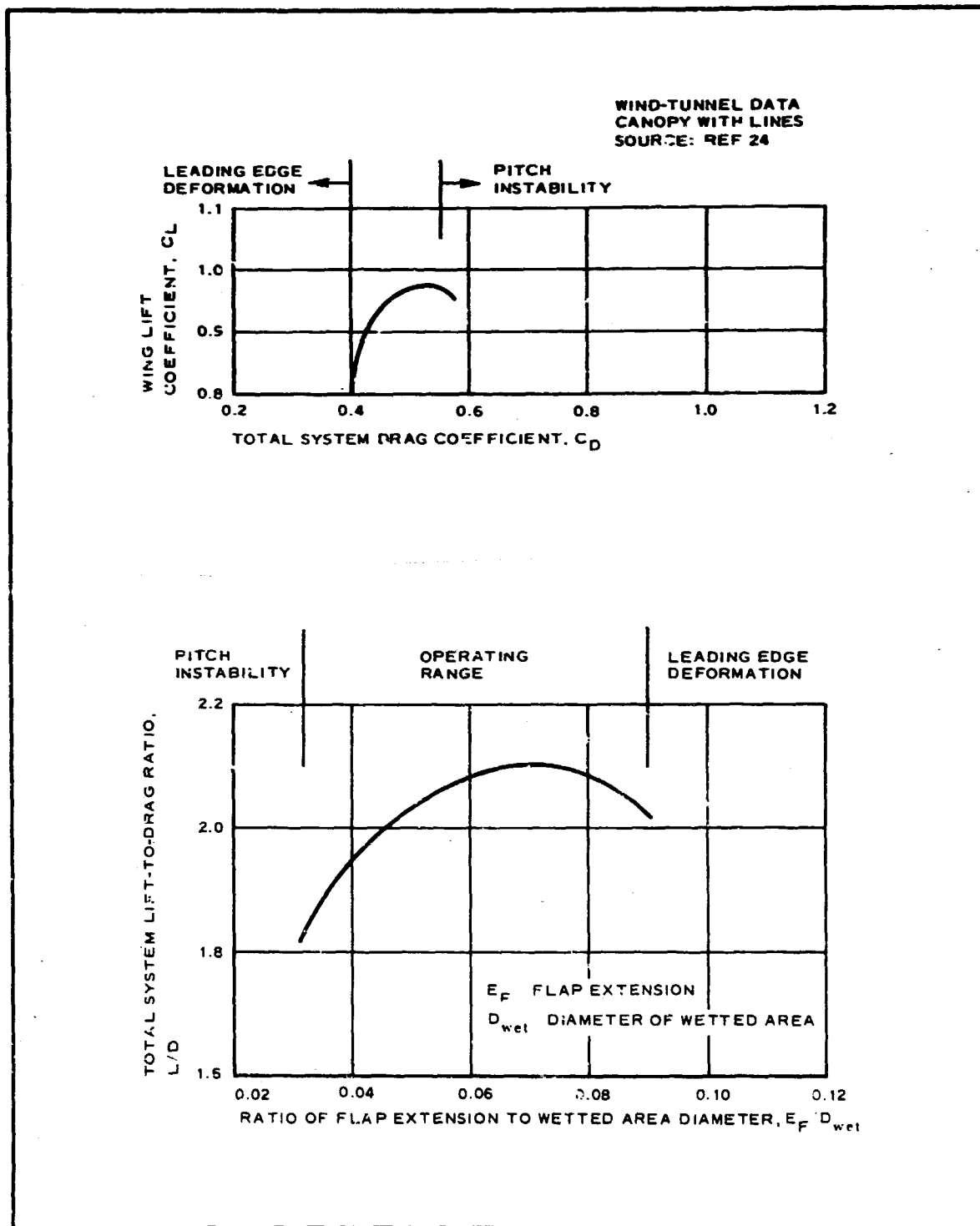


Figure 31 - Aerodynamic Characteristics of Cloverleaf Parachute

SECTION II - CONCEPT ANALYSIS

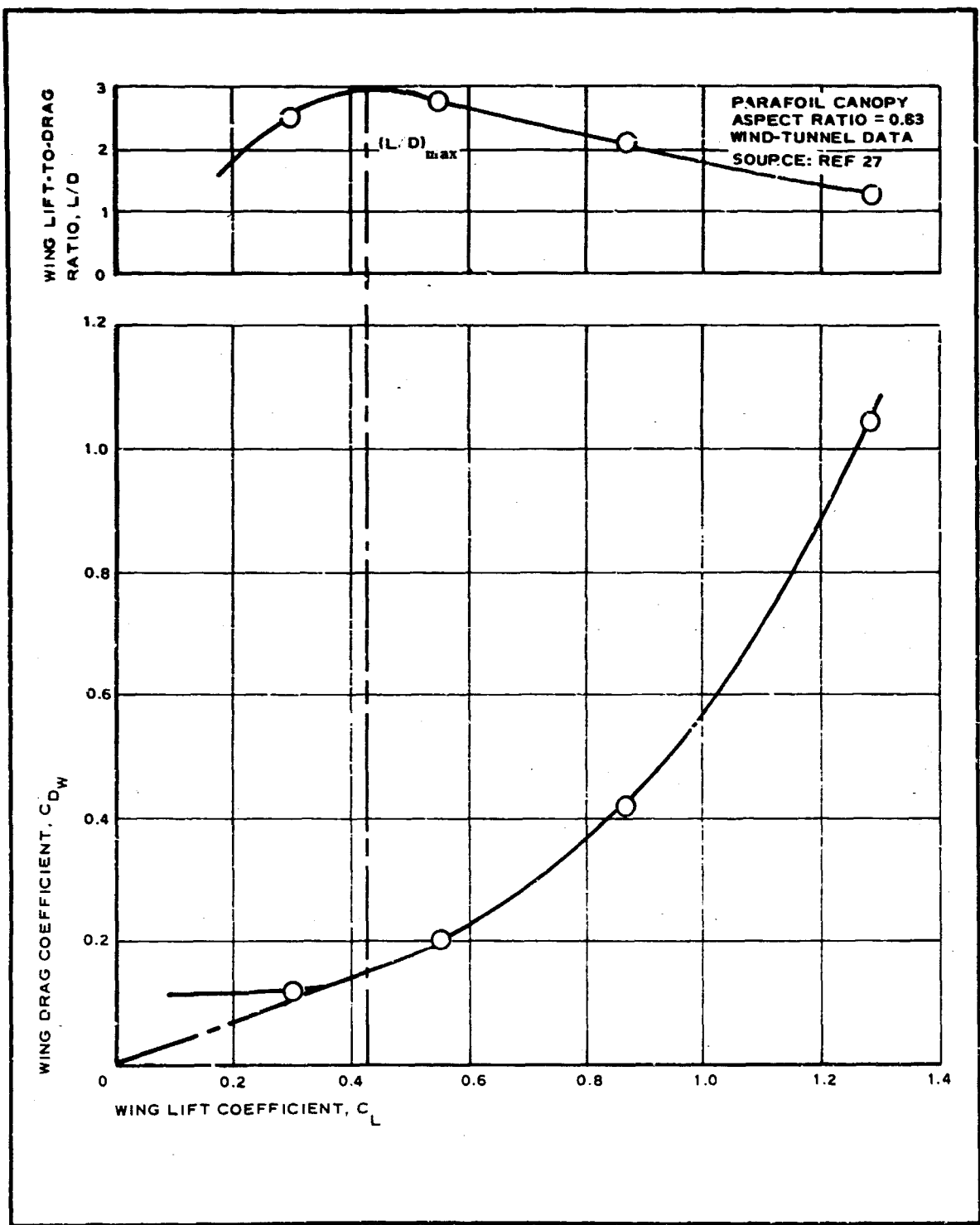


Figure 32 - Aerodynamic Characteristics of Wing-Alone Configuration

SECTION II - CONCEPT ANALYSIS

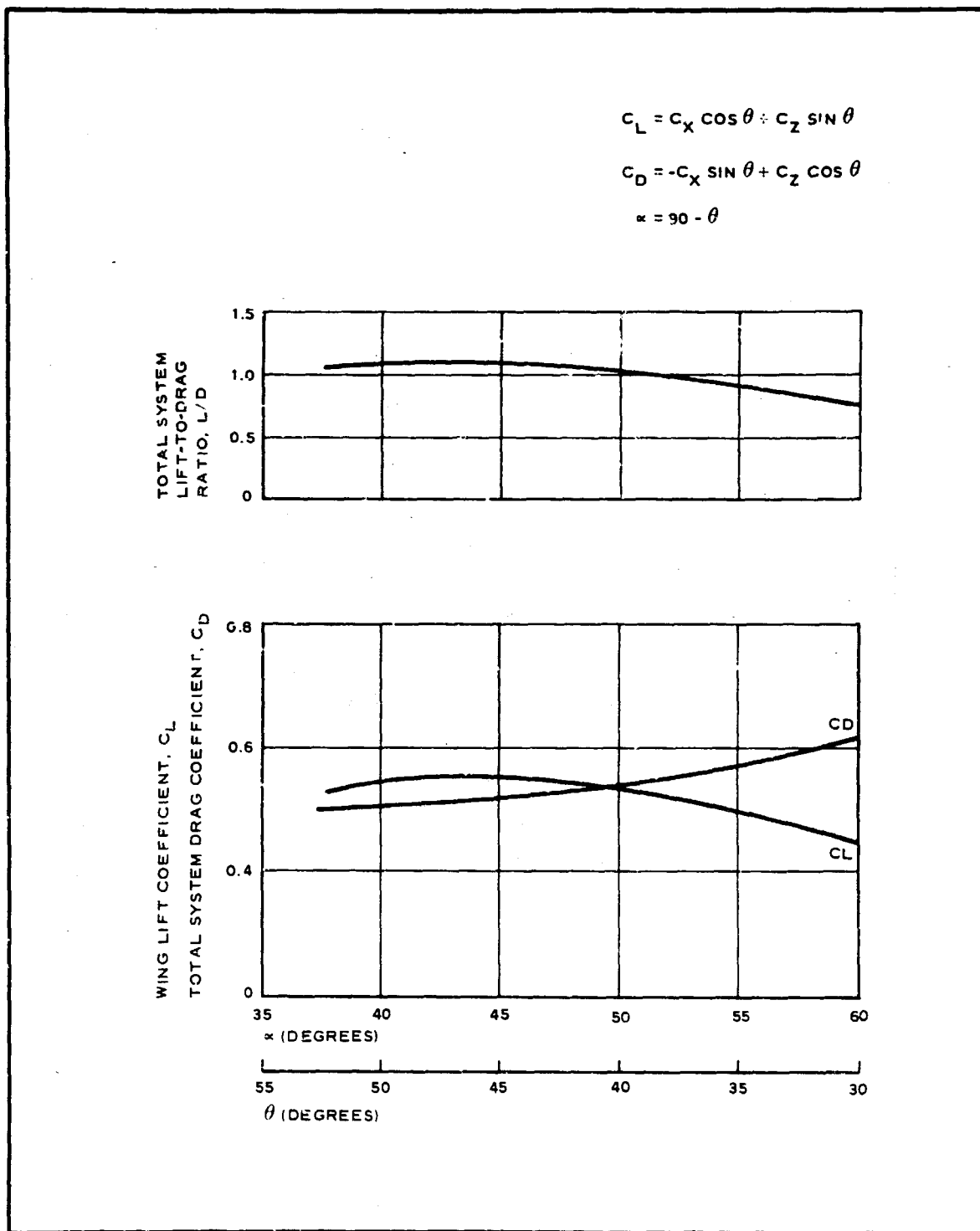


Figure 33 - Aerodynamic Characteristics of Parasail Canopy

SECTION II - CONCEPT ANALYSIS

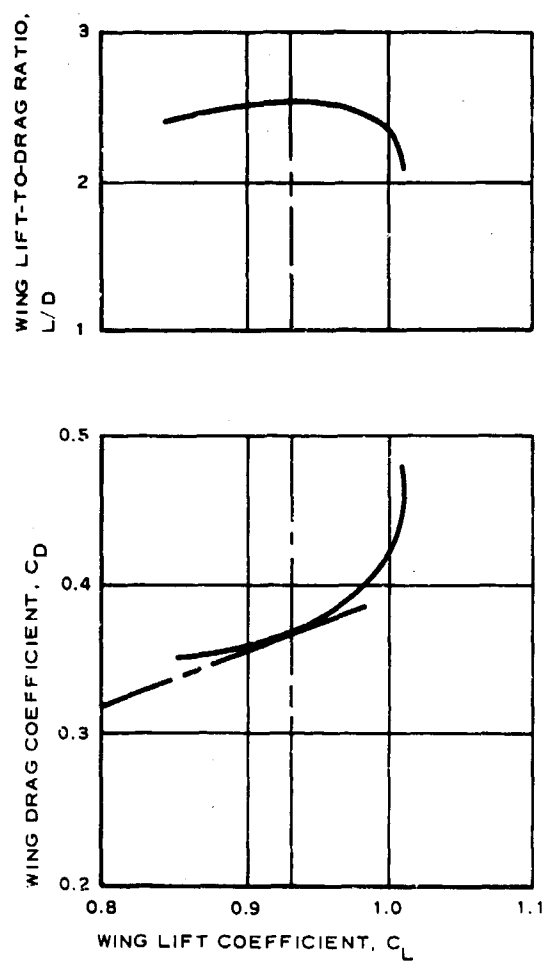


Figure 34 - Aerodynamic Characteristics of Cloverleaf Parachute
(Canopy Alone) without Lines

SECTION II - CONCEPT ANALYSIS

The Parafoil is controlled by using two lines attached at the aft end of the canopy at outboard stations along the span. By pulling a line toward the payload, lift on the deflected panel is spoiled and form drag on the panel is increased. The result is a yaw and rolling moment in the direction of the deflected panel. Pulling on both lines at once results in a loss of L/D and an aft pitching rotation.

Turn slots located on the side of the Parasail canopy are used to create a yawing moment and thereby provide a means of maneuverability and control as well as L/D modulation. Control flaps located at the slots can be differentially opened, closed, or fully inverted to modulate the turn rate. The simultaneous and equal operation of the flaps is used for L/D modulation.

Control of the Cloverleaf also is achieved by differentially operating the control flaps located on its trailing edge. These flaps are extended or retracted by control lines leading to the payload. The differential operation of the two flaps results in drag reduction on the extended side and drag increase on the retracted side. The result is a turning torque, which tends to roll the system toward the retracted side.

(4) Stability

Qualitative stability data for the three gliding parachute designs generally are unavailable. Results of wind-tunnel and free-flight tests, however, indicate all three to be basically stable configurations capable of being rigged for trim at positive lift coefficients.

Lateral-directional stability of the Parafoil is aided by a series of triangular-shaped fabric panels called flares, which are fastened to the canopy along the chord at every other air cell juncture. These panels also connect the suspension lines to the canopy.

Two diametrically opposite stabilizer panels are used on the Parasail to improve its performance. The panels constitute approximately four percent of the total canopy area. Canopy oscillations with the Parasail have been demonstrated as low as ± 3 deg with a 70-ft diameter canopy under a canopy loading of approximately 1.24.

(5) Estimated System Weight

Weights of the three candidate gliding parachutes will be determined to develop weight equations for parawings (see Item 4b, above). Using the same approach it can be shown that, for a given composite system weight, the weight of each gliding parachute can be expressed by

$$W_{\text{tot}} = C_5 S^{1/2}, \quad (34)$$

SECTION II - CONCEPT ANALYSIS

where W_{tot} is the total decelerator weight, C_5 is an appropriate constant, and S is the corresponding reference area. As in Item 4b, above, known parameter values will be used to determine the appropriate values of the constant C_5 . Unfortunately, insufficient data are available for the Parafoil canopy to permit comparison of its weight-size relationship to that relationship of other systems. The following weight analysis is limited to the Parasail and Cloverleaf configurations. The Parafoil weight will be discussed briefly at the end of this section.

Based on References 25 and 27, the following relevant parameter values for the Parasail and Cloverleaf are available:

Parasail canopy:

1. Canopy weight - 160 lb
2. Canopy diameter - 70-ft D_o
3. Canopy reference area - 3850 sq ft
4. Maximum design load - 16,000 lb
5. Safety factor - 1.5

Cloverleaf canopy:

1. Canopy weight - 168 lb
2. Canopy diameter - 56-ft D_{wet}
3. Canopy reference area - 2460 sq ft
4. Maximum design load - 16,000 lb^a
5. Safety factor - 1.5^a

The first step is to determine the theoretical weight requirements for structural integrity with the above configuration sizes under a maximum loading of 2400 lb. An 8-G load limit is assumed, and a safety factor of 2 is used. The calculations are:

$$W = (160) \left(\frac{2400}{16,000} \right) \left(\frac{2}{1.5} \right) = 32 \text{ lb}$$

and

^a Actual values are unknown; however, they are assumed the same as the corresponding values of the Parasail, since both configurations are being tested concurrently and compared for the same application.

SECTION II - CONCEPT ANALYSIS

$$W = (168) \left(\frac{2400}{16,000} \right) \left(\frac{2}{1.5} \right) = 33.6 \text{ lb} \quad (35)$$

The constant, C_5 , for each configuration now can be obtained by dividing the adjusted weight by $(S)^{1/2}$. Therefore, for the Parasail canopy:

$$W = C_5(S)^{1/2} \quad (36)$$

or

$$C_5 = \frac{32}{(3850)^{1/2}} = 0.516. \quad (36)$$

For the Cloverleaf canopy:

$$W = C_5(S)^{1/2}$$

or

$$C_5 = \frac{33.6}{(2460)^{1/2}} = 0.677. \quad (37)$$

Thus, the relationship for the two configurations between weight and reference area is expressed by

$$W = (0.516)(S)^{1/2} \quad (38)$$

for the Parasail canopy and for the Cloverleaf canopy:

$$W = (0.677)(S)^{1/2} \quad (39)$$

Figure 35 presents the results of Equations 35 through 39 for the Parasail and the Cloverleaf configurations for the conditions indicated. Figure 35 reflects the change in material weight with size to maintain structural integrity for configurations subjected to the same maximum opening force. For the size range given, considered potentially appropriate for personnel application, the Parasail has an indicated advantage over the Cloverleaf at corresponding sizes. Like the parawings, however, the size of each configuration is determined from landing requirements (see Item 4e, below). In general, the size requirements are not the same for the two configurations.

In discussing the weights of the Parasail and Cloverleaf, a 2.2 oz/sq yd minimum gage fabric will be assumed as a practical minimum. To

SECTION II - CONCEPT ANALYSIS

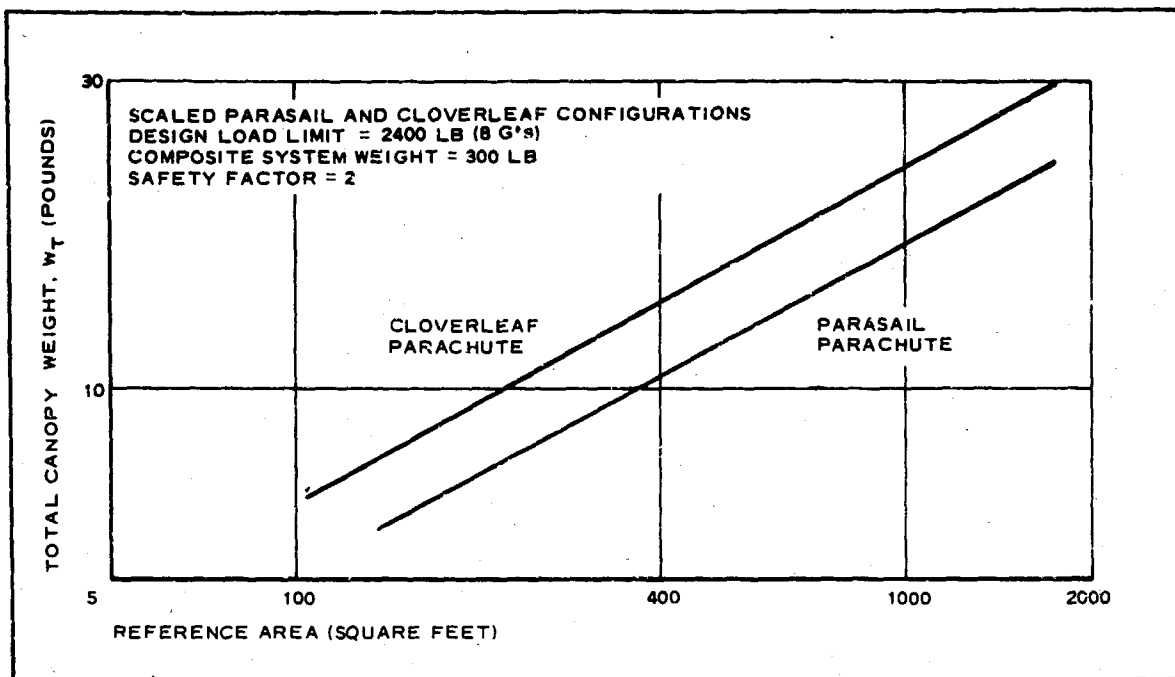


Figure 35 - Estimated Gliding Parachute Weight versus Reference Area

account for the additional weight of the suspension lines, standard personnel parachute lines at 0.0095 lb per running yard will be assumed. Based on References 24 and 27, suspension-line lengths approximately equal to the reference diameter (corresponding to the respective reference areas) are typical. The number of lines as a function of reference diameter, however, is not clearly indicated, and some assumptions are required to define this relationship. Construction details given in Reference 24 of a 16-ft D_{wet} Cloverleaf parachute indicate the configuration to have 61 suspension lines, or approximately 3.8 lines for every foot of reference diameter. This same relationship, for purposes of weight estimation, will be assumed for all configuration sizes. The Cloverleaf configuration apparently would have a comparatively large number of suspension lines due to its particular three-lobed design. For the Parasail, a more conventional parachute relationship will be assumed between the number of lines and the reference diameter due to its more conventional-appearing shape. One line for every foot of reference diameter (D_o) will be assumed. Photographs of specific configurations in Reference 27 also indicate this assumption to be reasonable.

The results of Figure 35 are presented in Figures 36 and 37 for the indicated configuration. Each configuration shows the appropriate plots of

SECTION II - CONCEPT ANALYSIS

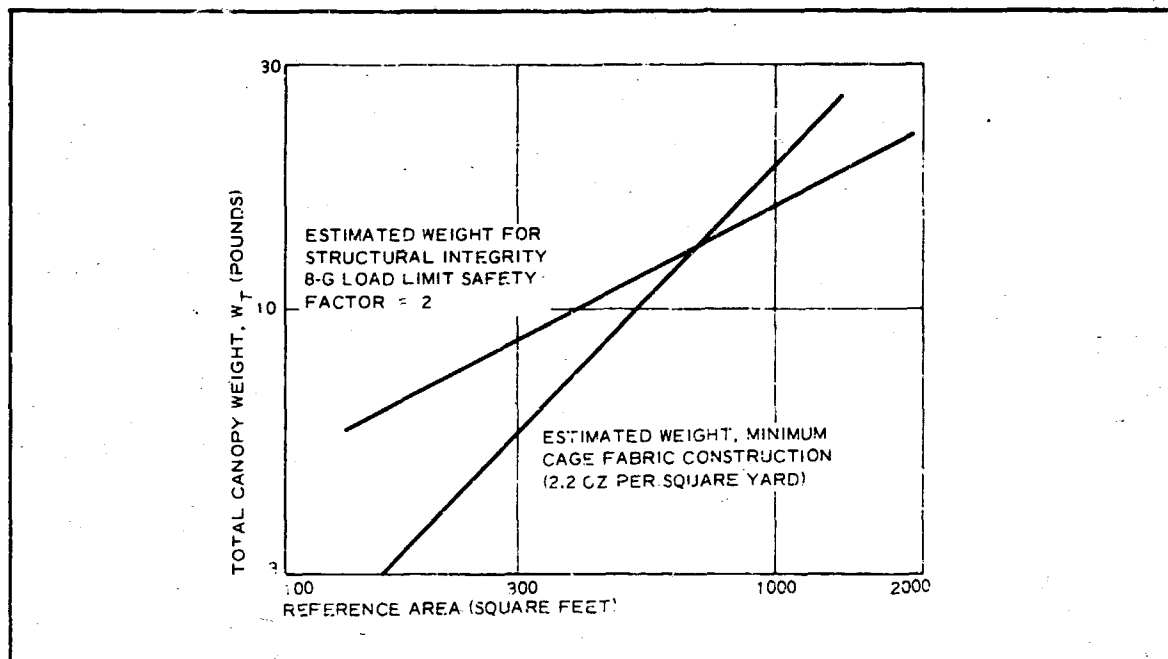


Figure 36 - Estimated Parasail Weight with Suspension Lines versus Nominal Reference Area

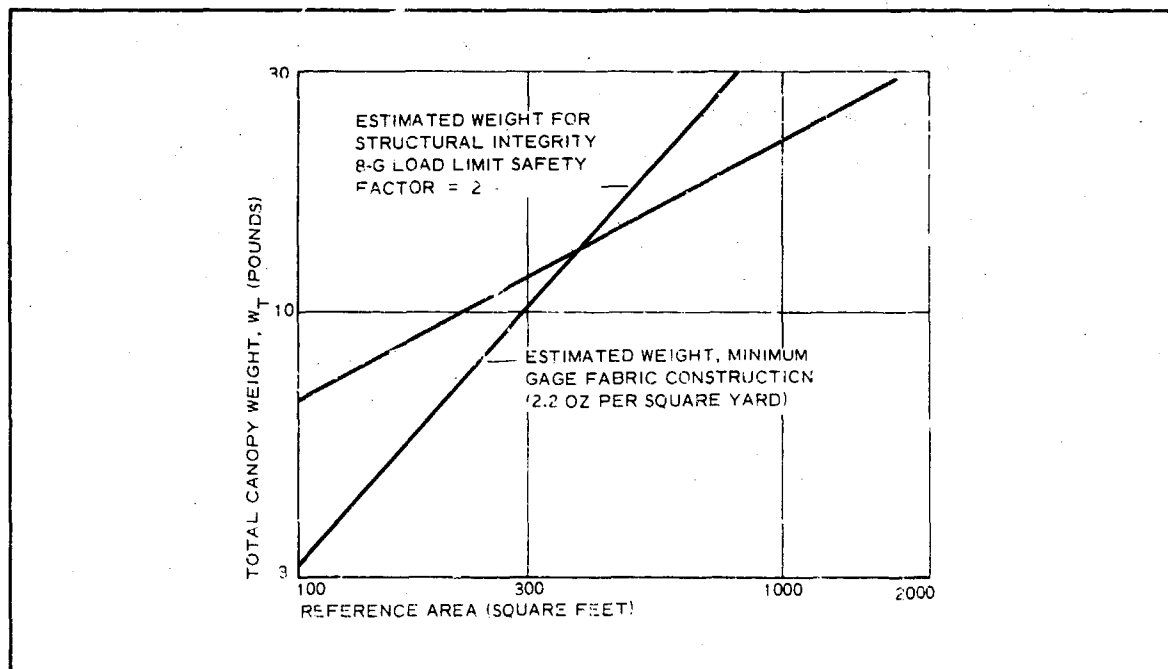


Figure 37 - Estimated Cloverleaf Weight with Suspension Lines versus Reference Wetted Area

SECTION II - CONCEPT ANALYSIS

weight versus reference area based on a 2.2 oz/sq yd minimum gage fabric construction. For the Cloverleaf design, the flat pattern area (neglecting seams and overlap material) is approximately 1.1 times the reference area. Accordingly, an adjustment on the minimum gage fabric weight has been made.

The intercept between the two plots on both Figures 36 and 37 occurs at reference areas significantly smaller than the corresponding points on the limp parawing plot (see Figure 28). For the Cloverleaf configuration, this can be attributed mostly to the rather large contribution of the suspension line weight (due to the comparatively large number of lines) included in the minimum gage fabric weight plot. If not required to maintain an adequate in-flight shape, many of these lines (and much of the resulting weight) presumably could be eliminated while an adequate safety factor is maintained. The low reference area value at which the intercept occurs on the Parasail plot can be attributed to its low weight requirement for structural integrity. This statement suggests that the Parasail is either a more structurally efficient recovery device or is less efficient performance-wise. Item 4e, below, will show that, in general, a comparatively large Parasail is required to effect the required landing velocity.

Insufficient Parafoil data are available for analyzing this configuration similar to the analysis made of the parawings, Parasail, and Cloverleaf. These insufficient data result because little has been given to packing and deployment of the Parafoil. In the parafoil's steady-state configuration, weight and size data are available on a limited basis, but they are given typically without clearly indicating the maximum design loads or the safety factor used. Table XI gives weight and size data for Parafoil configurations. Values for payload weight and canopy loading in Table XI do not necessarily represent the maximum possible loading situation but merely reflect available test configuration data and results. The Parafoil is a dual-walled structure. Where minimum gage fabric considerations become important, some weight penalty may be involved.

d. Ring Wing Airfoil

(1) Preliminary Design Analysis

Of the seven gliding-type designs considered in this study, the ring wing airfoil is the least well defined and developed. Due to lack of experimental data on the ring wing, development of a configuration will be discussed using available data and semiempirical techniques. The configuration to be developed is assumed supported in the ring shape in-flight by a pressurized torus at the leading edge and several pressurized chordwise ribs.

From Reference 28, the lift of a ring wing airfoil is expressed as

SECTION II - CONCEPT ANALYSIS

TABLE XI - AVAILABLE WEIGHT AND SIZE DATA FOR
PARAFOIL CONFIGURATIONS

Reference size (sq ft)	Configuration weight (lb)	Payload weight (lb)	Canopy loading (psf)*	Aspect ratio
...	0.25
66.0	5.50	160	2.40	...
39.7	...	10 to 29	0.25 to 0.73	0.74
45.5	...	25 to 30	0.55 to 0.66	0.61
76.3	...	25 to 58	0.33 to 0.76	1.30
90.5	...	30 to 57	0.33 to 0.62	1.89
108.0	...	50 to 100	0.47 to 0.94	0.75
313.0	19.50	42 to 700 ⁺	0.134 to 2.33	0.75

* Does not include canopy weight.

⁺ 700-lb weight broke loose.

$$L = \frac{4b/\pi C}{1 + (4b/\pi C)} (\alpha_{\mathcal{E}} \rho V^2 \pi^2 b C), \quad (40)$$

where $\alpha_{\mathcal{E}}$ is angle of attack, lift is referenced to an elliptical flat plate of span b , area $S = (\pi/2)bC$, and b and C are the ring wing radius and chord, respectively. Thus, the aspect ratio of the ring wing is defined by $AR = 8b/\pi C$ (see Figure 38). The theoretical lift curve slope is defined by

$$C_{L_{\alpha_{\mathcal{E}}}} = 4\pi [AR/(AR + 2)] \quad (41)$$

Experimental results from Horner (see Reference 29) give the lift curve slope as presented in Figure 39. From these data, the estimated induced drag associated with various lift coefficient values can be obtained. The parasite drag of the ring, resulting from both skin friction and leading edge thickness, then must be estimated to obtain a total wing profile drag. For the ring configuration, a leading edge thickness of 10 percent of the chord is considered adequate, when using a pressurized fabric torus structure, due to the high load-carrying capability of a torus. The parasite drag of the wing alone is estimated as follows:

SECTION II - CONCEPT ANALYSIS

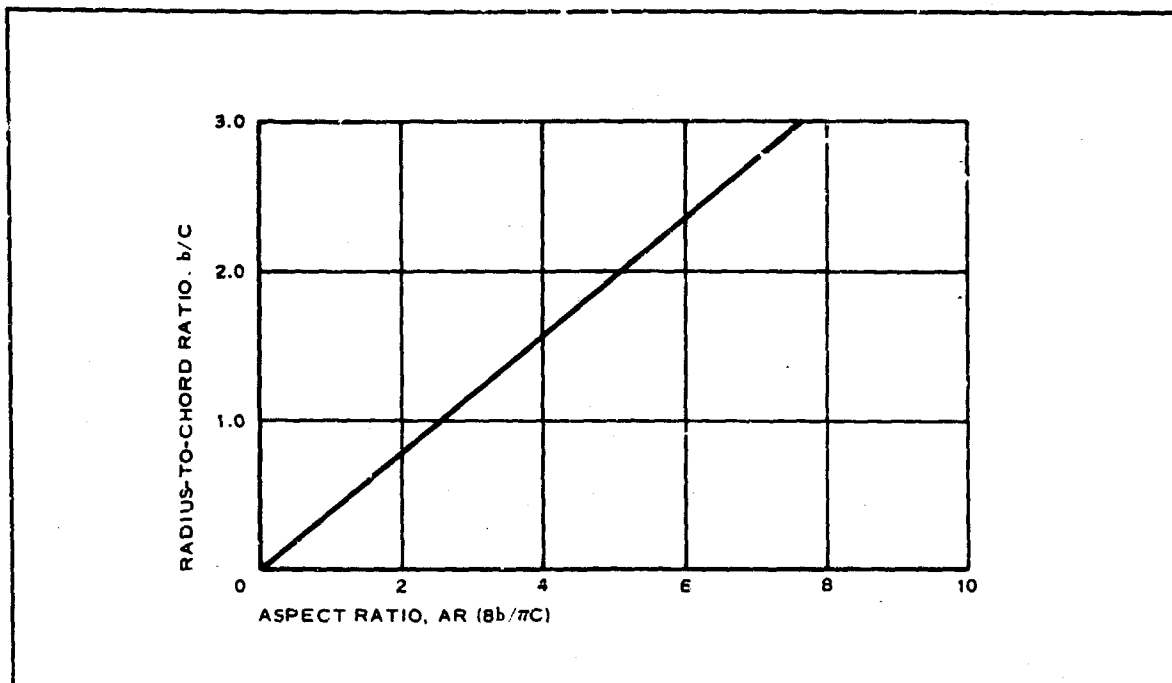


Figure 38 - Radius-to-Chord Ratio versus Aspect Ratio for a Ring Wing Airfoil

$$C_{D_W} = C_f \left(\frac{S_{wet}}{S} \right) + C_t \left(\frac{2\pi b t}{S} \right), \quad (42)$$

where

$$C_f = 0.003 \text{ (turbulent flow),}$$

$$S_{wet} = 8 S,$$

$$C_t = 0.04 \text{ (leading edge assumed faired into trailing cord),}$$

$$t = 0.1 C, \text{ and}$$

$$S = \pi/2 b C$$

Therefore,

$$C_{D_W} = (0.024 + 0.016) = 0.040. \quad (43)$$

SECTION II - CONCEPT ANALYSIS

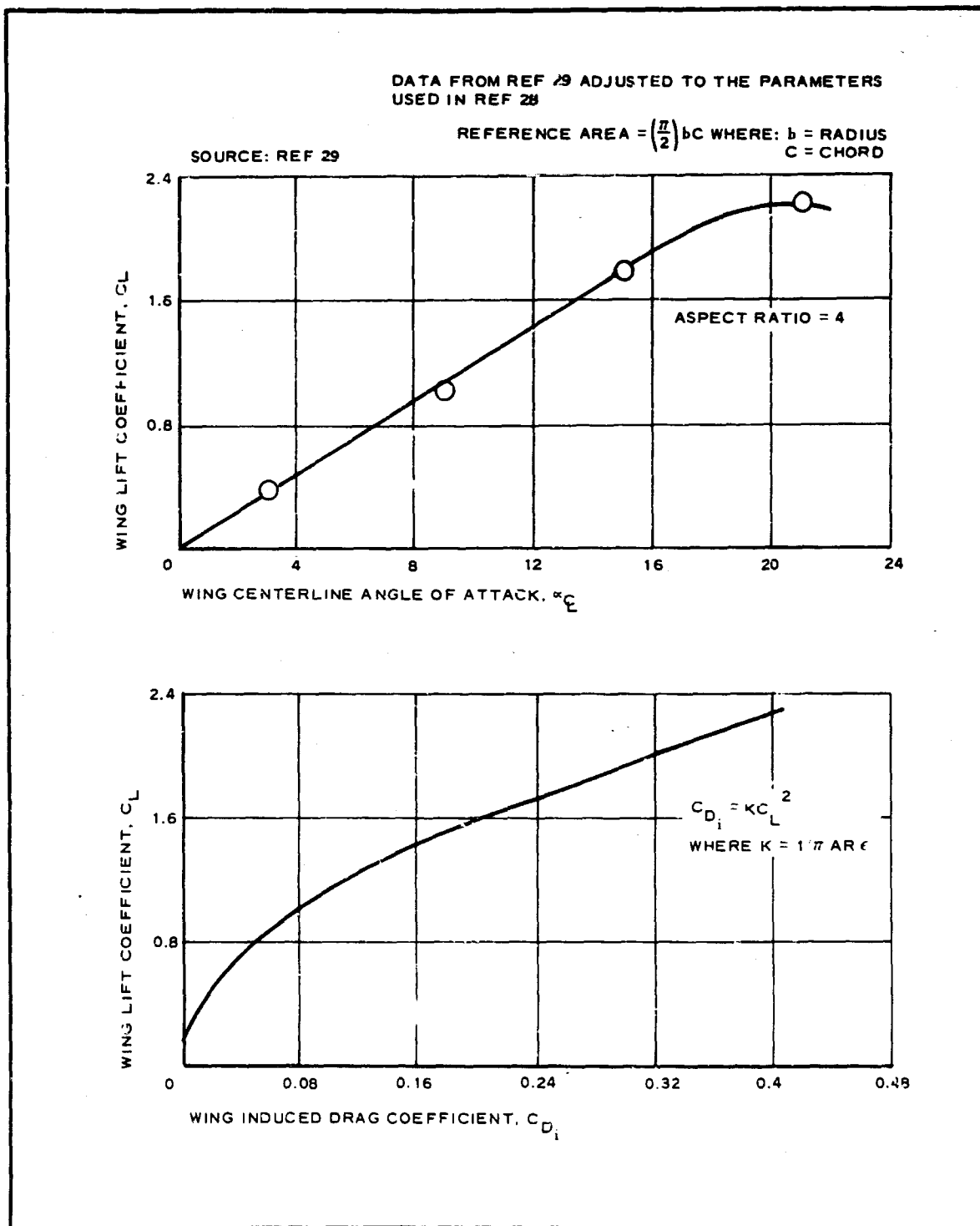


Figure 39 - Aerodynamic Characteristics of a Ring Wing Airfoil

SECTION II - CONCEPT ANALYSIS

Predicted characteristics of the ring-alone configuration now can be determined and are presented in Figure 40.

(2) Alternate Design

An alternate ring wing airfoil design possibility would have only a portion of the leading edge pressurized for wing support (see Figure 41). For this case, a half-torus, closed on the two ends, would be incorporated only into the lower half of the circular leading edge. The normal force generated, leading to collapse on the lower surface, then would be countered by this half torus. The normal force on the upper surface puts the fabric in tension and renders pressurized-tube support unnecessary. The upper surface, then, with proper rigging probably would function in a manner similar to that of the Barish sailing.

(3) Maneuverability and Control

Maneuverability of the ring wing could be achieved by a number of techniques, including extra control surfaces or local deflection of the ring itself. If the latter technique were used, maneuvers would be performed by spoiling the lift and increasing the drag on the deflected portion, in a manner similar to the maneuvers performed with a Parasail.

(4) Stability

The degree of stability that could be achieved with the ring wing airfoil for personnel delivery applications essentially is unknown. One apparent advantage is the definite feasibility of a design incorporating close coupling of the man and the ring. This close coupling could be achieved by attaching the lower portion of the ring to the man's back, with the main portion of the structure extending above his head. Suspension and control lines then would extend from the upper surface to maintain trimmed stable conditions and to enable control. Flow blockage effects on the ring due to the man's shoulders and head would be small, with insignificant effects on the performance characteristics.

(5) Estimated System Weight

No experimental data were found to base weight estimates for the ring wing airfoil. In general, the weight of a ring wing with an internal-source pressurized torus and chordwise ribs would be more than the weight of a conical parawing sized to effect the same delivery velocity. This weight difference is due primarily to the larger enclosed volume that must be inflated, which necessitates a somewhat larger and heavier inflation system. For sizes at which minimum gage fabrics govern the weight, the ring wing with its double-walled structure probably would be considerably heavier. A significant weight reduction undoubtedly could be achieved if the alternate ring wing design was feasible and could be used.

SECTION II - CONCEPT ANALYSIS

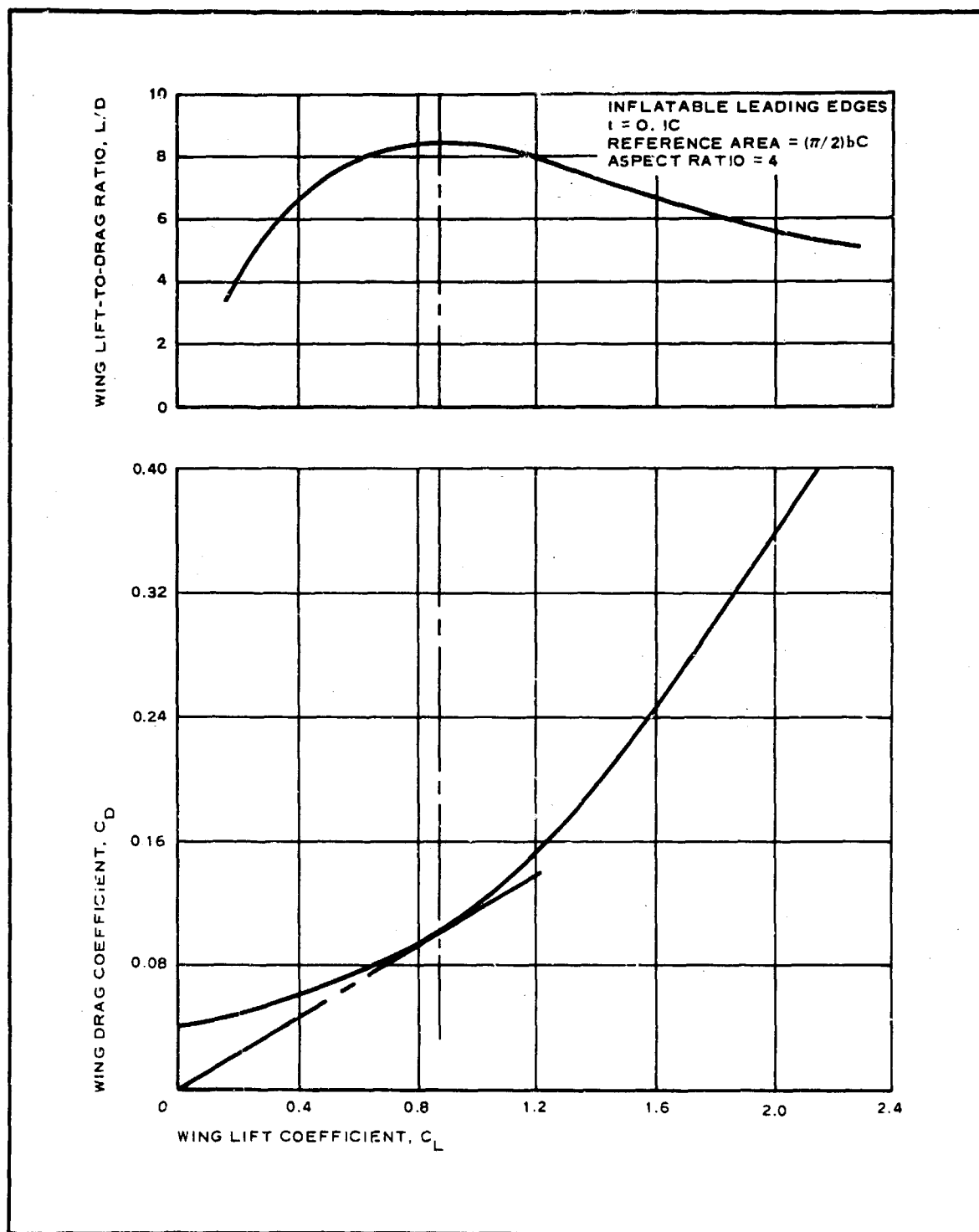


Figure 40 - Aerodynamic Characteristics of Ring Wing Airfoil (Ring Alone)

SECTION II - CONCEPT ANALYSIS

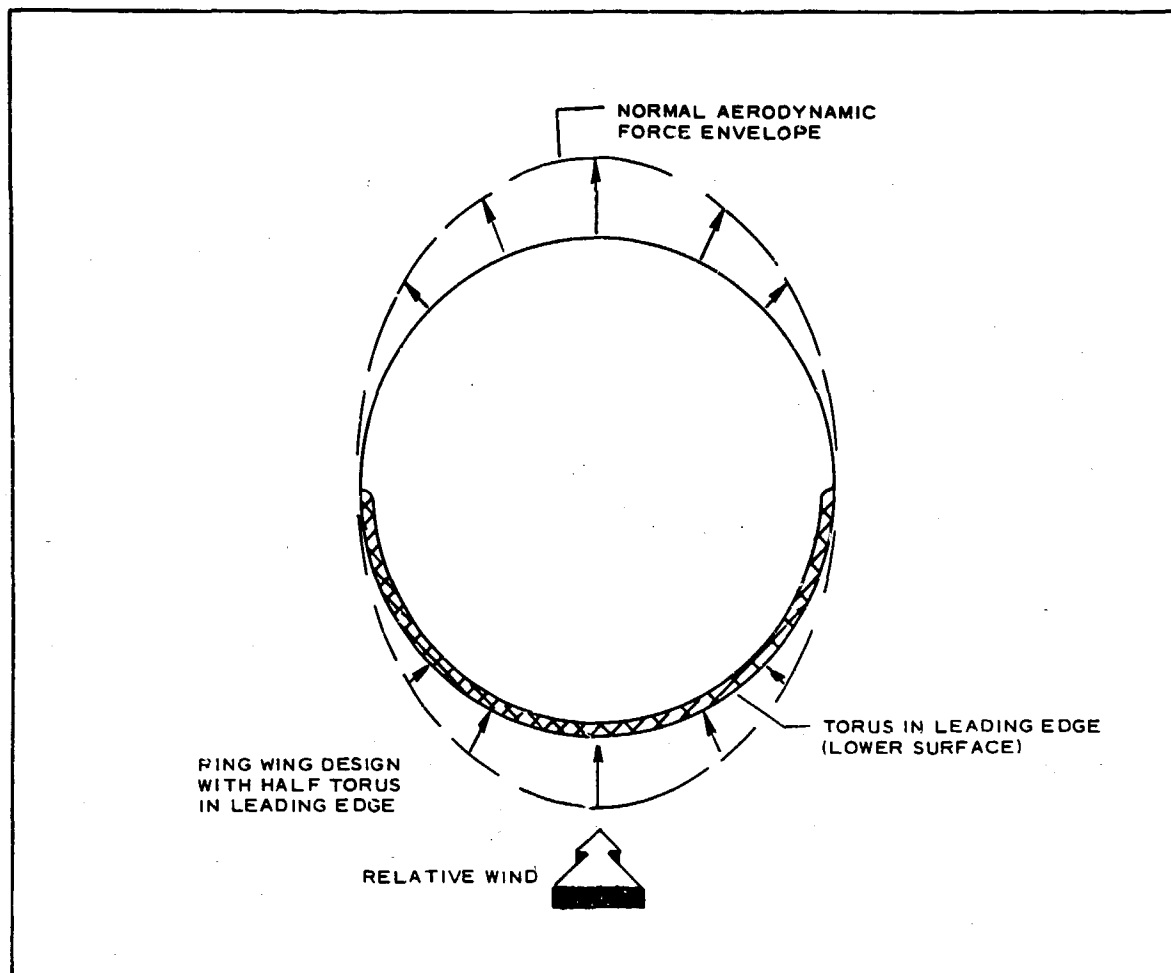


Figure 41 - Alternate Ring Wing Airfoil Design

e. Total System Design and Performance

Typical parachute landing experience has indicated that impact shock loads associated with a descent velocity of about 11 knots and ground winds of between 0 and 12 knots are acceptable for personnel delivery applications. A satisfactory gliding concept design would include comparable landing conditions. This design could be accomplished by sizing the configuration for a flared landing or by sizing and trimming the system for steady-state descent conditions suitable for landing. The former generally provides for a much more efficient structure in size and weight but would require additional manipulation. The dynamic response of a flared gliding configuration substantially reduces the preflare kinetic energy of the composite system and provides for a much more effective decelerator. This statement

SECTION II - CONCEPT ANALYSIS

is particularly true if the preflare C_L is considerably less than the C_L value in flare and if a high preflare total velocity is obtained, which would occur with high wing-loading values.

An indication of this capability is illustrated in Figure 42 for a low aspect ratio conical design. Unfortunately, as indicated in Figure 42, the dynamic response is a transient condition requiring precise and/or coordinated execution for maximum effectiveness and personnel safety. Trade-off then is indicated between size and performance and the effects of human error in judgment and execution. A possible compromise is a system that would limit the impact kinetic energy to a maximum design value, with the configuration operating under equilibrium conditions at a high C_L value (ideally, $C_{L_{max}}$). Thus, the configuration presumably could be

trimmed and operated at $C_{L(D)_{max}}$; landing would be achieved by flaring

to a higher trimmed C_L value, where tolerable landing loads would be experienced even under equilibrium descent conditions. With this approach, gliding systems can be sized for landing at any kinetic energy level within the constraints of allowable landing velocities for personnel parachute systems. This sizing is achieved using only static performance coefficients as given in the following analysis:

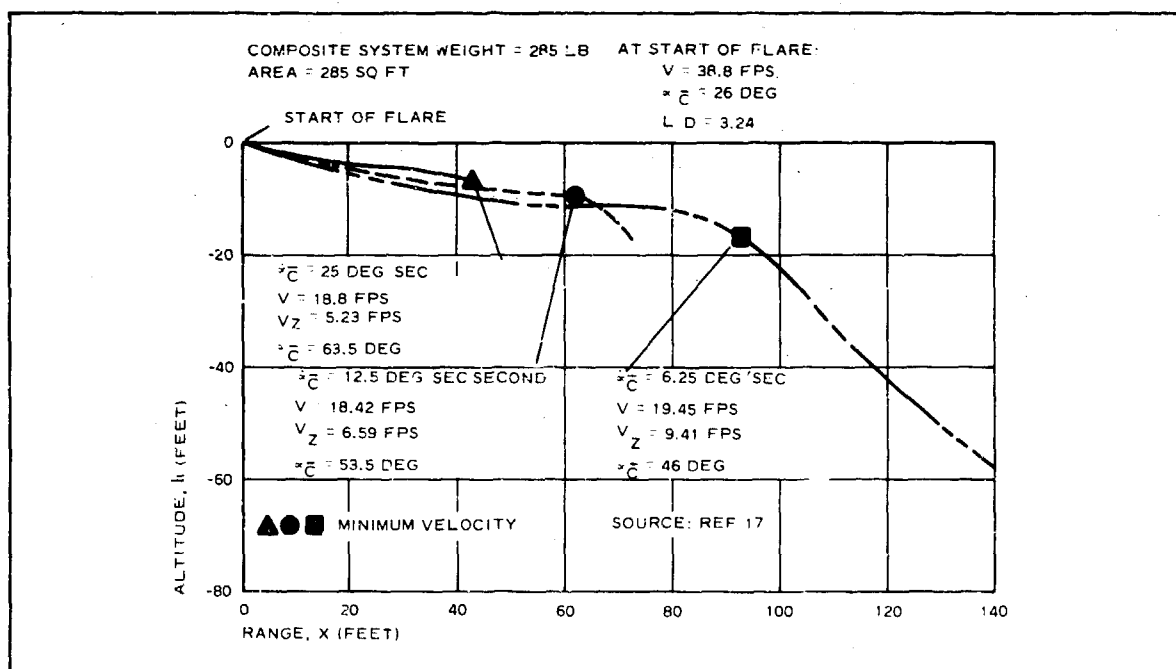
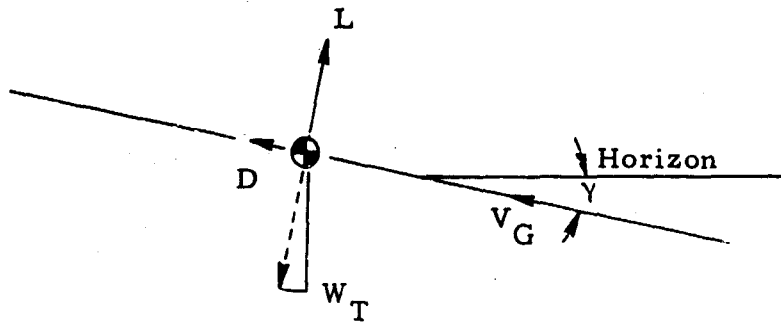


Figure 42 - Computed Paraglider Flare Trajectories

SECTION II - CONCEPT ANALYSIS



At equilibrium,

$$L = W_T \cos \gamma$$

$$V_Z = V \sin \gamma$$

$$L/D = \cot \gamma$$

$$D = W_T \sin \gamma$$

$$V_H = V \cos \gamma$$

$$\gamma = \cot^{-1} (L/D)$$

Therefore,

$$D = W \sin \gamma = C_D S \frac{\rho}{2} V^2 . \quad (44)$$

Solving for $C_D S$,

$$C_D S = W_T \sin \gamma / (\rho/2) V^2$$

or

$$S = \frac{W}{(\rho/2) V^2} \left(\frac{\sin \gamma}{C_D} \right) . \quad (45)$$

An example of this technique for each gliding configuration will be provided using the following parameters:

1. Composite system weight - 300 lb

SECTION II - CONCEPT ANALYSIS

2. Landing altitude (ground level) - 5000 ft
3. Design total landing velocity - 19 fps
4. Landing C_L value = $C_{L_{\max}}$ (of each gliding system)
5. Parasite drag area of man and suspension lines, $(C_D S)_P$ - 12 sq ft

With appropriate substitutions, the above equation reduces to

$$S = 812 \left(\frac{\sin \gamma}{C_D} \right) C_L = C_{L_{\max}} \quad (46)$$

Equation 46 cannot be directly solved now, since the contribution to C_D of the man and to the suspension lines (C_{D_P}) depends on the reference area, S . An iterative process can be applied to solve the equation, however, by first selecting some approximate value for S and then evaluating the right-hand side to obtain a new approximation. This process is continued using each successive approximation until sufficient agreement is obtained between the final two approximations. The required sizes were obtained and are presented in Table XII. Table XII also presents similar results for different landing velocities and landing altitudes.

TABLE XII - ESTIMATED REFERENCE AREA REQUIREMENTS FOR TWO LANDING VELOCITIES AT TWO GROUND-LEVEL ALTITUDES

Concept	Reference area (sq ft)			
	Ground level = 5000 ft		Ground level = sea level	
	V = 19 fps	V = 22 fps	V = 19 fps	V = 22 fps
Conical parawing	656	490	574	421
Cylindrical parawing	655	490	573	421
Limp parawing	684	513	588	442
Parafoil	496	370	426	318
Parasail	1060	790	912	680
Cloverleaf	765	570	660	490
Ring wing airfoil	394	292	339	251

Notes:

1. Main and suspension-line drag area = 12 ft
2. Composite system weight = 300 lb
3. $C_L = C_{L_{\max}}$ (of each gliding system)

SECTION II - CONCEPT ANALYSIS

Figure 43 gives the component velocities at landing for each configuration. Table XIII summarizes the descent and landing performance results. For the Parasail and Cloverleaf configurations, no apparent significant advantage is realized for a flare maneuver for the assumed conditions.

The flare requirement can be eliminated if the system is sized for descent and landing at the same L/D value. Table XIV lists approximate size requirements for landing at $(L/D)_{\max}$ with a 19-fps total velocity for assumed ground levels of zero and 5000 ft. The appropriate equation is

$$S = 812 \left(\frac{\sin \gamma}{C_{D_T}} \right) C_L \left[C_L \text{ at } (L/D)_{\max} \right] \quad (47)$$

For this situation, the exact reference area is more difficult to obtain since, in general, an effective change in C_{D_P} (and thus in C_D) also results in a change in C_L from the wing-alone value to maintain $(L/D)_{\max}$. Consequently, Table XIV neglects the contribution of $(C_D S)_P$. Since the error obtained is less than 5 percent due primarily to the comparatively large areas involved, these values are considered satisfactory.

Table XV summarizes the descent and landing performance results for configurations sized to effect landing at $(L/D)_{\max}$.

In the preceding analysis, a man and the suspension-line drag area, $(C_D S)_P$, of 12 sq ft were assumed and applied to obtain the results given in Tables XII through XV. The 12 sq ft assumed that both the man and the suspension lines each contributed approximately 6 sq ft of profile drag area. For the suspension lines, this number provides for a total length of approximately 480 ft, assuming the $(C_D S)_l$ of each suspension line to be 0.0125 sq ft per foot of length and their nominal diameter to be 1/8 in. As suggested in Items 4b and 4c, above, total line requirement for each system would not, in general, be equal. Table XVI indicates the effects of a variable amount of total suspension line on $(L/D)_{\max}$ using the largest reference areas given in Table XIV. The largest $(C_D S)_P$ value of 16 sq ft corresponds to a total line length of about 800 ft using the above criteria.

Figures 44 through 48 plot the variation in lift coefficient with angle of attack for those configurations for which this information has not been presented.

SECTION II - CONCEPT ANALYSIS

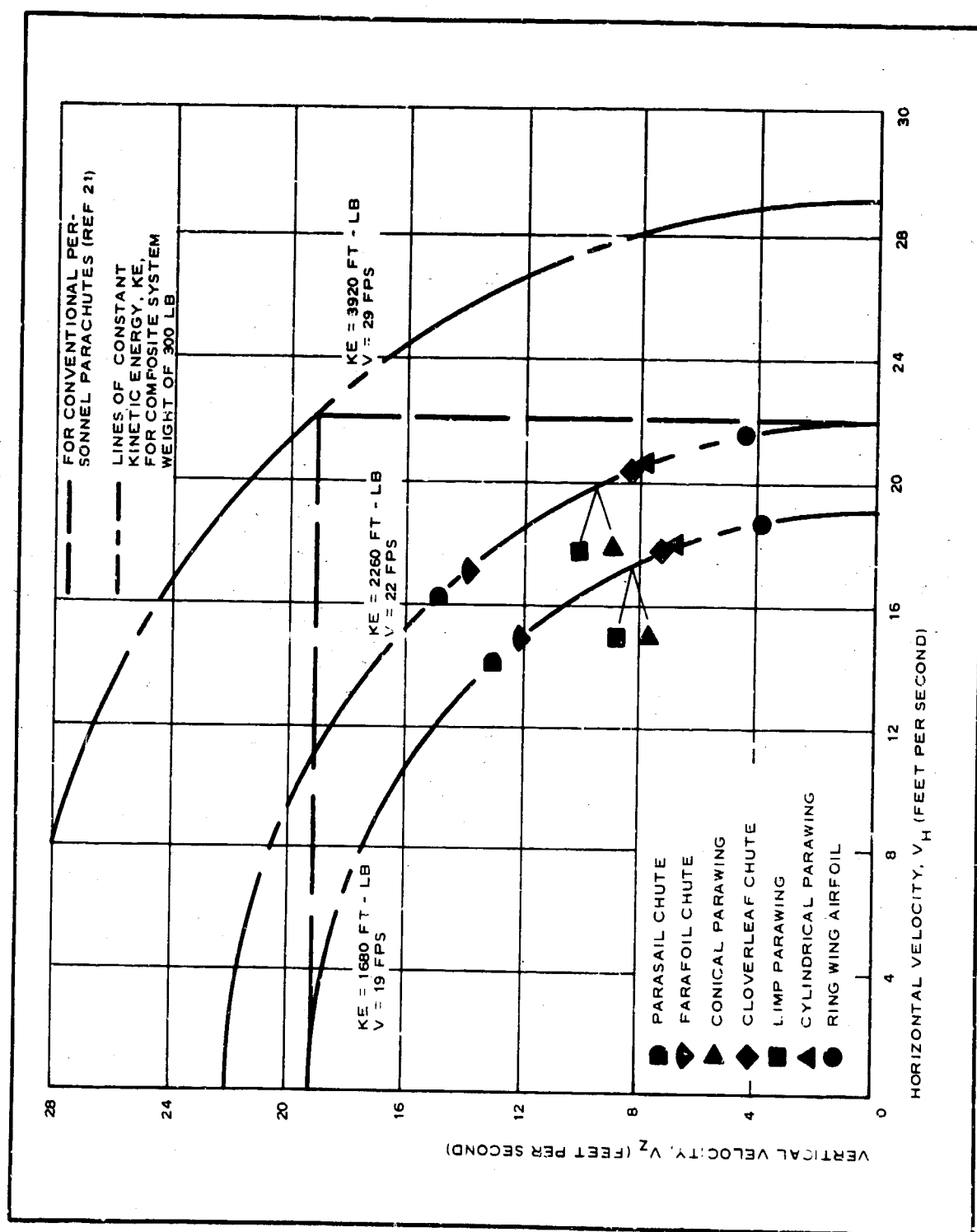


Figure 43 - Allowable Landing Velocities

SECTION II - CONCEPT ANALYSIS

TABLE XIII - PARAMETER VALUES FOR DESCENT AND LANDING WITH

$$C_L \text{ AT LANDING} = C_{L \text{ MAX}}$$

Configuration	Reference area (sq ft) ^a	(L/D) _{max} ^b	Total velocity (fps)	Vertical velocity (fps)	Horizontal velocity (fps)	(L/D) _{C_Lmax}	Total velocity (fps) at C _L max	Canopy loading (psi) ^c
Conical parawing	574 (656)	3.7	28.8	7.55	27.5	2.01	19	0.458
Cylindrical parawing	573 (655)	...	28.8	4.06	28.6	2.62	19	0.458
Limp parawing	588 (634)	2.8	26.5	8.9	25.0	2.02	19	0.439
Parafoil	426 (496)	2.0	36.3	13.0	33.9	1.21	19	0.605
Parasail	912 (1060)	1.96	19.0	13.0	13.6	1.96	19	0.283
Cloverleaf	660 (765)	2.4	19.6	7.53	18.1	2.40	19	0.302
Ring wing airfoil	339 (394)	6.7	28.0	4.06	27.2	4.80	19	0.162
Extended-skirt parachute	960 (1060)	0	19.0	19.0	0	0	19	0.278

^a Sized for landing at sea level (sized for landing at 5000 ft).

^b Composite value assuming drag area of suspended payload = 12 sq ft.

^c Composite system weight = 300 lb.

TABLE XIV - ESTIMATED REFERENCE AREA REQUIREMENTS

FOR A 19-FPS TOTAL LANDING VELOCITY AT TWO

GROUND-LEVEL ALTITUDES

Concept	Reference area (sq ft)	
	Ground level = 5000 ft	Ground level = sea level
Conical parawing	1575	1360
Cylindrical parawing	1420	1220
Limp parawing	1120	965
Parafoil	1770	1525
Parasail	1060	915
Cloverleaf	780	670
Ring wing airfoil	860	740

Notes:

1. Man and suspension-line drag area = 12 sq ft
2. Composite system weight = 300 lb
3. $C_L = C_{L \text{ at } (L/D)_{\text{max}}}$ (for each gliding system)

SECTION II - CONCEPT ANALYSIS

TABLE XV - PARAMETER VALUES FOR VARIOUS SYSTEM LANDINGS WITHOUT

FLARE AT $(L/D)_{MAX}$

Configuration	Reference area (sq ft) *	$(L/D)_{max}$ +	Total velocity (fps)	Vertical velocity (fps)	Horizontal velocity (fps)	Canopy load- ing (psf) †	Aspect ratio
Conical parawing	1360 (1575)	4.0	19	4.6	18.4	0.183	2.2
Cylindrical para- wing	1220 (1420)	8.0	19	2.36	18.8	0.180	5.46
Limp parawing	965 (1120)	2.8	19	6.4	17.8	0.254	2.9
Parafoil	1525 (1770)	2.8	19	6.4	17.8	0.160	0.83
Parasail	915 (1060)	1.06	19	13.0	13.8	0.283	1.27
Cloverleaf	670 (780)	2.4	19	7.3	17.5	0.355	1.85
Ring wing airfoil	740 (860)	7.8	19	2.4	18.7	0.322	4.0
Extended-skirt parachute	960 (1080)	0	19	19.0	0	0.278	1.27

* Sized for landing at sea level (sized for landing at 5000 ft).

† Composite value assuming drag area of suspended payload = 12 sq ft).

‡ Composite system weight = 300 lb.

TABLE XVI - EFFECTS OF ATTACHED PAYLOAD

PARASITE DRAG AREA,

$(C_D S)_P \text{ ON } (L/D)_{MAX}$

Payload drag area ($C_D S)_P$ (sq ft)	Gliding system concepts											
	Conical parawing ($S = 656$ sq ft)		Cylindrical parawing ($S = 655$ sq ft)		Limp parawing ($S = 684$ sq ft)		Parafoil ($S = 496$ sq ft)		Parasail ($S = 1860$ sq ft)		Cloverleaf ($S = 765$ sq ft)	
	ΔC_D	$(L/D)_{max}$	ΔC_D	$(L/D)_{max}$	ΔC_D	$(L/D)_{max}$	ΔC_D	$(L/D)_{max}$	ΔC_D	$(L/D)_{max}$	ΔC_D	$(L/D)_{max}$
0	...	4.2	...	9.5	...	3.0	...	3.0	...	1.06	...	2.5
8	0.0122	3.7	0.0122	7.6	0.0117	2.9	0.0161	2.8	0.0075	1.06	0.0104	2.5
16	0.0244	3.4	0.0244	6.7	0.0234	2.8	0.0322	2.7	0.0150	1.06	0.0208	2.4

Note:

$\Delta C_D = (C_D S)_P / S$

SECTION II - CONCEPT ANALYSIS

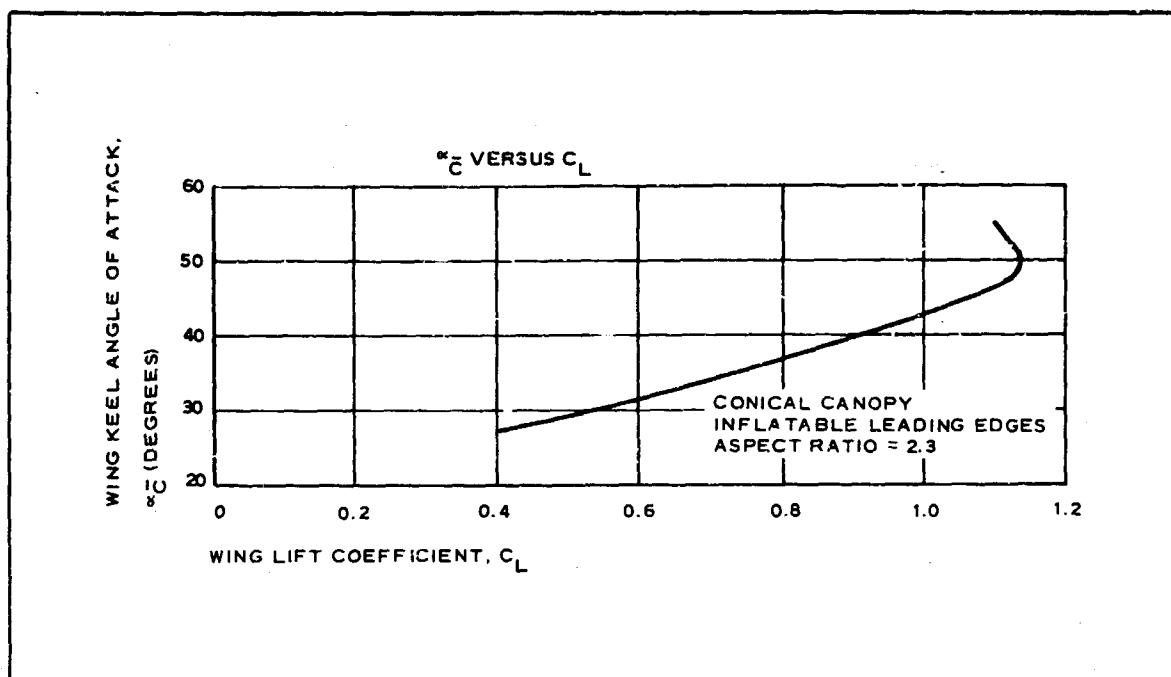


Figure 44 - Angle of Attack versus Lift Coefficient (Conical Parawing)

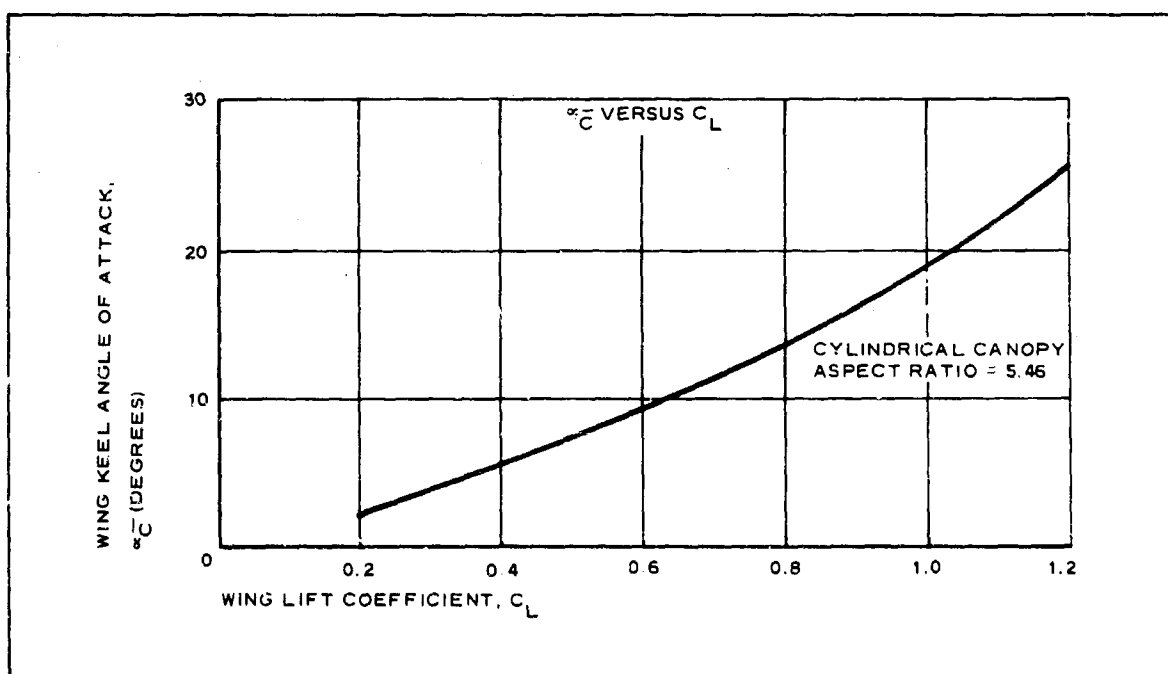


Figure 45 - Angle of Attack versus Lift Coefficient (Cylindrical Parawing)

SECTION II - CONCEPT ANALYSIS

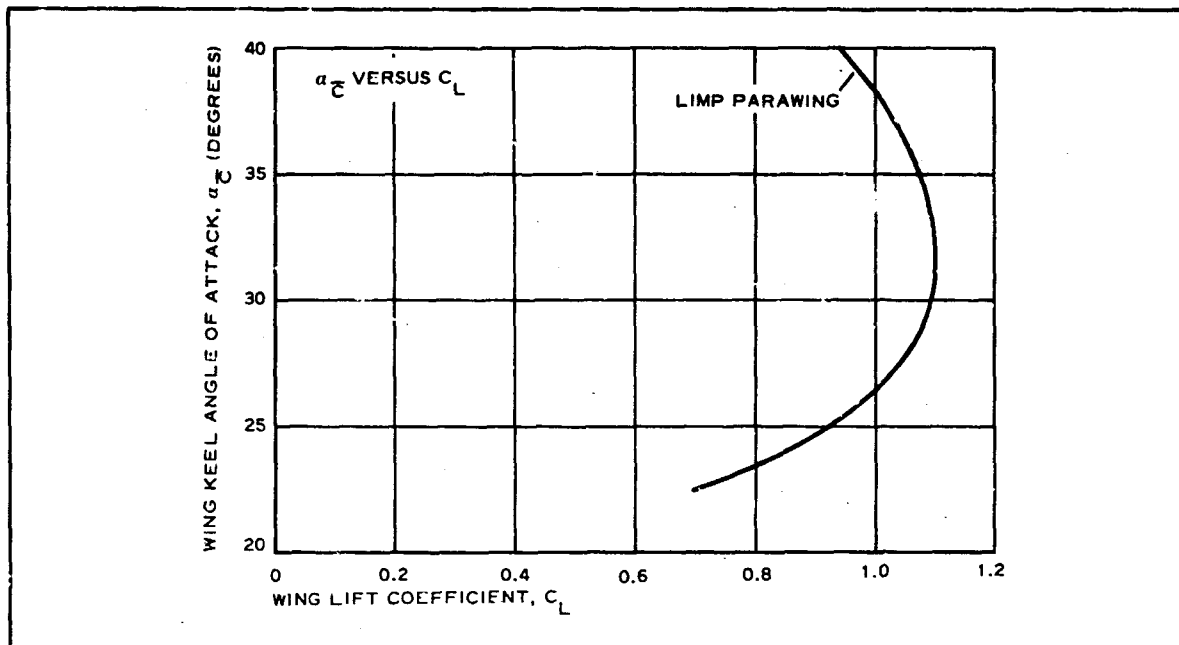


Figure 46 - Angle of Attack versus Lift Coefficient (Limp Parawing)

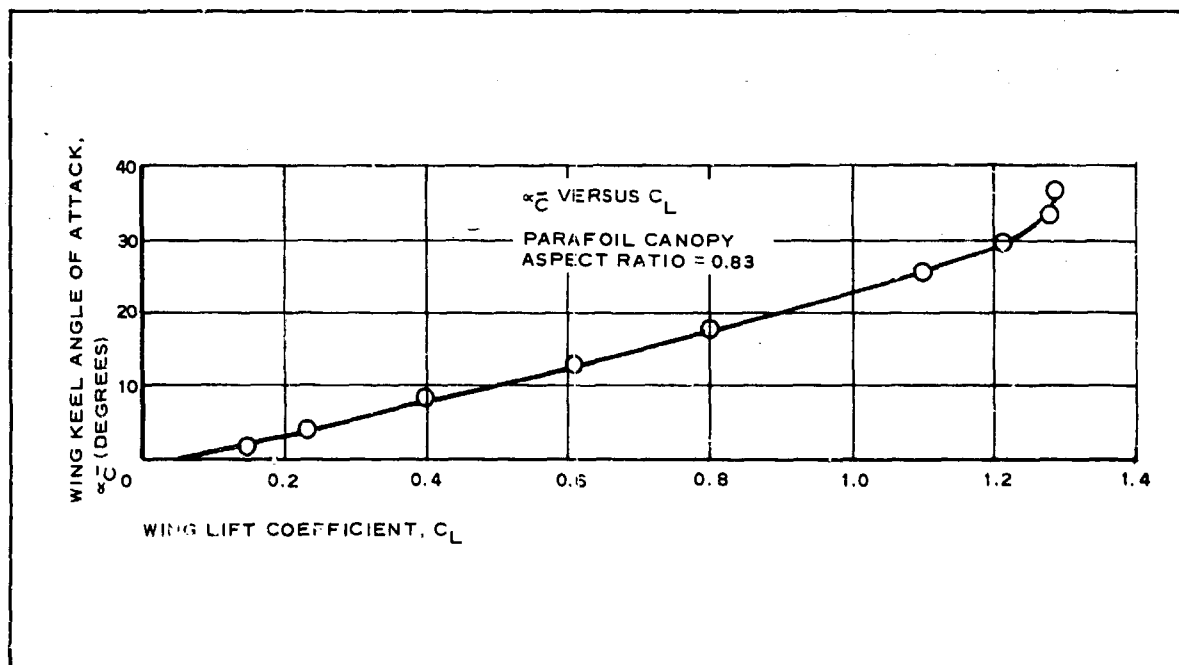


Figure 47 - Angle of Attack versus Lift Coefficient (Parafoil)

SECTION II - CONCEPT ANALYSIS

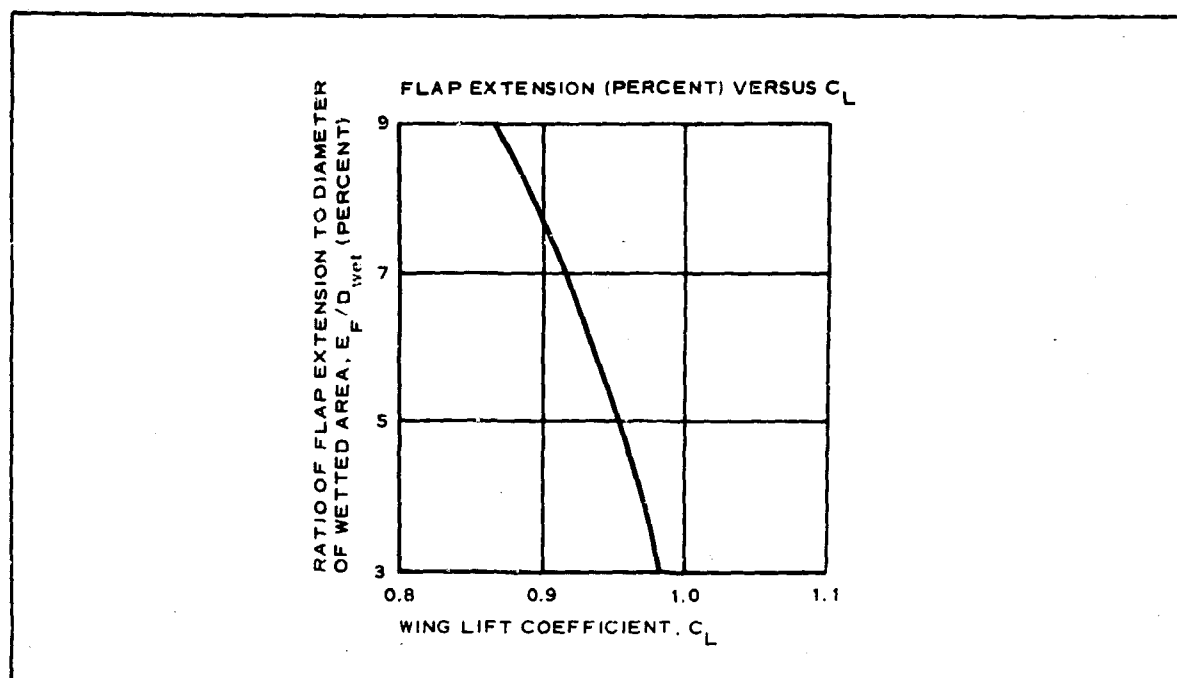


Figure 48 - Flap Extension versus Lift Coefficient (Cloverleaf)

SECTION III - SYSTEM CONCEPT RECOVERY PROFILES

1. GENERAL

A discussion and a pictorial representation of the recovery profile of each system will be presented in this section. Operations are based on the analysis of Section II and represent a single basic approach to applying the indicated system to the air delivery of personnel. The purpose of Section III is to indicate the general functional suitability and applicability of the individual system concepts and to indicate the associated problems and the advantages and disadvantages involved. Alternate recovery operations that may offer certain advantages also will be included.

2. FUNCTIONAL OPERATIONS

The functional operations and components of each system concept are summarized in Table XVII and are based on the conditions and assumptions of Section II. As indicated in Table XVII, most systems are assumed to have some initial drogue device to reduce the peak opening loads and/or to otherwise enhance their performance characteristics. For the gliding systems, the techniques indicated have been used with the conical parawing and with the gliding parachutes. The techniques indicated for the other systems are compatible with their conceptual design and operational requirements. For the rapid-opening concepts, either a one- or two-stage system may be possible conceptually. The alternatives will be more fully discussed in this item.

Figures 49 through 61 provide a general representation of the operational profile of each system concept based on Table XVII. With the exception of the lifting platform system and the ballistically deployed parachute system, all initial decelerators are considered to be static-line deployed. For each system then, with the above exceptions, the troops would line up in accordance with standard jumping procedures for exiting from either the side doors or the loading ramp of a C-130 aircraft (used for evaluation purposes). The troops then would secure their static lines to the proper anchor line cable. When the "go" command is given, the troops would begin exiting. System operations are described in Items 2a through 2j, below.

a. BALLUTE/Parachute (see Figure 49)

Following deployment of the payload suspension lines, the BALLUTE

SECTION III - SYSTEM CONCEPT RECOVERY PROFILES

would be deployed and inflated by either ram-air or by internal pressurization. The canopy stowed upon the BALLUTE could be either simultaneously deployed and inflated or, alternately, retained in its stored state until all deployment dynamics had been eliminated and the composite system had aligned itself along the flight path. In the first case, the smaller BALLUTE would inflate before the canopy and would divert the flow entering the canopy radially outward. This diversion would result in a more positive spreading of the inlet and a faster, more repeatable inflation process. In the alternate case, deployment and inflation of the canopy would be performed under more favorable conditions, with a potential reduction in line twists and canopy malfunctions. The alternate case would necessitate a small delay in the deployment of the canopy, which would be warranted only if its total opening characteristics were improved sufficiently. In either case, the BALLUTE would function as an inflation aid.

Following canopy inflation, the BALLUTE riser would be severed to allow the BALLUTE and canopy apex to move rearward (see Figure 49) and permit the canopy to assume its conventional inflated shape. Terminal deceleration and landing operations then would be performed in the conventional manner.

b. Internal Canopy System (see Figure 50)

As indicated in Figure 50, operations of this system would not be expected to differ substantially from operations of the T-10. At full-line stretch, inflation of the MC-1 canopy would occur in a typical manner, except for the effects of the small internal canopy. The internal canopy, having considerably less volume than the primary canopy, would inflate much more rapidly and would effect some flow blockage at the primary canopy inlet. The result would be the diversion of the flow radially outward, which would cause a comparatively rapid spreading of the primary canopy inlet and thus result in a faster inflation process. Descent and landing then would proceed in a conventional manner.

c. Ballistic Parachute (see Figure 51)

The system illustrated in Figure 51 incorporates a ballistically actuated device to effect the rapid spreading of the inlet and promote rapid, more positive canopy inflation. At full-line stretch, the separation of the deployment bag and the canopy would activate a small time-delay device that would allow the canopy to pass through its approximately 90-deg arc prior to spreading of the canopy inlet. This alignment of the composite system with the flow is considered necessary to permit a successful canopy inlet spreading without a subsequent recollapse of the canopy prior to inflation.

Following canopy inflation, the ballistic spreader would remain suspended

SECTION III

TABLE XVII - SYSTEM SEQUENCE AND OPERA

Concept	Initial device	Decelerator inflation	Primary re-covery device description	Decelerator inflation	Princip of operat
BALLUTE/Para-chutes	4-ft diam BALLUTE	Ram-air or internal pres-surization	35-ft extended skirt	Ram-air	Rapid inl opening, stabilizat
Quick-opening parachutes	Primary and secondary canopy	Ram-air	35-ft extended skirt	Ram-air	Rapid inl opening
Ultrafast-opening parachutes	Primary canopy	Ram-air	35-ft extended skirt	Ram-air	Rapid inl opening
Drag cones	Drogue para-chute or BALLUTE	Ram-air	Cone	Pressurized support torii	Drag and impact attenuatio
Canopy/explosives	Primary canopy	Ram air	24-ft D ₀ canopy with explosive charges	Ram-air	Linear impulse c canopy
Rotating decel-erators	4-ft rotating BALLUTE or rotofoil chute	Ram-air or internal pres-surization	Fabric rotor blades	Pressurized blades	Rotating lifting surfaces
Powered lifting devices	Parachute	Ram-air	Teeter-rotor or rocket lifting device	Not applicable	Specific impulse o rotor lift
Paragliders	Primary re-covery device in parachute mode 1	Ram-air	Conical, cylindrical, or limp	Pressurized booms and keel	Lift/drag surfaces
Gliding para-chutes	Primary re-covery device (reefed)*	Ram-air	Parasail, Parafoil, or Cloverleaf	Ram-air	Lift/drag surfaces
Ring wing airfoil	3-ft drogue parachute (minimum)	Ram-air	Circular airfoil	Pressurized leading edge and ribs	Lift/drag surfaces

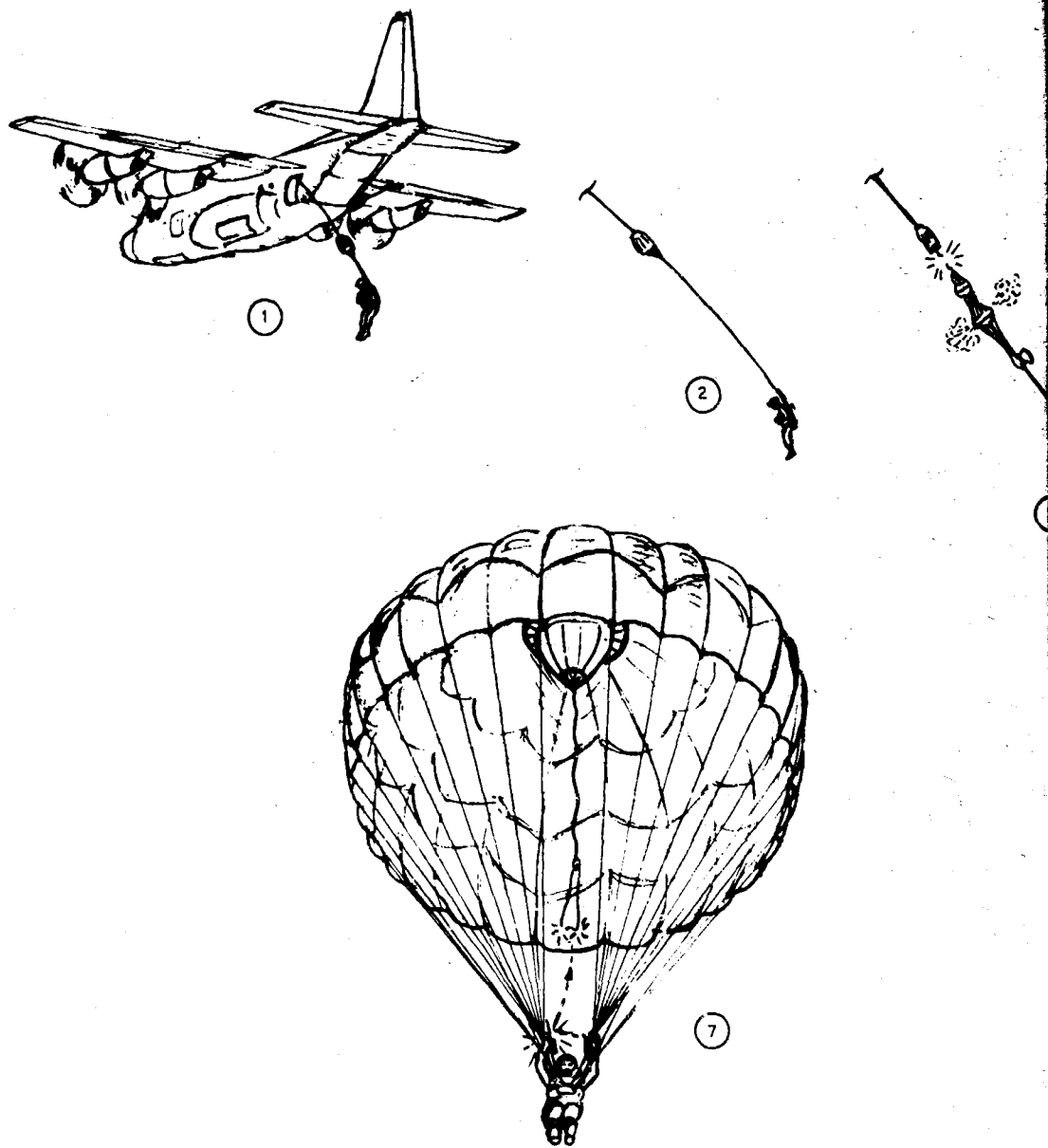
* Deployment sleeve may be required.

A.

SECTION III - SYSTEM CONCEPT RECOVERY PROFILES

SYSTEM SEQUENCE AND OPERATIONS

Primary recovery device description	Decelerator inflation	Principal of operation	Steady-state descent	Control	Landing
Extended	Ram-air	Rapid inlet opening, stabilization	Vertical, conventional	None	Conventional
Extended	Ram-air	Rapid inlet opening	Vertical, conventional	None	Conventional
Extended	Ram-air	Rapid inlet opening	Vertical, conventional	None	Conventional
	Pressurized support structure	Drag and impact attenuation	Vertical, high speed	None	Impact attenuation
Explosive canopy	Ram-air	Linear impulse on canopy	Vertical	None	Upward impulse on canopy
Rotor	Pressurized blades	Rotating lifting surfaces	Vertical or glide	Effective cyclic pitch	Collective and cyclic flare
Rotor jet device	Not applicable	Specific impulse or rotor lift	Vertical and/or lateral	Thrust vectoring	Upward impulse or touchdown
Parachute, aerial	Pressurized booms and keel	Lift/drag surfaces	Glide	Center-of-gravity shift, control straps	Conventional
Parachute, aerial, or leaf	Ram-air	Lift/drag surfaces	Glide	Control flaps	Flare
Parachute	Pressurized leading edge and ribs	Lift/drag surfaces	Glide	Control lines and surfaces	Flare



A.

SECTION III - SYSTEM CONCEPT RECOVERY PROFILES

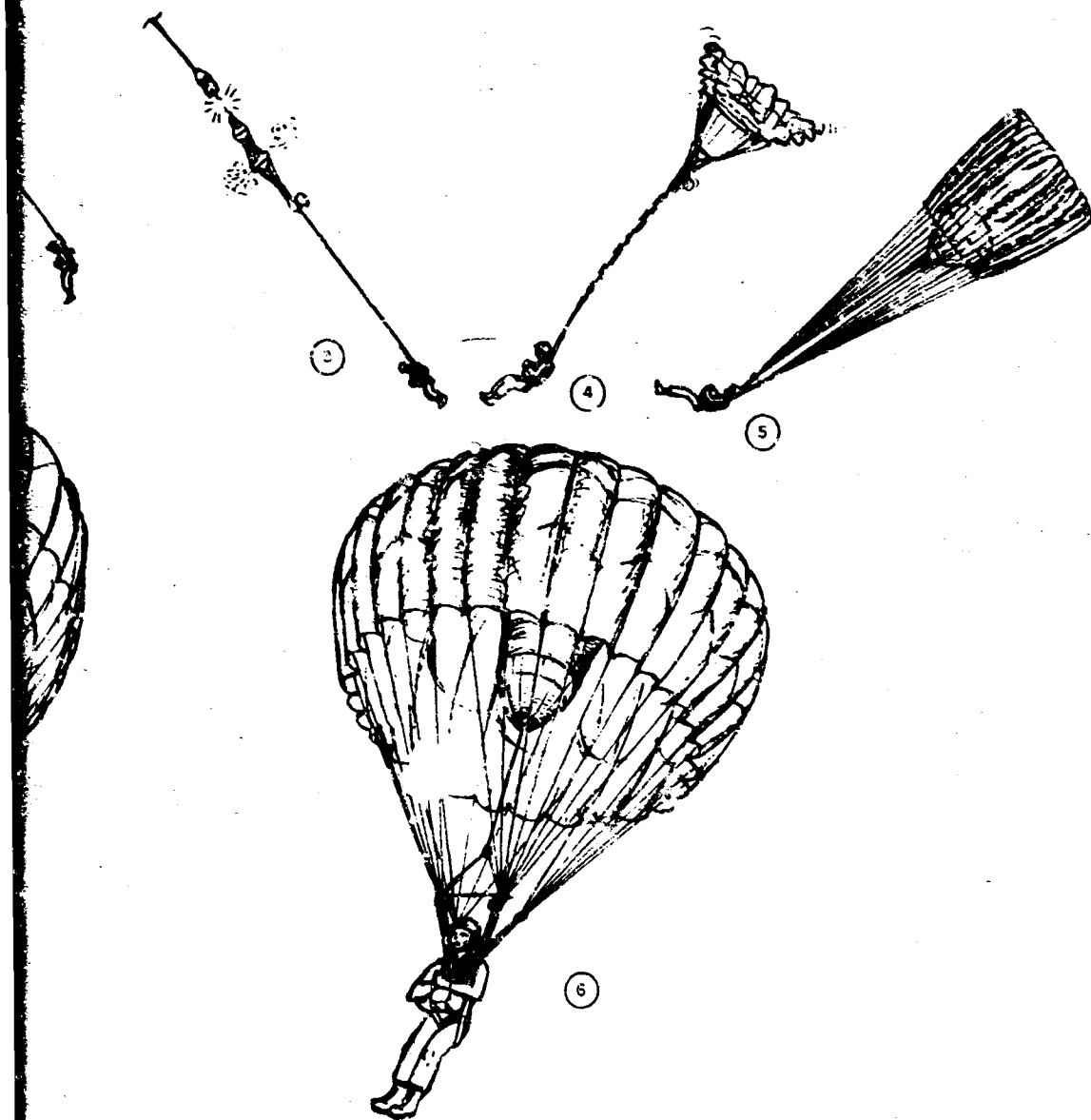
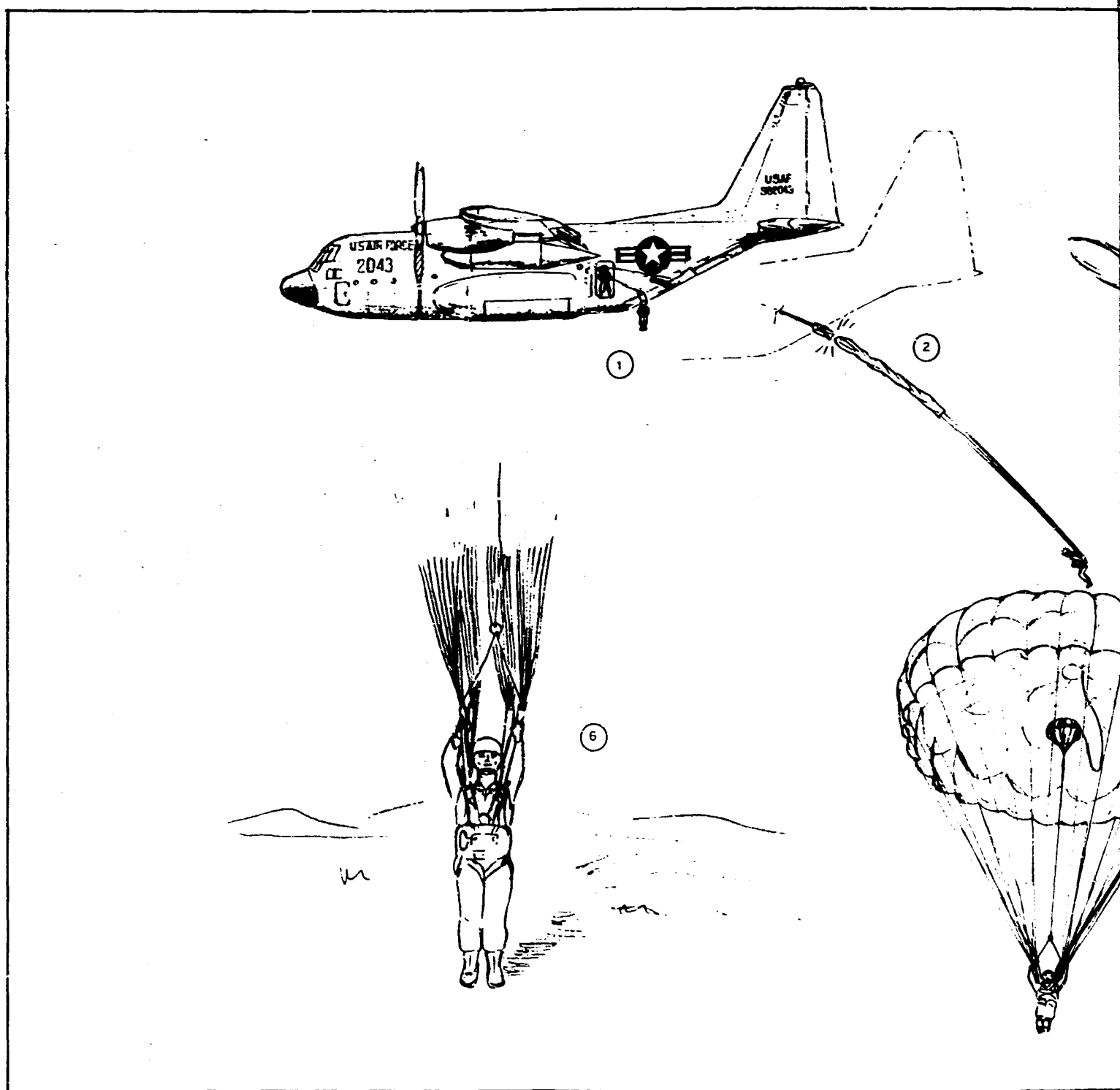


Figure 49 - BALLUTE/Parachute Operational Profile



A.

SECTION III - SYSTEM CONCEPT RECOVERY PROFILES

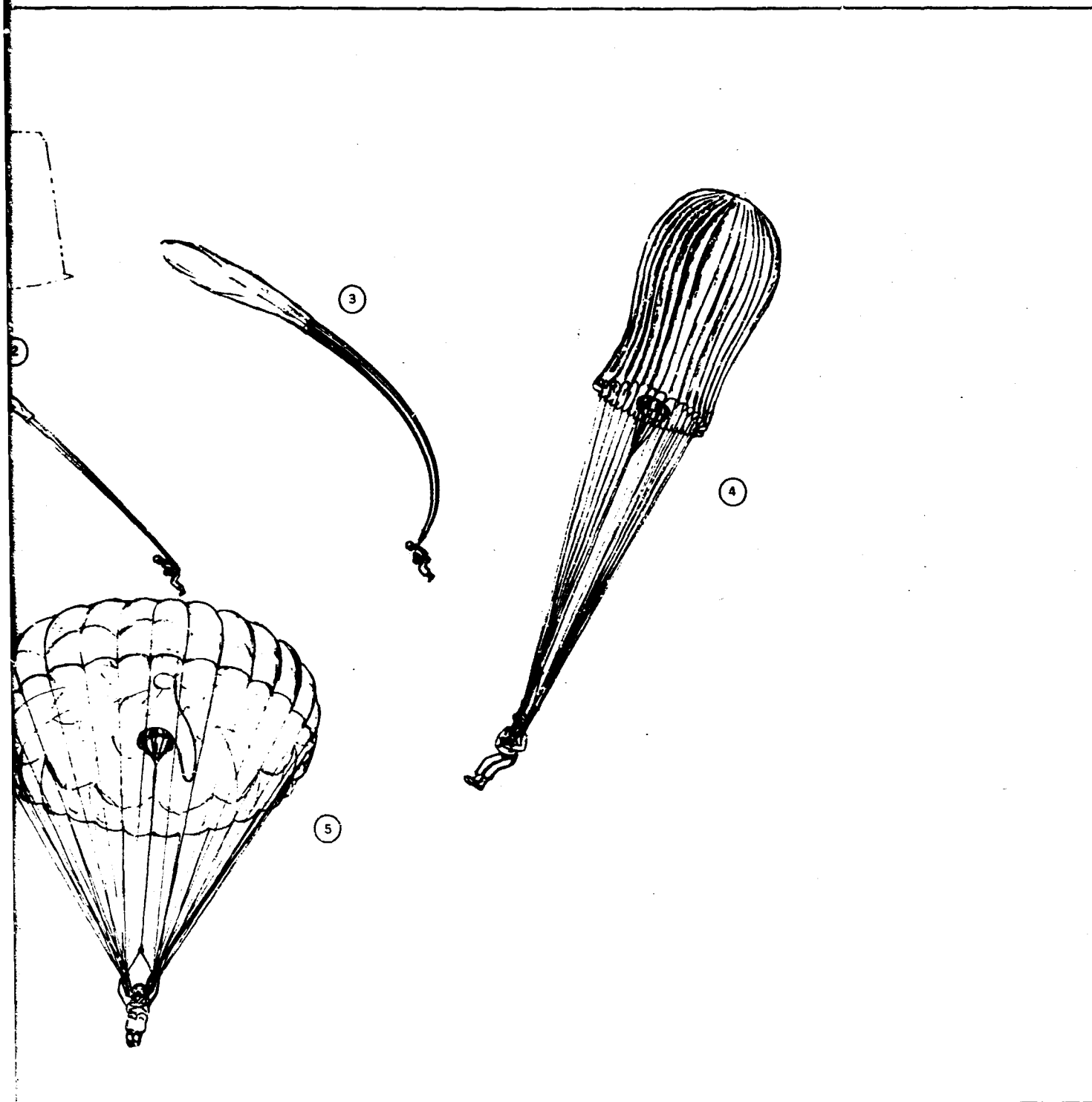
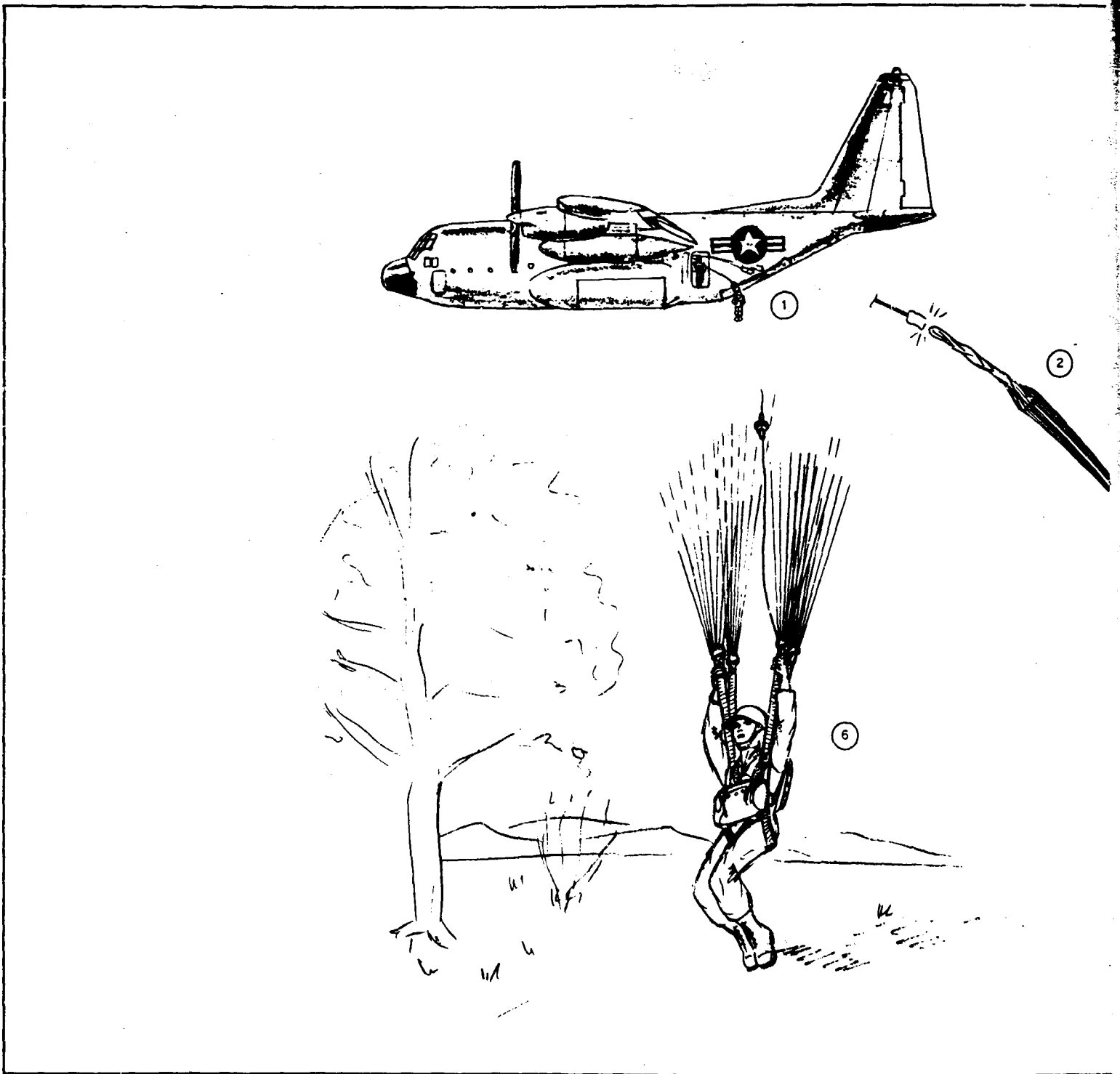


Figure 50 - Internal Canopy System Operational Profile

B.



A.

SECTION III - SYSTEM CONCEPT RECOVERY PROFILES

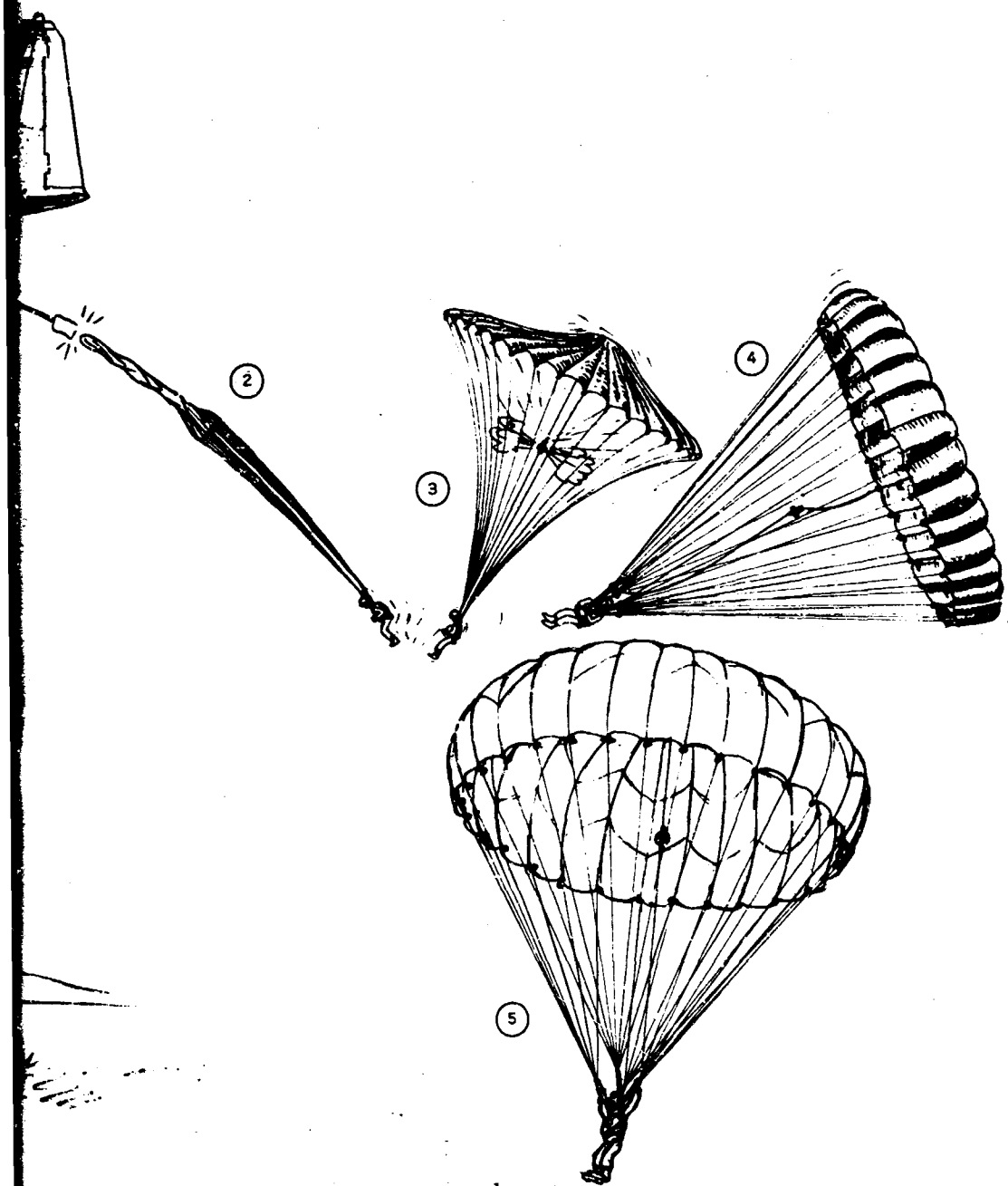
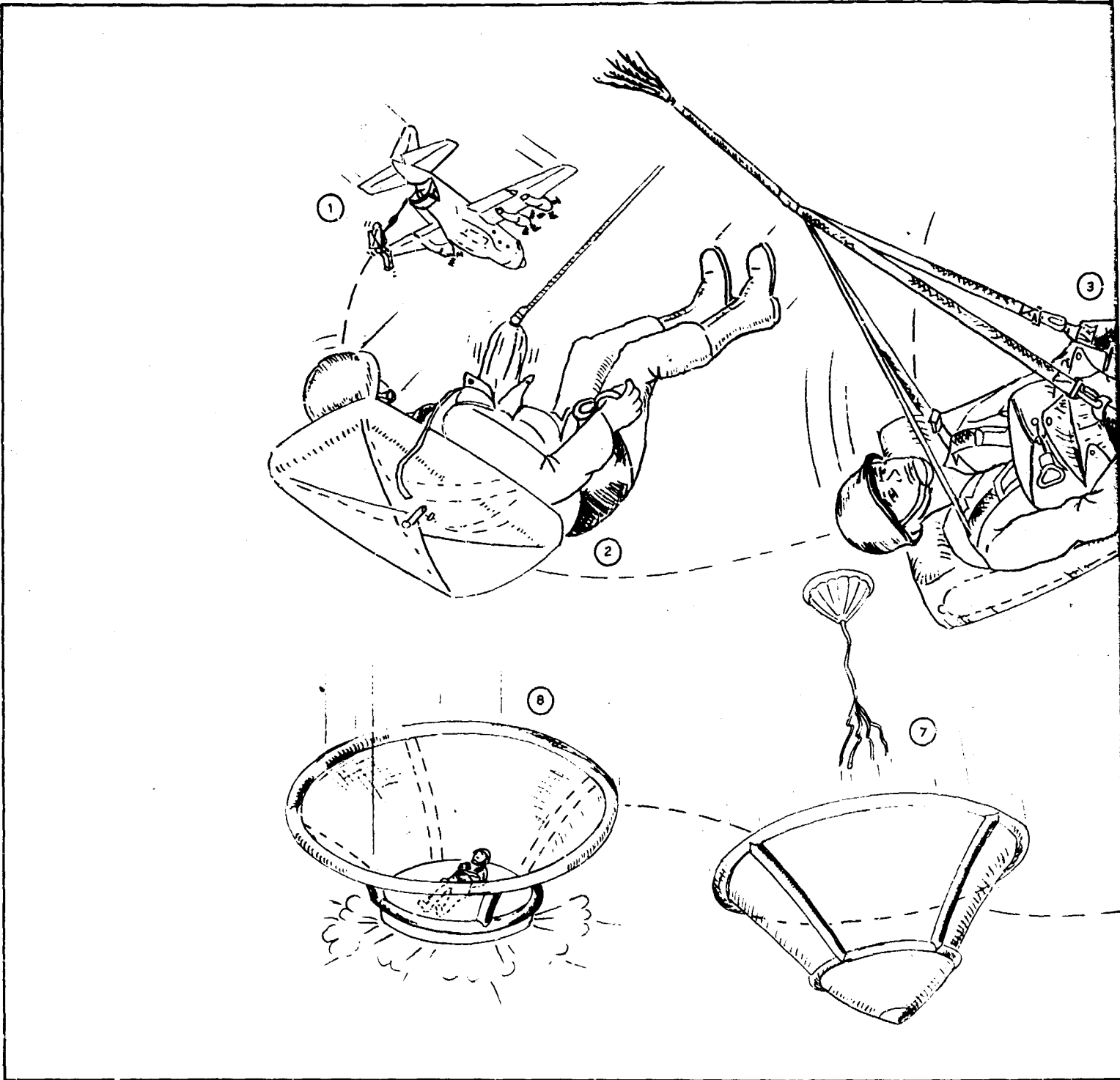


Figure 51 - Ballistic Parachute Operational Profile



A.

SECTION III - SYSTEM CONCEPT RECOVERY PROFILES

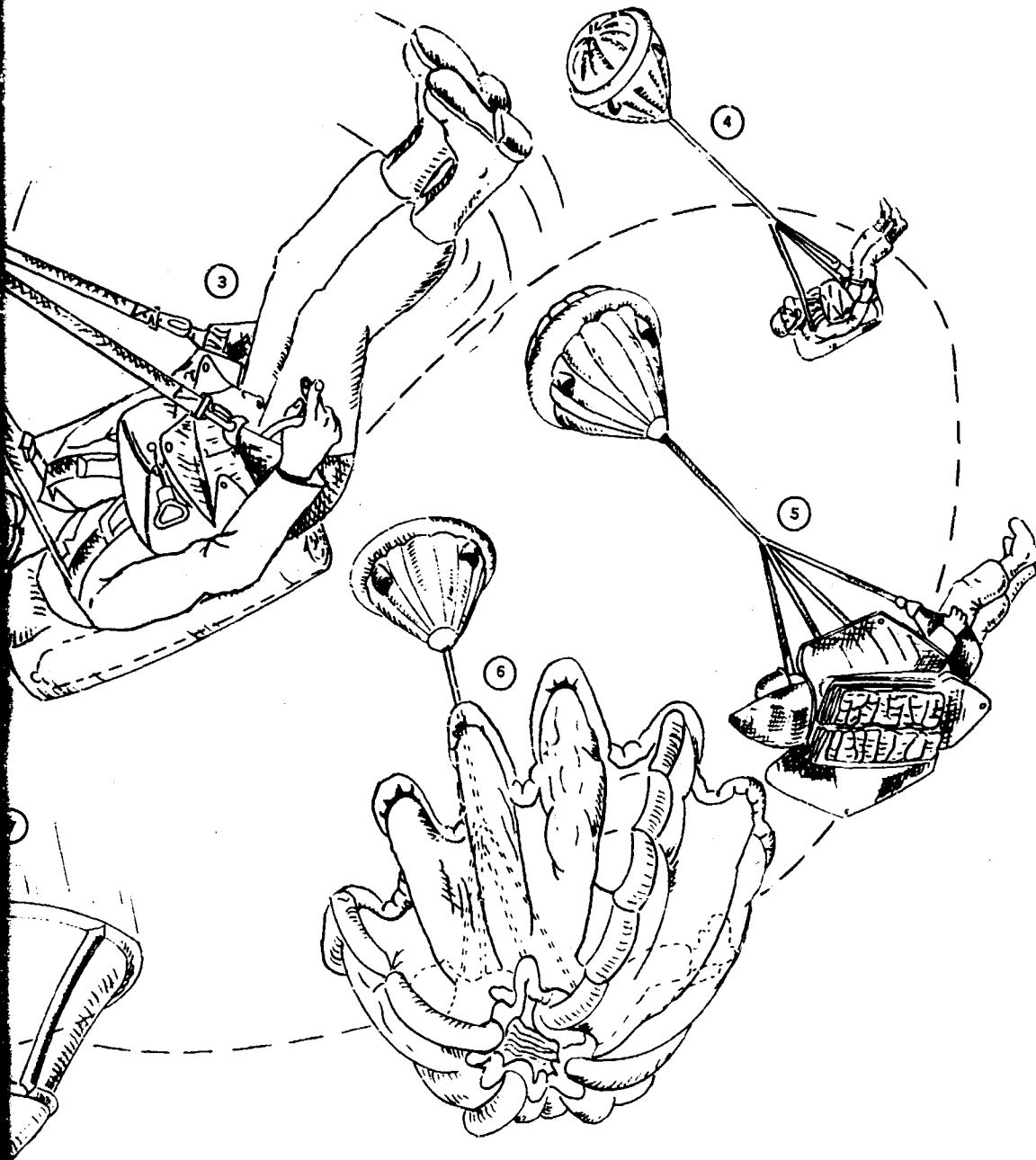
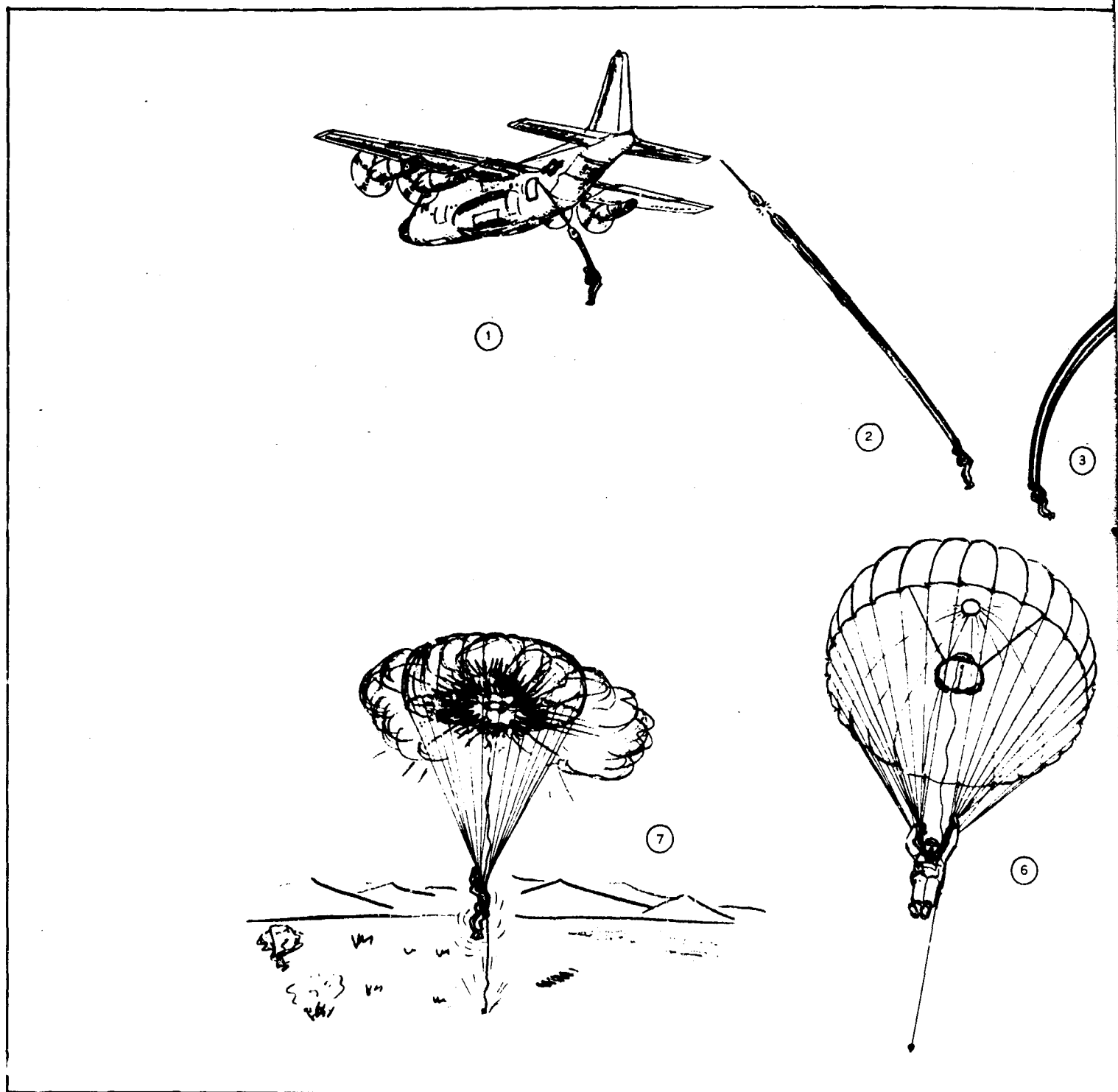


Figure 52 - Drag Cone Operational Profile



A.

SECTION III - SYSTEM CONCEPT RECOVERY PROFILES

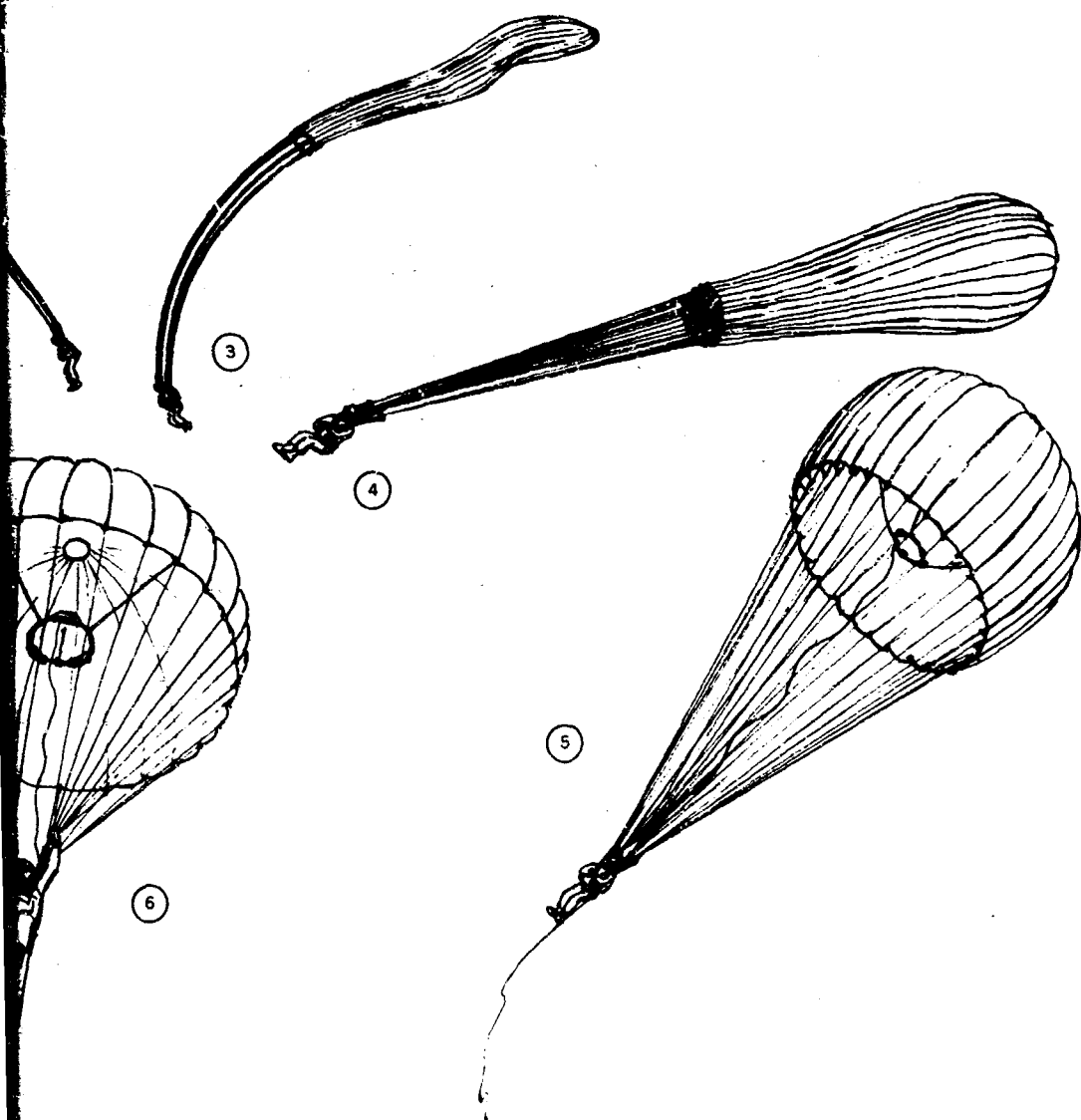
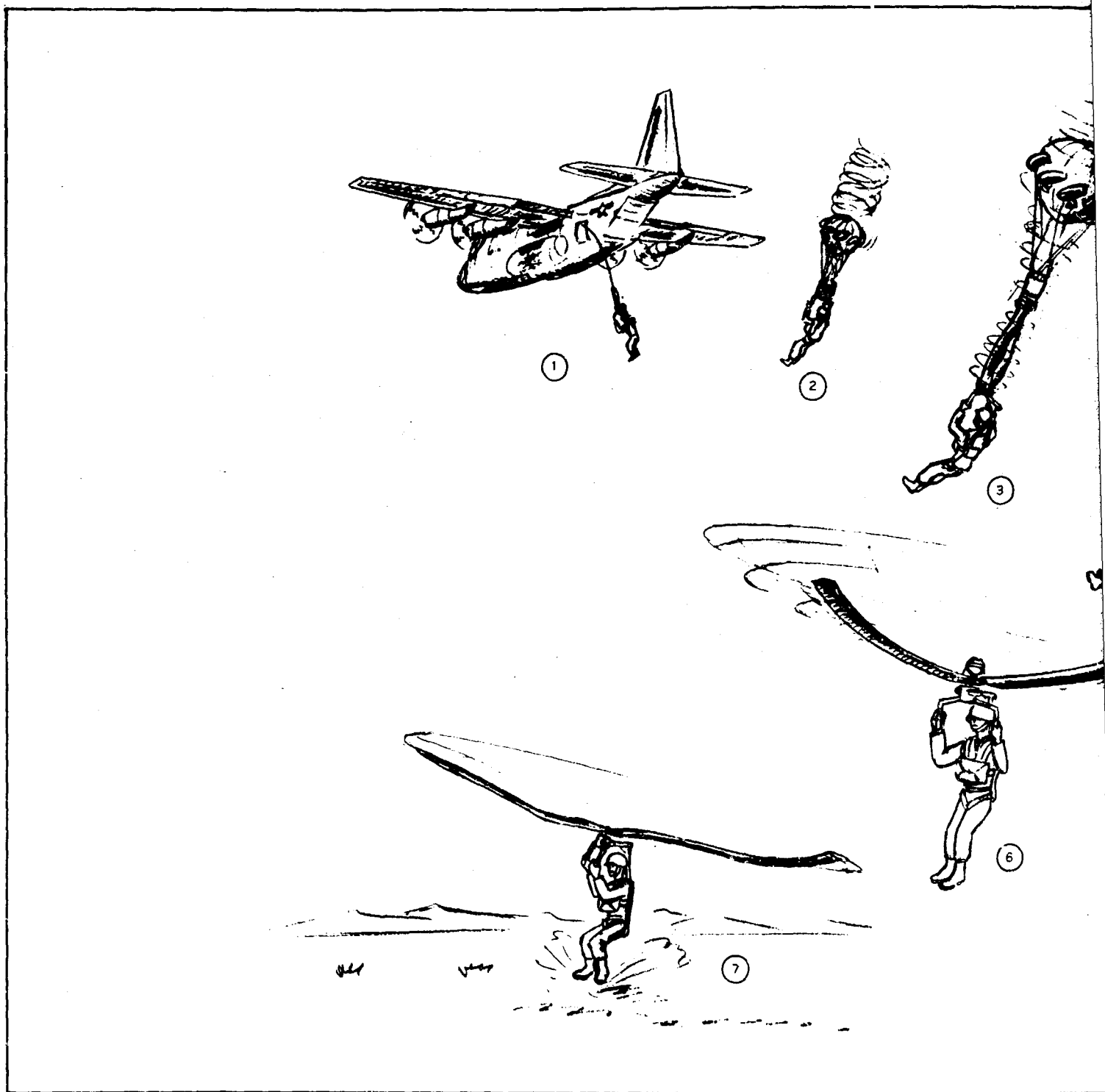


Figure 53 - Canopy/Explosive System Operational Profile



A.

SECTION III - SYSTEM CONCEPT RECOVERY PROFILES

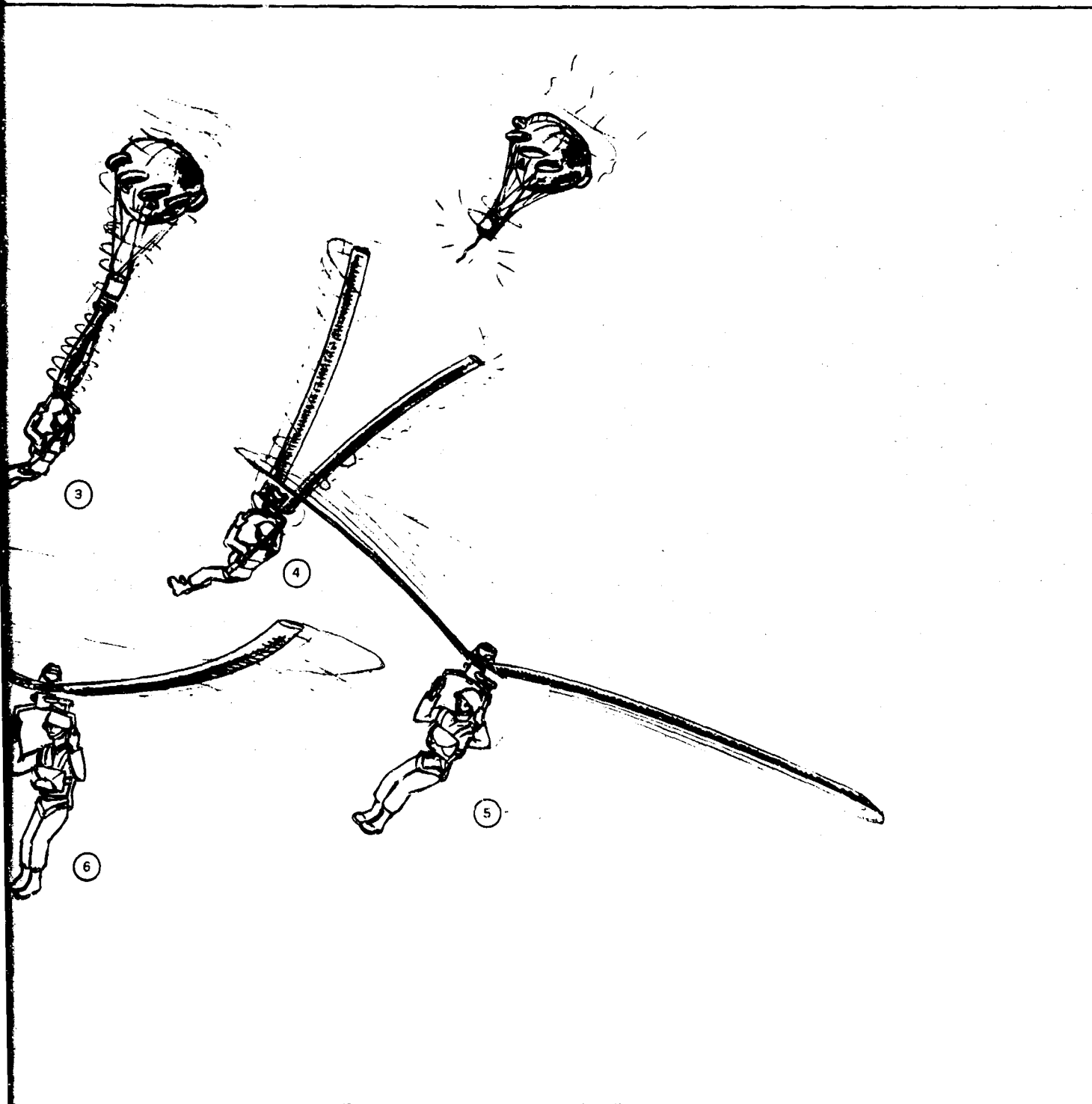
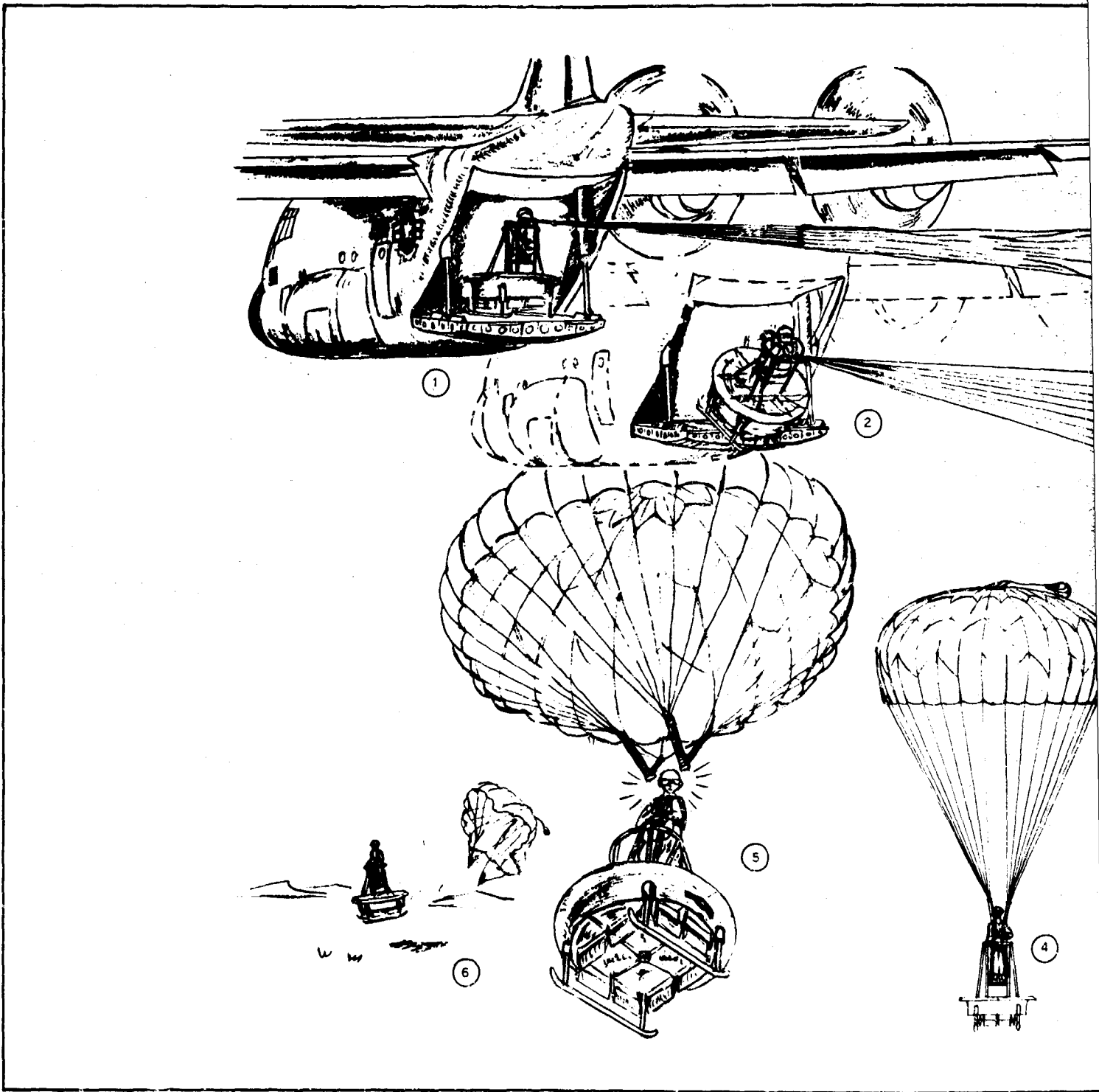


Figure 54 - Rotating Decelerator Operational Profile



A.

SECTION III - SYSTEM CONCEPT RECOVERY PROFILES

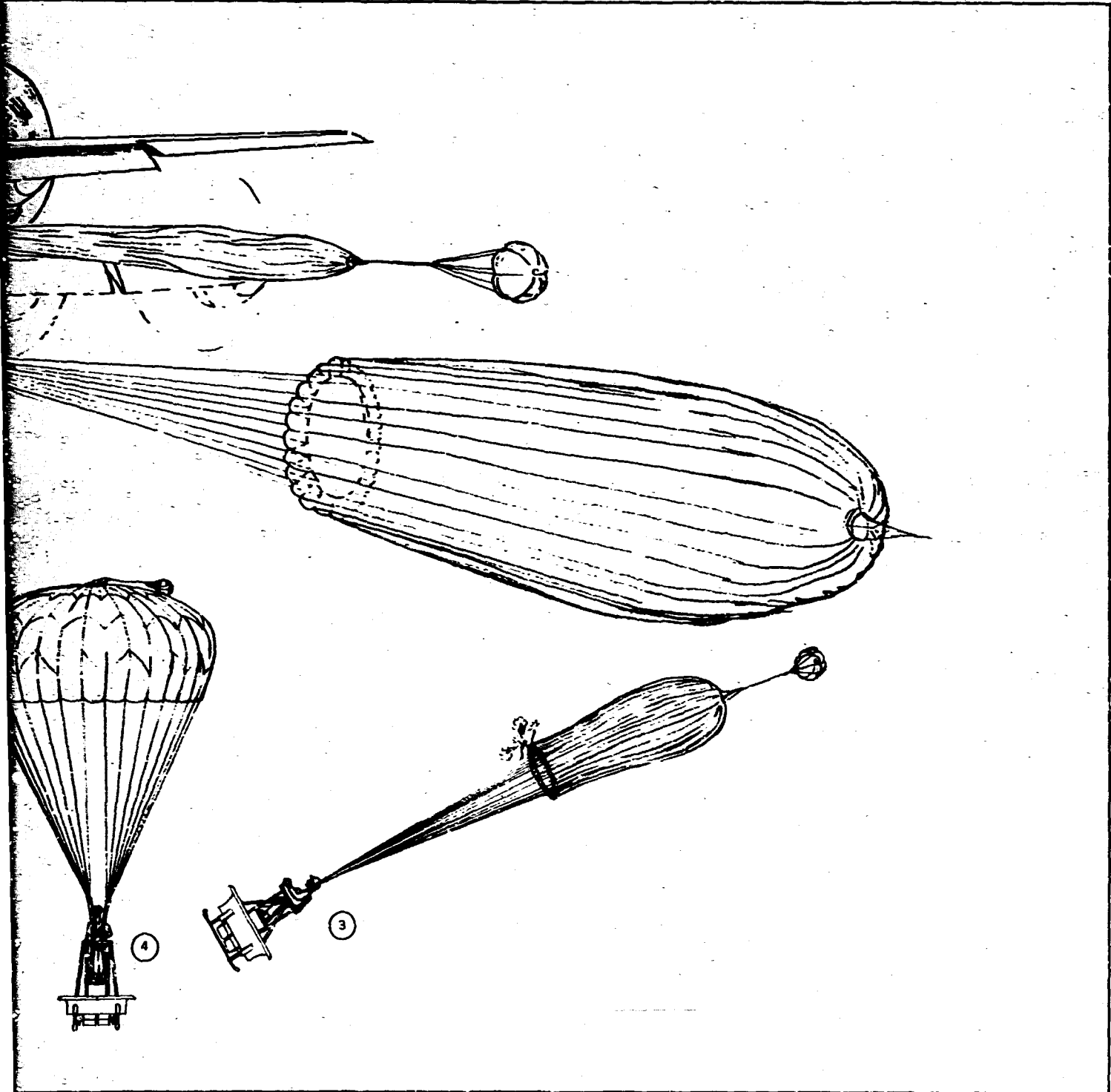
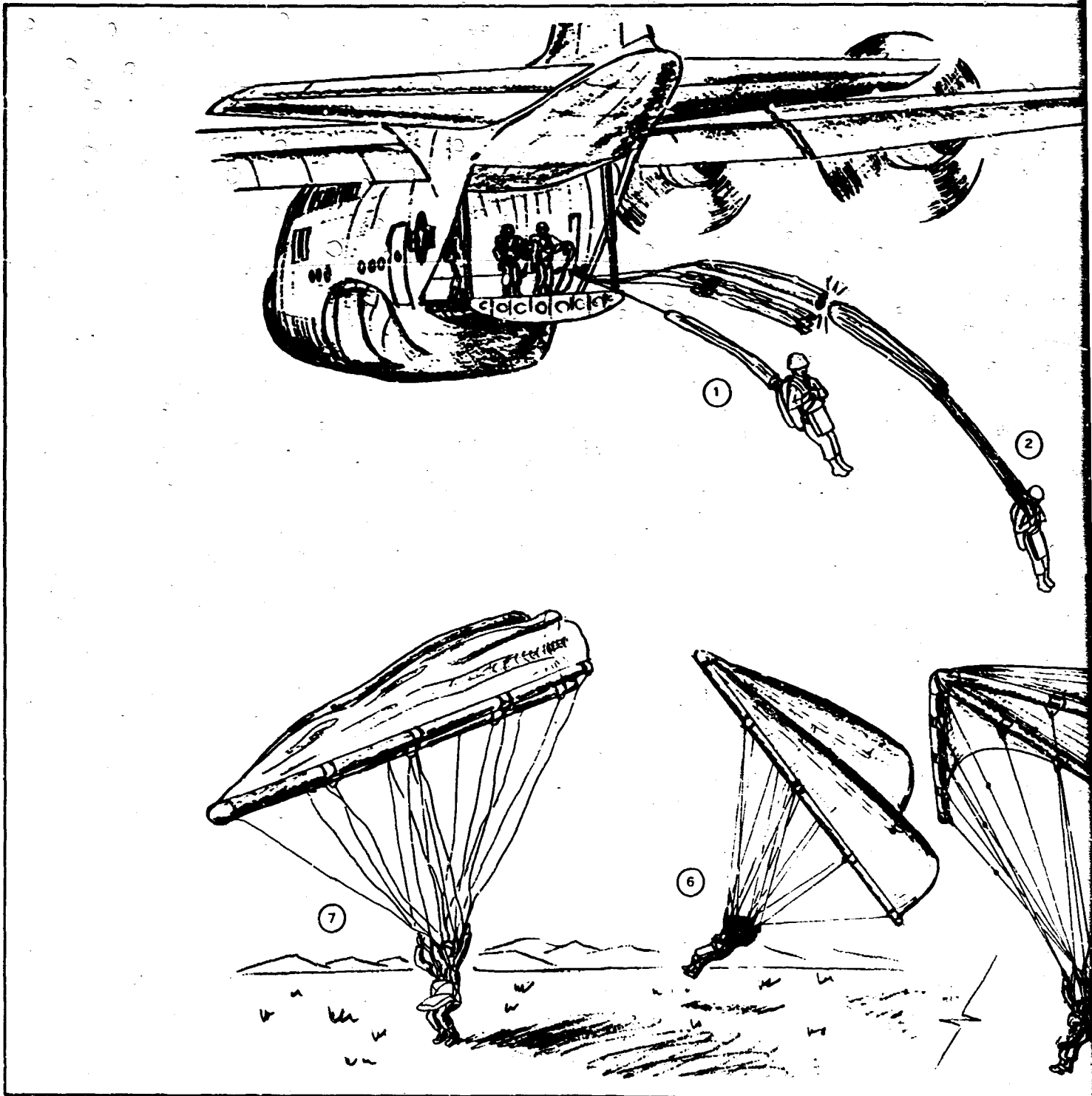


Figure 55 - Lift Platform Operational Profile



A.

SECTION II - SYSTEM CONCEPT RECOVERY PROFILES

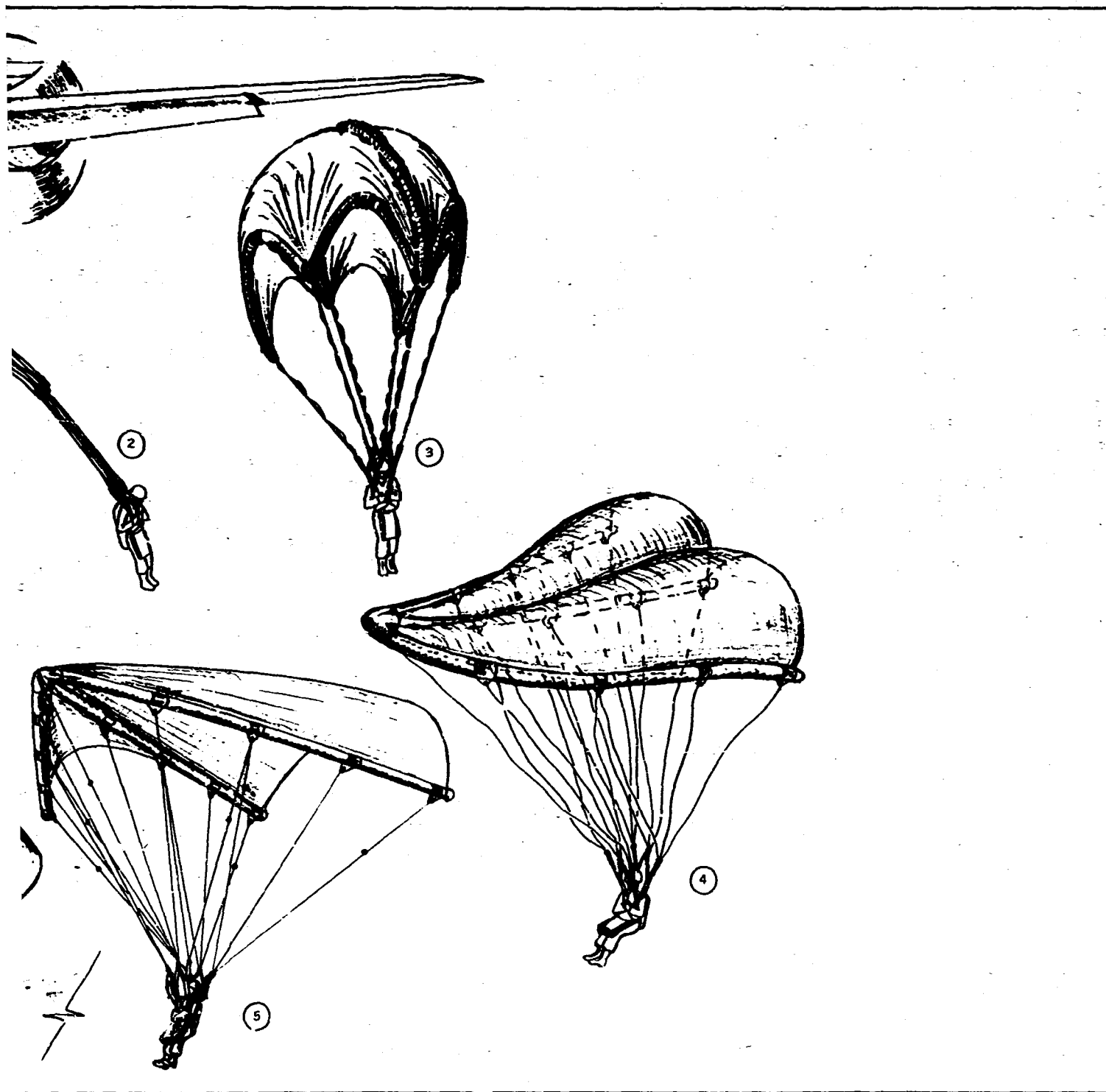
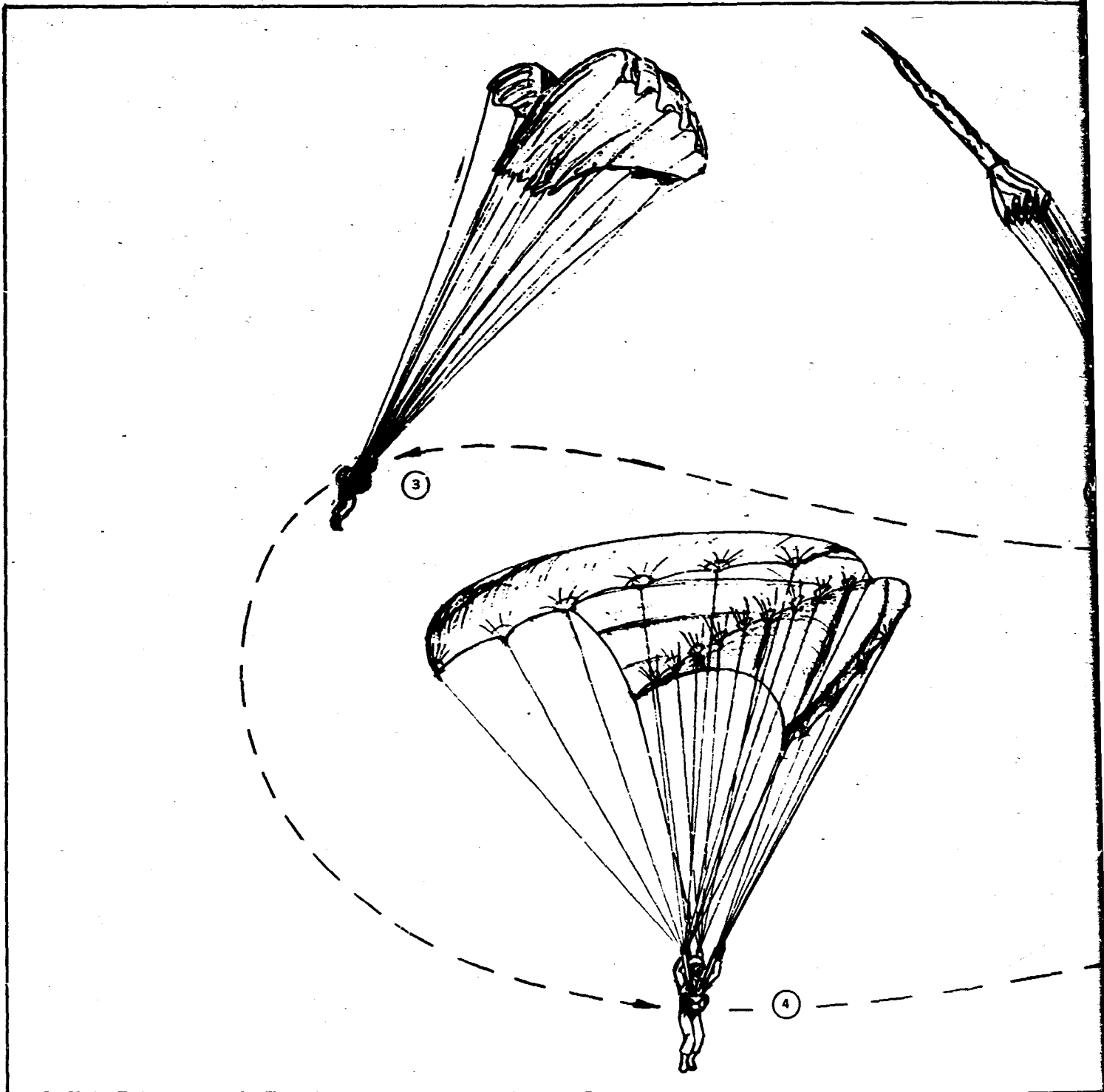


Figure 56 - Conical Parawing Operational Profile



A.

SECTION III - SYSTEM CONCEPT RECOVERY PROFILES

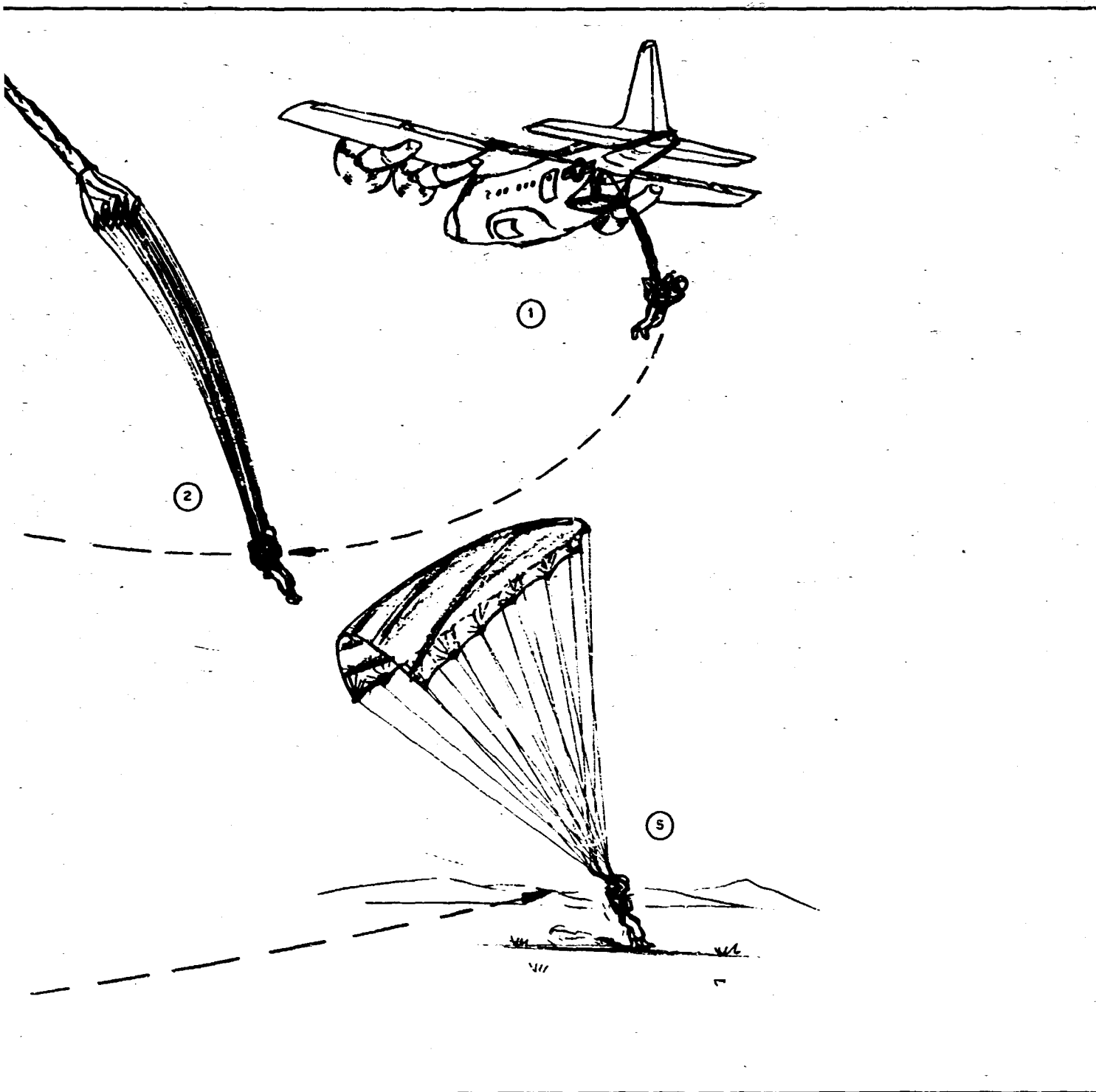
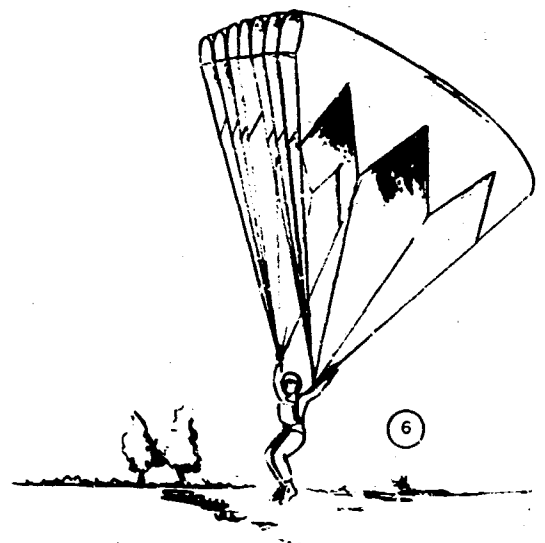
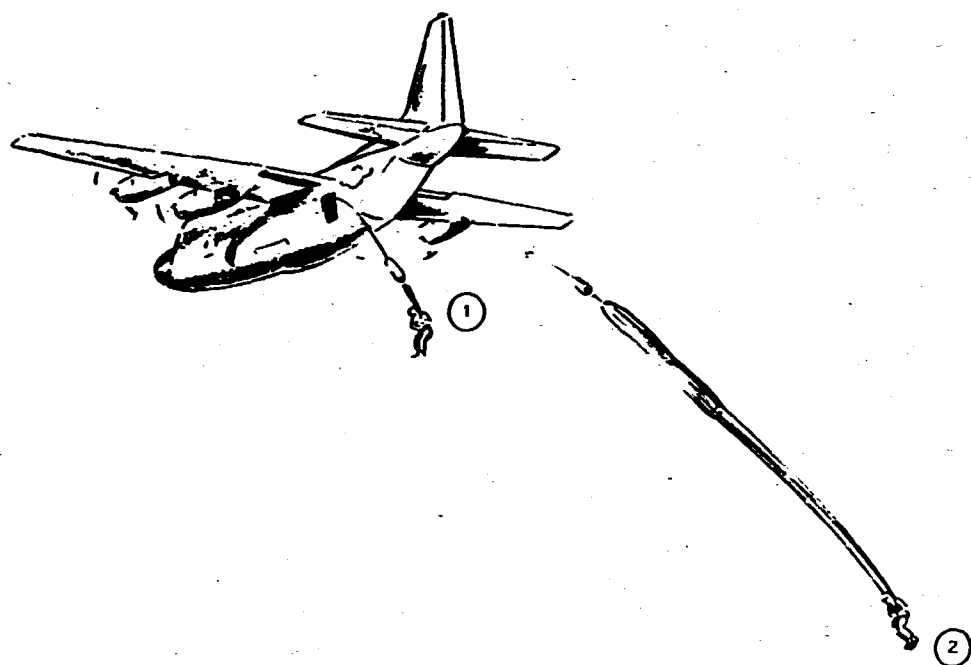


Figure 57 - Limp Parawing Operational Profile



A.

SECTION III - SYSTEM CONCEPT RECOVERY PROFILES

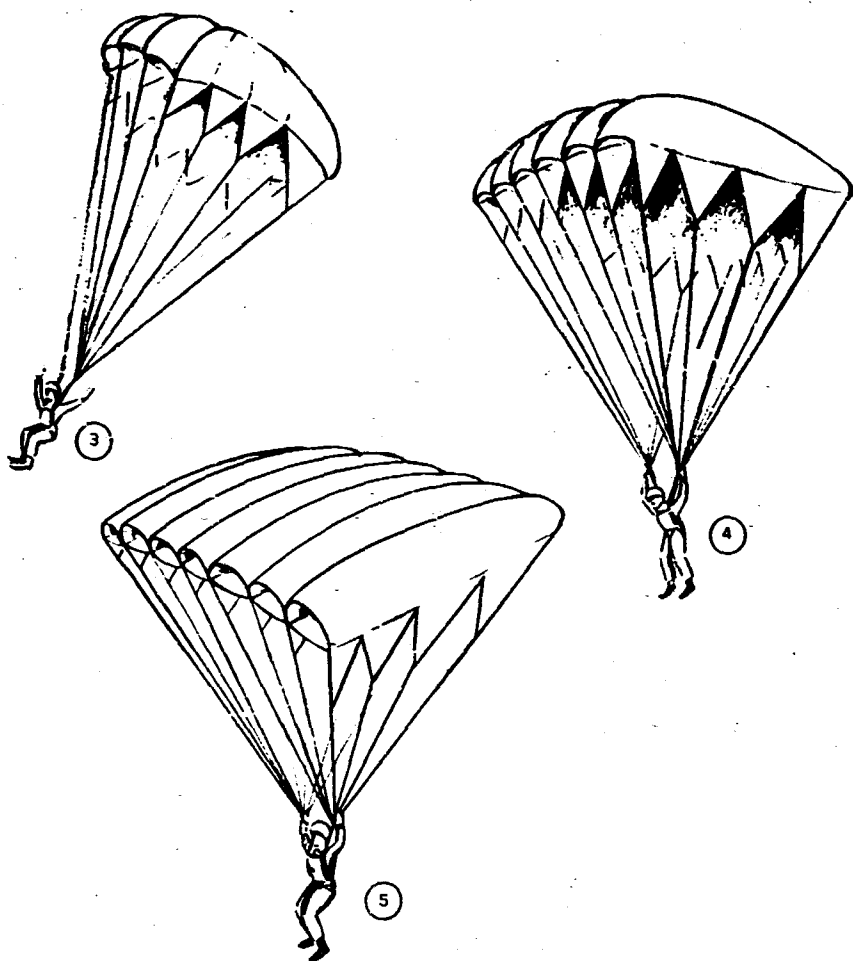
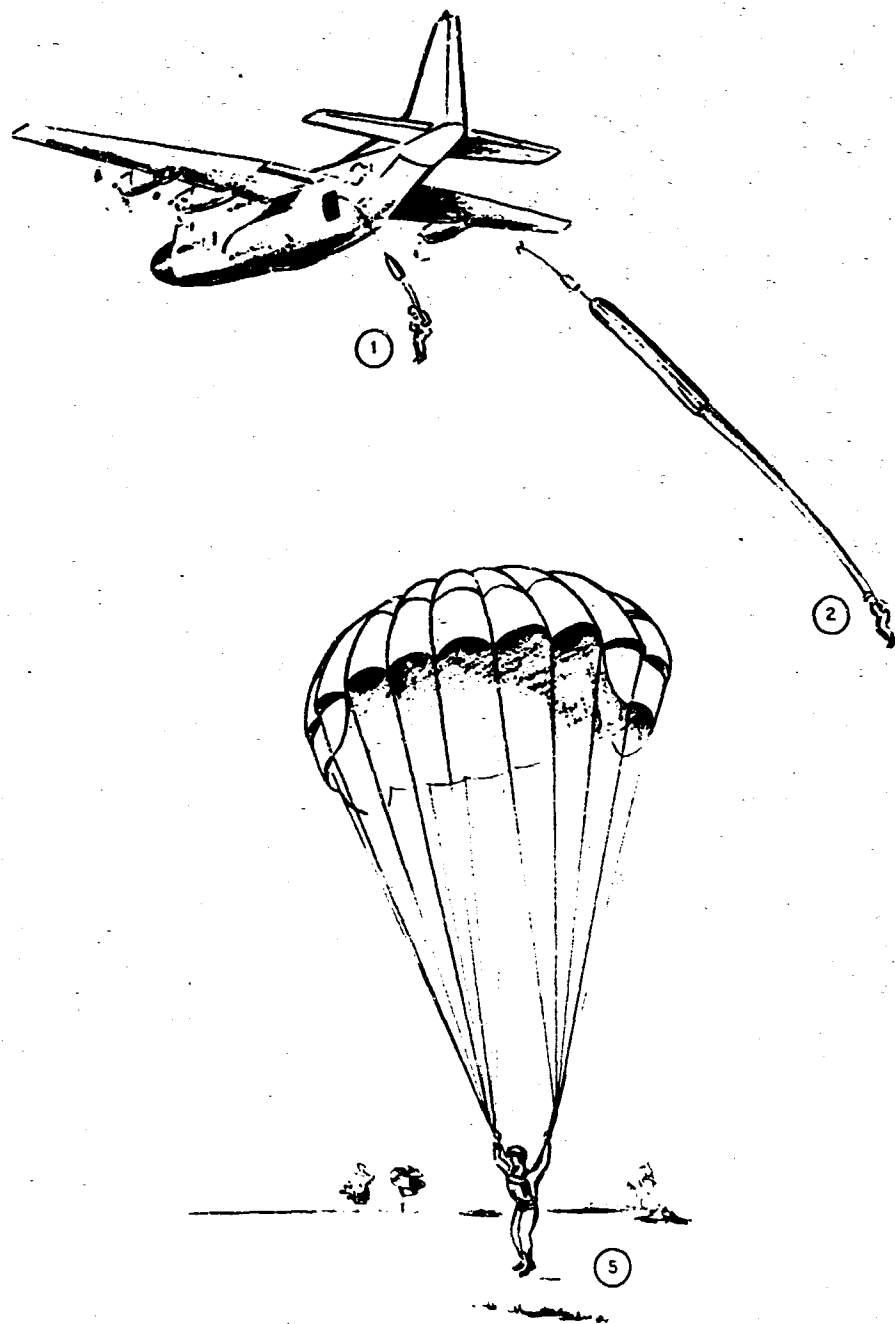


Figure 58 - Parafoil Parachute Operational Profile



A.

SECTION III - SYSTEM CONCEPT RECOVERY PROFILES

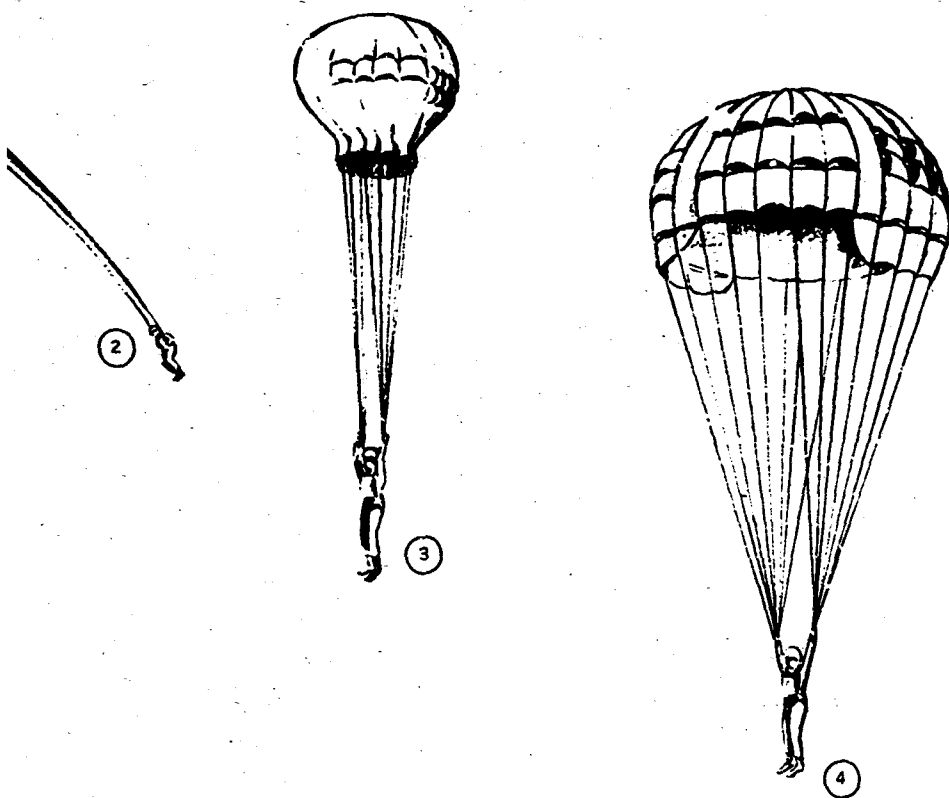
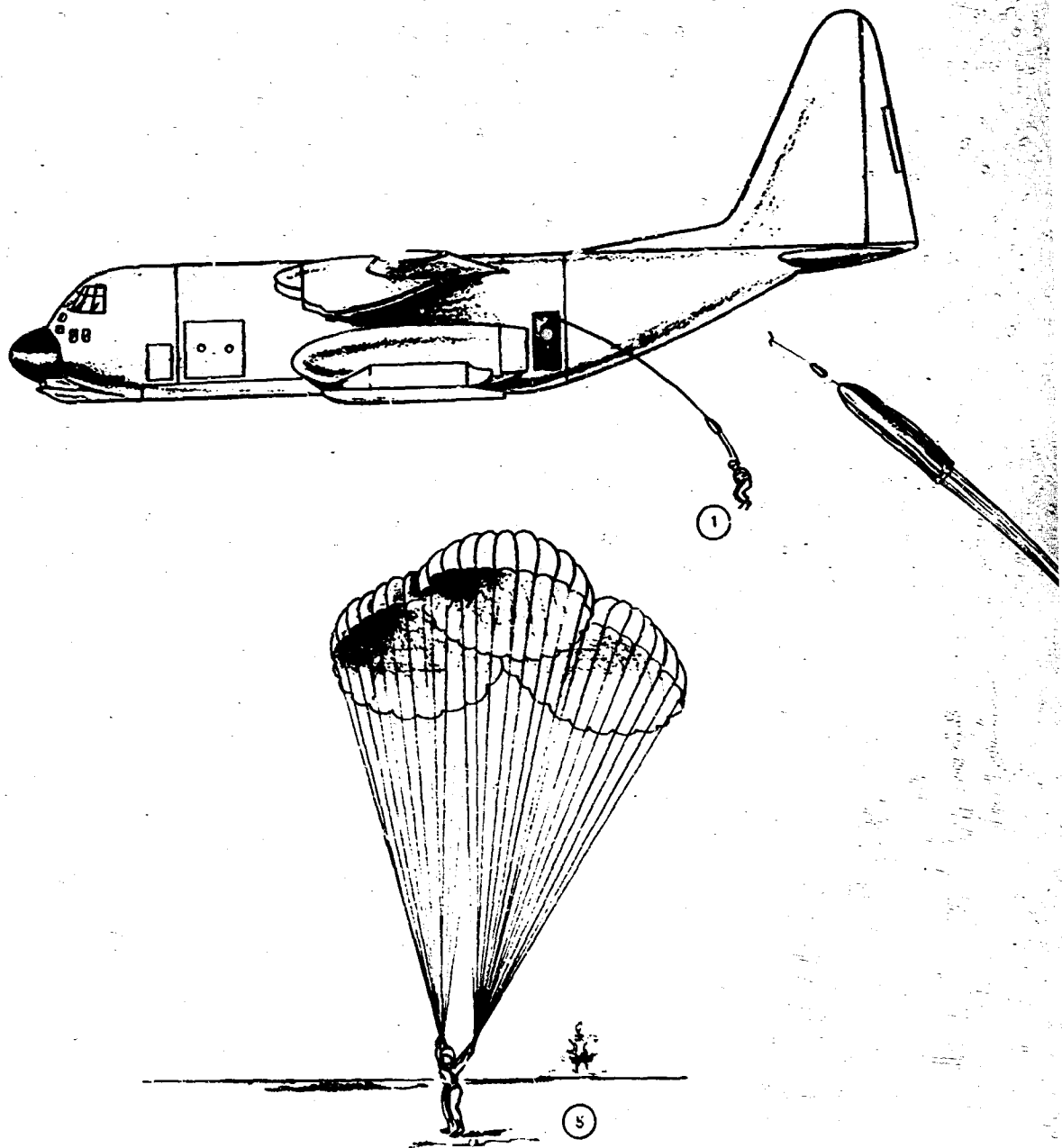


Figure 59 - Parasail Parachute Operational Profile



A.

SECTION III - SYSTEM CONCEPT RECOVERY PROFILES

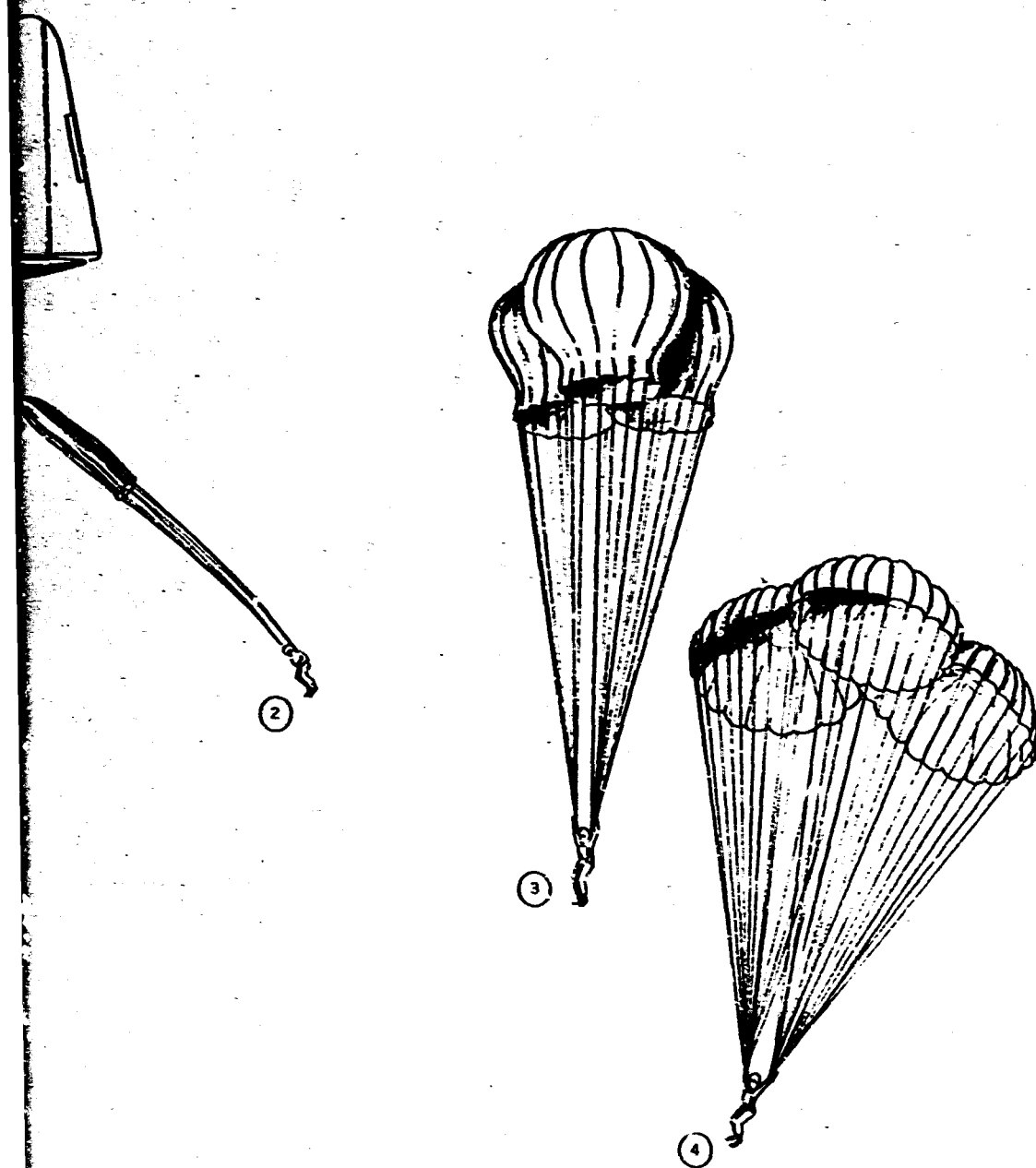
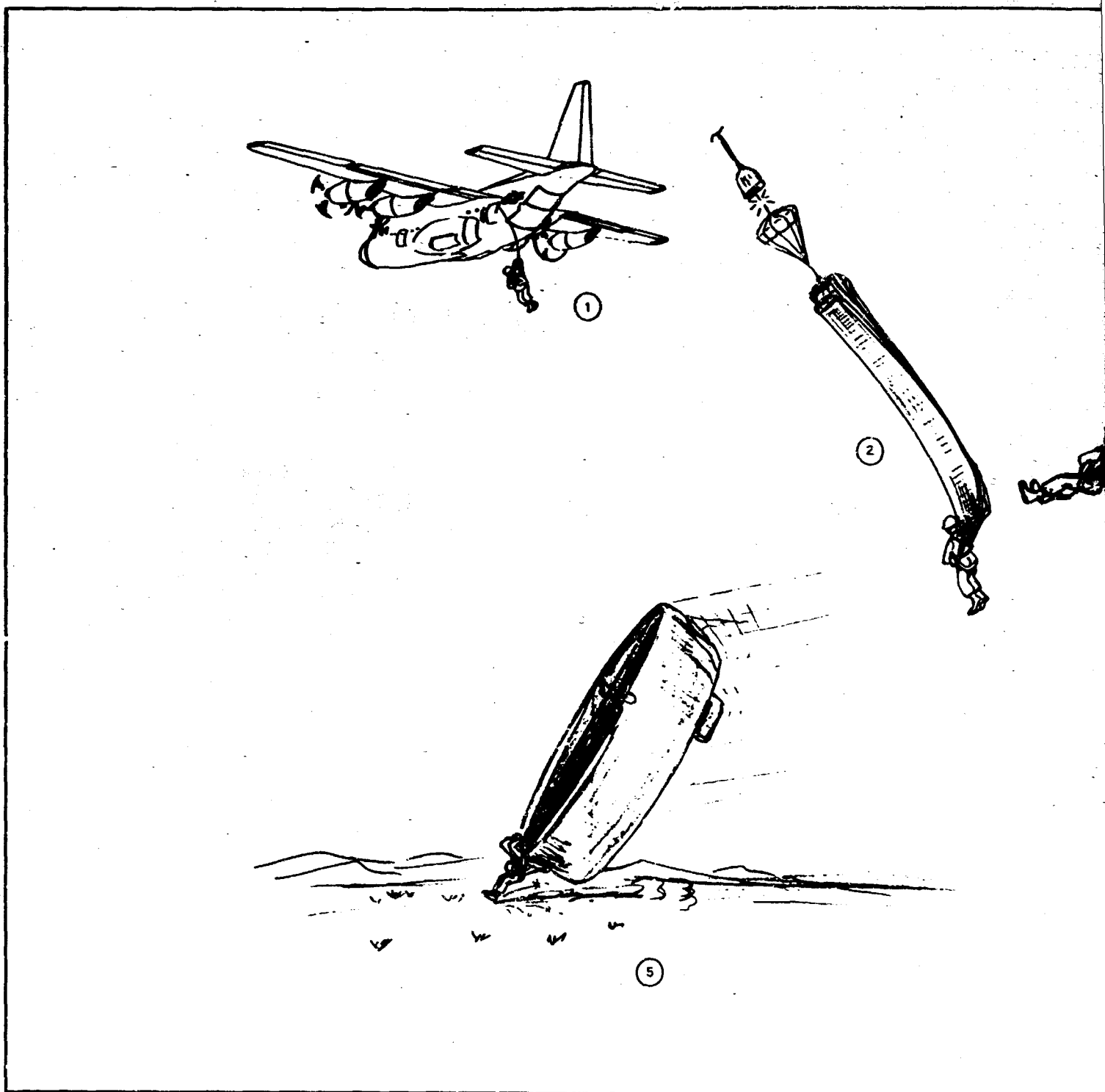


Figure 60 - Cloverleaf Parachute Operational Profile



A.

SECTION III - SYSTEM CONCEPT RECOVERY PROFILES

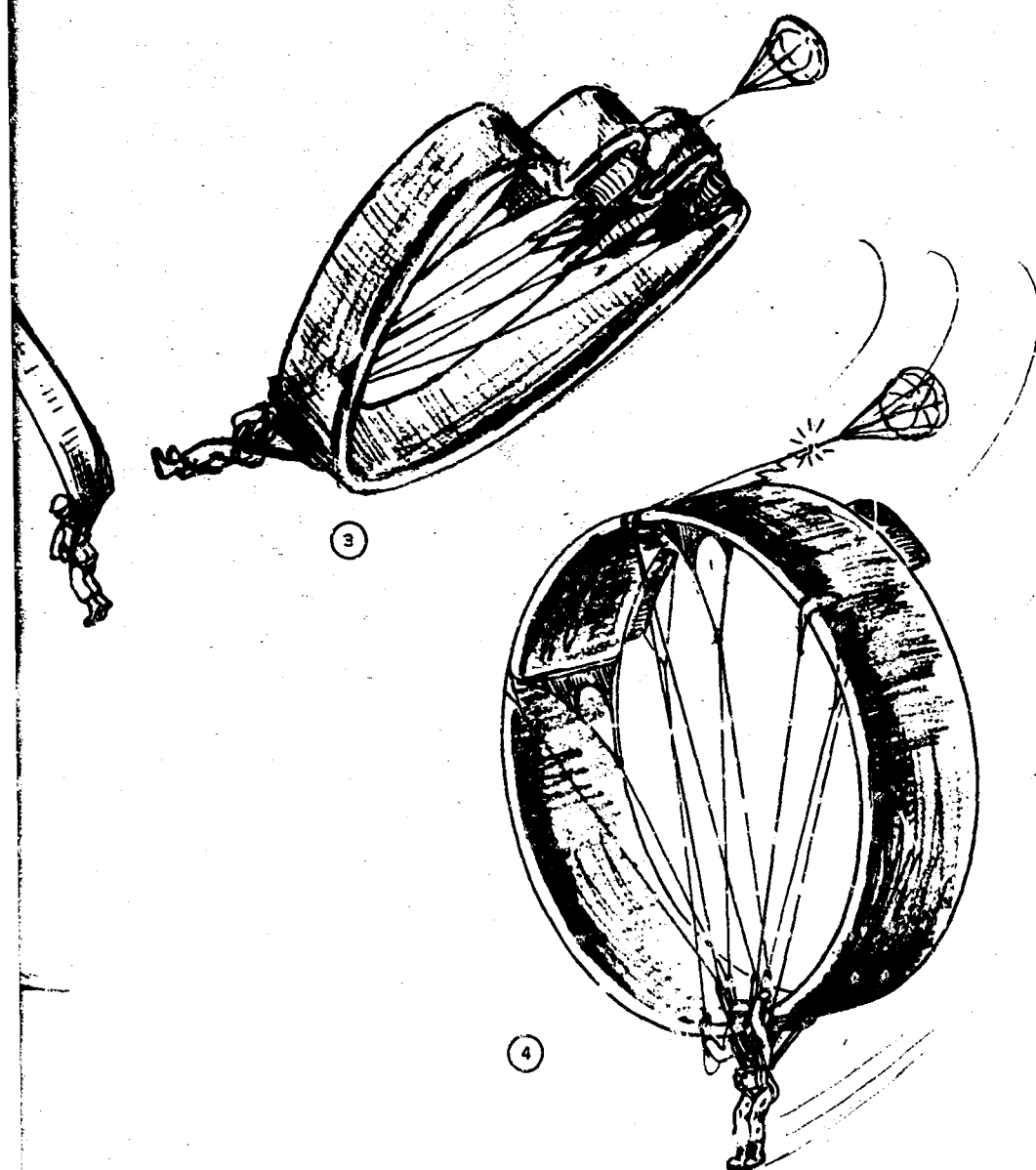


Figure 61 - Ring Wing Airfoil Operational Profile

SECTION III - SYSTEM CONCEPT RECOVERY PROFILES

between the canopy and the man, and terminal descent operations would be the same as those operations now used.

A similar system is the ballistically deployed, ballistically spread parachute. This system would introduce the additional complexity and weight of a timed ballistic canopy projection mechanism as well as problems associated with recoil and unique canopy stowage requirements. A possible advantage, however, is the capability of canopy deployment under somewhat more favorable conditions than those conditions existing in the deployment of a conventional system. Such deployment, as with the BALLUTE/parachute system, conceivably could aid in eliminating line twists and substantially reduce the required minimum operational altitude.

Both ballistic parachute systems would apparently improve the opening characteristics of the canopy itself; however, the reliability of the ballistic mechanism also must be considered.

d. Drag Cone (see Figure 52)

The drag cone offers potential advantages in terms of drop-zone geography and descent downtime. Basically conical in shape, from which it obtains its aerodynamic drag, the drag cone has a blunted nose-apex section that serves as an impact attenuator. Thus, a rapid terminal descent rate and a high-speed land impact presumably could be successfully tolerated.

After leaving the aircraft, a first-stage drogue BALLUTE or parachute would deploy from the trooper's chest pack. This device would orient the trooper (back to earth) for the subsequent deployment of the drag cone. During its inflation, the drag cone would envelop the trooper and provide him with some protection from many normal landing hazards. Consequently, considerable freedom in drop-zone geography, land or water, may be possible.

e. Canopy/Explosive System (see Figure 53)

The canopy/explosive concept uses a small charge or series of small charges incorporated within a relatively small personnel canopy (for example, a 24-ft D_0 standard flat canopy). At the proper intervals, the charges are ignited, and the resulting explosion imparts an upward impulse on the canopy. The intrinsic reaction force is dissipated into the atmosphere beneath the canopy and above the trooper.

In this concept, a reserve-sized canopy is static-line deployed in a conventional manner (see Figure 53). After canopy inflation, the explosives, suspended within the canopy, drop to approximately the canopy inlet. The initial descent phase of the mission is considered unaffected by the charges within the canopy, and the parachute performs in a conventional manner.

SECTION III - SYSTEM CONCEPT RECOVERY PROFILES

When the trooper's feet are approximately three feet above the ground, the explosive charges would be detonated, with a resulting velocity reduction. Failure of the charges to detonate would result in landing conditions typical for a reserve system.

f. Rotating Decelerator (see Figure 54)

Following trooper deployment from the aircraft, a BALLUTE drogue is deployed and ram-air inflated. The drogue is equipped with small canted fabric blades that impart a torque to the BALLUTE, which causes it to rotate. This initial rotation also is imparted to the rotor blades, which then are deployed from their stowed position. The angular momentum imparted from the BALLUTE decreases the transient time necessary for steady-state autorotation of the rotor blades. As the blades deploy, the initial spinup and the autorotative characteristics of the rotor itself would effect the completion of the deployment process. Inflation of the fabric blades also would be initiated with the deployment. Once the inflated operational configuration has been obtained, a controlled descent can be achieved. A maneuverable gliding trajectory then could be obtained by personnel using cyclic pitch control or rotor shaft tilt (see Figure 54) to place the rotor disk at an angle of attack. Operating personnel also could effect a pure vertical descent by maintaining the rotor disk at zero angle of attack. Just prior to landing, flare maneuvers (if required) would be used to obtain the desired touchdown conditions. Cyclic flare first would be necessary to reduce the horizontal velocity component if a gliding approach were made. Collective flare that results in transient increase in lift then would be used to obtain the desired impact velocity.

Two possible approaches for BALLUTE deployment of the rotor blades are available. In the first approach, depicted in Figure 54, the blades initially would be folded and stowed within a deployment bag that is attached to the BALLUTE or rotating-type parachute by a geodetic line suspension system. At deployment, the decelerator separates from the rotor system. The second approach would use a BALLUTE fairing in which the rotor hub would be enclosed. The uninflated blades, attached to the hub, then would extend through slots in the BALLUTE fairing and would be stowed on the BALLUTE's outer surface. In this manner, the BALLUTE fairing would not provide structural support at the root fitting but would perform as a first-stage deceleration and spinup device. At blade deployment, however, the BALLUTE fairing would remain with the rotor system and would spin with the blades about the hub structure.

g. Powered Lifting Systems (see Figure 55)

Stand-on platforms apparently are not compatible with personnel air delivery applications, although delivery using this system conceivably could be performed in a manner similar to the system used for cargo delivery.

SECTION III - SYSTEM CONCEPT RECOVERY PROFILES

A small pilot parachute would deploy a large drogue parachute, which would extract the platform through the cargo-loading doors. The drogue would be reefed initially to keep the suspension lines taut. After extraction, the drogue would be disreefed in one or more stages until it was fully opened and equilibrium conditions had been obtained. At this point, the drogue would be released and the thrust-producing unit, operating since extraction, would be used to generate the lift necessary to provide terminal low-speed descent and possible limited forward flight. Control theoretically would be achieved "kinesthetically" - that is, by the man controlling the thrust vector by shifting his weight and using his instinctive balancing reactions.

Figure 55 shows that the stand-on platform and the trooper are both attached to the parachute. With this arrangement, the trooper could release the platform, in the event of a malfunction, and descend with the parachute. For complete release of the parachute and the conceptual operation of the platform, two releases (one for the man and one for the platform) would have to be activated.

Delivery using either the SRLD or a retrorocket system presumably could be performed in a more conventional manner. A parachute could be deployed during initial delivery to serve as a first-stage decelerator. Prior to landing, the parachute would be separated from the user for subsequent operations of the SRLD or retained to aid in landing with the retrorocket system.

h. Parawing (see Figures 56 and 57)

The technique illustrated in Figures 56 and 57 for deploying the paraglider follows the technique used by Ryan for deploying the individual drop glider. After the trooper clears the aircraft, his static line would extract the sleeve containing the wing. After sleeve extraction, the trooper's momentum would effect the deployment of the wing into the parachute mode. This configuration would provide initial stabilization and deceleration to the composite system and, theoretically, would allow the smooth transition from the parachute mode to the wing configuration. After transition, the trooper would descend in a steady-state glide while preparing for landing. Maneuverability could be achieved by the differential action of the control line. For landing in the drop zone, the trooper would flare the wing. This flaring would decrease both the horizontal and vertical velocities to values compatible with landing requirements. Landing into the wind would reduce or eliminate the effects of ground wind.

For the conical configuration (see Figure 56) and the cylindrical configuration, wing deployment also would activate a short time-delay device connected to the inflation bottles. While in the parachute mode, the inflatable leading edge booms and the keel would be pressurized for the

SECTION III - SYSTEM CONCEPT RECOVERY PROFILES

subsequent transition to the wing configuration. For the limp configuration, this additional system complexity would not be required, and direct deployment to the glide mode may be possible (see Figure 57).

i. Gliding Parachutes (see Figures 58, 59, and 60)

The Parafoil, Parasail, and Cloverleaf would be deployed and operated in a manner similar to the operation of the parawings. First, a sleeve containing the canopy would be extracted from the trooper's backpack and stretched out. The gliding configuration then would be deployed from the sleeve and ram-air inflated into an initial stabilization and deceleration mode. For the Parafoil, the suspension lines are foreshortened; this results in a parachute mode similar to the mode of the parawings. The Parasail and the Cloverleaf both are deployed with their canopies in a reefed state. For transition to the gliding mode, each configuration would be oriented with its leading edge into the wind. Following the initial deceleration phase, transition to the gliding mode would be effected for steady-state gliding descent.

Maneuverability of the Parafoil would be achieved by deflection of the rearward tips using currently applied methods. Control flaps would be used on both the Parasail and the Cloverleaf.

Landing could be accomplished by a flare technique similar to the technique used with the Ryan configuration. With the Parafoil, while operating at $(L/D)_{\max}$, this technique definitely would be desirable for reducing size and weight. For both the Cloverleaf and the Parasail, no substantial advantage is gained apparently by the flare maneuver from steady-state descent at $(L/D)_{\max}$. Consequently, the flare pattern for these configurations probably would not be desirable to eliminate this additional operational requirement.

j. Ring Wing Airfoil (see Figure 61)

Figure 61 gives the personnel air delivery approach for the ring wing airfoil. The ring wing and a drogue parachute would be deployed from a deployment bag. Separation of the bag would activate the inflation apparatus, which would pressurize the leading edge torus and chordwise ribs (or AIRMAT construction) during first-stage descent. During this phase, the small drogue parachute would decelerate and stabilize the composite system while maintaining tension on the stretch-out wing. Tie cords connecting each side of the band also would aid in keeping it from flapping during pressurization. When the configuration is sufficiently pressurized, these ties could be released (see Figure 61) to allow the configuration to take its ring shape. At this time, the drogue chute either could be released or could be retained to aid in trimming the configuration.

SECTION III - SYSTEM CONCEPT RECOVERY PROFILES

The ring shape is maintained throughout the steady-state recovery operation by a pressurized leading edge structure and several chordwise ribs. This configuration has a demonstrated high lift-to-drag ratio and, when properly trimmed, should exhibit good maneuverability potential. As envisioned in this application, control would be achieved by manipulating control lines that attach either to control surfaces on the configuration or directly to the lifting surface fabric.

SECTION IV - CONCEPT EVALUATION

1. GENERAL

System concepts for personnel delivery applications will be evaluated preliminarily in Section IV. Concept evaluation will be in accordance with the criteria discussed in Section I and the concept characteristics discussed in Sections II and III. To a large extent, the evaluation process necessarily is somewhat subjective. This statement is particularly true of operational suitability and reliability, where insufficient data generally are available to establish these characteristics in a quantitative manner. While many of the system concepts have been tested rather extensively, other concepts either have not been tested or the test results, if available, are of limited applicability. Consequently, the evaluation process also will include a qualitative appraisal of the current developmental status of the systems involved.

2. PERFORMANCE AND OPERATIONAL SUITABILITY

One necessary prerequisite to the selection of any system concept for further development is a potential low-altitude delivery capability. Of the concepts considered, only the rapid-opening systems are conceptually designed specifically for this purpose. Nominal opening characteristics of these systems can be determined directly from the opening characteristics of the MC-1 canopy by using the results of Section II. Figure 62 gives the average MC-1 opening times obtained from Reference 30. Only the canopy filling time is assumed to be affected by the inflation aids of the rapid-opening systems (see Figure 63). For the BALLUTE/-parachute system and the internal canopy system, an 18 percent reduction in the inflation time of the standard canopy was used at all airspeeds (see Table IV). For the ballistic system, the reference curve of Figure 6 was used.

Figure 63 shows that the rapid-opening concepts do reduce the inflation time and the corresponding altitude lost. In addition, the rapid-opening concepts provide for a more repeatable inflation time (see Table IV and Figure 6). Despite this, however, the potential altitude reduction does not appear to be large, except for the ballistic parachute system at airspeeds below approximately 100 knots. At 130 knots, the average inflation altitude requirement with the standard system is about 80 ft (see Appendix A). Based on the inflation times given in Figure 63, the potential altitude reduction during inflation with the rapid-opening concepts is only about 15 ft. The estimated inflation time of the ballistic parachute

SECTION IV - CONCEPT EVALUATION

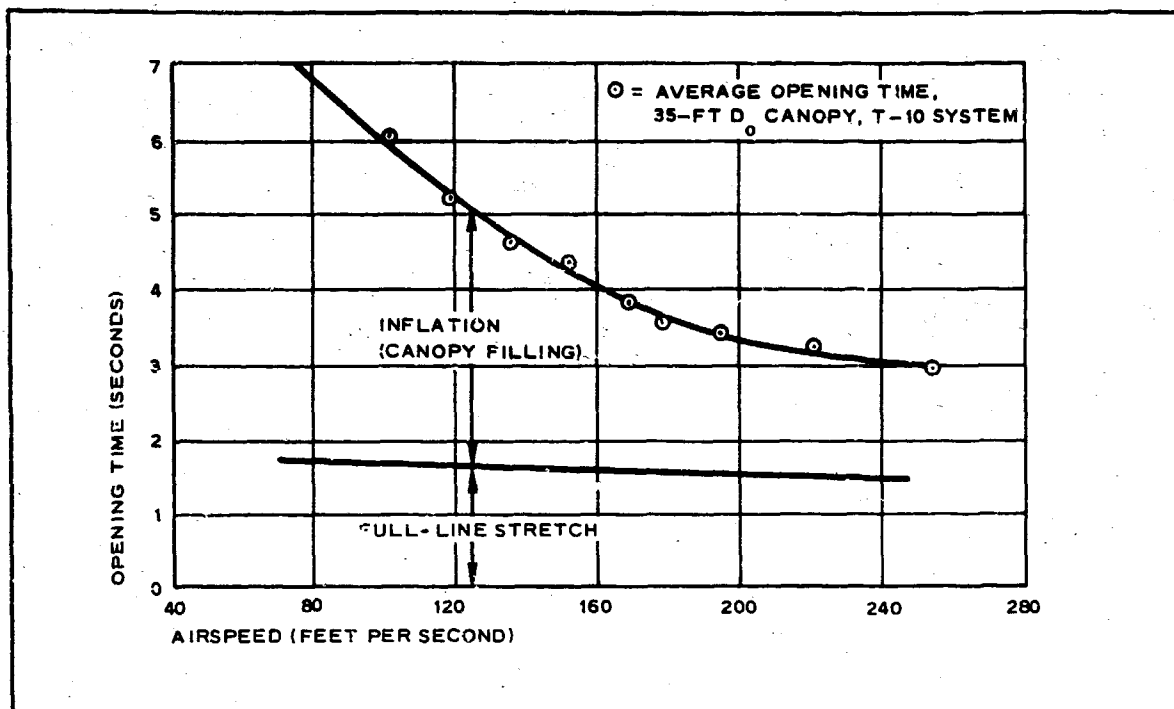


Figure 62 - Opening Time versus Airspeed (T-10 System, MC-1 Canopy)

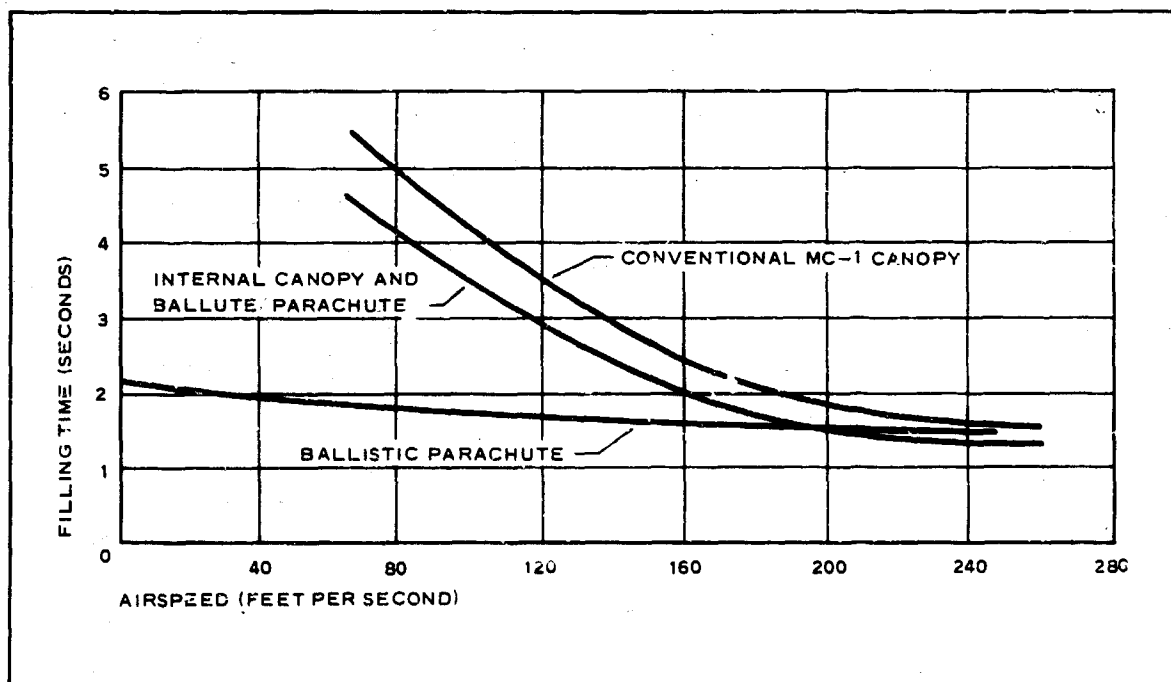


Figure 63 - Inflation Time versus Airspeed

SECTION IV - CONCEPT EVALUATION

(see Figure 6), however, appears repeatable enough that some reduction in the delayed-opening altitude requirement of the standard system also may be possible. This potential advantage, however, could be nullified since ballistic spreading of the canopy cannot be achieved until the canopy has essentially aligned with the flow to preclude its recollapse.

Based on Appendix A, a rather large altitude requirement is necessary with the standard T-10 assembly to compensate for line twists. In this respect, both the BALLUTE/parachute and the ballistic parachute have some potential advantage for reducing this altitude requirement.

Although not conceptually designed specifically for low-altitude application, other system concepts also offer some potential for reducing the present altitude requirement. This statement is true of those systems that achieve terminal equilibrium descent with a canopy smaller than the MC-1 canopy (such as a canopy/explosive system) and, in general, of the completely flexible gliding concepts sized for landing at $C_{L_{max}}$. The comparatively small inflatable volume of these concepts would reduce the necessary inflation time and the corresponding altitude lost. Moreover, with the gliding concepts the comparatively low porosity designs would also promote more rapid inflation, although some tradeoffs between opening shock and inflation time probably would be required. With the rapid-opening concepts, however, the potential altitude reduction may not be large, especially at the higher deployment velocities. Concepts with components that must be inflated from some internal source are expected to require more altitude than the current system.

Table XVIII summarizes the concept performance characteristics. Parameter values given were based on delivery at an initial airspeed of 130 knots. Corresponding values for the MC-1 canopy also are presented for comparison. The table is self-explanatory, except that the operational altitude requirement needs to be clarified. Indicated altitude requirements for the completely flexible gliding systems reflect their generally smaller size, compared with the MC-1 canopy, and their relatively low porosity. The rapid inflation of these configurations, however, would tend to increase the opening shock to possibly a higher level than the level experienced with the T-10 system under comparable conditions. To reduce this load, additional altitude, not reflected in Table XVIII, would be required. The indicated altitude requirements for the rapid-opening systems, in particular the BALLUTE/parachute and the ballistic parachute, reflect potential improvements in the performance characteristics of the T-10 system. According to Reference 31, as much as 220 ft of altitude may be required to discover and to remove completely one- to eight-line twists. These twists often are experienced with the standard canopy system. To a large extent, these line twists occur during the initial canopy-filling stages when the canopy pulls loose from the static line and sails back over the using personnel. With the BALLUTE/parachute system

SECTION IV - CONCEPT EVALUATION

the BALLUTE conceivably could be used to decelerate initially and to stabilize the composite system. Then, after the composite system had aligned with the flight path, the parachute could be released for inflation. This release would permit canopy inflation under more favorable conditions and may reduce substantially or eliminate line twists and the compensating altitude requirement. The same effect may be possible with a ballistically deployed ballistic parachute system by ejecting the parachute after the composite system has aligned with the flight path. In this case, however, no first-stage drogue device would be used to aid in initial stabilization.

Table XIX summarizes the estimated operational characteristics for the system concepts. Estimated system weight and maximum shock loads imposed were obtained from the analyses of Section II, where a composite system design weight of 300 lb was used. A 24-ft D₀ solid flat parachute was assumed, where indicated in Table XIX, since this parachute is the reserve parachute that is readily available and provides a descent rate acceptable in an emergency. Other operational characteristics were obtained from a qualitative analysis of each system (see Section III).

3. NONOPERATIONAL SUITABILITY AND RELIABILITY

Table XX indicates the reliability, current status, and economy of the system concepts. Status of the system concepts reflects their current development in terms of air-to-ground delivery applications, including spacecraft, cargo, and/or personnel. Costs are intended to reflect the relative economics of developing a personnel system for possible wide-spread usage.

TABLE XVIII - ESTIMATED PERFORMANCE CHARACTERISTICS

System concepts	Minimum operational altitude (ft)	Target intercept capability	Inflatable repeat of prior deceleration
Drag concepts:			
BALLUTE/parachute	300 to 500	Fair (subject to wind drift)	Good Table
Internal canopy system	486	Fair (subject to wind drift)	Good Table
Ballistic parachute	300 to 500	Fair (subject to wind drift)	Good Figure
Drag cone	1000	Potentially fair (subject to wind drift)	Unknown
Canopy/explosives	460	Fair (subject to wind drift)	Fair
Thrust-lift concepts:			
Rotating decelerators	800	Apparent controllability	Potential fair
Lift platforms	500	Poor (low control power)	...
Small rocket lift device	460	Controllable	...
Retrorocket system	460	Fair (subject to wind drift)	...
Gliding concepts:			
Conical parawing	800	Controllable	Fair to poor
Cylindrical parawing	500	Controllable	Unknown
Limp parawing	Possibly < 500	Controllable	Fair to good
Parafoil parachute	Possibly < 500	Controllable	Fair
Parasail parachute	500	Controllable	Fair
Cloverleaf parachute	Possibly < 500	Controllable	Fair
Ring wing airfoil	500	Apparent controllability	Unknown
T-10 System (MC-1 canopy)	500	Fair (subject to wind drift)	Fair

A.

SECTION IV - CONCEPT EVALUATION

PERFORMANCE CHARACTERISTICS OF SYSTEM CONCEPTS FOR DELIVERY AT 130 KNOTS

Target intercept capability	Inflation repeatability of primary decelerator	Stability in free descent	Nominal range capability	Remarks
Fair (subject to wind drift)	Good (see Table IV)	Adequate	None	Altitude requirement reflects potential reduction in line twists. Canopy oscillations are ± 10 to ± 20 deg (see Reference 6).
Fair (subject to wind drift)	Good (see Table IV)	Adequate	None	Canopy oscillations are ± 10 to ± 20 deg (see Reference 6).
Fair (subject to wind drift)	Good (see Figure 6)	Adequate	None	Altitude requirements reflect potential reduction in line twists. Canopy oscillations are ± 10 to ± 20 deg (see Reference 6).
Potentially fair (subject to wind drift)	Unknown	Apparently adequate	None	Configuration is statically stable; tube inflation time is approximately 6 sec.
Fair (subject to wind drift)	Fair	Adequate	None	24-ft D_0 solid flat canopy; ± 30 deg oscillations.
Apparent controllability	Potentially fair	Possible instabilities in glide	Low	Blade inflation time requirement is approximately 6 sec.
Poor (low control power)	. . .	Dynamically unstable	None	Configurations not stable enough for general usage in forward flight. Altitude requirement reflects parachute requirement.
Controllable	. . .	Adequate	Moderate	Adequate control obtained kinesthetically. Thrust duration is 20 to 30 sec.
Fair (subject to wind drift)	. . .	Adequate	None	Rockets assist parachute in landing
Controllable	Fair to poor	Adequate	Moderate	Individual drop glider design (see Reference 21); tube inflation time is approximately 6 sec.
Controllable	Unknown	Poor (tendency toward lateral instability)	High	Tube inflation time is approximately 6 sec
Controllable	Fair to good	Adequate	Moderate	Comparatively small inflatable volume (see Table X); low porosity configuration. No tube inflation time requirement.
Controllable	Fair	Adequate	Moderate	Comparatively small inflatable volume (see Table X); low porosity configuration. No tube inflation time requirement.
Controllable	Fair	Adequate	Low	Comparable in size to the MC-1 canopy (see Table X); relatively high total porosity due to vents.
Controllable	Fair	Adequate	Moderate	Less inflatable volume than MC-1 canopy (see Table X); low porosity configuration. No tube inflation time requirement.
Apparent controllability	Unknown	Unknown	High	Tube inflation time requirement is approximately 6 sec.
Fair (subject to wind drift)	Fair	Adequate	None	See Appendix A for altitude requirements. Canopy oscillation = ± 10 to ± 20 deg (see Reference 6).

B.

TABLE XIX - ESTIMATED OPERATIONAL SUITABILITY CHARACTERISTICS

System concepts	Operational hazards	Total recovery system weight (lb)*	Maximum shock load (G's)	Landing velocity (fps)	Compatible with mass air-assault operations	Comments
Drag concepts:						
BALLUTE/parachute	No	41 (ram-air inflated BALLUTE)	6	19	Yes	Yes
Internal canopy system	No	40	5.5 to 6.5	19	Yes	Yes
Ballistic parachute	Yes (ballistic hazard)	48	3	19	Yes	Yes
Drag cone	No	≈ 64 (including initial drogue device)	≈ 29 to 40 (landing impact)	43 to 50	Yes	Yes
Canopy/explosives	Yes (explosive hazard)	≈ 42	8 (with 24-ft D ₀ solid flat parachute)	≈ 19	Yes	Yes
Thrust-lift concepts:						
Rotating decelerators	Yes	54	4	19	No (danger from rotating blades)	Yes
Lift platforms	Yes	70 to 225 (minimum)	6 (drogue parachute)	≈ 0	No (large and bulky, would reduce troop-carrying capability of aircraft)	Yes
Small rocket lift device	No	≈ 150 (including 24-ft D ₀ drogue)	8 (with 24-ft D ₀ solid flat parachute)	≈ 0	Yes	Yes
Retrorocket system	No	43 (at 28-fps equilibrium descent)	8 (with 24-ft D ₀ solid flat parachute)	≈ 0	Yes	Yes
Gliding concepts:						
Conical parawing	No	75 ⁺	8 (design)	19	No (high possible collision rate)	Yes
Cylindrical parawing	No	≥ 75 ⁺	8 (design)	19	No (high possible collision rate)	Yes
Limp parawing	No	≈ 43 ⁺	8 (design)	19	No (high possible collision rate)	Yes
Parafoil parachute	No	≈ 50 ⁺	8 (design)	19	No (high possible collision rate)	Yes
Parasail parachute	No	45 ⁺	8 (design)	19	No (high possible collision rate)	Yes
Cloverleaf parachute	No	52 ⁺	8 (design)	19	No (high possible collision rate)	Yes
Ring wing airfoil	No	50 to 75 ⁺	6 to 8 (design)	19	No (high possible collision rate)	Yes
T-10 system (MC-1 canopy)	No	39	6	19	Yes	Yes

*Includes approximate weight of reserve parachute and other required components that complement the MC-1 canopy.

⁺Configuration size obtained from Table XII and assumes sea-level descent.

A.

SECTION IV - CONCEPT EVALUATION

CHARACTERISTICS OF SYSTEM CONCEPTS FOR DELIVERY AT 130 KNOTS

Compatible with mass e-assault operations	Compatible with emergency procedures	System complexity	Compatible with existing aircraft	Control complexity	Drop zone preparations	All-weather/night operations	Alternate load configurations
	Yes	Low to medium	Yes	Low	No	Yes	Yes
	Yes	Low	Yes	Low	No	Yes	Yes
	Yes	High	Yes	Low	No	Yes	Yes
	Yes	High	Yes	Low	No	Yes	Yes
	Yes	Medium	Yes	Low	No	Yes	Yes
(danger from rotating blades)	Yes	High	Yes	High	No (in vertical descent)	Limited	Yes
(large and heavy, would reduce troop-carrying capacity of aircraft)	Yes	High	No	High	No	Limited	No
	Yes	High	Yes	Medium	No	Limited	No
	Yes	High	Yes	Low	No	Yes	Yes
High possible mission rate)	Yes	High	Yes	High	Some (clear approach	No	Yes
High possible mission rate)	Yes	High	Yes	High	Some (clear approach)	No	Yes
High possible mission rate)	Yes	Low to medium	Yes	Medium	Some (clear approach)	No	Yes
High possible mission rate)	Yes	Medium	Yes	Medium	Some (clear approach)	No	Yes
High possible mission rate)	Yes	Medium	Yes	Medium	Some (clear approach)	No	Yes
High possible mission rate)	Yes	Medium	Yes	Medium	Some (clear approach)	No	Yes
High possible mission rate)	Yes	High	Yes	High	Some (clear approach)	No	Yes
	Yes	Low	Yes	Low	No	Yes	Yes

Element the MC-1 canopy in the T-10 assembly (= 24 lb).

B

TABLE XX - NONOPERATIONAL SUITABILITY AND RE

System concepts	Status *	Reliability			Maintenance and service (inspection, replacement, repair)	D o
		Component complexity	Operational failure susceptibility	Sequencing		
Drag concepts:						
BALLUTE/parachute	Feasibility demonstrated	Low	Low	Good	Low	L
Internal canopy system	Operational	Low	Low	Good	Low	L
Ballistic parachute	Operational	Low	Medium	Good	Medium	L
Drag cone	Study	Medium	Medium	Fair	Medium	M
Canopy/explosive	Feasibility demonstrated	Medium	Medium	Fair	Medium	M
Thrust-lift concepts:						
Rotating decelerators	Feasibility demonstrated (with fabric blades)	High	Medium to high	Fair	Medium	H
Lift platforms	Currently not suitable	High	High	Poor	High	H
Small rocket lift device	Feasibility demonstrated	High	Medium	Fair	High	M
Retrorocket system	Feasibility demonstrated	Medium	Medium	Fair	Medium	M
Gliding concepts:						
Conical parawing	Operational	Medium	Medium	Good	Medium	M
Cylindrical parawing	Currently not practical	High	High	Good	Medium	H
Limp parawing	Early development	Low	Low	Good	Low	L
Parafoil parachute	Early development	Low	Low	Good	Low	L
Parasail parachute	Operational	Low	Low	Good	Low	L
Cloverleaf parachute	Final development	Low	Low	Good	Low	L
Ring wing airfoil	Preliminary study	Medium	Medium	Good	Medium	H
T-10 system (MC-1 canopy)	Operational	Low	Low	Good	Low	.

* Status for aerial delivery applications (not necessary for personnel delivery).

A.

SECTION IV - CONCEPT EVALUATION

ABILITY AND RELIABILITY OF SYSTEM CONCEPTS

Concept	Maintenance and service (inspection, replacement, repair)	Costs			Remarks
		Development	Manufacture	Training requirements	
1	Low	Low	Low	Low	BALLUTE and canopy extensively developed individually. Limited number of drop tests with integral system.
2	Low	Low	Low	Low	Applied to cargo delivery and other applications.
3	Medium	Low	Low	Low	Various successful tests conducted. Ballistically deployed reserve operational.
4	Medium	Moderate	Moderate	Moderate	Has not been tested. Feasibility studies have been conducted.
5	Medium	Moderate	Moderate	Low	Feasibility tests have been conducted.
6	Medium	High	Moderate	High	Feasibility tests with small models have been conducted.
7	High	High	High	High	Development to date indicates unsatisfactory dynamic stability characteristics.
8	High	Moderate	High	Low	Demonstrated ground-to-ground feasibility with the SRLD.
9	Medium	Moderate	Moderate	Low	Technique previously used in recovery applications.
10	Medium	Moderate	Moderate	Moderate	Extensive tests conducted on conical parawings. Deployment and opening of IDG about 25 percent successful in free-flight test (see Reference 21).
11	Medium	High	Moderate	Moderate	Additional surfaces required for lateral directional stability.
12	Low	Low	Low	Moderate	Successfully deployed and operated in both personnel and cargo delivery tests.
13	Low	Low	Moderate	Moderate	Limited wind-tunnel and free-flight drop tests conducted.
14	Low	Low	Moderate	Moderate	Considerable wind-tunnel and drop tests conducted. Demonstrated reliability in recent NASA large parasail drop tests (see Reference 27).
15	Low	Low	Moderate	Moderate	Successfully deployed and operated in various test programs.
16	Medium	High	Moderate	Moderate	Only limited aerodynamic performance data available.
17	Low	...	Low	Low	Proved reliability and delivery capability.

SECTION V - CONCLUSIONS AND RECOMMENDATIONS

1. DRAG SYSTEMS

The BALLUTE/parachute and the ballistic parachute apparently best satisfy, with minimum compromises, the basic requirements for personnel and cargo delivery applications in mass air-assault operations. Both concepts have a potential advantage for substantially reducing the present altitude delivery requirement. Reducing this requirement would lessen delivery aircraft vulnerability and provide for less troop dispersion in the drop zone. Further investigation of these system concepts for the personnel and cargo delivery applications is recommended. For example, a test program with the BALLUTE/parachute seems desirable to substantiate possible performance improvements by aligning the system to the free-stream flow prior to canopy inflation to reduce the number of line twists and the current compensating altitude margin for removal. Further investigation of the ballistic parachute is recommended to determine whether a low-altitude system can be developed with adequate design and operational simplicity and safety. Other drag concepts offer little or no improvements in the performance characteristics of the present system and, in some cases, introduce undesirable operational complexities and safety hazards.

2. THRUST-LIFT SYSTEMS

Thrust-lift systems considered generally do not satisfy the basic requirements of a low-altitude personnel system. For example, present systems of this type are potentially hazardous to personnel and have a comparatively high degree of design and operational complexity. The powered maneuverable lifting systems are, in addition, currently not compatible with the mass air-assault criterion and are heavier than the desired maximum system weight.

3. GLIDING SYSTEMS

Gliding systems in general do not appear particularly suitable for high-density troop deployment until the potentially high personnel collision rate can be satisfactorily resolved. Additional operational training requirements also would be necessary with a gliding system, although a potentially high drop-zone accuracy presumably could be achieved even with high troop dispersion at deployment and/or in ground winds. Although

SECTION V - CONCLUSIONS AND RECOMMENDATIONS

not within the scope of this program, it is noted that the completely flexible (nonrigidized) gliding systems are potentially suitable for special tactical missions, including possible remote delivery applications, where a limited number of highly trained personnel are involved. For this type of application, the limp parawing may be particularly well suited due to its basic design simplicity, performance characteristics, and flare capability.

LIST OF SYMBOLS

NOTE: (Units as given unless otherwise specified in text.)

I - SYMBOLS USED THROUGHOUT REPORT

V = velocity (fps)

V_Z = vertical velocity component (fps)

V_H = horizontal velocity component (fps)

A, S = reference area (sq ft)

q = dynamic pressure (psf)

G = deceleration force per unit weight, F/W

F = force (lb)

W = weight (lb)

$C.S.W.$ = composite system weight for 300-lb design (lb)

L = lift force (lb)

D = drag force (lb), D/qS

C_L = lift coefficient, L/qS

CG = center of gravity

R, r = radius (ft)

D = diameter

D_o = diameter referenced to nominal surface area of parachute canopy (ft)

h = altitude (ft)

AR = aspect ratio, $\frac{b^2}{S}$

LIST OF SYMBOLS

- b = span of reference area (ft)
- C_R, \bar{C} = root chord or keel (ft)
- p = pressure (psf)
- $\frac{L}{D}$ = lift-to-drag ratio of wing or total system as indicated
- $(L/D)_{\max}$ = Optimized lift-to-drag ratio for maximum range
- M = moment (ft-lb)
- C_m = coefficient of moment, $\frac{M}{qS\bar{C}}$
- $(C_D S)_P$ = parasite drag area of attached payload (sq ft)
- $(C_L S)_1$ = parasite drag area per foot of one suspension line (sq ft)
- ΔC_D = attached payload parasite drag coefficient referenced to the wing reference area, $\frac{(C_D S)_P}{S}$
- α = angle of attack (deg) or "is proportional to" for parawings
- $\dot{\alpha}$ = time rate change of angle of attack, $\frac{d\alpha}{dt}$ (deg/sec)
- γ = total system flight-path angle measured from local horizon (deg)
- ρ = air density (slugs/cu ft)

II - SYMBOLS USED WITH SPECIFIC CONCEPTS

A. BALLUTE/Parachute

- $(C_D A)_{\text{man}}$ = drag area of man (sq ft)
- T_i = time at jump
- V_i = jump velocity (fps)

LIST OF SYMBOLS

h_i = jump altitude (ft)

γ_i = total system flight-path angle at jump measured from local horizon (deg)

$(C_D A)_{MB}$ = drag area of man and inflated BALLUTE in combination (sq ft)

B. Internal Canopy System

D_P = projected diameter of parachute (ft)

D_1 = diameter of primary canopy inlet area (ft)

D_2 = diameter of secondary canopy inlet area (ft)

L' = location of secondary canopy with respect to the primary canopy as measured from their respective inlet area planes (ft)

D_{o1} = nominal diameter of primary canopy (ft)

F_C = inflation force of primary canopy without secondary canopy (lb)

t_C = inflation time of primary canopy without secondary canopy (sec)

F = inflation force of primary canopy with secondary canopy (lb)

t = inflation time of primary canopy with secondary canopy (sec)

C. Ballistic Parachute

t_1 = inflation time of LS-1 ballistic parachute (sec)

t_2 = calculated inflation time of ballistically spread personnel canopy, $D_o = 35$ ft (sec)

V_1 = inflatable volume of LS-1 ballistic parachute (knots)

LIST OF SYMBOLS

V_2 = inflatable volume of ballistically spread personnel canopy, $D_0 = 35$ ft (knots)

A_{i1} = inlet area of LS-1 ballistic parachute canopy (sq ft)

A_{i2} = inlet area of 35-ft D_0 personnel parachute canopy (sq ft)

D_{o1} = nominal diameter of LS-1 ballistic parachute canopy (sq ft)

D_{o2} = nominal diameter of 35-ft D_0 personnel parachute canopy (sq ft)

t_a = time at which inlet-spreader gun is fired (sec)

G_1 = G-load with LS-1 ballistic parachute

G_2 = calculated G-load with 35-ft D_0 ballistic parachute

W_1 = LS-1 ballistic parachute composite (total) system weight (lb)

W_2 = 35-ft D_0 ballistic parachute composite (total) system weight (lb)

a_1 = LS-1 total system acceleration (ft/sec²)

a_2 = calculated 35-ft D_0 total system acceleration (ft/sec²)

m_1 = LS-1 total system mass (slugs)

m_2 = 35-ft D_0 total system mass (slugs)

D. Drag Cone

C_{DB} = Drag coefficient referenced to base area

R_B = radius of base (ft)

LIST OF SYMBOLS

r_{MT} = radius of man-torus (ft)

l = length (ft)

C_P = center of pressure

L_C = aerodynamic compressive load in radial torii
(lb/in.)

a = cone angle factor

D_T = torus diameter (ft)

P_{cr} = critical load in inflated torus due to internal
pressure (lb/in.)

E = modulus of elasticity (psi)

I = moment of inertia

r_t = torus tube radius (in.)

t = material thickness (in.)

R_T = torus radius (in.)

θ = cone semiapex angle (deg)

E. Canopy/Explosive System

ΔV = change in velocity (fps)

Δt = change in time (sec)

V_f = final velocity (fps)

W_T = total system weight (lb)

$m_{C.S.}$ = mass of composite system (slugs)

LIST OF SYMBOLS

F. Thrust-Lift Concepts

C_{D_R} = rotor drag coefficient referenced to disk area

$(L/D)_R$ = rotor lift-to-drag ratio

$(L/D)_T$ = total system lift-to-drag ratio

C_T = thrust coefficient

C_{D_P} = attached body parasite drag

W_{BB} = blade weight requirement for pressure (lb)

W_{air} = weight of air required to inflate one blade (lb)

$W_{\bar{C}}$ = weight of coating on one blade (lb)

W_2 = weight of blade section aft of quarter-chord line (lb)

W_1 = weight of blade section forward of quarter-chord line including leading edge material (lb)

W_B = weight of one blade without tip weight (lb)

W_{BT} = weight of one blade including tip weight (lb)

Q = tip weight (lb)

R_R = radius of disk area (ft)

N = number of rotor blades

L_B = rotor lift per blade (lb)

V_t = tip velocity (fps)

β = rotor coning angle (deg)

LIST OF SYMBOLS

$I_{SP.}$ = specific impulse (sec)

V_f = final velocity (fps)

σ = rotor disk solidity

μ = advance ratio

G. Parawings

X_{CG} = distance from the juncture of the leading edges along the keel to a line passing through the center-of-gravity normal to the keel (ft)

Z_{CG} = perpendicular distance from the keel to the center of gravity (ft)

$C_{m\frac{\bar{C}}{2}}$ = coefficient of moment at 50-percent keel

$C_{m\frac{\bar{C}}{4}}$ = coefficient of moment at quarter keel

$C_{Y\beta}$ = rate of change of side-force coefficient C_Y with side-slip angle β

$C_{m\beta}$ = rate of change of yawing-moment coefficient C_m with side-slip angle β

$C_{l\beta}$ = rate of change of rolling-moment coefficient C_l with side-slip angle β

f_m = fabric hoop load in membrane (lb/ft)

P_m = pressure on membrane (psi)

R_m = inflight lobe radius of membrane (ft)

W_m = membrane weight (lb)

k = fabric strength-to-weight ratio $\left(\frac{\text{lb/ft}}{\text{psf}} \right)$

LIST OF SYMBOLS

C_i = constants of proportionality where $i = 1, 2, 3,$
or 4 (lb/ft)

$p_{\bar{C}}$ = internal keep pressure (psf)

$M_{\bar{C}}$ = maximum keel bending moment (ft-lb)

$R_{\bar{C}}$ = keel tube radius (ft)

W' = load parameter; $W' = \frac{(0.546)(C.S.W.)}{\bar{C}}$
 $= \frac{164}{\bar{C}}$ (lb/ft)

$f_{\bar{C}}$ = fabric hoop load in keel (lb/ft)

W_t = weight sum of leading edge and keel tubes

W_{misc} = miscellaneous component weight (lb)

V_t = volume sum of inflatable tubes (cu ft)

p_t = internal pressure in inflatable tubes (psf)

W_{air} = total air weight in tubes (lb)

p_{atm} = atmospheric pressure (psf)

m_{air} = air weight per unit volume (pcf)

α = "is proportional to"

$\alpha_{\bar{C}}$ = keel angle of attack (deg)

$\dot{\alpha}_{\bar{C}}$ = time rate change in $\alpha_{\bar{C}}$, $\frac{d\alpha_{\bar{C}}}{dt}$ (deg/sec)

H. Gliding Parachutes

D_{wet} = diameter of upper surface wetted area, cloverleaf canopy (ft)

LIST OF SYMBOLS

C_X = horizontal-force coefficient

C_Z = vertical-force coefficient

E_F = flap extension for cloverleaf canopy

C_5 = constant of proportionality (lb/ft)

θ = parasail inflow angle measured from a vertical (deg)

I. Ring Wing Airfoil

b = radius of ring and span of the elliptical flat-plate reference area (ft)

C = chord (ft)

$C_{L\alpha_{\mathcal{L}}}$ = rate of change of lift coefficient C_L with angle of attack $\alpha_{\mathcal{L}}$ (1/deg)

C_{D_W} = wing parasite drag coefficient

C_f = skin friction drag coefficient

C_t = drag coefficient due to leading edge thickness

S_{wet} = total surface wetted area (sq ft)

t = leading edge thickness (ft)

C_{D_i} = induced drag coefficient due to lift

$\alpha_{\mathcal{L}}$ = angle of attack of axial centerline of ring (deg)

LIST OF REFERENCES

1. GER-11538: Gemini Ballute System Developments - Final Report. Akron, Ohio, Goodyear Aerospace Corporation, January 1965.
2. GER-11961: Wind-Tunnel Test Report of Ballute Trajectory Control System for Snakeye II Weapon. Akron, Ohio, Goodyear Aerospace Corporation, January 1965.
3. Heinrich, H., and Niccum, R.: A Method to Reduce Parachute Inflation Time with a Minor Increase of Opening Force. Minneapolis, Minn., University of Minnesota, Department of Aeronautical Engineering, August 1960.
4. Murray, E.: Ultrafast Opening Personnel Parachute Type XMP-2. WADD Technical Report (USAF) 60-485, April 1961.
5. Peck, W.: "Application of Ballistics to Precisely Control the Opening of Parachutes, the Ultraprecision Parachute." Symposium on Parachute Technology and Evaluation, El Centro, Calif., Flight Test Center, Edwards Air Force Base, FTC-TDR-64-12, Vol I, September 1964.
6. Performance of and Design Criteria for Deployable Aerodynamic Decelerators. ASD-TR-61-579, December 1963.
7. Kendall, R.: "The Paracone - A Replacement for the Parachute." Symposium on Parachute Technology and Evaluation, El Centro, Calif., Flight Test Center, Edwards Air Force Base, FTC-TDR-64-12, Vol I, September 1964.
8. Study of Saturn S-1C Recovery and Reusability (Vol II), Document No. D2-23233-2. Seattle, Wash., The Boeing Co., December 1964.
9. Handbook for the Design of Guided Missile Recovery Systems (U), Report R-65. Van Nuys, Calif., Radioplane Co., March 1951.
10. Barzda, J.: "Rotary Wing Decelerators." Symposium on Parachute Technology and Evaluation, El Centro, Calif., Flight Test Center, Edwards Air Force Base, FTC-TDR-64-12, Vol I, December 1964.
11. Investigation of Stored Energy Rotors for Recovery. ASD-TDR-63-745, December 1963.

LIST OF REFERENCES

12. GER-12970: Preliminary Investigation of a Ballute-Flexible-Rotor for Low-Altitude Cargo Airdrop. U.S. Army Contract No. DA 19-129-AMC-857(N), Project IM121401 D195, final report. August 1966.
13. GER-12665: Investigation of Ballute-Flexible-Rotor Concept for Low-Altitude Cargo Airdrop; November 30, 1965 to March 31, 1966. Akron, Ohio, Goodyear Aerospace Corporation, May 1966.
14. Hill, P., and Kennedy, T.: Flight Tests of a Man Standing on a Platform Supported by a Teetering Rotor. NACA Research Memorandum RM L54B12a. May 1955.
15. Greenman, R., and Gaffney, M.: Dynamic Stability Analysis of Ducted Fan Type Flying Platforms, Report No. ARD-233. Palo Alto, Calif., Hiller Aircraft Corp., May 1959.
16. Parlett, L.: Hoovering Flight Investigation of Two Methods of Controlling a Man-Carrying Ducted-Fan Vehicle of the Flying-Platform Type. NASA TN D-841, June 1961.
17. Small Rocket Lift Device. TCREC Technical Report 61-123, November 1961.
18. Rocket Motor Manual (U), Vol II. Compiled and edited by the Chemical Propulsion Information Agency, the Johns Hopkins University Applied Physics Laboratory, Baltimore, Md., October 1966 (CONFIDENTIAL).
19. Bradfield, T.: "R. C. D. - An Automatic Touchdown System for the Complete Elimination of Landing Impacts." Symposium on Parachute Technology and Evaluation, El Centro, Calif., Flight Test Center, Edwards Air Force Base, FTC-TDR-64-12, Vol I, September 1964.
20. Rogallo, F.; Sleeman, W.; and Croom, D: Résumé of Recent Parawing Research. Presented at the Course on Aerodynamic Deceleration at the Center for Continuation Study, University of Minnesota, July 1965.
21. Flexible-Wing Individual Drop Glider - Final Report. TRECOM TR 63-26, July 1963.
22. Polhamus, E., and Naeseth, R.: Experimental and Theoretical Studies of the Effects of Camber and Twist on the Aerodynamic Characteristics of Parawings Having Nominal Aspect Ratios of 3 and 6. NASA TN D-972, January 1963.
23. Nicolaides, J., and Knapp, C.: A Preliminary Study of the Aerodynamics and Flight Performance of the Parafoil. Presented at the Course on Aerodynamic Deceleration at the Center for Continuation Study, University of Minnesota, July 1965.

LIST OF REFERENCES

24. Riley, V., and Linhart, E.: Investigation of Various Textile Parachutes and Control Systems to Achieve Steerability - Phase I. FDL-TDR-64-81, October 1964.
25. "Parachutes Tested to Drop Astronauts Softly on Land" from Product Engineering, Vol 37, No. 12, June 6, 1966.
26. Vickery, E.: Aerodynamics of the Parasail. Presented at the Course on Aerodynamic Deceleration at the Center for Continuation Study, University of Minnesota, July 1965.
27. Everett, W.: The Design and Development of the Parasail Parachute. Presented at the Course on Aerodynamic Deceleration at the Center for Continuation Study, University of Minnesota, July 1965.
28. Ribner, H.: "The Ring Airfoil in Non-Axial Flow" from the Journal of the Institute of Aeronautical Science, September 1947.
29. Hoerner, C.: Fluid Dynamic Drag. Published by the author, 1958.
30. Technical Training of Parachutists. Department of the Army Technical Bulletin TM-57-220, January 1966.
31. Memorandum AHBFQS-EA from Col. C. R. Church to members, CINSTRIKE, Air Movements Board: "High Density of Paratroopers on the Drop Zone and More Rapid Assembly."
32. Alexander, W.: Investigation to Determine the Feasibility of Using Inflatable Balloon-Type Drag Devices for Recovery Applications in the Transonic, Supersonic, and Hypersonic Flight Regime; Part II - Mach 4 to Mach 10 Feasibility Investigation. ASD-TDR-62-707 Part II, October 1962.

APPENDIX A - PERFORMANCE CHARACTERISTICS OF THE T-10

PERSONNEL DELIVERY SYSTEM

To facilitate system concept analyses, performance characteristics of the T-10 assembly were studied. This study provides a basic reference frame for system concept evaluation.

Figure A-1 presents opening time requirements for the MC-1 canopy obtained from Reference 30. Figure A-1 also includes the estimated time to canopy full-line stretch, with time zero being the instant of departure from the aircraft. Full-line stretch was assumed to occur when the total separation distance between the man and the aircraft was 45 to 50 ft. Two times were obtained from computer trajectories at 40 and 130 knots, respectively. For the computer trajectories, straight flight and level flight at deployment were assumed, and a constant drag area of six square feet was used to simulate a man in free-fall to full-line stretch.

Figure A-2 shows the estimated total altitude loss when a 300-lb system is delivered. Average altitude requirements for inflation, delayed opening, and line twist removal were obtained from Reference 31. Data from Reference 31 indicate that from one to eight line twists are prevalent in 60 percent of the jumps. Although the data presented in Figure A-2 is at relatively high deployment airspeeds, trends indicate that a substantial altitude increase will be required at lower delivery velocities.

Figure A-3 gives opening force data for the MC-1 canopy. Opening force data with a 200-lb payload were obtained from Reference 6. These data were adjusted by the ratio of system weights to obtain the estimated opening force curve for the 300-lb system. These data were then converted to opening G-load.

Since a 24-ft D_0 solid flat canopy is used as a reserve canopy in the T-10 system, opening force and shock data for this configuration are presented in Figure A-4. The same procedure used in Figure A-3 to obtain estimated opening loads for a 300-lb system also was used in Figure A-4. A higher opening load is encountered with the reserve canopy than with the MC-1 canopy at corresponding airspeeds. This higher opening load is encountered because the reserve canopy has a higher opening shock factor resulting from its different design and its more rapid inflation.

APPENDIX A

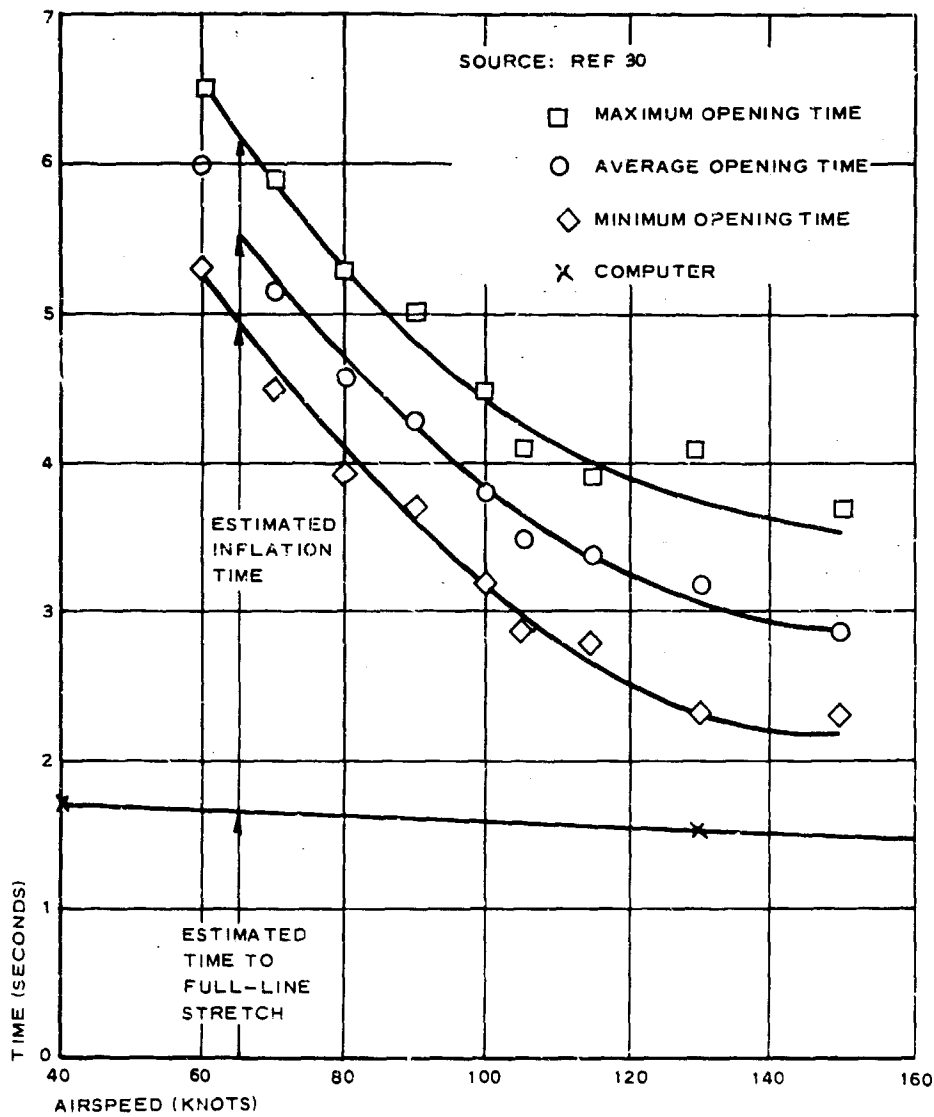


Figure A-1 - Opening Time Characteristics of the MC-1

APPENDIX A

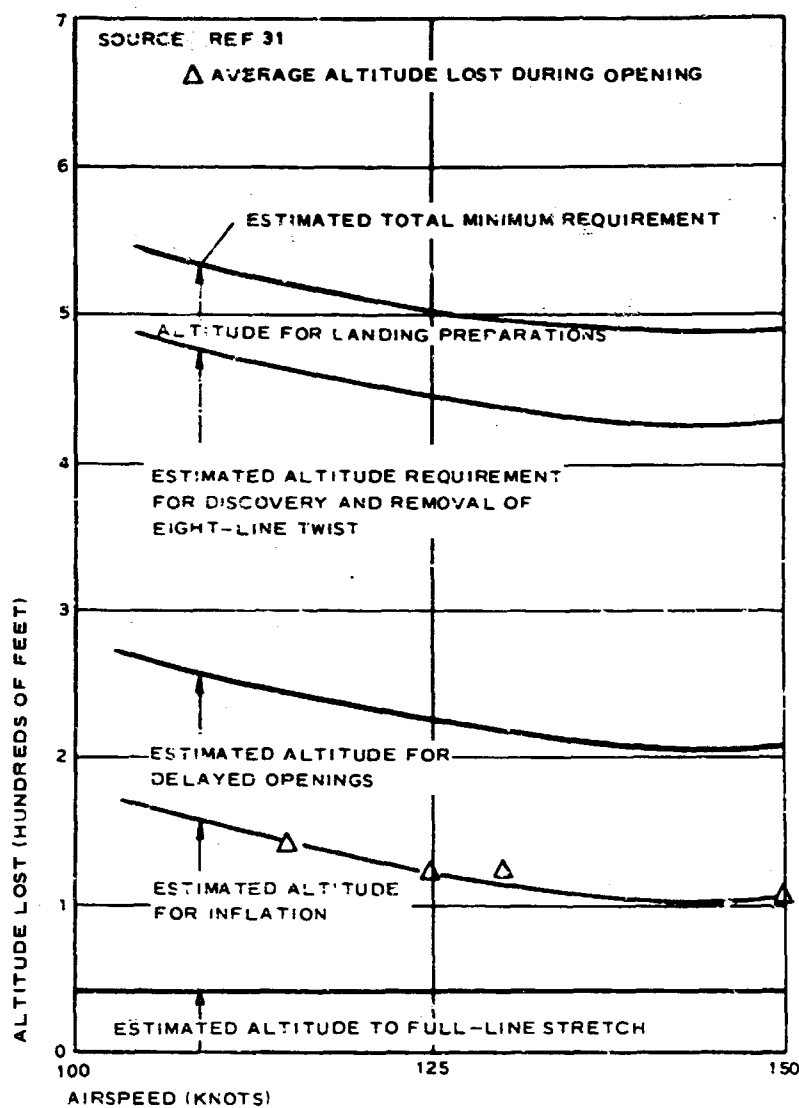


Figure A-2 - Estimated Altitude Lost versus Aircraft Delivery Speed for a 300-Lb System

APPENDIX A

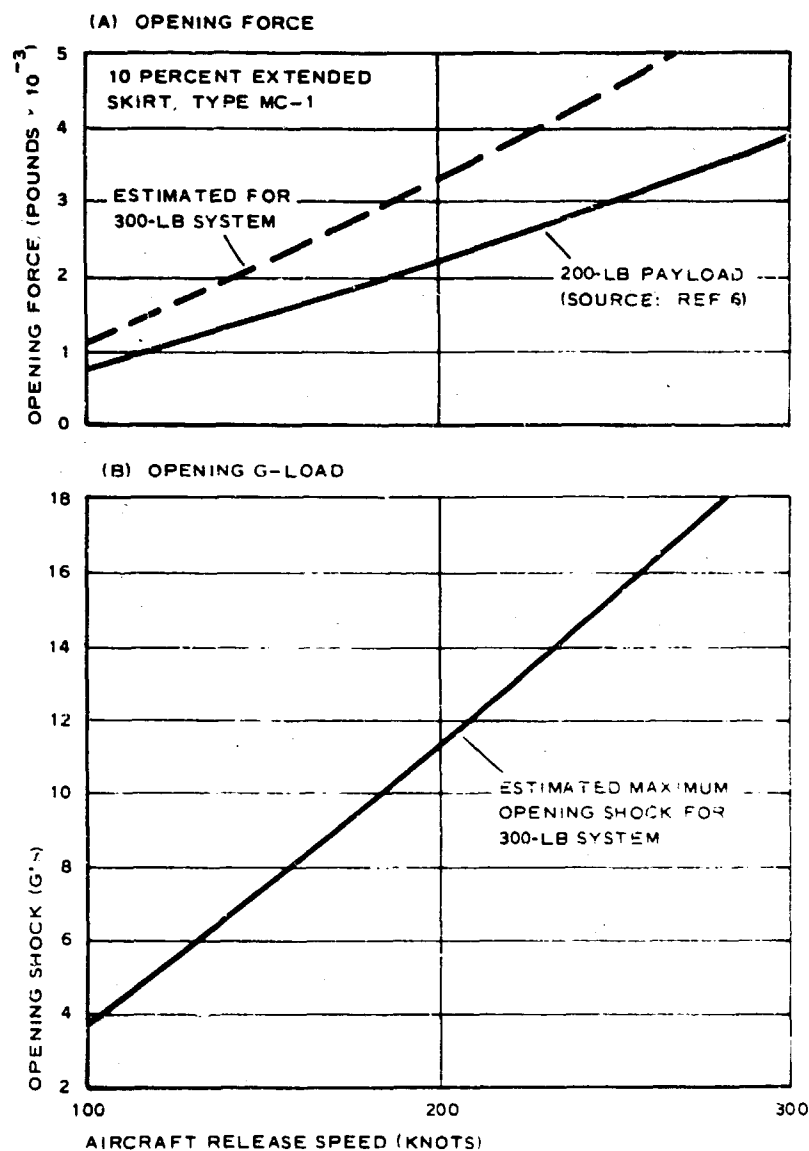


Figure A-3 - Characteristics of a 10-Percent Extended-Skirt Canopy (Type MC-1, 35-Ft D_o)

APPENDIX A

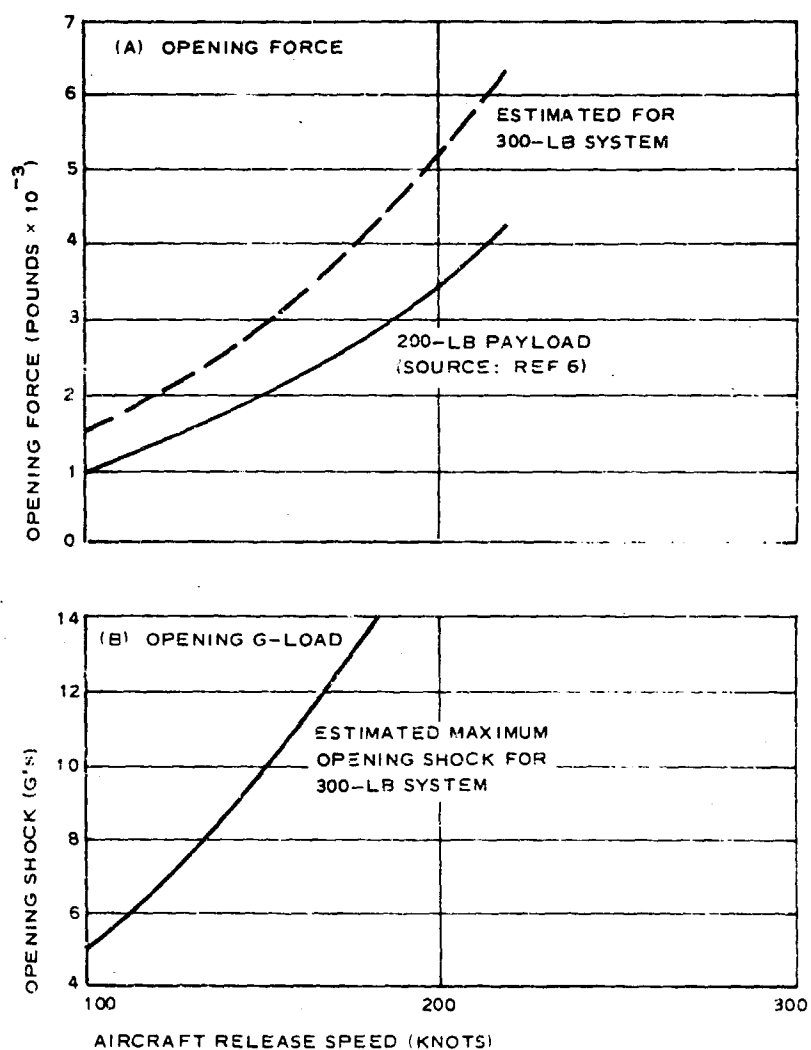


Figure A-4 - Characteristics of a 24-Ft D₀ Solid Flat Canopy

APPENDIX B - INFLATION SYSTEM STUDY (see Reference 32)

1. GENERAL

With any airborne system, weight is one of the prime considerations in determining an optimum design. Figure B-1 summarizes the most feasible methods of system inflation versus weight with internal sources.

The following systems were found worth considering:

1. Compressed gas in pressure vessels
2. Gas generation by burning fuel

2. COMPRESSED GAS IN PRESSURE VESSELS

Probably the most widely used method of producing large volumes of gas at relatively low pressures is storage at high pressures and small volumes in steel, wire-wound, and fiberglass bottles. The state of the art in this area is progressing with the development of higher strength metals and compression equipment. Associated hardware in the form of tubing, solenoids, and pyrotechnic valves is available as an off-the-shelf item. Inflation rates can be controlled easily by metering with standard hardware.

The weight curves for the steel bottle systems and the fiberglass bottle systems shown in Figure B-1 are based on catalog weights for commercially available bottles. The titanium sphere weight curve was calculated from data obtained from a nomograph published by the Titanium Metals Corporation of America. Heat-treated Ti-6A-4V alloy was selected; the design conditions for the bottles were assumed to be 7000 psi of pressure and 100,000 psi of design stress. This stress level gives a safety factor of 1.6 at 70-deg F.

In the three gas bottle systems, the total system weight was determined by adding the weight of the compressed air and the weight of the control valve. The control valve was assumed to be simple, and its weight was estimated to vary from one to three pounds over the range of bottle sizes. A major disadvantage of using this system for personnel delivery applications is the inherent danger in prolonged close contact with high-pressure bottles.

APPENDIX B

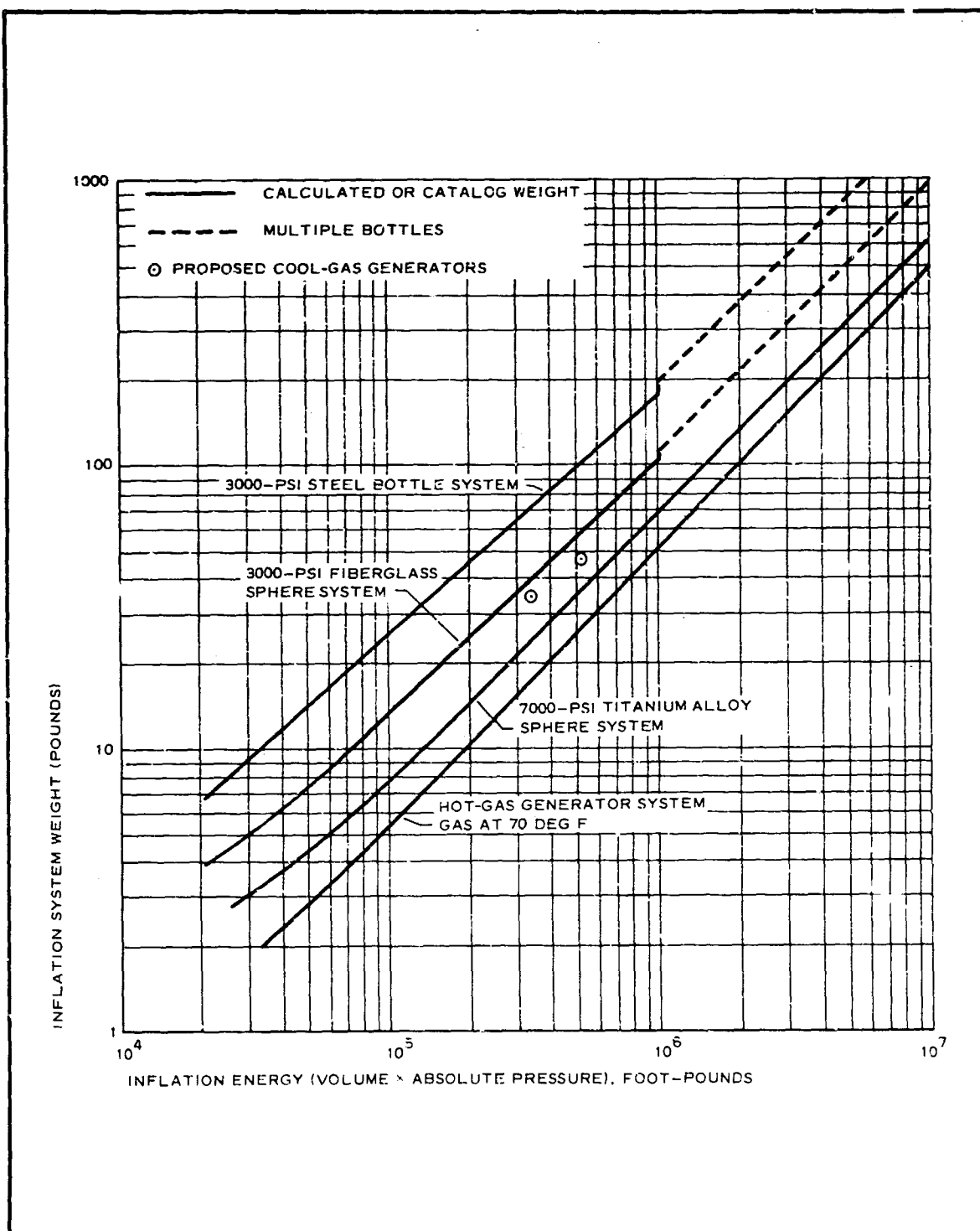


Figure B-1 - Inflation System Weights

APPENDIX B

3. GAS GENERATION BY BURNING SOLID FUEL

Chemical generation of gas by burning explosive-type materials is a very reliable system that is being continuously refined. Hot-gas and cool-gas generators are available in some small sizes as off-the-shelf items. Custom-made gas generators can be procured to fulfill almost any pressure volume requirement. Firing of these devices can be done either electrically or mechanically.

The gas-generator curve in Figure B-1 was calculated from the equation

$$P_v = W r T,$$

where

P_v = energy (lb-ft),

W = propellant weight (lb),

T = gas temperature (deg R), and

r = energy constant = 55 ft/deg R (a good average value for present-day ballistic generators).

The total weight of the gas-generator systems was determined by arbitrarily multiplying the propellant weight by 1.5 to include the weight of the case and hardware. The 1.5 factor was estimated from limited data on hot-gas generators; it assumes that the gas is generated hot and then cooled to 70 deg F for entry into the inflatable structure. Thus, the relationship shown in Figure B-1 has been corrected for the energy loss due to cooling of the gas.

Packaging densities for various pressure bottle and gas-generator systems are given in Table B-I. The density of a typical hot-gas generator was determined from limited data on a generator proposed by the Frankford Arsenal. The density of the cool-gas generator system was determined from data on a McCormick-Selph proposal drawing. Bottle volumes were estimated from catalog data; total weights, including the weight of the compressed air, were used in determining densities.

TABLE B-I - TYPICAL PACKAGING FACTORS

Type of system	Density (pcf)
Hot-gas generator	60
Cool-gas generator	95
Fiberglass sphere, air at 3000 psi	35
Titanium sphere, air at 7000 psi	59
Steel bottle, air at 3000 psi	63

Unclassified

Security Classification *

DOCUMENT CONTROL DATA - R&D		
(Security classification of title, body of abstract and indexing annotation must be entered when the overall report is classified)		
1. ORIGINATING ACTIVITY (Corporate author) Goodyear Aerospace Corp. U.S. Army Natick Laboratories Akron, Ohio and Natick, Massachusetts		2a. REPORT SECURITY CLASSIFICATION Unclassified
		2b. GROUP
3. REPORT TITLE Preliminary Investigation of Concepts For Low Altitude Airdrop of Personnel Exploratory Development		
4. DESCRIPTIVE NOTES (Type of report and inclusive dates) Analytical Study Report 30 Nov 65 - 1 Nov 66		
5. AUTHOR(S) (Last name, first name, initial) Lau, Richard A.		
6. REPORT DATE 30 December 1966	7a. TOTAL NO. OF PAGES 167	7b. NO. OF REFS 32
8a. CONTRACT OR GRANT NO. DA 19-129-AMC-855 (N)	8a. ORIGINATOR'S REPORT NUMBER GER-12888	
b. PROJECT NO. 1M121401D195		
c. Reference No. 65-41	9b. OTHER REPORT NO(S) (Any other numbers that may be assigned this report) 68-43-AD	
10. AVAILABILITY/LIMITATION NOTICES THIS DOCUMENT HAS BEEN APPROVED FOR PUBLIC RELEASE AND SALE AND DISTRIBUTION IS UNLIMITED Qualified requestors may obtain copies of this report from DDC		
11. SUPPLEMENTARY NOTES		12. SPONSORING MILITARY ACTIVITY U. S. Army Natick Laboratories Natick, Massachusetts 01760
13. ABSTRACT This report presents the results of an analytical study that was conducted of various aerodynamic decelerators, to determine the feasibility of use, during mass troop jumps, at altitudes of 500 feet or below, from fixed and rotary wing aircraft flying at speeds of 40 to 150 knots. Of the systems investigated, only two appeared to offer any potential improvement over the present standard system. Of the thrust-lift devices, weight was the major factor for the non-compatibility with mass airdrop operations. The gliding concepts presented many problems when consideration was given to high density troop use during mass airdrop operations. Of the drag concepts investigated, only two appear to reduce the total altitude requirement. These were the internal ballute/parachute system, the internal parachute/parachute system, and the ballistic parachute concept.		

Security Classification

Unclassified
Security Classification

14. KEY WORDS	LINK A		LINK B		LINK C	
	ROLE	WT	ROLE	WT	ROLE	WT
Deceleration	8					
Airdrop operations	9					
Low Altitude	9					
500 Feet	0					
Drag	10					
Gliding	10					
Thrust	10					
Lift	10					
Delivery	8,4					
Military personnel	9,4					

INSTRUCTIONS

1. **ORIGINATING ACTIVITY:** Enter the name and address of the contractor, subcontractor, grantee, Department of Defense activity or other organization (*corporate author*) issuing the report.

2a. **REPORT SECURITY CLASSIFICATION:** Enter the overall security classification of the report. Indicate whether "Restricted Data" is included. Marking is to be in accordance with appropriate security regulations.

2b. **GROUP:** Automatic downgrading is specified in DoD Directive 5200.10 and Armed Forces Industrial Manual. Enter the group number. Also, when applicable, show that optional markings have been used for Group 3 and Group 4 as authorized.

3. **REPORT TITLE:** Enter the complete report title in all capital letters. Titles in all cases should be unclassified. If a meaningful title cannot be selected without classification, show title classification in all capitals in parenthesis immediately following the title.

4. **DESCRIPTIVE NOTES:** If appropriate, enter the type of report, e.g., interim, progress, summary, annual, or final. Give the inclusive dates when a specific reporting period is covered.

5. **AUTHOR(S):** Enter the name(s) of author(s) as shown on or in the report. Enter last name, first name, middle initial. If military, show rank and branch of service. The name of the principal author is an absolute minimum requirement.

6. **REPORT DATE:** Enter the date of the report as day, month, year, or month, year. If more than one date appears on the report, use date of publication.

7a. **TOTAL NUMBER OF PAGES:** The total page count should follow normal pagination procedures, i.e., enter the number of pages containing information.

7b. **NUMBER OF REFERENCES:** Enter the total number of references cited in the report.

8a. **CONTRACT OR GRANT NUMBER:** If appropriate, enter the applicable number of the contract or grant under which the report was written.

8b, 8c, & 8d. **PROJECT NUMBER:** Enter the appropriate military department identification, such as project number, subproject number, system numbers, task number, etc.

9a. **ORIGINATOR'S REPORT NUMBER(S):** Enter the official report number by which the document will be identified and controlled by the originating activity. This number must be unique to this report.

9b. **OTHER REPORT NUMBER(S):** Enter any other report number(s) by which the document may be identified and controlled by the originating activity.

10. **AVAILABILITY/LIMITATION NOTICES:** Enter any limitations on further dissemination of the report, other than those imposed by security classification, using standard statements such as:

- (1) "Qualified requesters may obtain copies of this report from DDC."
- (2) "Foreign announcement and dissemination of this report by DDC is not authorized."
- (3) "U. S. Government agencies may obtain copies of this report directly from DDC. Other qualified DDC users shall request through _____."
- (4) "U. S. military agencies may obtain copies of this report directly from DDC. Other qualified users shall request through _____."
- (5) "All distribution of this report is controlled. Qualified DDC users shall request through _____."

If the report has been furnished to the Office of Technical Services, Department of Commerce, for sale to the public, indicate this fact and enter the price, if known.

11. **SUPPLEMENTARY NOTES:** Use for additional explanatory notes.

12. **SPONSORING MILITARY ACTIVITY:** Enter the name of the departmental project office or laboratory sponsoring (paying for) the research and development. Include address.

13. **ABSTRACT:** Enter an abstract giving a brief and factual summary of the document indicative of the report, even though it may also appear elsewhere in the body of the technical report. If additional space is required, a continuation sheet shall be attached.

It is highly desirable that the abstract of classified reports be unclassified. Each paragraph of the abstract shall end with an indication of the military security classification of the information in the paragraph, represented as (TS), (S), (C), or (U).

There is no limitation on the length of the abstract. However, the suggested length is from 150 to 225 words.

14. **KEY WORDS:** Key words are technically meaningful terms or short phrases that characterize a report and may be used as index entries for cataloging the report. Key words must be selected from a controlled vocabulary, such as the *Index Medicus* or *Index Medicus* or *Index Medicus*. The assignment of links, rules, and weights is optional.